Doctoral Dissertation
Doctoral Program in Chemical Engineering (38th Cycle)

Improving biomass waste upcycling by process intensification in two-stage anaerobic digestion

Gaia Mazzanti
* * * * * *

Supervisors
Prof. Tonia Tommasi, Supervisor
Prof. Francesca Demichelis, Co-Supervisor

Politecnico di Torino
January 31, 2026

I hereby declare that, the contents and organisation of this dissertation constitute my own original work and does not compromise in any way the rights of third parties, including those relating to the security of personal data.

…….....

Gaia Mazzanti

Turin, January 31, 2026

Summary

This PhD project is developed within the framework of the *National Recovery and Resilience Plan* (PNRR) and is funded through the NODES project, an innovative ecosystem designed to foster collaboration between research institutions and industry. NODES is structured into seven thematic spokes, and this research is carried out within Spoke 7, which focuses on the agri-food system, with particular emphasis on sustainability, circularity, and innovation along the supply chain.

In line with these objectives, this thesis investigates how agro-industrial residues can be converted into renewable energy, with a focus on anaerobic digestion and two-stage anaerobic digestion (TSAD). Large amounts of agro-industrial waste are still underutilized, and improving their valorization can support circular economy goals while increasing renewable energy production.

The study combines experimental work with process optimization and preliminary techno-economic and environmental assessments. Following a literature review on TSAD and digestate valorization, the application of TSAD to fruit and vegetable waste (FVW) and jam wastewater (JWW) is explored. To address the potential of hydrogen production, inoculum selection and thermal pretreatment are first evaluated. Key operational parameters are then studied, including substrate-to-inoculum ratio, organic loading rate, and reactor scale. The results show that JWW can be successfully co-digested with FVW, improving overall energy recovery. To extend the range of usable substrates, glucose-rich residues from starch syrup production are also tested. They are evaluated both alone and in combination with conventional feedstocks. The results highlight the flexibility of TSAD in treating unconventional biomass streams. The research also investigates process intensification strategies in TSAD, including thermophilic conditions, biochar addition, and water reuse. Digestate valorization is assessed

through the extraction of humic-like substances, showing potential for additional resource recovery.

A preliminary techno-economic analysis and life cycle assessment of a full-scale TSAD plant identify key limitations, particularly low hydrogen yields and high energy demand.

For substrates not suitable for dark fermentation, alternative single-stage digestion strategies are explored. Animal-based waste, including primary sludge, is tested in continuous systems. Strategies such as optimized feeding, hyper-thermophilic hydrolysis, and bioaugmentation are applied. These improve methane production but also reveal challenges in maintaining long-term microbial stability.

Overall, the study shows that TSAD is a promising approach for biomass waste valorization. It can enhance energy recovery and support circular systems. Further optimization and scale-up are still required to improve performance and feasibility.

Acknowledgment

This thesis is part of the project NODES which has received funding from the MUR – M4C2 1.5 of PNRR funded by the European Union - NextGenerationEU (Grant agreement no.ECS00000036).

I would like to dedicate this thesis to my loving parents

Contents

List of Tables

List of Figures

Abbreviation list

AD, Anaerobic Digestion
BC, Biochar
BEP, Break Even Point
BMP, Biochemical Methane Potential
BOD, Biological Oxygen Demand
C, Carbon
CAS, Cow-Agricultural Sludge
CM, Cow Manure
C/N, Carbon-to-Nitrogen
COD, Chemical Oxygen Demand
CSTR, Continuous Stirred-Tank Reactor
DF, Dark Fermentation
DPS, Digested Primary Sludge
FA, Fulvi Acids
FC, Fixed Costs
HA, Humic Acids
FVW, Fruit and Vegetable Waste
HRT, Hydraulic Retention Time
HTH, Hyper-Thermophilic Hydrolysis
I, Inoculum
JWW, Jam Wastewater
LCA, Life Cycle Analysis
MWW, Milk Wastewater
N, Nitrogen
NPV, Net Present Value
OFMSW, Organic Fraction of Municipal Solid Waste
OLR, Organic Loading Rate
P, Phosphorous
PBT, Payback Time
PS, Primary Sludge
ROI, Return on Investment
S:I, Substrate-to-Inoculum
SCOD, soluble COD
SN, Soluble Nitrogen
TEA, Techno-Economic Assessment
TC, Total Costs
TCOD, Total COD
TRL, Technology Readiness Level
TN, Total Nitrogen
TS, Total Solids
TSAD, Two-Stage Anaerobic Digestion
TSS, Total Suspended Solids
UASB, Upflow Anaerobic Sludge Blanket
UASR, Up-flow Anaerobic Staged Reactor
VC, Variable Costs
VFAs, Volatile Fatty Acids
VS, Volatile Solids
VSS, Volatile Suspended Solids

Chapter 1

1. Introduction

The material presented in this chapter has been published in the article:
Gaia Mazzanti, Francesca Demichelis, Debora Fino, Tonia Tommasi,
"**A closed-loop valorization of the waste biomass through two-stage anaerobic digestion and digestate exploitation**"
Renewable and Sustainable Energy Reviews, Volume 207, 2025, 114938,
ISSN 1364-0321, https://doi.org/10.1016/j.rser.2024.114938.

1.1 Sustainability

The concept of sustainability has gained increasing relevance in recent years; however, defining it in a single, universally accepted manner remains challenging. According to the *Oxford English Dictionary*, the term sustainable refers to something that can be maintained over time. Although this definition appears broad, its significance becomes clearer when sustainability is considered within the framework of interactions between human activities and natural systems. In this context, sustainability addresses the impacts of anthropogenic pressures on the environment and promotes the development of technological solutions that minimize negative effects while avoiding the replication of unsustainable practices adopted in the past.

In recent decades, natural ecosystems have undergone profound changes, accompanied by a growing number of environmental challenges that threaten not only ecological stability but also the social and economic structures that support modern societies. Sustainability, therefore, integrates three strongly interconnected dimensions (environmental protection, economic viability, and social equity) that must be addressed simultaneously. Several studies have identified key objectives within this framework, including the long-term support of human populations, the sustainable management of biological and agricultural resources, the stabilization of population growth, the reduction of economic imbalances, the promotion of decentralized production systems, and the

preservation of environmental quality and ecosystem functionality. From an engineering perspective, the goal of sustainability is the long-term maintenance of human societies while ensuring a quality of life that extends beyond basic survival and includes access to energy, materials, and services. Achieving this objective requires the protection of the environmental systems that support life on Earth, alongside the implementation of infrastructures and technologies capable of producing goods in a manner compatible with ecosystem conservation and resource regeneration (B. J. Brown et al. 1987).

Environmental preservation plays a central role in sustainable development. Historically, human progress has relied on the extensive exploitation of natural resources to improve living conditions. Over the past century, technological advancement and industrial growth have been largely driven by the widespread use of fossil resources, including oil, natural gas, and coal, which remain the dominant sources of global energy. These resources, however, were formed over geological timescales and have been depleted at a rate far exceeding their natural regeneration. In addition to their finite availability, fossil resources contribute significantly to disturbances in the global carbon cycle. Their use in combustion processes releases large quantities of carbon dioxide into the atmosphere, increasing greenhouse gas concentrations and intensifying the greenhouse effect, which in turn leads to global warming. Fossil fuels therefore, present two major limitations: their rapid depletion and their contribution to climate change through carbon cycle imbalance.

These issues raise a fundamental question central to sustainable process engineering: is it possible to replace fossil resources with alternatives that regenerate on timescales compatible with consumption and that do not exacerbate greenhouse gas emissions?

One promising pathway involves the production of energy carriers, fuels, and chemical compounds from renewable biological feedstocks, such as plants and photosynthetic microorganisms. Ideally, these feedstocks should exhibit high growth rates, low water and nutrient requirements, and compatibility with existing biological conversion technologies (Saracco 2017). In this context, organic waste streams represent particularly attractive resources, as their valorization simultaneously addresses waste management challenges and renewable energy production.

1.2 Green chemistry and green engineering

Sustainability is often closely associated with complementary concepts aimed at environmental protection, most notably *green chemistry* and *green engineering*.

Green chemistry was formally introduced in 1998 by Paul Anastas and John Warner in their seminal work *Green Chemistry: Theory and Practice*. It represents an ethical and scientific approach that, through a set of guiding principles, directs the chemical industry toward reducing or eliminating the generation and use of hazardous substances in the design of chemical products and processes. In close analogy with the broader concept of sustainability, the

primary objective of green chemistry is environmental protection through prevention, achieved by promoting the synthesis of safer chemicals and the adoption of environmentally benign reaction pathways.

In addition to minimizing toxicity, green chemistry also aims to improve energy efficiency by optimizing process performance, which in turn is often associated with reduced operational costs. The framework of green chemistry is structured around twelve fundamental principles that provide practical guidance for sustainable chemical design:

1. Prevention: as stated by Benjamin Franklin, "An ounce of prevention is worth a pound of cure." In chemical processing, avoiding waste generation eliminates the need for treatment and disposal and reduces safety requirements, resulting in simpler and more cost-effective processes. The prevention principle is directly implemented by treating organic residues through Dark Fermentation (DF) and Anaerobic Digestion (AD). By converting these residues into H_2, CH_4, and intermediate compounds, the process exploits waste-biomass that would otherwise require disposal or energy-intensive treatment.
2. Atom economy: synthetic methods should maximize the incorporation of all materials into the final product, thereby minimizing waste generation and unnecessary reaction steps.
3. Less hazardous chemical syntheses: chemical routes should be designed to reduce or eliminate the use and generation of hazardous substances, favoring safer alternatives whenever possible. The design of less hazardous chemical processes is intrinsically satisfied in AD and DF systems, which operate in aqueous environments and do not require toxic reagents or aggressive solvents.
4. Designing safer chemicals: chemical products should be effective while minimizing toxicity, achieved by modifying molecular structures to remove harmful functional groups without compromising functionality.
5. Safer solvents and auxiliaries: the use of solvents and auxiliary substances should be avoided or minimized, and when necessary, non-toxic alternatives should be employed.
6. Energy efficiency: processes should be designed to minimize energy consumption and environmental impact, for example, through energy integration strategies. The mild operating conditions typically employed in biological processes, such as mesophilic or thermophilic temperature ranges and atmospheric pressure, contribute to energy efficiency, another key objective of green chemistry.
7. Use of renewable feedstock: renewable raw materials should be preferred whenever technically and economically feasible, alongside the recycling and reuse of non-renewable resources such as metals. In this thesis, all substrates investigated originate from biomass residues with regeneration times compatible with their consumption rates. This approach minimizes the need for additional feedstock and reduces reliance on fossil-based energy sources.

8. Reduce derivatives: unnecessary derivatization steps should be avoided, as they often generate additional waste and require extra reagents.
9. Catalysis: catalytic reagents are preferred over stoichiometric ones, as they reduce material consumption, enhance reaction rates, and improve selectivity.
10. Design for degradation: chemical products should break down into innocuous substances after use and not persist in the environment.
11. Real-time analysis for pollution prevention: continuous monitoring enables early detection of hazardous by-products and timely adjustment of operating conditions.
12. Inherently safer chemistry for accident prevention: using less hazardous substances reduces the risk of releases, explosions, and fires.

The core philosophy of green chemistry, therefore lies in reducing risks at the design stage rather than mitigating damage after it has occurred. This preventive approach avoids hazardous substances and processes that are often associated with higher disposal and safety costs. However, while green chemistry focuses strongly on hazard reduction, it does not explicitly address the overall environmental impact of chemical processes.

This gap is addressed by *green engineering*, an ethical and technical approach also structured around twelve principles, specifically developed to reduce the environmental and health impacts of chemical and industrial systems. Green engineering acknowledges that risk, defined as a function of hazard and exposure, is inherent to chemical production, and therefore emphasizes its control and minimization rather than its complete elimination. Based on this assumption, the twelve principles of green engineering were formulated:

1. Inherent rather than circumstantial: processes should be designed so that material and energy inputs and outputs are intrinsically less hazardous, minimizing risks to both people and the environment.
2. Prevention instead of treatment: waste generation leads to additional processing steps, reagent consumption, and energy use, making waste minimization a critical design objective.
3. Design for separation: developing efficient separation techniques can significantly reduce material and energy consumption, as separation often dominates process costs.
4. Maximize efficiency: inefficiencies frequently arise from excessive use of time, space, materials, and energy; smaller, well-optimized systems operating under mild conditions often offer superior performance. AD efficiency is achieved through the selection of operating parameters such as organic loading rate (OLR) and hydraulic retention time (HRT), which are optimized to balance microbial activity, gas production, and process stability.
5. Output-driven design: production systems should be designed based on desired outputs and demand, avoiding overproduction and excessive resource use.
6. Conserve complexity: reusing complex materials is often more energy-efficient than breaking them down into simpler components unnecessarily.

7. Durability rather than immortality: products should be designed for a defined service life, followed by recycling or reuse, as excessive persistence poses environmental risks.
8. Minimize excess: overdesign should be avoided by tailoring system capacity and flexibility to actual operating requirements.
9. Minimize material diversity: reducing material complexity facilitates assembly, recycling, and reuse across multiple applications.
10. Integrate material and energy flows: a holistic view of processes enables internal reuse and optimization of material and energy streams.
11. Design for commercial end of life: modular design allows recovery and reuse of components even if the primary product reaches the end of its life prematurely.
12. Renewable rather than depleting resources: the origin of raw materials is fundamental to sustaining natural cycles, and renewable resources should be prioritized whenever possible.

Together, green chemistry and green engineering form the foundation of a technological transition aimed at reducing environmental and human health impacts using renewable resources and sustainable process design. These principles were central to the development of this thesis. By employing agro-industrial biomass waste as feedstocks for new processes, the system was designed to be as simple as possible, to minimize solvent use, and to incorporate recirculation strategies to reduce waste (Marteel-Parrish and Abraham 2013).

1.3 Biomass waste as a renewable resource

As mentioned before, the energy economy is facing the depletion of fossil fuels, which are essential in the production of chemicals and energy carriers (Gawel Sołowski 2018). Moreover, the massive exploitation of fossil resources contributes to the greenhouse effect. Renewable resources could partially replace fossil ones by providing energy supplies in a lower environmentally impactful way (Shanmugam et al. 2021). Intergovernmental Panel on Climate Change (IPCC) of the United Nations (UN) elaborated statistical data on CO_2 equivalent emitted per kilowatt hour of electricity options (Schlömer et al. 2014). From this study, based on life cycle analysis (LCA), it is evident how renewable energy production is associated with lower CO_2 equivalent emissions compared to fossil fuels, as shown in *Figure 1.1*. However, renewable energy systems are not always the lowest-impactful solution in terms of emissions. As illustrated by Amponsah et al. (2014), biomass-based technologies can emit a high quantity of CO_2 equivalent/kWh depending on biomass type, the treatment chosen, and boundaries considered in LCA. Sustainable and renewable are not synonyms because, as demonstrated before, there are lots of variables to consider in sustainability analysis, which should be contextualized in the specific case study.

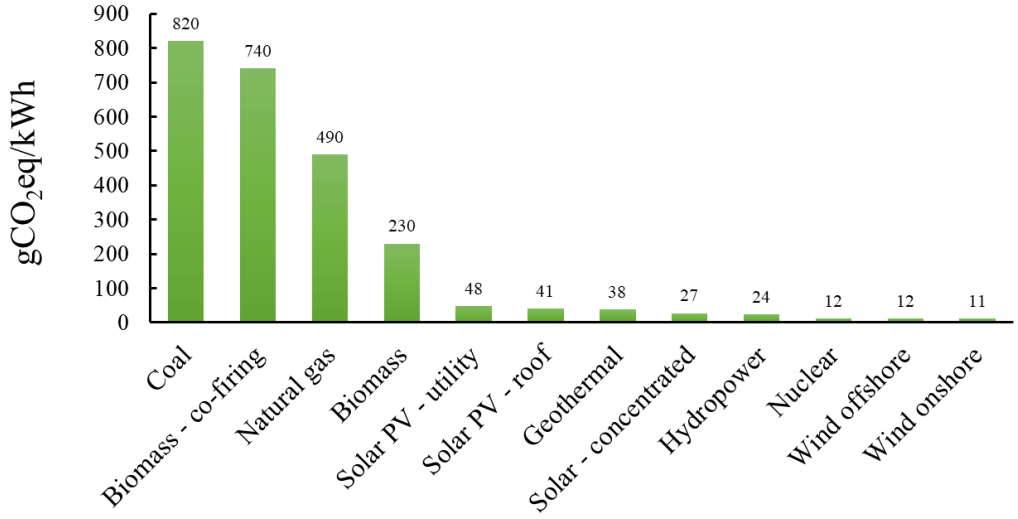

Figure 1.1 Global warming potential of different technologies to produce energy.

Among renewable resources, waste-biomasses represent a feasible and carbon-neutral alternative to fossil fuels according to circular economy pillars, since they can be employed to produce both high- added value chemicals products and bio-energy by developing the waste management systems in agreement with the Waste Framework Directive 2008/98/EC of the European Parliament and of the Council (Gaweł Sołowski et al. 2020; European Council 2008). Waste-biomasses, which are the organic fraction of industrial, agricultural, and urban waste, present environmental, economic, and social issues. From an environmental perspective, they are often subjected to improper management which can cause the release of greenhouse gases emissions, contaminants, and odors depending on their composition. From an economic point of view, waste-biomasses management represents a cost, while from a social perspective waste-treatment plants, and disposal sites are considered not safe and consumed edible areas.

The exploitation of waste-biomasses as secondary -raw materials to produce bio-energy converts them from problem to resource, by enhancing their life cycle according to bioeconomy principles (Geisendorf and Pietrulla 2018). From waste-biomasses, different types of second-generation biofuels could be produced as biodiesel, biogas, bioethanol, and biohydrogen.

Among them, hydrogen has gained interest as both a fuel and a chemical. It is considered a promising fuel because of its high heating value (~120 kJ/g) and low density while it is a key reagent in several production processes like ammonia, methanol, and oils. However, it presents a low boiling point which imposes the storage of the gas at very high pressure to avoid losses (Gawel Sołowski 2018). In addition, hydrogen is not a source ready to use as it is often generated from natural gas. The conventional processes associated with hydrogen production are steam reforming of methane or hydrocarbons, noncatalytic partial oxidation of fossil fuels, autothermal reforming, and coal gasification. The raw materials employed in these conventional techniques are non-renewable and do not observe sustainability principles. Hence, to overcome the global crisis concerning the

depletion of fuels and climate change, an alternative approach is necessary. Among the alternative approaches, the development of methods that use renewable resources as waste biomass may contribute to the satisfaction of the global hydrogen demand (Habashy et al. 2021).

In 2021, Italian government approved the "National Recovery and Resilience Plan" (PNRR), a program containing measures against the economic collapse caused by the COVID-19 pandemic. The plan is part of the Next Generation EU (NGEU) program which is associated to a fund of 806.9 billion € for the transformation of economies and society to make Europe a healthier and greener continent. Italy gathered these goals in two words: recovery and resilience. The first one refers to the willingness to create occupation, invest in healthcare and school, and improve the quality of work; the second one stands for the reinforcement of the ability to respond to economic, social, and environmental shocks and changes in a fair, sustainable, and inclusive way. The PNRR consists of four missions. Among them, Mission 2 concerns the ecological transition of Italy in terms of improvement of waste recycling, protection of waste resources to produce renewable energy, construction of more efficient private and public buildings, and support for research on the use of hydrogen in industry and transport. The second and the latter points confirm once again the central role of hydrogen generated from biomass wastes. Italy allocated a fund of 23.78 billion € for the development of innovative techniques aimed at the ecological transition which affects energy and chemical production ("Italia Domani, Il Piano Nazionale Di Ripresa e Resilienza" 2021).

1.3.1 Biohydrogen production

The most effective routes for biohydrogen production from biomass include thermochemical processes, such as pyrolysis, and electrochemical approaches, as well as biological pathways, including biophotolysis, dark fermentation, and photofermentation.

In pyrolysis, organic materials are subjected to heat in the absence of oxygen to obtain high-value energy products. Three products are generated from the degradation of biomass: biochar, a solid with a high content of carbon; a liquid fraction called bio-oil, composed of oxygenated compounds and condensed gases; a non-condensable fraction rich mostly in CO and H_2 and a small quantity of CO_2, H_2O, N_2, and light hydrocarbons (Sharma et al. 2015; Jahirul et al. 2012). Compared to biological processes, thermochemical ones require a temperature between 400 and 500 °C to achieve a high yield in H_2 (J. Z. Zhang 2014). This requirement is associated with a high energy demand. Pyrolysis is an endothermic process, which makes it energetically costly and more complex in terms of equipment design and operating conditions (Aziz et al. 2021).

Among electrochemical techniques, microbial electrolysis is the most discussed in the literature. In an electrochemical cell, biomass is deteriorated by bacteria to release CO_2, protons, and electrons. Bacteria, which are in the anodic compartment with culture medium, fix electrons to the anode. They arrive at the

cathode through an external wire where they generate hydrogen reacting with protons. The latter ones reach the cathode passing through a membrane. The oxidation of organic matter is not spontaneous, hence voltage should be applied to ensure charges motion. The energy input should be 0.123 V which is considerably lower compared to the redox potential necessary in water electrolysis. However, this technique is the coupling of two opposite processes: on one hand the solution should be conductive to let charges move; on the other hand, high conductive solution is not the ideal environment for the growth of bacteria which needs a neutral pH and rich media. For this reason, scaling up the process is challenging, and its feasibility as an industrial technology remains uncertain (Rousseau et al. 2020). Moreover, the efficiency at an industrial scale remains limited, and the use of platinum cathodes is both costly and environmentally unsustainable (Senthil Rathi et al. 2022).

Biological and photobiological systems are particularly interesting since they are less energy intensive, as they are performed by microorganisms which go through metabolic pathways related to several products. They can be divided in light-independent and light-dependent. Biophotolysis stands among the latter as it is a process where hydrogen is generated from the dissociation of water. The microorganisms involved are photosynthetic bacteria and photoautotrophic green algae (J. Z. Zhang 2014). They absorb light to activate photosystem I and II which transfer light energy through the movement of electrons. These charges reach the hydrogenase enzyme, leading to the formation of hydrogen (Azwar et al. 2014). The main issues related to this technique are the inhibition of hydrogenase in presence of oxygen, the low hydrogen production compared to other processes, and the non-utilization of biomass wastes (Kapdan and Kargi 2006).

Photo-fermentation is another light-dependent technique, and it is based on the utilization of purple non-Sulfur bacteria. H_2 production is possible through the degradation of organic acids in a N_2-deficient environment. Sunlight spreads energy, which is employed to generate electrons from organic matter. Through the action of the nitrogenase enzyme, protons pass a membrane and are reduced by electrons to form H_2 (Kanwal and Torriero 2022). A wide range of biomass can be degraded through this method even if high molecular weight bio-waste needs pre-treatment as in case of lignocellulosic material. Pre-treatments are necessary as lignocellulosic biomass is composed by complex polymers not easy to break. A high efficiency is obtained in the absence of oxygen and with good access to sunlight (Senthil Rathi et al. 2022). In addition, the process is sensitive to the presence of ammonia, which inhibits nitrogenase and stops the fermentation (Habashy et al. 2021).

Each technique presents specific advantages and limitations; therefore, the selection of an appropriate method is not straightforward. With the increasing development of renewable energy technologies, benchmarking tools have been introduced to assess the relevance and feasibility of emerging processes. Among these, the technology readiness level (TRL) is a widely used indicator for evaluating and comparing the maturity of technological developments. Biohydrogen production from biomass is a relatively recent research area, driven

largely by concerns over fossil fuel depletion. Consequently, most of the proposed technologies are characterized by relatively low TRL values. Pyrolysis represents a notable exception, with a TRL of approximately 7. However, despite the identification of optimal operating conditions, this technology is currently limited to pilot-scale applications, as the underlying reaction kinetics and mechanisms are not yet fully understood (Beims et al. 2019). Both microbial electrolysis and photofermentation are currently characterized by a TRL of approximately 4. Microbial electrolysis has predominantly been investigated in small-scale systems, typically using reactors with volumes around 0.5 L. However, industrial applications require operation at significantly larger scales; therefore, demonstrating stable and efficient performance in larger reactors is essential to advance the TRL of this technology (Roy et al. 2022). Photofermentation, on the other hand, is strongly dependent on light availability, with higher H_2 yields generally achieved under artificial illumination. Nevertheless, satisfactory yields have not yet been demonstrated at larger scales, which contributes to the persistently low TRL of this process (Melitos et al. 2021).

Photocatalytic H_2 production exhibits an even lower maturity level, with TRL values up to 3. This is primarily due to the high complexity of the process, which has so far been successfully demonstrated only under laboratory-scale conditions (Frowijn and van Sark 2021). Overall, these considerations highlight that biohydrogen production technologies are not yet applicable at large scale. Although numerous innovative approaches have been proposed, they are currently unable to replace conventional hydrogen production routes based on fossil fuels.

1.3.2 Dark fermentation and anaerobic digestion

AD is a biological conversion process in which organic biomass is decomposed under oxygen-free conditions, resulting in the production of a biogas phase rich in methane. The overall process proceeds through four sequential and metabolically interconnected stages, namely hydrolysis, acidogenesis, acetogenesis, and methanogenesis, whose efficient operation relies on a delicate syntrophic balance among different microbial consortia (Wirth et al. 2012). Disruption of this microbial cooperation can significantly impair system performance and stability.

The initial hydrolysis step involves the breakdown of complex organic polymers into simpler, soluble compounds that can be assimilated by microorganisms. During this stage, hydrolytic bacteria secrete extracellular enzymes that convert carbohydrates, lipids, and proteins into monosaccharides, long-chain fatty acids, and amino acids, respectively. Hydrolysis is often the rate-limiting step of the anaerobic digestion process, particularly when treating substrates rich in structurally complex components, and it is generally favored under operating conditions of 30-50 °C and pH values between 5 and 7. The presence of lignocellulosic biomass further slows hydrolysis due to the recalcitrant nature of lignin, which restricts enzymatic accessibility to fermentable fractions (Zamri et al. 2021).

Following hydrolysis, acidogenesis occurs, during which acidogenic microorganisms metabolize soluble intermediates into volatile fatty acids (VFAs), primarily acetic, propionic, and butyric acids, along with smaller quantities of ethanol and lactic acid. The relative distribution of these fermentation products depends strongly on operating parameters such as pH, temperature, and substrate composition. However, excessive accumulation of VFAs can lead to acidification of the system, resulting in microbial inhibition and, in severe cases, process failure. In the case of protein-rich substrates, amino acid degradation also generates ammonia, which may exert an inhibitory effect on the anaerobic digestion process when present at elevated concentrations (Zamri et al. 2021).

The subsequent acetogenesis stage involves the further conversion of VFAs into acetate, H_2, and CO_2. Although acetic acid can inhibit acetogenic microorganisms, its continuous consumption by methanogens maintains favorable thermodynamic conditions for acetogenesis. Lipid degradation proceeds through acidogenesis followed by β-oxidation, producing acetate from glycerol and long-chain fatty acids (Zamri et al. 2021). This stage is thermodynamically constrained and highly sensitive to H_2 partial pressure, which must be maintained below approximately 10^{-4} atm to ensure process feasibility (Uddin and Wright 2023).

H_2 accumulation is prevented by the activity of methanogenic archaea during the final methanogenesis step, in which H_2 is utilized as an electron donor in the hydrogenotrophic pathway to reduce carbon dioxide to methane. In parallel, acetoclastic methanogens convert acetate directly into methane through an energy yielding reaction (Cai et al. 2016). Methanogenic microorganisms are particularly sensitive to environmental disturbances, including oxygen exposure, and exhibit narrow substrate specificity. They generally require neutral to slightly alkaline pH conditions and low redox potentials. Methanogenesis typically represents the slowest phase of anaerobic digestion, lasting approximately 5–16 days, and in batch systems, the digestion process is considered complete when biogas production ceases, usually after around 40 days.

DF encompasses the first three stages of anaerobic digestion (hydrolysis, acidogenesis, and acetogenesis) and represents the most widely studied biological route for H_2 production from organic substrates. Unlike conventional AD, DF deliberately suppresses methanogenesis, allowing H_2 to accumulate as the primary gaseous product. DF is a light-independent process where the final products of fermentation are H_2, CO_2 and VFAs such as acetic acid, butyric acid, and propionic acid. Considering 1 mol of glucose, 4 mol of H_2 are obtained when the product is acetic acid (CH_3COOH). On the other hand, if butyrate (CH_3CH_2COOH) is generated, 2 mol of hydrogen are produced, following the reactions:

$$C_6H_{12}O_6 + 2\,H_2O \rightarrow 2\,CH_3COOH + 2\,CO_2 + 4\,H_2 \quad (1.1)$$

$$C_6H_{12}O_6 \rightarrow CH_3CH_2COOH + 2\,CO_2 + 2\,H_2 \quad (1.2)$$

In real conditions, both reactions take part in H_2 production together with the small contribution of propionate reaction (J. Z. Zhang 2014). To obtain the highest H_2 yield, the acetate path should be maximized. Moreover, oxygen inhibits hydrogenate enzyme so its presence should be avoided (Kanwal and Torriero 2022). When acidogens reach a steady production of VFAs, their accumulation leads to lower pH and disturbs the activity of microorganisms. VFAs are released in the medium to preserve cell stability. However, if they accumulate in the surrounding environment, cytosol of biocatalysts may be penetrated causing the lysis of cells wall (Dahiya et al. 2021). A wide range of biomass wastes can be treated through DF due to the high flexibility of the process. Moreover, compared with other biohydrogen production technologies, DF is economically advantageous, as it does not require sterile conditions and operates under relatively simple and low-energy-demand conditions (Ubando et al. 2022).

Nevertheless, it is associated with low production, ranging from 10 to 180 mL/g_{VS}, depending on the substrate, which limits its industrial application and scale up (Osman et al. 2023). The VFAs produced during DF, may act as substrate in a further step where methanogens bacteria are able to produce methane. Moreover, their dispersion in the environment should be avoided as they generate pollution while their employment as raw material is completely in agreement with circular economy principles (Y. Zheng et al. 2022). DF shows the second highest TRL between biohydrogen production techniques, which amounts to 5. This value has not risen yet as the process is efficient at laboratory scale, but optimizations are necessary to make it suitable at industrial scale (Buffi et al. 2022).

1.3.3 Two-stage anaerobic digestion

A two-stage process configuration, consisting of DF for H_2 production followed by AD of the remaining solid residue rich in VFAs for CH_4 generation, represents an effective strategy to maximize the valorization of waste biomass. This integrated approach is commonly referred to as two-stage anaerobic digestion (TSAD). In TSAD, the biological phases of acidogenesis–acetogenesis and methanogenesis are spatially separated, as these stages require distinct optimal operating conditions in terms of pH, temperature, and hydraulic retention time, as schematically illustrated in *Figure 1.2*.

The use of two dedicated reactors allows for improved control over process parameters and microbial activity, thereby enhancing overall gas yields and process stability. This configuration enables the simultaneous production of two energy carriers, H_2 and CH_4, while ensuring efficient exploitation of carbon-based biomass. When energy recovery is evaluated considering methane production, conventional single-stage anaerobic digestion achieves an efficiency of approximately 84 % when glucose is used as the substrate. In contrast, TSAD exhibits higher energy recovery, ranging from 86.3 % to 89 %, depending on the specific metabolic pathway governing glucose degradation. These results

demonstrate the superior energy recovery performance of TSAD compared to conventional anaerobic digestion (Ruggeri et al. 2015).

Beyond its enhanced energetic efficiency, TSAD is particularly attractive for biohydrogen production due to its ability to couple H_2 generation with CH_4 recovery and the production of digestate. This residual material represents a valuable secondary stream that can be further processed or upgraded into high-added value products, thereby strengthening the overall sustainability and circularity of the process.

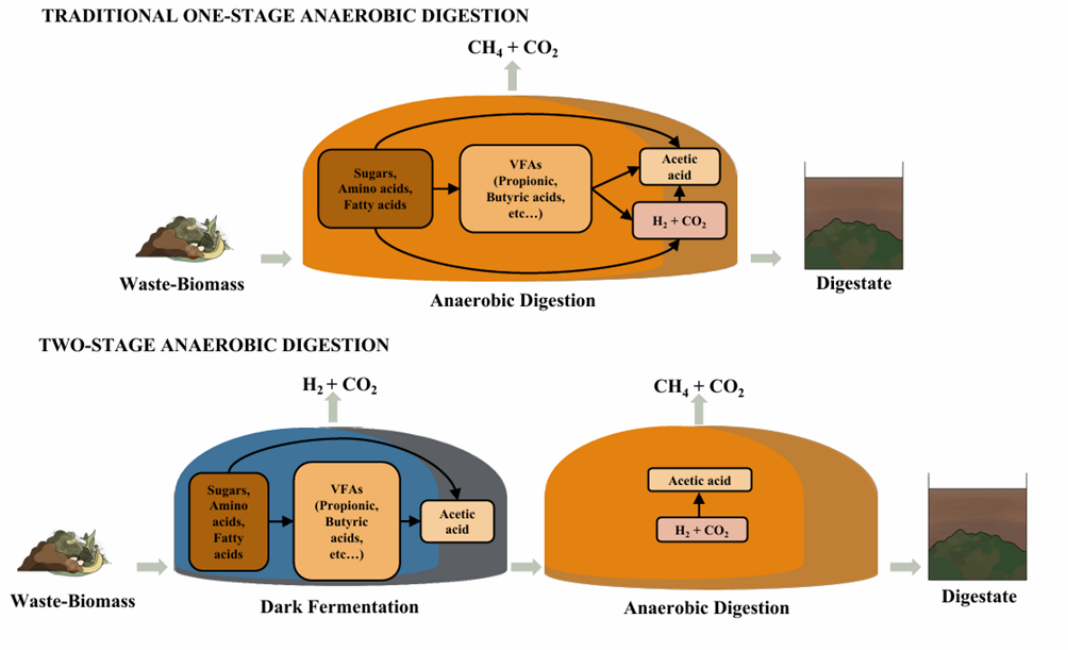

Figure 1.2 Scheme of one-stage and two-stage anaerobic digestion: in the first case, waste biomass undergoes three degradation steps producing a mixture of CH_4 and CO_2; in the second case the process is carried out in two reactors: in the first, dark fermentation takes place producing a mixture of H_2 and CO_2 while its residue is fed to the second reactor where, through methanogenesis, biogas is produced.

1.3.3.1 Main process conditions

The main operational parameters governing TSAD include process conditions such as pH, HRT, OLR, total solids (TS) content, and temperature, as schematically summarized in *Figure 1.3*. In addition to these operational variables, TSAD performance is strongly influenced by the amount of TS fed to the reactors, the type and composition of the processed biomasses, any applied pre-treatment strategies, and the availability of essential nutrients.

pH control is a critical factor, as microbial activity and metabolic pathways are highly dependent on the acidity or alkalinity of the environment. DF operates optimally under mildly acidic conditions, typically within a pH range of 5.0-6.5, whereas methanogenic anaerobic digestion requires near-neutral to slightly alkaline conditions, with optimal performance between pH 6.5 and 8.0 (Kobayashi et al. 2012). The separation of the two stages in TSAD allows each microbial consortium to operate under its respective optimal pH range, thereby improving overall process efficiency.

HRT represents another key parameter, as H_2-producing microorganisms exhibit significantly faster growth kinetics than methanogens. Consequently, DF and AD must be operated with different HRTs to avoid washout of slow-growing methanogens and to maximize gas yields. Typical HRTs range from 2 to 5 d for H_2 production in the first stage and from 10 to 20 d for CH_4 production in the second stage (Bertin et al. 2013; Lembo et al. 2022; O-Thong et al. 2016).

OLR, defined as the amount of organic matter biodegraded per unit reactor volume and time, is inversely related to HRT and commonly ranges from 1.2 to 12 kg_{VS}/m^3 d. An insufficient OLR results in suboptimal substrate utilization and low gas production, whereas excessive OLR can lead to the accumulation of inhibitory intermediates, such as VFAs, ultimately causing process instability or failure (Krishnan et al. 2016).

Temperature strongly affects microbial growth rates and metabolic activity in TSAD systems, which can be operated under psychrophilic (<20 °C), mesophilic (20-45 °C), or thermophilic (55-70 °C) conditions (Cremonez et al. 2021). Increasing temperature generally enhances microbial metabolism and biogas production but also promotes VFAs accumulation, which may result in microbial inhibition if not properly controlled (S. Wang et al. 2019). For this reason, different temperature regimes can be applied in the two stages to optimize volatile solids (VS) removal and CH_4 yield. Nabaterega et al. (2021) demonstrated the benefits of operating the first stage under thermophilic conditions and the second stage under mesophilic conditions, while emphasizing the need to carefully assess the additional energy demand associated with elevated temperatures.

Based on TS content, AD processes are classified as either dry or wet. Dry anaerobic digestion typically operates with TS concentrations between 20-40 % w/w, whereas wet digestion involves TS contents below 15 % w/w (Benbelkacem et al. 2015). Dry digestion offers advantages such as reduced reactor volume, greater flexibility in feedstock selection, and lower water and energy consumption (Angelonidi and Smith 2015). However, limited mass transfer in dry systems can lead to VFAs accumulation, pH reduction, and inhibition of microbial activity (Thaemngoen et al. 2020). Additionally, dry digestion is often associated with lower biogas yields, longer digestion times, and the generation of unpleasant odors (M. Zhou et al. 2019). In contrast, wet digestion requires larger volumes of water and higher energy input for biomass handling, but it ensures improved nutrient diffusion and microbial accessibility, resulting in higher biogas production and potentially greater economic benefits compared to dry digestion (Panigrahi and Dubey 2019; Angelonidi and Smith 2015).

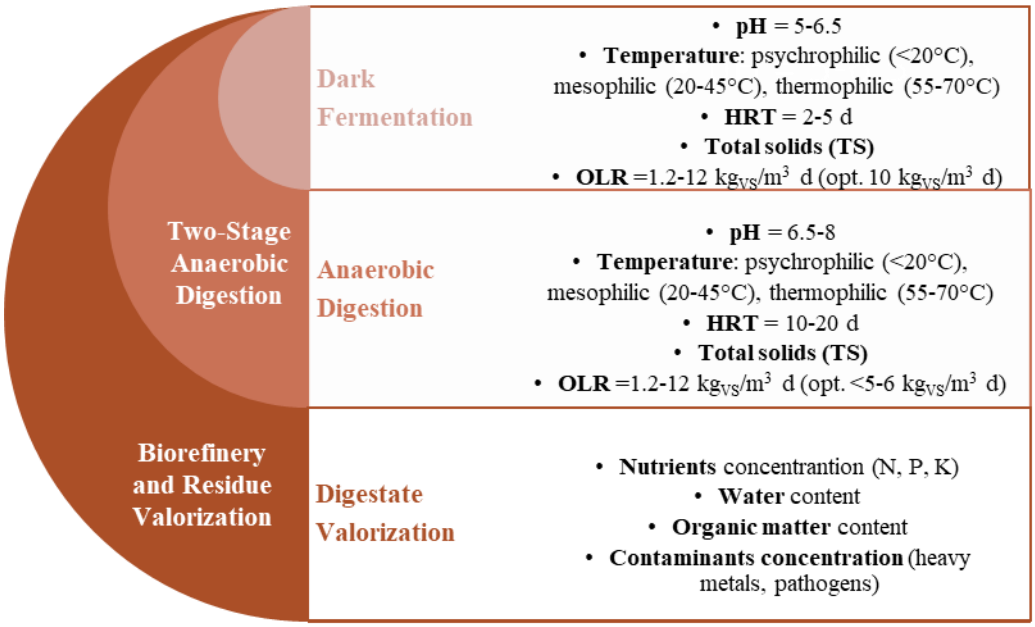

Figure 1.3 Main parameters of dark fermentation and anaerobic digestion to perform two-stage anaerobic digestion followed by digestate valorization and its main parameters.

1.3.3.2 Waste biomass type and characteristics

TSAD can be applied to a wide variety of waste biomasses, which differ in chemical composition, geographical availability, seasonal fluctuations, and rates of biodegradation. The primary constituents of biomass are carbohydrates, lipids, and proteins and they are metabolized by microorganisms at different rates. Simple sugars, mainly mono- and disaccharides, are rapidly consumed, whereas lipids and proteins degrade more slowly. Complex organic polymers, such as hemicellulose and lignin, are broken down even more gradually due to their structural recalcitrance. Although waxes and greases are highly biodegradable, they can generate inhibitory compounds during lipid digestion, potentially halting microbial activity and affecting the production of energy carriers H_2 and CH_4 (Rasit et al. 2015; Cremonez et al. 2021). Seasonal variability further influences feedstock availability; for example, residues from breweries are produced intermittently, whereas agro-industrial and municipal residues are generated continuously and can reliably support H_2 and CH_4 production (Petta et al. 2017).

Table 1.1 summarizes the waste biomasses used in biological processes such as DF, AD and TSAD, grouped into four categories: urban biomass, animal-based agro-biomass, cereal agro-biomass, and industrial biomass. For each biomass, European availability, physical characteristics, elemental and biochemical composition, and the theoretical biomethane potential calculated using the Buswell and Neave equation, indicating the expected CH_4 yield are reported.

This classification follows EU 2009/28/CE and the Eurostat database. Urban biomasses include organic fraction of municipal solid waste (OFMSW), food waste and sewage sludge; animal-based agro-biomasses include manure and animal wastewater; cereal agro-biomasses include rice residues and wheat straw;

and industrial biomasses include bakery waste, dairy residues, olive pomace, oil mill wastewater, and wine industry residues.

Food waste is often degraded through DF or AD because of its easily biodegradable compounds and availability as it is mostly composed of 95 % VS and 85 % moisture (Dinesh et al. 2018). It can be treated in mesophilic (Nathao et al. 2013; Xinyuan Liu et al. 2013; D. Liu et al. 2006; Gómez Camacho et al. 2019) or thermophilic conditions (Lukitawesa et al. 2018; Zhu et al. 2022; Kobayashi et al. 2012) even if there is not a visible improvement in passing from one condition to another.

Manure is another promising substrate, and its composition varies greatly depending on the species of animal, geographical location, and climate but it consists mostly of organic compounds which are rich in both carbon and nitrogen (Risberg et al. 2017). The latter is a nutrient easily detected in sewage sludge, a large part of which originates from wastewater treatment plants hence it is characterized by a high moisture (94 % weight basis) and low volatile solids (3.5 % weight basis) content. It contains organic compounds, microorganisms, and inorganic matter hence it acts as an interesting substrate for digestion (Alrawashdeh et al. 2017). Several components present in sludge are non-easily biodegradable through DF and AD, so pre-treatments are necessary to improve biogas yield (Lee et al. 2023; Akcakaya et al. 2022).

Lignocellulosic biomass, the most abundant waste stream in Europe, has a complex crystalline structure mainly composed of cellulose, hemicellulose, and lignin (B. Liu et al. 2022; Francesca Demichelis et al. 2020). This recalcitrance limits enzymatic accessibility and reduces biodegradability even when pre-treatments are applied. Consequently, TSAD using purely lignocellulosic biomass is rarely reported; it is typically co-digested with more easily degradable substrates such as food waste or cheese whey to enhance microbial conversion to H_2 in the first stage and CH_4 in the second stage (Aravani et al. 2023; Margarita Andreas Dareioti and Kornaros 2015a; Zhu et al. 2022). Pre-treatments are commonly applied to increase digestibility and facilitate microbial access to complex organic matter. By improving hydrolysis rates, these pre-treatments enhance the subsequent conversion of biomass carbon into H_2 and CH_4, ultimately maximizing energy recovery from waste streams.

Table 1.1 Waste biomasses are classified into four categories and for each waste biomass physical, chemical, and biochemical compositions are reported. The acronyms adopted are organic fraction of municipal solid waste (OFMSW), total solids (TS), and volatile solids (VS).

Category	Name	EU Availability (Mt/y)	TS %	VS/TS %	Elemental Composition on TS basis %						Biochemical Composition %			CH_4 (Nm^3/ kgvs)	References
					C	N	S	H	O	C/N	Lipid	Protein	Carbohydrate		
Urban biomass	OFMSW	177	19.32	96.76	48.42	6.76	2.97	0.2	41.65	7.16	11.90	5.40	55.00	0.28	(F. Demichelis et al. 2022; Francesca Demichelis et al. 2023)
	Sewage sludge	550	2.00	65	50.00	3.00	1.9	8.6	36.5	16.67	12.00	9.90	27.30	0.57	(Gebreeyessus and Jenicek 2016; Pellegrini et al. 2016; N. Parmar et al. 2001)
Animal-based agro-biomass	Manure	1400	33.15	59.13	67.87	2.90	0.63	4.87	58.53	11.40	0.40	9.55	41.15	0.22	(Setyobudi et al. 2017; Tsai et al. 2019; Margarita A. Dareioti et al. 2022)
	Broiler and slaughter house litter	N.A.	18.53	89.4	54.90	5.90	1.00	8.50	29.70	9.31	N.A.	N.A.	N.A.	0.62	(Jeon et al. 2013)

Cereal agro-biomass	Rice residues	3.35	94.00	98	36.02	1.12	0.38	6.63	55.85	32.16	1.61	4.12	71.47	0.32	(Izzatie et al. 2016; Pattarapisitporn et al. 2021)
	Wheat straw	144	27.2	84.6	46.60	2.90	0.30	6.60	43.60	16.07	1.38	7.92	36.22	0.45	(Campuzano and González-Martínez 2016; Gaitán-Hernández and Mata 2004; "Wheat Straw Waste Could Be Basis for Greener Chemicals" 2017)
Industrial biomass	Bakery waste	N.A.	74.1	N.A.	N.A.	N.A.	N.A.	N.A.	N.A.	NA	3.00	10.50	46.00	N.A.	(Haque et al. 2016; C. S. K. Lin et al. 2013)
	Dairy residues	192.5	12.5	97	46.50	4.90	5.62	8.43	34.55	9.49	13.50	29.5	45.50	0.55	(Stasinakis et al. 2022; Vidal et al., n.d.; Nečemer et al. 2016)
	Oil pomace	36.69	90.00	86.1	51.28	0.95	0.11	5.86	41.8	53.98	2.33	2.48	29.48	0.50	(Cravotto et al. 2022;

														Sert et al. 2018; Selim et al. 2020)
	Oil mill wastewater	23.35	12.00	75.00	N.A.	N.A.	N.A.	N.A.	N.A.	NA	2.14	5.345	6.86	N.A.	(Solomakou and Goula 2020; Cravotto et al. 2022; Gomec et al. 2007; Foti et al. 2021)
	Wine residues	24750	0.40	87.20	49.80	2.00	0.00	5.80	42.40	24.9	N.A.	N.A.	N.A.	0.47	(Vlyssides et al. 2005; Link et al. 2018; Miklas et al. 2022)

1.3.3.3 Substrate pre-treatments

Pre-treatments are generally classified into four main categories: physical, chemical, enzymatic, and hybrid methods, the latter combining two or more approaches. They are selected depending on different factors as efficiency, environmental impact, cost and complexity of the process. Easily degradable biomasses, such as food waste and OFMSW, typically require only mild physical pre-treatments, including shredding or dilution with water, to enhance microbial access. In contrast, lignocellulosic biomasses, with their complex and cross-linked polymeric structures, demand more intensive treatments to overcome physical and chemical barriers that limit microbial degradation and reduce H_2 and CH_4 yields (S. R. Paudel et al. 2017). By-products may be generated while treating biomass which may inhibit the whole digestion. Evaluating benefits and disadvantages of every technique is mandatory to perform a sustainable process.

Among chemical methods, there are acidic, alkaline, oxidative and ionic-liquid pretreatments. Chemical pretreatments aim to enhance biofuel yield through the disruption of hydrogen and covalent bond between the main components of biomass. They include the employment of inorganic or organic acids to disaggregate structure of biomass. Hemicellulose and then lignin are solubilized to make cellulose more accessible. Typical inorganic acids used to treat biomass are strong as nitric, phosphoric, hydrochloric and sulfuric. Concentrated acids allow to gain a higher yield of biogas but they are also related to harmful effects as the formation of hydroxymethyl furfural which damage biological and enzymatic activity. Moreover, acids can corrode equipment which should be constructed with resistant material, directly associated to an increase in capital cost and maintenance. On the other hand, diluting acids allows to perform a less dangerous, toxic and corrosive digestion associated to easier scale up of the process (Lorenci Woiciechowski et al. 2020). Organic acids represent an alternative to mineral acids as they are environmentally friendly and non-toxic. Furthermore, sugar degradation is minimized together with the formation of inhibitors (Dharmalingam et al. 2022). However, using concentrated organic acids is not ideal as they can penetrate cell membrane and cause a drop in internal pH leading to growth inhibition. They should be diluted even if their concentration in pretreatment is usually higher with respect to mineral acids (Amnuaycheewa et al. 2016).

Alkaline pretreatments act mostly on lignin which is dissolved because of the degradation of ester and glycosidic side chains. Cellulose structure loses crystallinity and it is broken while hemicellulose is degraded. Alkaline substance is mixed with water and then sprayed onto biomass. Among basic components, the most employed are NaOH, KOH, lime, ammonia and urea (Loow et al. 2016). NaOH efficiently degrades biomass but it is expensive, corrosive and hazardous to the environment. Moreover, its recovery and recycle are not easy and can act as an inhibitor to microorganisms. KOH results less toxic and more efficient. It can be employed as fertilizer or in agriculture hence its disposal is much easier (Yu et al. 2019). Lime can be used in the form of CaO or $Ca(OH)_2$ and it enhances

enzymatic hydrolysis and limits toxic inhibitors generation. However, NaOH, KOH and lime are not ideal as additives as they are not renewable. Ammonia and especially urea are proposed for alkaline pretreatments. While liquid ammonia is used at high temperature and pressure, urea can be added to biomass at 55°C and it has a control effect on process pH. Zhu et al. (2022) pretreated corn straw with urea to perform a codigestion with food waste and chicken manure obtaining a CH_4 yield of 106 ml/g_{VS}.

Oxidative pretreatment involves chemical agents as peroxides, alcohol acidic solution, ozone, oxygen or air to dissolve lignin and degrade hemicellulose. On the other hand, cellulose is not affected by the agent and remains undissolved in its crystalline structure. Oxidizing agents are expensive while their efficiency in biomass degradation are not much higher with respect to alkaline and acid pretreatments (Gaweł Sołowski et al. 2020). Between oxidizing agents, hydrogen peroxide (H_2O_2) plays an important role as it can be used at ambient pressures and low temperature. Also ozone can be employed to degrade mostly lignin as it specifically acts on aromatic ring, leaving hemicellulose and cellulose almost intact. Ozone is not associated to the generation of toxic inhibitors so post treatment can be avoided and the process can be considered environmentally friendly. However, acceptable efficiencies are reached with a large amount of ozone making the process too expensive for industrial scale (Norrrahim et al. 2021). Ion-liquid pretreatments employ liquid salts with a melting point below 100 °C, high thermal and chemical stability, low viscosity, toxicity and flammability. They are efficient and eco-friendly but also quite expensive which makes them unfeasible for industrial scale processes. Their efficiency could be optimized by improving their rheological properties or by coupling them with other treatments. However further investigations are necessary to refine their action on lignocellulosic biomasses (Amini et al. 2021).

Physical pretreatments are employed to break lignin barrier and make sugars accessible for digestion. Surface area increase, crystallinity modifications and size reduction are the main effects of physical pretreatments which make biomass amorphous and available for hydrolysis. These techniques are convenient due to no weight loss and no inhibitor formation. However, they required a large amount of energy and are not efficient as chemical pretreatments. To achieve particles reduction, milling should be performed in different forms such as ball milling, wet disk milling, roll milling, grinding and chipping. Extrusion is a more recent process which modifies lignocellulosic structure due to high-power rotation of screws mounted on a grooved shaft. Through this action, an increase in temperature and pressure changes the physical properties of biomass. Compared to other technique, extrusion can occur at relatively low temperature which avoids further degradation of biomass and positively affects the cost of the process (Akobi et al. 2016). Microwave irradiation acts on biomass intra-water which is evaporated altering the cellulose crystallinity. This pretreatment exploits a constant power between 300 and 700 W for a period from 2 to 20 min (Jianwei Liu et al. 2020; Xuran Liu et al. 2019; Feng et al. 2019). Microwaves are suitable for allowing uniform heating even in deeper layers. The solubility of organic

compounds present in biomass is strongly enhanced and they become more available to microorganism (Beszédes et al. 2011). Microwave irradiation also presents some issues related to the scale-up of the process as costs are too high to make the operation profitable. Microwave technique is often coupled to another method, for example acid or alkaline pretreatment, to achieve a convenient and efficient system (Yu et al. 2019). Ultrasound-assisted technique is a physical pretreatment which consists in propagating ultrasound waves, which have a frequency higher than 20 kHz, generating a phenomenon called cavitation. Biomass is crossed by waves while gas bubbles are formed. They to a critical point which is characterized by the implosion of bubbles. Temperature and pressure undergo a local increase which causes the releasing of intracellular compounds due to the damage in cellulose and hemicellulose structure. Another effect of the pretreatment is the enhancement of porosity originated by the disruption of complex polymers. Sugars result more accessible to microorganism thanks to an improvement of the contact area between substrate and microbial population. Biomass volume strongly influences pretreatment as it dilutes ultrasound power mitigating its effect. Some economic analysis manifest profitability in ultrasound waves pretreatment. However, a balance between biomass disintegration and power consumption is necessary to minimize costs. In addition, better results may be achieved combining ultrasound technique and other pretreatments as chemical ones to gain a higher yield in biogas production (Shukla et al. 2023; Mudhoo 2012).

Thermal pretreatments often involve the utilization of additives such as water, air or CO_2 to modify biomass structure at high temperature. Employing those compounds respect sustainability goals as they are environmentally friendly (Antczak et al. 2022). However, heating the system may be very expensive in terms of energy. A deep economic and sustainability analysis should be performed to evaluate the worthiness of the pretreatment. Furthermore, high temperatures may damage some biomasses depending on their heat-sensibility. Steam explosion is one of the alternatives and it consists in two stages: firstly, lignocellulosic biomass is heated with sub-critical water at 170-210 °C at high pressure to cause the hydrolytic disruption of cell wall; afterwards, steam undergoes an expansion due to a sudden pressure drop which allows vapor accesses the fibrous structure and its breakage. An enhancement of porosity and surface area of the substrate is obtained because of changes in lignin and solubilization of hemicellulose. The main issue is the control of process parameters even if it is already employed at industrial scale (Ziegler-Devin et al. 2021). Liquid hot water pretreatment involves the utilization of water at elevated temperature and pressure to overcome lignocellulosic recalcitrance. It is an eco-friendly technique as it avoids hazardous chemicals and corrosion of equipment (Shang et al. 2019). Hemicellulose is dissolved, lignin is broken and positioned differently while cellulose is slightly disintegrated to avoid sugars loss (M. Li et al. 2017). Water is heated up to 120-230 °C under subcritical conditions and is applied to biomass from 2 min to 6 h. Some inhibitors are generated, especially at higher temperature as furfurals, 5-hydroxymethylfurfurals and melanoidins which can affect substrate degradation

(González and Heiermann 2021). Among green solvents, CO_2 is an attractive alternative to treat biomass. It is economic, non-flammable, inertness, non-toxic, ubiquitous and recyclable. In addition, it is characterized by moderate supercritical properties (7.38 MPa, 31.05 °C) compared to water ones. Supercritical CO_2 is employed in CO_2 explosion due to its low viscosity, zero surface tension and gas-like diffusivity (Zabihi et al. 2021). CO_2 diffuses through micropores and when pressure is released, a breakage in cellulose makes sugars more accessible to microorganism action. Moreover, its dissolution in water causes a rise in system acidity which contributes to biomass degradation and explain why dry biomass is not suitable for this pretreatment (Gu et al. 2013). Supercritical CO_2 pretreatments are commonly carried out for about 5-60 min, at 60-150 °C and 120-240 bar (Navarro et al. 2021). Specific equipment should be used to bear high pressure which is often related to elevated costs. Furthermore, extreme conditions could also cause degradation of the final product (Arumugham et al. 2022). Wet air oxidation is a thermal pretreatment which consists in oxidizing biomass under sub-critical conditions. A temperature between 125 °C and 320 °C together with pressure goes from 0.5 MPa to 2 MPa are commonly used. Oxygen is the main gaseous source even if air is usually used as oxidizing agent (Banerjee et al. 2009). Pressurized wet air cause hemicellulose and lignin dissolution and easier access to cellulose. A lower amount of furfural and HMF are formed compared to steam explosion. On the other hand, organic acids are produced to start the degradation process producing lower molecular weight components (Z. Zhou et al. 2023). This pretreatment can be also employed to completely degrade biomass to CO and CO_2 even if in AD system, that transformation is undesired. Furthermore, wet air oxidation can be enhanced through catalysts as metal ions, noble metal-based catalysts, transition metal-based catalysts (Ansaloni et al. 2018).

Biological pretreatments require lower energy consumption and complexity as there are not chemicals to be recycled and toxic compounds emissions are avoided. They allow to achieve a high sugar degradation and digestible solids in mild conditions (Kocher et al. 2017). Biological pretreatments employ fungi, bacteria and enzymes. Among fungi, filamentous white rot fungi are efficient as they usually grow on dead or living wood producing enzymes in nitrogen deficiency (Terasawat and Phoolphundh 2021). Microorganisms generate enzymes which allow hydrolysis of the substrate. The most important lignolytic enzymes produced by fungi are manganese peroxidase (MnP), lignin peroxidase (LiP) and laccase. The first two degrade biomass oxidizing lignin while laccase is activated in presence of oxidizers as 2,2'-azinobis-(3)-ethylbenzylthiazoline-6-sulphonate (ABTS) and acts on phenolic compounds, anilines and aromatic thiols through copper ions (Bak et al. 2010). On the other hand, cellulose is degraded by cellulase which breaks β-1,4 linkages. Cellulase activity is directly affected by cellulose accessibility which is hindered by xylan. The latter one is the main component of hemicellulose which participates to cell structure as it creates a cross linked network. Xylanase is an enzyme present in multiple forms with different characteristics and actions. Biological pretreatments show some issue

mainly related to enzyme production costs which are not feasible for industrial scale applications (Hosseini Koupaie et al. 2019). In addition, process stability and high efficiency are not guaranteed. Further research is needed to optimize the process and make it convenient (de Freitas et al. 2021).

1.3.3.4 Inoculum pretreatment in dark fermentation

The microbial communities involved in DF must be completely free of methanogens, which consume H_2 and inhibit its recovery. To achieve this, pretreatment of the inoculum is necessary to eliminate these microorganisms, encouraging the proliferation of H_2-producing bacteria.

Common pretreatment techniques include thermal and chemical methods. Thermal technique involves microbial heating at temperatures between 60 and 120 °C during a period of 15-240 min. Ravindran et al. (2010) investigated the effect of thermal pretreatment on the isolation of hydrogen-producing microorganisms by applying five different temperatures (65, 80, 95, 105, and 120 °C) for one hour to forest soil. The highest hydrogen production was observed at 95 °C, followed by 105 °C. Lower temperatures were not conducive to the sporulation of additional strains, which were instead present under more extreme conditions.

Similarly, Hidalgo et al. (2023) evaluated the impact of inoculum thermal pretreatment at 60, 80, and 100 °C. Their findings indicated that while there was no significant difference in hydrogen production among these temperatures, residence time played a crucial role. A 30-minute treatment enhanced biogas production at 80 and 100 °C, whereas a one-hour treatment was more effective at 60 °C. Various time-temperature combinations have been tested, suggesting that mild conditions are preferable to prevent the complete deactivation of microbial cultures.

Although thermal pretreatment is a straightforward process, it does not always fully eliminate hydrogen-consuming microorganisms. Some may sporulate, while others are only temporarily suppressed and can re-emerge over time. Therefore, periodic thermal pretreatment may be necessary to sustain hydrogen production. This limitation also impacts on the economic feasibility of the process, which must be carefully assessed (Bundhoo et al. 2015).

Chemical pretreatment involves the modification of inoculum pH to stimulate H_2-producer development. Strong acids such as HCl, H_2SO_4, and HNO_3 can be added to the culture until a certain pH is reached. Lee et al. (2009) evaluated the use of HCl, H_2SO_4, and HNO_3 for acid pretreatment of inoculum sourced from an anaerobic digester. Each acid was added to the inoculum until the pH reached 2, and then adjusted to 5.5 after 24 hours. HNO_3 had an inhibitory effect on the process due to excessive nitrate accumulation in the reactor, which exceeded the acceptable threshold by a factor of 3.5. Similarly, H_2SO_4 led to high sulfate concentrations, which were toxic and inhibited fermentation. Among the acids tested, HCl was identified as the most suitable option for enhancing hydrogen-producing microorganisms. In a separate study, Hidalgo et al. (2023) also explored the use of strong acids for inoculum pretreatment. Their results indicated

that H_2SO_4 did not cause any significant adverse effects on biogas production compared to HCl. Nonetheless, both studies concluded that HCl is the most effective acid for chemical pretreatment. While acid pretreatments are generally simple, cost-effective, and efficient, they also present some limitations. These include the necessity of pH adjustment post-treatment, the potential formation of undesirable by-products that may require disposal, and the need for periodic repetition to maintain efficacy on the microbial culture (Bundhoo et al. 2015). As previously mentioned, thermal and acid pretreatments are the most commonly used techniques in dark fermentation processes. However, in recent years, several alternative methods have been proposed, making it difficult to determine a universally superior approach (Bundhoo et al. 2015). While some studies have identified chemical pretreatment as the most effective, others have highlighted heat shock treatment as the best strategy for eliminating methanogens and enhancing hydrogen production (Al-Haddad et al. 2023; Chen et al. 2021).

1.3.3.5 Nutrients balance

Nutrient balance, such as nitrogen (N) and phosphorous (P), is an important parameter to guarantee process control and it can be achieved through the addition of artificial nutrients or through simultaneous digestion of different substrates by performing a co-digestion. This approach aims to maximize the process energy production by creating a suitable environment for microorganisms' growth. This condition is possible when a proper C:N:P is reached.

Nitrogen is important for microorganisms' propagation because of its buffering capacity, which is essential during VFAs production, but nitrogen in the form of ammonia can inhibit the process. On the other hand, nitrogen is essential in amino acids production by microorganisms (Tufaner and Avşar 2016). Reaching an ideal ratio between carbon and nitrogen content, around 20-30, can enhance digestion performance (Esposito et al. 2012; Z. Zheng et al. 2021). Phosphorous is essential too for an optimal microbial growth and a good control of pH and its quantity should account for 15 % of N content in a reaction environment (Hussain et al. 2015). Finding a unique value of C:N:P is hard as several different values are reported in the literature. Comparing them, a ratio C:N:P equal to 200:7:1 can be adopted in the digestion design. Even if N and P presence enhances biogas yield, their concentration should not be too high because it is associated to with inhibition phenomena, precipitation of N and P salts which make nutrients no more available, higher costs, and release of N and P compounds in waterways, causing pollution (Gil et al. 2019).

When the correct nutrients are provided, microorganism activity is maximized, and this condition can be reached by mixing feedstocks with different compositions. Co-digestion technique is quite popular adopted in DF and AD since most biomass wastes do not contain the adequate amount of nutrients.

1.3.3.6 Co-digestion

Co-digestion consists of combining different biomasses to achieve a more balanced nutrient composition, while simultaneously providing several operational advantages. One of the main benefits is the possibility of regulating pH by blending acidic, carbon-rich substrates with alkaline biomasses rich in nitrogen, thereby improving process stability. In addition, the moisture content of the feedstock can be optimized without the need for fresh water addition, or by minimizing its use, through the selection of inherently humid substrates that help achieve the desired TS content (Esposito et al. 2012).

Biomasses rich in phosphorus, such as sewage sludge or food waste, are often combined with substrates that are poor in this element to avoid nutrient imbalance (Lan et al. 2022). Food waste, although rich in carbon, may lack sufficient nitrogen and can therefore lead to excessive acidification and inhibition of microbial growth. For this reason, it is frequently co-digested with nitrogen-rich biomasses such as manure or sludge, which enhance the buffering capacity of the system and mitigate acidification caused by fatty acid accumulation (Alrawashdeh et al. 2017).

Similarly, dairy residues can serve as suitable substrates for microbial activity; however, the digestion of whey often results in rapid acidification of the process environment. To counteract this effect, whey is commonly combined with nitrogen-rich biomasses, such as manure or sludge, which help maintain stable operating conditions and improve overall performance (Bertin et al. 2013; Dareioti e Kornaros 2015).

Table 1.2 summarizes selected two-stage anaerobic digestion studies applied to different substrates. The first section of the table reports mono-digestion process conditions and corresponding yields, while the second section focuses on co-digestion configurations. The data clearly show that a wide range of substrate combinations can be employed; however, the common characteristic among effective mixtures is the pairing of carbon-rich substrates with feedstocks rich in nitrogen or phosphorus. At the same time, co-digestion does not always guarantee higher H_2 and CH_4 yields, as certain biomasses, such as spent mushroom substrate, are not well suited for this approach. Household solid waste and OFMSW often exhibit the highest H_2 and CH_4 yields under mono-digestion conditions, although their performance can be further enhanced when co-digested with nitrogen-rich biomasses.

As previously discussed, the first and second stages of TSAD may be operated at different temperatures, as reported in several studies listed in *Table 1.2*. Nevertheless, increasing temperature does not always result in a significant improvement in H_2 production, and when an enhancement is observed, it is often limited in magnitude.

There are very few examples in the literature of TSAD applied exclusively to lignocellulosic biomasses, as these substrates are poorly suited to biological degradation. More commonly, lignocellulosic materials are co-digested with manure or readily degradable substrates such as food waste or cheese whey (Zhu

et al. 2022; Margarita Andreas Dareioti and Kornaros 2015a; Aravani et al. 2023). Under these conditions, TSAD often yields promising H_2 and CH_4 production, in some cases outperforming other co-digestion configurations.

Finally, nutrient balance may also be achieved through the direct addition of elements to the reaction environment. From a circular economy perspective, these nutrients can be recovered from waste streams, particularly digestate, which represents the solid and liquid residues of digestion and is rich in nitrogen, phosphorus, and potassium. In this context, digestate can be reintegrated into a virtuous cycle, shifting from a waste product to a valuable secondary raw material.

Table 1.2 Examples of two-stage anaerobic digestion applied on the different types of feedstocks under different operative conditions. The first part of the table contains modo- digestion process conditions and yield. In the second part, co-digestion processes are presented.

Substrate	Pre-treatments	COD content	Operative conditions	H_2 and CH_4 yields	References
			Mono-digestion		
Food waste	Ground and diluted with water	57 g/L	1st stage: 37°C, pH = 6, HRT = 35 h 2nd stage: 37°C, pH = 7, HRT = 72 h	H_2: 55 mL/g_{VS} CH_4: 94.8 mL/g_{VS}	(Nathao et al. 2013)
Cheese whey	Diluted with phosphate buffer	60-80 g/L	1st stage: HRT = 1 d 2nd stage: HRT = 7.5 d	H_2: 120 mL/g_{VS} CH_4: 340 mL/g_{VS}	(Lembo et al. 2022)
Sewage sludge	None	42.3 g/L	1st stage: 35°C, pH = 5.5, HRT = 2 d 2nd stage: 35°C, pH = 7, HRT = 12 d	CH_4: 200 mL/g_{VS}	(Maspolim et al. 2015)
Raw tomato plant waste	Dried, milled and sieved	N.A.	1st stage: 37°C, pH =6, HRT = 14 d 2nd stage: 37°C, pH = 6, HRT = 28 d	H_2: 11.6 mL/g_{VS} CH_4: 252.3 mL/g_{VS}	(Ruiz-Aguilar et al. 2022)
Cattle manure	Thawed, blended, and diluted with tap water	N.A.	1st stage: 68°C, HRT = 3 d 2nd stage: 55°C, HRT = 12 d	CH_4: 260 mL/g_{VS}	(Nielsen et al. 2004)
OFMSW	Milled and diluted with water	52 g/L	1st stage: 55°C, pH = 5.5, HRT = 2 d 2nd stage: 55°C, pH = 7.3, HRT = 10 d	H_2: 20-85 mL/g_{VS} CH_4: 329-364 mL/g_{VS}	(Chu et al. 2012)
Household solid waste	Shredded and diluted with water	N.A.	1st stage: 37°C, pH = 5.5, HRT = 2 d 2nd stage: stage: 37°C, pH = 7.5, HRT = 15 d	H_2: 43 mL/g_{VS} CH_4: 500 mL/g_{VS}	(D. Liu et al. 2006)
Organic market waste	Grounded and diluted with water	N.A.	1st stage: 35°C, pH = 5.5, HRT = 12 d 2nd stage: 35°C, pH =7-7.5, HRT = 12 d	H_2: 50 mL/g_{VS} CH_4: 179 mL/g_{VS}	(Gómez Camacho et al. 2019)
Peach waste	Diluted with tap water	21.2 g/L	1st stage: 30°C, pH = 5.5, HRT = 1 d 2nd stage: 30°C, pH =7-7.5, HRT = 5 d	CH_4: 320 mL/g_{COD}	(Carvalheira et al. 2018)
Vinasse	Diluted with tap water	20 g/L	1st stage: 55°C, pH = 5.5, HRT = 4 h 2nd stage: 30°C, pH =7-7.5, HRT = 18 h	H_2: 150 mL/g_{COD} CH_4: 240 mL/g_{VS}	(Ramos et al. 2021)
Palm oil mill effluent	None	85.85 g/L	1st stage: 55°C, pH = 6.5, HRT = 2 d 2nd stage: 35°C, pH =7.5, HRT = 15 d	H_2: 135 mL/g_{VS} CH_4: 414 mL/g_{VS}	(O-Thong et al. 2016)
Bagasse bioethanol	Centrifuged and supernatants discarded	30.6 g/L	1st stage: 37°C, pH = 6, HRT = 9 h 2nd stage: 37°C, HRT = 8 h	H_2: 8.24 mL/g_{COD} CH_4: 345.2 mL/g_{COD}	(Cheng et al. 2016)

fermentation residue					
			Co-digestion		
Food waste, corn straw, chicken manure	Food waste crushed and sieved, corn straw crushed, sieved, and treated with urea	5.75 g/L (soluble)	1st stage: 55°C, pH= 5.5 2nd stage: 55°C, pH= 7	H_2: 106 mL/g_{VS} CH_4: 515.9 mL/g_{VS}	(Zhu et al. 2022)
Food waste and brown water	Food waste is sorted out and blended with tap water	127 g/L	1st stage: 37°C, pH= 5-5.5, HRT = 8 h 2nd stage: 37°C, pH=7-7.5, HRT = 20 d	H_2: 99.8 mL/g_{VS} CH_4: 728 mL/g_{VS}	(S. Paudel et al. 2017)
Sludge and food waste	None	23.6 g/L	1st stage: 37°C, pH= 5.5 2nd stage: 37°C, pH=7	H_2: 106.4 mL/g_{VS} CH_4: 353.5 mL/g_{VS}	(Xinyuan Liu et al. 2013)
Sludge and wine vinasse	None	63.8 g/L	1st stage: 35°C, pH= 5.5, HRT = 4 d 2nd stage: 35°C, pH=7, HRT = 4 d	H_2: 16.4 mL/g_{VS} CH_4: 159.5 mL/$g_{CODremoved}$	(Tena et al. 2021)
Corn silage, cattle manure, olive pomace, orange peels	None	N.A.	1st stage: 37.5°C, HRT = 15 d 2nd stage: 37.5°C, HRT = 15 d	CH_4: 570 mL/g_{VS}	(Aravani et al. 2023)
Corn silage, cattle manure, malt	None	N.A.	1st stage: 37.5°C, HRT = 20 d 2nd stage: 37.5°C, HRT = 20 d	CH_4: 370 mL/g_{VS}	(Aravani et al. 2023)
Cheese whey and cattle manure	Diluted with water and sieved	35.3 g/L	1st stage: 35°C, pH= 5, HRT = 5 d 2nd stage: 35°C, pH=7.5, HRT = 20 d	H_2: 84 mL/g_{VS} CH_4: 258 mL/g_{VS}	(Bertin et al. 2013)
Sorghum and cow manure	Sorghum shredded/sieved, diluted with water, alkaline on ensiled sorghum	N.A.	1st stage: 37°C, pH= 5, HRT = 5 d 2nd stage: 37°C, pH=7.5-8, HRT = 25 d	H_2: 209 mL/$g_{Carbohydrates}$ CH_4: 295.3 mL/g_{VS}	(Margarita A. Dareioti et al. 2022)
Leachate and starch waste	Crushed, blended, and homogenated	5.84 g/L	1st stage: 35°C, HRT = 5 d 2nd stage: 35°C, pH=7.5, HRT = 25 d	CH_4: 125.1 mL/g_{VS}	(Darwin et al. 2019)
Seaweed and solid cow manure	Seaweed grinded and both diluted with water	11.8 g/L	1st stage: 37°C, pH= 7 2nd stage: 37°C, pH=7.5	CH_4: 110 mL/g_{VS}	(Nkemka et al. 2014)
Spent mushroom substrate and chicken manure	Spent mushroom substrate crushed, ground, treated with acid	N.A.	1st stage: 35°C, pH= 7 2nd stage: 55°C, pH=7	CH_4: 84.3 mL/g_{VS}	(Shu et al. 2022)

Cheese whey, cow manure, and ensiled sorghum	Sorghum ensiled, grounded and alkaline pretreated	80 g/L	1st stage: 37°C, pH =5.5, HRT = 0.5 d 2nd stage: 37°C, pH = 8, HRT = 24 d	H_2: 0.7 $mol/mol_{CarbohydratesConsumed}$ CH_4: 326 mL/g_{VS}	(Margarita Andreas Dareioti and Kornaros 2015a)

1.4 Digestate management

At the end of the second stage of the process, digestate can no longer be biologically degraded by microorganisms; however, it still contains a significant fraction of carbon as well as essential elements such as nitrogen, phosphorus, and trace metals. Digestate is a solid–liquid material whose water content strongly depends on the operating conditions adopted during AD. When digestion is carried out under wet conditions, a substantial amount of water can be recovered from the digestate and subsequently reused within the AD process or alternatively applied as irrigation water or liquid fertilizer (Khan and Nordberg 2018).

In recent years, several innovative recovery strategies have been developed to enhance the valorization of both nutrients and water from digestate. In parallel, the solid fraction can be further upgraded and reintroduced into the digestion chain after thermal treatment, which promotes the formation of biochar or hydrochar (D. C. Shin et al. 2022). These process intensification strategies may be implemented either individually or in combination, with the overall objective of improving resource efficiency and advancing the circularity of anaerobic digestion systems.

1.4.1 Digestate composition and conventional utilization

Digestate represents the solid-liquid residue obtained after DF and AD processes (Czekała 2019). Its chemical and physical composition is strongly influenced by the nature of the feedstock and by the operating conditions applied throughout the process. Digestate typically contains between 15-55 % of carbon, originating from both the substrate and the inoculum. During biological conversion, organic matter is progressively stabilized, resulting in a reduction of chemical oxygen demand (COD) and biological oxygen demand (BOD_5), while more recalcitrant compounds accumulate in the digestate matrix.

Advanced spectroscopic analyses have shown that, when comparing substrates before and after digestion, digestate exhibits an increased abundance of carboxyl carbon, aromatic carbon, and aliphatic carbon, accompanied by a decrease in alkyl compounds, which suggests the preferential degradation of alkanes during the process (Adani et al. 2009). In addition to organic carbon, digestate also contains inorganic elements such as nitrogen, phosphorus, and potassium, which are considered non-renewable resources whose long-term availability depends on efficient recycling strategies (Battista et al. 2021).

Digestate can be utilized in three main forms: as a whole material, as a liquid fraction rich in nitrogen and potassium, or as a solid fraction enriched in carbon and phosphorus (W. Wang et al. 2023b). These fractions are obtained through separation processes that include mechanical separation, centrifugation, stripping, drying, or evaporation. Precipitation and flocculation are commonly applied techniques that promote the aggregation of fine particles, thereby facilitating phase separation (Chozhavendhan et al. 2023). Alongside physical methods,

chemical treatments can also be employed to enhance particle coagulation through the neutralization of surface charges (Beggio et al. 2022).

One of the most widespread applications of digestate is land application, as it represents a valuable source of nutrients for agricultural crops and can function as an organic fertilizer (Czekała 2022). However, nutrient concentrations in digestate are highly variable, and excessive accumulation of specific elements in soil may result in environmental pollution. For example, surplus nitrogen can lead to eutrophication or nutrient overloading, which restricts digestate land application in certain areas. Moreover, logistical constraints related to transportation costs, farmer preferences for low-cost mineral fertilizers, and regulatory limitations often hinder large-scale digestate use in agriculture (W. Wang et al. 2023a).

Until recently, direct land application was the predominant management strategy for digestate, but regulatory frameworks governing its use were limited. In 2019, the European Union introduced Regulation 1009/2019 on fertilizing products, which addressed previous legislative gaps and promoted safer and more sustainable utilization of organic fertilizers, thereby supporting the circular management of digestate (Rizzioli et al. 2023).

Despite its nutrient value, digestate may also contain undesirable contaminants. Heavy metals are generally not abundant in fresh substrates, yet they can accumulate in digestate due to anthropogenic activities (Makádi et al. 2012). Elements such as Ni, Zn, Cu, Pb, Cd, Cr, and Hg are commonly detected, although their concentrations vary depending on feedstock composition (Demirel et al. 2013). Zn, Cu, and AS are frequently associated with manure, as they originate from animal feed additives and veterinary treatments. Their concentrations in digestate are often higher than in raw manure due to mass reduction during biological degradation (Govasmark et al. 2011). As is of particular concern because it is not only unnecessary for microbial metabolism but also highly toxic. When digestate is applied to soil, metals may become more stable and bioavailable, highlighting the need for strict concentration control (H. Jin and Chang 2011).

Digestate may also contain organic contaminants, including pathogens, pesticides, and steroid hormones (F. Monlau et al. 2015). Pesticides, such as fungicides and insecticides, along with pathogenic microorganisms derived mainly from animal and human waste streams, represent significant risks. If digestate is improperly treated and applied to soil, these contaminants may spread through crops, posing threats to plant, animal, and human health (Bonetta et al. 2014).

Due to the potential presence of both inorganic and organic contaminants, direct land application of digestate is increasingly being reconsidered. As a result, recent research and industrial practices have shifted toward targeted nutrient recovery strategies, which allow better control over nutrient dosage, fertilizer quality, and environmental safety.

1.4.2 Liquid phase valorization

Liquid fraction originates from separation processes where it is divided from a thicker fraction. It contains less than 3% of total suspended solids (Jin Lu and Xu 2021). Improper use of liquid digestate in land disposal can cause soil pollution hence alternative applications have been developed. Among them, the extraction of nutrients represents an alluring option for avoiding pollution associated to with their release. Moreover, they can be employed to balance nutrients in digestion or be applied as fertilizer.

1.4.2.1 Nitrogen recovery

Nitrogen is the most present element in liquid digestate and 70-80% of its dissolvable fraction can be found in the liquid phase (Jin Lu and Xu 2021). N is mineralized to ammonia which affects the alkalinity of the residue (Möller and Müller 2012). Some N recovery techniques employ a chemical approach such as ozonation or stripping while others use physical methods such as microwave irradiation, vacuum evaporation, or membrane. Biological processes are also considered as they present a higher yield concerning other methods. Among nitrogen recovery techniques, more traditional methods are joined by innovative technologies, as reported in *Table 1.3*. They differ in TRL as new processes are mostly operated at laboratory scale as they are not ready to be scaled up.

Ammonia-nitrogen stripping is the most developed process, with a TRL around 8-9 (Samarina et al. 2022). It consists in capturing compounds of interest present in the liquid phase through the contact with a gas. Desired components are released in the latter one which is then treated in a scrubber to separate ammonia and stripping gas. This process is convenient when the direct utilization of digestate in land disposal can be harmful for to crops due to excessive nitrification of soil (K. Jin et al. 2022). Nitrogen released is controlled while the low ammonia digestate can be recirculated to the digester to adjust the alkalinity of the system. The most common stripping gas is air even if oxygen is known to have and an inhibitory effect on microbial consortium. However, this effect is not that serious to lead to different gases which are probably more expensive or dangerous than air. After nitrogen-ammonia has been captured, inorganic acid solution solutions such as sulphates sulphates or nitrates are employed during the scrubbing step. However, they are expensive and associated with the formation of wastes that must be disposed of. To replace inorganic acid, nitrified solution has gained attention as it absorbs ammonia generating a stable fertilizer that is more valuable (Bousek et al. 2016).

Biological processes represent another well-known solution to extract elements present in liquid digestate. When nitrogen is the principal target of microbial degradation, autotrophic nitrification and heterotrophic denitrification can be performed to oxidize ammonia. Bacterial activity can be enhanced through the addition of further carbon sources as organic wastes (Chuda and Ziemiński 2021). Unfortunately, they are associated with leachate and odours (Eraky et al. 2022).

Innovative methods comprehend microwave irradiation, ozonation, vacuum evaporation and membranes. TRL of these techniques cannot be higher than 4-5 as all of them are currently being tested in the laboratory to evaluate their performances as they often present limitations which do not allow an easy scale up (Rizzioli et al. 2023).

Through microwave radiations, digestate is warmed up and a molecular moment is generated causing the evaporation of volatile ammonia molecules in solution (La et al. 2014). On the other hand, ozonation is often employed in wastewater treatment to remove pathogens, organic matter, and inorganic contaminants. Ozone is a strong oxidant that decomposes pollutants to make their recovery easier (Yunpeng Yang and Liu 2022). When ammonia is oxidized, the main products are nitrates which are removed (Ruffino and Zanetti 2012). Nonetheless, these techniques are hardly employed on a large scale because of their cost and reagent requirements.

Vacuum evaporation can be employed to concentrate digestate. Water evaporates in negative-pressure conditions at the boiling temperature associated with that pressure. Then it is collected in tanks after condensation (Chiumenti et al. 2013). This method is linked to elevated operational costs and great variability in ammonia content in the two phases which depend on digestate characteristics (Simonič and Simonič 2018).

Membrane technology represents another option for nutrient capture. As mentioned before, recovery processes are often energy-expensive or rely on additives. On the other hand, membranes are gaining interest due to the sustainable approach. They are mostly used to obtain ammonia-nitrogen through hydrophobic polymers which compose the membrane. Nitrogen easily permeates through them and from liquid digestate it is transferred to an acid solution. Sulfuric acid is typically employed as receiving liquid even if phosphoric or nitric acid can be used too. They react with ammonia forming salts which are commercial fertilizers (Rivera et al. 2022). Membrane technology is associated to a high yield of nutrients, but it presents some issues related to fouling because of the high concentration of dry matter in digestate. Enzymatic pre-treatment of the substrate could reduce the dimension of the molecule in the liquid phase and minimize this effect (Gienau et al. 2018).

Table 1.3 Pros and cons of nitrogen recovery techniques from digestate.

Technique	Benefits	Disadvantages	Removal efficiency (on total N-compound content)	TRL	References
Microwave radiations	• High removal efficiencies • Fast and easy to control	• High energy cost	82.6 %	4-5	(La et al. 2014)
Ozonation	• Removal of pathogens, organic matter, and inorganic contaminants	• Ozone requirements	85%	4-5	(Yunpeng Yang and Liu 2022)
Biological processes	• Degradation of unstable biomass	• Not complete consumption • Leachate and odors	83.7%	4-5	(Eraky et al. 2022; Okolie et al. 2022)
Vacuum evaporation	• Concentration of ammonia	• Elevated operational costs • Great variability	97.5%	4-5	(Chiumenti et al. 2013)
Stripping	• High degree of development • High efficiency	• Scrubbing step is necessary • Production of wastes	70-80%	8-9	(Rizzioli et al. 2023; Alhelal et al. 2022; Bousek et al. 2016; Samarina et al. 2022)
Membranes	• High removal efficiencies	• Not selective • Fouling	70-75%	4-5	(Rizzioli et al. 2023; Rivera et al. 2022)

1.4.3 Phosphorous recovery

Phosphorous compounds are concentrated mainly in solid digestate (55-65 %), but the liquid phase contains a significant percentage (35-45 %) (Logan and Visvanathan 2019). Traditional phosphate rock extraction for P production is unsustainable since, according to the European Commission, P is a critical raw material (Golroudbary et al. 2019). Precipitation is widely employed in P recovery, and it can be applied in different forms as illustrated in *Table 1.4*.

The simultaneous recovery of multiple nutrients can be achieved through the formation of struvite, a crystalline mineral generated via a precipitation process involving nitrogen, phosphorus, and magnesium. Struvite is of particular interest not only as a nutrient recovery pathway but also as a fertilizer, owing to its slow and controlled release of nutrients, which makes it well suited for agricultural applications (Vidlarova et al. 2017). The precipitation reaction occurs when ammonium, magnesium, and phosphate ions are present in sufficient concentrations to exceed the solubility product of the mineral. Under these conditions, an equimolar ratio of the three elements leads to the formation of a crystalline solid with the chemical composition $MgNH_4PO_4$ H_2O. In addition to ionic concentrations, struvite precipitation is strongly influenced by pH, which must be maintained under alkaline conditions to favor crystal formation (Lorick et al. 2020).

Despite its advantages, the practical implementation of struvite recovery from digestate presents several challenges. Digestate is often characterized by insufficient Mg concentrations, requiring the addition of external Mg sources. Furthermore, alkaline conditions are necessary to promote precipitation, which typically entails the use of chemical additives to increase pH, thereby increasing operational costs and potentially compromising process sustainability.

Several strategies have been proposed to address these limitations. Siciliano e De Rosa (2014) suggested the use of magnesium-rich waste materials as alternative sources of magnesium. In their study, seawater bittern, a by-product of the marine salt industry, was employed as a magnesium supplier. Phosphorus deficiency in liquid digestate was addressed through the addition of bone meal, a residue derived from the thermal treatment of meat-processing waste. Both approaches are particularly relevant from a circular economy perspective, as they promote the valorization of waste streams while reducing the need for virgin raw materials.

An alternative to struvite formation is the precipitation of vivianite, a mineral with the chemical formula $Fe(PO_4)_2$ $8H_2O$, which can be produced under less restrictive operational conditions than struvite and can be used as a phosphorus fertilizer. Vivianite precipitation does not require elevated pH values and can therefore be more easily integrated into existing treatment schemes. This approach can be combined with membrane separation processes to achieve phosphorus removal efficiencies close to 100%, although further research is required to demonstrate its feasibility at larger scales (Piash et al. 2022).

Calcium phosphate precipitation represents another potential pathway for phosphorus recovery. However, this process is characterized by complex reaction mechanisms and requires highly supersaturated conditions and alkaline pH values. In wastewater treatment applications, sodium hydroxide is often added to promote precipitation, as organic acids and carbonates present in digestate tend to lower pH and hinder crystal formation. The use of hydroxide, however, significantly increases operational costs. For this reason, electrochemical precipitation has been proposed as an alternative, as it enables pH control without the addition of chemical reagents (Lei et al. 2017). Nevertheless, additional research is needed to assess the long-term sustainability and economic viability of this technique.

As previously discussed, membrane technologies can be employed for ammonia recovery, but they can also be integrated with precipitation processes to enable the simultaneous recovery of nitrogen and phosphorus. In such integrated systems, liquid digestate is first subjected to membrane separation to capture ammonia, which results in a reduction of system alkalinity. This change in chemical conditions favors subsequent phosphorus precipitation (González-García et al. 2023). Magnesium chloride is commonly added at this stage to promote the formation of magnesium phosphate precipitates, thereby enabling efficient phosphorus recovery (Vanotti et al. 2017).

Finally, vacuum membrane distillation can be combined with phosphate precipitation to enhance ammonia recovery. This process operates under relatively mild conditions, with temperatures in the range of 50–60 °C and vacuum pressures between 50 and 100 mbar. Under these conditions, ammonia permeates through the membrane following the evaporation of the liquid phase induced by vacuum. Recovery efficiencies approaching 90% have been reported; however, further investigations are necessary to optimize process performance and assess scalability (Karanasiou et al. 2023).

Table 1.4 Pros and cons of phosphorous recovery techniques from digestate.

Technique	Benefits	Disadvantages	Removal efficiency (on total P content)	TRL	References
Struvite precipitation	• Simultaneous recovery of N, Mg, and P	• Need for high Mg concentration • Alkaline chemicals required	88%	7-9	(Vidlarova et al. 2017; Lorick et al. 2020; Saerens et al. 2021)
Vivianite precipitation	• Simpler conditions of production	• New technology to be further deepened	~100%	6	(Uzkurt Kaljunen et al. 2022; Piash et al. 2022)
Calcium phosphate precipitation	• Efficient and economic	• Complex process conditions	57%	6-7	(Martín-Hernándaez et al. 2021; Lei et al. 2017)

1.4.4 Humic and fulvic acids

Recently, earth population has grown exponentially hence intensive crops have become necessary to satisfy food requirements. Bio-stimulants are substances which acts on plant growth enhancing productivity and tolerance to damaging events. Among them, humic (HA) and fulvic acids (FA) are interesting as they can be obtained from digestate. They differ in molecular weight as humic acids are heavier compared to fulvic acids. Moreover, the first ones are soluble in alkaline solutions while the second ones are soluble in both alkaline and acid solutions (Canellas et al. 2015; Khan and Nordberg 2018). These acids can be employed in returning carbon to soil improving its quality (Slepetiene et al. 2020). Furthermore, they have several beneficial effects on soils and plants. Humic acids act on roots root growth as they include metals in their structure which are essential in plant development. They also concur in optimizing nutrients nutrient absorption and resilience to salinity sources such as NaCl (Adil Aydin 2012). Fulvic acids influence micronutrients micronutrient uptake too. They facilitate the mobilization and transport of iron and other nutrients. They are also responsible for optimum plant growth together with an increasing in fruit yield and quality (Calvo et al. 2014). Their action on soils includes an improvement in its water retention and structure. Humic and fulvic acids are typically removed from digestate through and acid-alkali method (X. Wang et al. 2021). These substances can be released by degrading flocs and cells which constitute digestate. Alkaline method through NaOH or KOH is recommended as it is the easiest and most efficient (H. Li et al. 2014). Base solution is coupled to centrifugation to allow a separation between insoluble and soluble humin particles. The second ones remain in a supernatant which is treated through an ultrafiltration membrane. This step is necessary to recover low molecular weight fulvates which are in the permeate. The concentrate is acidified with HCl to obtain humic and fulvic acids (Sarlaki et al. 2019).

1.4.5 Solid phase valorization

The carbon content in the solid fraction of digestate typically ranges between 15-55 % w/w and represents a valuable resource that can be exploited as a carbon source in subsequent fermentation processes, such as bioethanol or biomethane production (Sambusiti et al. 2015; W. Wang et al. 2023a). To enhance the biodegradability of this fraction, several pre-treatment strategies can be applied, including mechanical, thermal, chemical, and biological methods (Sambusiti et al. 2016).

Mechanical pre-treatments are particularly advantageous because they do not require chemical additives and therefore avoid the formation of inhibitory compounds such as furans and polyphenols. These substances are commonly generated during thermal or chemical pre-treatments and are known to negatively affect microbial activity. Mechanical approaches promote particle size reduction and decrease polymer crystallinity, thereby improving substrate accessibility and

biodegradability. Among size-reduction technologies, mills and extruders are the most frequently employed (Florian Monlau et al. 2019).

Chemical pre-treatments involve the addition of acidic or alkaline reagents, such as sulfuric acid or sodium hydroxide. Alkaline pre-treatments are generally more effective in promoting saccharification, particularly for lignocellulosic residues, as they facilitate lignin solubilization and structural disruption. In contrast, acidic pre-treatments mainly cause fiber disintegration but may limit sugar release and increase the risk of inhibitor formation (Stoumpou et al. 2020).

Pre-treatment strategies can also be combined to enhance overall process efficiency. For example, Wang et al. (2016) applied a sequential ozone and aqueous ammonia pre-treatment to digestate derived from rice straw anaerobic digestion, achieving significant degradation of residual fibers and improved ethanol production through subsequent digestate fermentation. Conversely, when the carbon-rich solid fraction is not intended for further biological conversion, thermochemical pathways should be considered. These processes, which enable the production of char-based materials, represent a promising valorization route and have gained increasing attention in recent decades due to their potential contribution to resource recovery and circular economy strategies.

1.4.5.1 Char from the solid fraction of digestate

Thermochemical processes such as pyrolysis, gasification, and hydrothermal carbonization enable the valorization of solid digestate.

Pyrolysis is a promising technique for the efficient degradation of biomass under oxygen-free conditions. This process generates three main products: bio-oil (liquid), biochar (solid), and pyrogas, which is a gaseous mixture mainly composed of CO, H_2, CH_4, ethylene, and C3 compounds (Nanda et al. 2014). Pyrolysis typically operates at temperatures ranging from 300 to 1000 °C. Based on the heating rate and residence time, it can be classified as slow or fast. Slow pyrolysis is characterized by long residence times, from minutes to hours, and low heating rates between 0.1 and 10 °C per minute, leading to higher biochar yields, typically between 25-35 % of the initial biomass. Fast pyrolysis, on the other hand, operates with short residence times, between 0.5-5 seconds, and high heating rates ranging from 10 to 10000 °C per minute (Tan et al. 2021; Nanda et al. 2014).

Gasification is another thermochemical process that degrades biomass under sub-stoichiometric oxygen conditions. It is typically carried out at temperatures between 600-1300 °C, resulting in the formation of syngas, a tar-rich liquid phase composed mainly of aromatic compounds, and a solid char fraction (Pecchi and Baratieri 2019). Both pyrolysis and gasification require biomass with low moisture content to minimize energy losses due to water evaporation. As a consequence, a drying step is often required prior to treatment (Wišniewski et al. 2015).

Humid digestate can instead be treated through hydrothermal carbonization or hydrothermal liquefaction, which take place in the aqueous phase. Hydrothermal carbonization is generally performed at mild temperatures, typically between 180-

250 °C, with reactor pressure governed by steam and gas formation (Xie et al. 2022). The process produces a gas phase mainly composed of CO_2, a liquid fraction containing water and soluble organic compounds, and a solid product known as hydrochar. Hydrochar is often rich in phosphorus, which can be recovered through precipitation or extraction techniques (X. Zhao et al. 2018).

When higher temperatures, between 200-380 °C, are applied, the process shifts toward hydrothermal liquefaction. This pathway sterilizes the residue and generates a larger amount of liquid products compared to hydrothermal carbonization (Azargohar and Dalai 2008). The liquid fraction can be separated into a bio-oil phase, characterized by a high heating value comparable to fossil fuels, and an aqueous phase rich in nutrients that can be recycled back into the digestion process or used for nutrient recovery. A solid residue is still produced and is commonly applied as a soil amendment (Farghali et al. 2022; Okoro and Sun 2021).

Char materials are porous solids that contribute to climate change mitigation through carbon sequestration, making them valuable for carbon capture strategies. When applied to soils, char improves nutrient retention, water-holding capacity, and microbial activity. In both DF and AD systems, the addition of char has been shown to enhance microbial performance and nutrient release (J. Tang et al. 2013). The chemical structure of char contains a wide variety of functional groups, making it a versatile material that can be further modified through physical or chemical activation to improve its properties (Sajjadi, Zubatiuk, et al. 2019). Physical activation increases surface area and porosity by exposing char to gases such as steam or CO_2, leading to the formation of micropores and oxygen-containing functional groups that enhance contaminant adsorption from water and soil (Sajjadi, Chen, et al. 2019). Chemical activation involves the impregnation of char with activating agents such as zinc chloride, phosphoric acid, or potassium hydroxide, which modify surface functional groups. These treatments generally require lower temperatures and shorter processing times compared to physical activation (Williams and Reed 2004). A subsequent thermal treatment is often applied to dehydrate the material, enhance porosity, reduce tar content, and generate volatile compounds (Azargohar and Dalai 2008).

The properties of biochar and hydrochar vary significantly depending on the production process, as summarized in *Table 1.5*. Biochar produced via pyrolysis or gasification generally exhibits a higher ash content than hydrochar due to the retention of inorganic fractions at high temperatures. This difference results in distinct pH values, with biochar typically showing alkaline characteristics, reaching pH values up to 9 or 10, while hydrochar is usually acidic, with pH ranging between 4 and 7 (Fuertes et al. 2010). Differences are also observed in morphology, as the higher temperatures and gas flow involved in pyrolysis and gasification promote greater surface area development in biochar (J. Fang et al. 2018). Compared to hydrochar, biochar exhibits higher aromaticity, larger H over C and O over C ratios, and electrical conductivity, enabling it to act as an electron shuttle between syntrophic bacteria and methanogens (Z. Liu et al. 2010; Sun et al. 2022).

Table 1.5 Characteristics of char obtained through hydrothermal carbonization (HTC) and pyrolysis (PY) in terms of process temperature, char yield, char pH, % of fixed carbon, specific surface area (SSA), porosity, and application. N.A =not available.

Type	Substrate	T (°C)	Yield (wt%)	pH	Fixed carbon (%)	SSA (m^2/g)	Pore volume (cm^3/g)	Application	References
HTC	Digestate from AD of sewage sludge	220	73.4	7.14	9.05	N.A.	N.A.	In addition to the anaerobic digestion of process water from HTC	(Aragón-Briceño et al. 2017)
HTC	Digestate from AD of corn silage, grass silage, and cattle manure	190	70.0	N.A.	19.40	14	0.35	Upgrading to activated carbons to adsorb CO_2 in biogas purification	(Rodriguez Correa et al. 2017)
HTC	Digestate from AD of maize silage	190	72.0	5	N.A.	12.3	0.096	N.A.	(Mumme et al. 2011)
HTC	Digestate from AD of sewage sludge	150	90.0	6.5	6.60	N.A.	N.A.	Soil amendment	(K. R. Parmar and Ross 2019)
PY	Digestate from AD of food waste	400	44.3	N.A.	29.49	73.99	0.1	N.A.	(Jingxin Liu et al. 2020)

PY	Digestate from AD of food waste	600	33.6	N.A.	13.09	89.23	0.07205	Adsorbent for pollutants, soil amendment catalyst to enhance the biorefinery	(N. Wang et al. 2022)
PY	Digestate from AD of food waste	400	73.0	9.81	4.65	53.13	0.1	N.A.	(C. Li et al. 2020)
PY	Digestate from AD of sewage sludge	550	63.0	10.3	N.A.	58.6	0.065	Soil amendment	(Pituello et al. 2015)

1.5 Aim of the work

The aim of this PhD thesis is to investigate the valorization of biomass waste for sustainable bioenergy production through integrated biological conversion pathways. To this purpose, different waste streams were treated using DF, AD, and TSAD, with the objective of intensifying conventional biological processes, increasing energy yields, and simultaneously addressing waste management challenges, which have become increasingly critical in recent years.

Both plant-based and animal-based residues were considered to evaluate the flexibility and robustness of the proposed approach. Plant-derived substrates included fruit and vegetable waste, wastewater from the jam industry, and a by-product stream from syrup production. Animal-based matrices comprised cow manure, dairy processing wastewater, and primary sludge from a municipal wastewater treatment plant. TSAD was applied to plant-based feedstocks to enable the sequential production of H_2 and CH_4, thereby maximizing energy recovery from carbon-rich biomass. In contrast, animal-derived residues were mainly treated through conventional anaerobic digestion combined with process intensification strategies aimed at improving overall performance. In particular, post-digestion treatments were investigated to enhance the biodegradation of substrates characterized by a high content of lignocellulosic compounds.

In addition to bioenergy production, digestate valorization was explored to further strengthen the circular economy framework of the system. Specifically, humic acids were extracted from the digestate obtained after TSAD of fruit and vegetable waste and jam industry wastewater, to assess the feasibility of an integrated biorefinery concept capable of generating value-added products alongside energy carriers.

To evaluate the practical applicability of the proposed solutions, a techno-economic assessment (TEA) and LCA were carried out. These analyses were used to investigate the economic feasibility and environmental sustainability of an integrated plant designed for the simultaneous production of bioenergy and soil- and plant-enhancing products, as well as to quantify the associated emissions and environmental impacts.

Overall, this research proposes an integrated and sustainable system for biomass waste valorization, combining waste reduction, renewable energy generation, and resource recovery. The ultimate goal is to contribute to the mitigation of fossil fuel depletion while meeting current sustainability requirements through the development of circular and environmentally responsible bioenergy pathways.

References

Adani, Fabrizio, Barbara Scaglia, Andrea Schievano, et al. 2009. *WHAT IS THE DIGESTATE?*

Adil Aydin. 2012. "Humic Acid Application Alleviate Salinity Stress of Bean (Phaseolus Vulgaris L.) Plants Decreasing Membrane Leakage." *AFRICAN JOURNAL OF AGRICULTURAL RESEEARCH* 7 (7). https://doi.org/10.5897/ajar10.274.

Ahmad, Talha, Rana Muhammad Aadil, Haassan Ahmed, et al. 2019. "Treatment and Utilization of Dairy Industrial Waste: A Review." *Trends in Food Science and Technology* 88 (June): 361–72. https://doi.org/10.1016/j.tifs.2019.04.003.

Akcakaya, Merve, Sera Tuncay, and Bulent Icgen. 2022. "Two-Stage Anaerobic Digestion of Ozonated Sewage Sludge Predominantly Took over by Acetotrophic Methanogens with Increased Biogas and Methane Production." *Fuel* 317 (June). https://doi.org/10.1016/j.fuel.2022.123434.

Akobi, Chinaza, Hyeongu Yeo, Hisham Hafez, and George Nakhla. 2016. "Single-Stage and Two-Stage Anaerobic Digestion of Extruded Lignocellulosic Biomass." *Applied Energy* 184 (December): 548–59. https://doi.org/10.1016/j.apenergy.2016.10.039.

Al-Haddad, Saleh, Cynthia Kusin Okoro-Shekwaga, Louise Fletcher, Andrew Ross, and Miller Alonso Camargo-Valero. 2023. "Assessing Different Inoculum Treatments for Improved Production of Hydrogen through Dark Fermentation." *Energies* 16 (3). https://doi.org/10.3390/en16031233.

Alhelal, Ismail I., Lucas H. Loetscher, Sybil Sharvelle, and Kenneth F. Reardon. 2022. "Nitrogen Recovery from Anaerobic Digestate via Ammonia Stripping and Absorbing with a Nitrified Solution." *Journal of Environmental Chemical Engineering* 10 (3). https://doi.org/10.1016/j.jece.2022.107826.

Alrawashdeh, Khalideh Al Bkoor, Annarita Pugliese, Katarzyna Slopiecka, et al. 2017. "Codigestion of Untreated and Treated Sewage Sludge with the Organic Fraction of Municipal Solid Wastes." *Fermentation* 3 (3). https://doi.org/10.3390/fermentation3030035.

Amini, Elahe, Cristina Valls, and M. Blanca Roncero. 2021. "Ionic Liquid-Assisted Bioconversion of Lignocellulosic Biomass for the Development of Value-Added Products." *Journal of Cleaner Production* 326 (December). https://doi.org/10.1016/j.jclepro.2021.129275.

Amnuaycheewa, Plaimein, Rotchanaphan Hengaroonprasan, Kittipong Rattanaporn, Suchata Kirdponpattara, Kraipat Cheenkachorn, and Malinee Sriariyanun. 2016. "Enhancing Enzymatic Hydrolysis and Biogas Production from Rice Straw by Pretreatment with Organic Acids." *Industrial Crops and Products* 87 (September): 247–54. https://doi.org/10.1016/j.indcrop.2016.04.069.

Amponsah, Nana Yaw, Mads Troldborg, Bethany Kington, Inge Aalders, and Rupert Lloyd Hough. 2014. "Greenhouse Gas Emissions from Renewable Energy Sources: A Review of Lifecycle Considerations." *Renewable and Sustainable Energy Reviews* 39: 461–75. https://doi.org/10.1016/j.rser.2014.07.087.

Angelonidi, Eleni, and Stephen R. Smith. 2015. "A Comparison of Wet and Dry Anaerobic Digestion Processes for the Treatment of Municipal Solid Waste and Food Waste." *Water and Environment Journal* 29 (4): 549–57. https://doi.org/10.1111/wej.12130.

Ansaloni, Simone, Nunzio Russo, and Raffaele Pirone. 2018. "Wet Air Oxidation of Industrial Lignin Case Study: Influence of the Dissolution Pretreatment and Perovskite-Type Oxides." *Waste and Biomass Valorization* 9 (11): 2165–79. https://doi.org/10.1007/s12649-017-9947-4.

Antczak, Andrzej, Jan Szadkowski, Dominika Szadkowska, and Janusz Zawadzki. 2022. "Assessment of the Effectiveness of Liquid Hot Water and Steam Explosion Pretreatments of Fast-Growing Poplar (Populus Trichocarpa) Wood." *Wood Science and Technology* 56 (1): 87–109. https://doi.org/10.1007/s00226-021-01350-1.

Aragón-Briceño, C., A. B. Ross, and M. A. Camargo-Valero. 2017. "Evaluation and Comparison of Product Yields and Bio-Methane Potential in Sewage Digestate Following Hydrothermal Treatment." *Applied Energy* 208 (December): 1357–69. https://doi.org/10.1016/j.apenergy.2017.09.019.

Aravani, Vasiliki P., Konstantina Tsigkou, Vagelis G. Papadakis, Wen Wang, and Michael Kornaros. 2023. "Anaerobic Co-Digestion of Agricultural Residues Produced in Southern and Northern Greece." *Fermentation* 9 (2). https://doi.org/10.3390/fermentation9020131.

Arumugham, Thanigaivelan, Jawaher AlYammahi, K. Rambabu, Shadi W. Hassan, and Fawzi Banat. 2022. "Supercritical CO2 Pretreatment of Date Fruit Biomass for Enhanced Recovery of Fruit Sugars." *Sustainable Energy Technologies and Assessments* 52 (August). https://doi.org/10.1016/j.seta.2022.102231.

Azargohar, R., and A. K. Dalai. 2008. "Steam and KOH Activation of Biochar: Experimental and Modeling Studies." *Microporous and Mesoporous Materials* 110 (2–3): 413–21. https://doi.org/10.1016/j.micromeso.2007.06.047.

Aziz, Muhammad, Arif Darmawan, and Firman Bagja Juangsa. 2021. "Hydrogen Production from Biomasses and Wastes: A Technological Review." *International Journal of Hydrogen Energy* 46 (68): 33756–81. https://doi.org/10.1016/j.ijhydene.2021.07.189.

Azwar, M. Y., M. A. Hussain, and A. K. Abdul-Wahab. 2014. "Development of Biohydrogen Production by Photobiological, Fermentation and Electrochemical Processes: A Review." *Renewable and Sustainable Energy Reviews* 31 (March): 158–73. https://doi.org/10.1016/j.rser.2013.11.022.

Bak, Jin Seop, Myoung Dong Kim, In Geol Choi, and Kyoung Heon Kim. 2010. "Biological Pretreatment of Rice Straw by Fermenting with Dichomitus Squalens." *New Biotechnology* 27 (4): 424–34. https://doi.org/10.1016/j.nbt.2010.02.021.

Banerjee, Saumita, Ramkrishna Sen, R. A. Pandey, et al. 2009. "Evaluation of Wet Air Oxidation as a Pretreatment Strategy for Bioethanol Production from Rice Husk and Process Optimization." *Biomass and Bioenergy* 33 (12): 1680–86. https://doi.org/10.1016/j.biombioe.2009.09.001.

Battista, Federico, Chiara Masala, Anita Zamboni, Zeno Varanini, and David Bolzonella. 2021. "Valorisation of Agricultural Digestate for the Ammonium Sulfate Recovery and Soil Improvers Production." *Waste and Biomass Valorization* 12 (12): 6903–16. https://doi.org/10.1007/s12649-021-01486-y.

Beggio, Giovanni, Wei Peng, Fan Lü, Andrea Cerasaro, Tiziano Bonato, and Alberto Pivato. 2022. "Chemically Enhanced Solid–Liquid Separation of Digestate: Suspended Solids Removal and Effects on Environmental Quality of Separated Fractions." *Waste and Biomass Valorization* 13 (2): 1029–41. https://doi.org/10.1007/s12649-021-01591-y.

Beims, R. F., C. L. Simonato, and V. R. Wiggers. 2019. "Technology Readiness Level Assessment of Pyrolysis of Trygliceride Biomass to Fuels and Chemicals." *Renewable and Sustainable Energy Reviews* 112 (September): 521–29. https://doi.org/10.1016/j.rser.2019.06.017.

Benbelkacem, H., J. Bollon, R. Bayard, R. Escudié, and P. Buffière. 2015. "Towards Optimization of the Total Solid Content in High-Solid (Dry) Municipal Solid Waste Digestion." *Chemical Engineering Journal* 273 (August): 261–67. https://doi.org/10.1016/j.cej.2015.03.048.

Bertin, Lorenzo, Selene Grilli, Alessandro Spagni, and Fabio Fava. 2013. "Innovative Two-Stage Anaerobic Process for Effective Codigestion of Cheese Whey and Cattle Manure." *Bioresource Technology* 128: 779–83. https://doi.org/10.1016/j.biortech.2012.10.118.

Beszédes, Sándor, Zsuzsanna László, Gábor Szabó, and Cecilia Hodúr. 2011. "Effects of Microwave Pretreatments on the Anaerobic Digestion of Food Industrial Sewage Sludge." *Environmental Progress and Sustainable Energy* 30 (3): 486–92. https://doi.org/10.1002/ep.10487.

Bonetta, Silvia, Sara Bonetta, Elisa Ferretti, Giorgio Fezia, Giorgio Gilli, and Elisabetta Carraro. 2014. "Agricultural Reuse of the Digestate from Anaerobic Co-Digestion of Organic Waste: Microbiological Contamination, Metal Hazards and Fertilizing Performance." *Water, Air, and Soil Pollution* 225 (8). https://doi.org/10.1007/s11270-014-2046-2.

Bousek, J., D. Scroccaro, Jan Sima, Norbert Weissenbacher, and W. Fuchs. 2016. "Influence of the Gas Composition on the Efficiency of Ammonia Stripping of Biogas Digestate." *Bioresource Technology* 203 (March): 259–66. https://doi.org/10.1016/j.biortech.2015.12.046.

Brown, Becky J., Mark E. Hanson, Diana M. Liverman, and Robert W. Merideth. 1987. "Global Sustainability: Toward Definition." *Environmental Management* 11 (6): 713–19. https://doi.org/10.1007/BF01867238.

Buffi, Marco, Matteo Prussi, and Nicolae Scarlat. 2022. "Energy and Environmental Assessment of Hydrogen from Biomass Sources: Challenges and Perspectives." *Biomass and Bioenergy* 165 (October). https://doi.org/10.1016/j.biombioe.2022.106556.

Bundhoo, M. A. Zumar, Romeela Mohee, and M. Ali Hassan. 2015. "Effects of Pre-Treatment Technologies on Dark Fermentative Biohydrogen Production: A Review." *Journal of Environmental Management* 157 (July): 20–48. https://doi.org/10.1016/j.jenvman.2015.04.006.

Cai, Mingwei, David Wilkins, Jiapeng Chen, et al. 2016. "Metagenomic Reconstruction of Key Anaerobic Digestion Pathways in Municipal Sludge and Industrial Wastewater Biogas-Producing Systems." *Frontiers in Microbiology* 7 (MAY). https://doi.org/10.3389/fmicb.2016.00778.

Calvo, Pamela, Louise Nelson, and Joseph W. Kloepper. 2014. “Agricultural Uses of Plant Biostimulants.” *Plant and Soil* 383 (1–2): 3–41. https://doi.org/10.1007/s11104-014-2131-8.

Campuzano, Rosalinda, and Simón González-Martínez. 2016. “Characteristics of the Organic Fraction of Municipal Solid Waste and Methane Production: A Review.” *Waste Management* 54 (August): 3–12. https://doi.org/10.1016/j.wasman.2016.05.016.

Canellas, Luciano P., Fábio L. Olivares, Natália O. Aguiar, et al. 2015. “Humic and Fulvic Acids as Biostimulants in Horticulture.” *Scientia Horticulturae* 196 (November): 15–27. https://doi.org/10.1016/j.scienta.2015.09.013.

Carvalheira, Mónica, Joana Cassidy, João M. Ribeiro, et al. 2018. “Performance of a Two-Stage Anaerobic Digestion System Treating Fruit Pulp Waste: The Impact of Substrate Shift and Operational Conditions.” *Waste Management* 78 (August): 434–45. https://doi.org/10.1016/j.wasman.2018.06.013.

Chen, Hong, Jun Wu, Hong Wang, et al. 2021. “Dark Co-Fermentation of Rice Straw and Pig Manure for Biohydrogen Production: Effects of Different Inoculum Pretreatments and Substrate Mixing Ratio.” *Environmental Technology (United Kingdom)* 42 (28): 4539–49. https://doi.org/10.1080/09593330.2020.1770340.

Cheng, Hai Hsuan, Liang Ming Whang, Man Chien Chung, and Kun Chi Chan. 2016. “Biological Hydrogen and Methane Production from Bagasse Bioethanol Fermentation Residues Using a Two-Stage Bioprocess.” *Bioresource Technology* 210 (June): 49–55. https://doi.org/10.1016/j.biortech.2015.12.084.

Chiumenti, A., F. da Borso, R. Chiumenti, F. Teri, and P. Segantin. 2013. “Treatment of Digestate from a Co-Digestion Biogas Plant by Means of Vacuum Evaporation: Tests for Process Optimization and Environmental Sustainability.” *Waste Management* 33 (6): 1339–44. https://doi.org/10.1016/j.wasman.2013.02.023.

Chozhavendhan, S., G. Karthigadevi, B. Bharathiraja, et al. 2023. “Current and Prognostic Overview on the Strategic Exploitation of Anaerobic Digestion and Digestate: A Review.” *Environmental Research* 216 (January). https://doi.org/10.1016/j.envres.2022.114526.

Chu, Chun Feng, Kai Qin Xu, Yu You Li, and Yuhei Inamori. 2012. “Hydrogen and Methane Potential Based on the Nature of Food Waste Materials in a Two-Stage Thermophilic Fermentation Process.” *International Journal of Hydrogen Energy* 37 (14): 10611–18. https://doi.org/10.1016/j.ijhydene.2012.04.048.

Chuda, Aleksandra, and Krzysztof Ziemiński. 2021. “Challenges in Treatment of Digestate Liquid Fraction from Biogas Plant. Performance of Nitrogen Removal and Microbial Activity in Activated Sludge Process.” *Energies* 14 (21). https://doi.org/10.3390/en14217321.

Cravotto, Christian, Anne Sylvie Fabiano-Tixier, Ombéline Claux, et al. 2022. “Higher Yield and Polyphenol Content in Olive Pomace Extracts Using 2-Methyloxolane as Bio-Based Solvent.” *Foods* 11 (9). https://doi.org/10.3390/foods11091357.

Cremonez, Paulo André, Joel Gustavo Teleken, Thompson Ricardo Weiser Meier, and Helton José Alves. 2021. “Two-Stage Anaerobic Digestion in Agroindustrial Waste Treatment: A Review.” *Journal of Environmental Management* 281 (March). https://doi.org/10.1016/j.jenvman.2020.111854.

Czekała, Wojciech. 2019. “Biogas Production from Raw Digestate and Its Fraction.” *Journal of Ecological Engineering* 20 (6): 97–102. https://doi.org/10.12911/22998993/108653.

Czekała, Wojciech. 2022. “Digestate as a Source of Nutrients: Nitrogen and Its Fractions.” *Water (Switzerland)* 14 (24). https://doi.org/10.3390/w14244067.

Dahiya, Shikha, Sulogna Chatterjee, Omprakash Sarkar, and S. Venkata Mohan. 2021. “Renewable Hydrogen Production by Dark-Fermentation: Current Status, Challenges and Perspectives.” *Bioresource Technology* 321 (February). https://doi.org/10.1016/j.biortech.2020.124354.

Dareioti, Margarita A., Konstantina Tsigkou, Aikaterini I. Vavouraki, and Michael Kornaros. 2022. “Hydrogen and Methane Production from Anaerobic Co-Digestion of Sorghum and Cow Manure: Effect of pH and Hydraulic Retention Time.” *Fermentation* 8 (7). https://doi.org/10.3390/fermentation8070304.

Dareioti, Margarita Andreas, and Michael Kornaros. 2015. “Anaerobic Mesophilic Co-Digestion of Ensiled Sorghum, Cheese Whey and Liquid Cow Manure in a Two-Stage CSTR System: Effect of Hydraulic Retention Time.” *Bioresource Technology* 175 (January): 553–62. https://doi.org/10.1016/j.biortech.2014.10.102.

Darwin, Ulfa Triovanta, and Ridho Rinaldi. 2019. “Two-Stage Anaerobic Co-Digestion of Landfill Leachate and Starch Wastes Using Anaerobic Biofilm Reactor for Methane Production.” *Progress in Agricultural Engineering Sciences* 15 (1): 53–70. https://doi.org/10.1556/446.15.2019.1.4.

Demichelis, F., T. Tommasi, F. A. Deorsola, D. Marchisio, G. Mancini, and D. Fino. 2022. "Life Cycle Assessment and Life Cycle Costing of Advanced Anaerobic Digestion of Organic Fraction Municipal Solid Waste." *Chemosphere* 289 (February). https://doi.org/10.1016/j.chemosphere.2021.133058.

Demichelis, Francesca, Fabio Alessandro Deorsola, Elisa Robotti, et al. 2023. "Experimental and Modelling Optimisation of Sustainable Techniques for the Pre-Treatment of the Organic Fraction Municipal Solid Waste to Improve Anaerobic Digestion." *Journal of Cleaner Production* 399 (May). https://doi.org/10.1016/j.jclepro.2023.136594.

Demichelis, Francesca, Maddalena Laghezza, Marco Chiappero, and Silvia Fiore. 2020. "Technical, Economic and Environmental Assessement of Bioethanol Biorefinery from Waste Biomass." *Journal of Cleaner Production* 277 (December): 124111. https://doi.org/10.1016/j.jclepro.2020.124111.

Demirel, Burak, Nefise Pinar Göl, and Turgut Tüzün Onay. 2013. "Evaluation of Heavy Metal Content in Digestate from Batch Anaerobic Co-Digestion of Sunflower Hulls and Poultry Manure." *Journal of Material Cycles and Waste Management* 15 (2): 242–46. https://doi.org/10.1007/s10163-012-0107-4.

Dharmalingam, Babu, Prapakorn Tantayotai, Elizabeth Jayex Panakkal, et al. 2022. "Organic Acid Pretreatments and Optimization Techniques for Mixed Vegetable Waste Biomass Conversion into Biofuel Production." *Bioenergy Research*, ahead of print. https://doi.org/10.1007/s12155-022-10517-y.

Dinesh, G. Kumaravel, Rohit Chauhan, and Sankar Chakma. 2018. "Influence and Strategies for Enhanced Biohydrogen Production from Food Waste." *Renewable and Sustainable Energy Reviews* 92 (September): 807–22. https://doi.org/10.1016/j.rser.2018.05.009.

Eraky, Mohamed, Mahdy Elsayed, Muhammad Abdul Qyyum, Ping Ai, and Ahmed Tawfik. 2022. "A New Cutting-Edge Review on the Bioremediation of Anaerobic Digestate for Environmental Applications and Cleaner Bioenergy." *Environmental Research* 213 (October). https://doi.org/10.1016/j.envres.2022.113708.

Esposito, G., L. Frunzo, A. Giordano, F. Liotta, A. Panico, and F. Pirozzi. 2012. "Anaerobic Co-Digestion of Organic Wastes." *Reviews in Environmental Science and Biotechnology* 11 (4): 325–41. https://doi.org/10.1007/s11157-012-9277-8.

European Council. 2008. *DIRECTIVE 2008/98/EC OF THE EUROPEAN PARLIAMENT AND OF THE COUNCIL of 19 November 2008 on Waste and Repealing Certain Directives*. Official Journal of European Union.

Fang, June, Lu Zhan, Yong Sik Ok, and Bin Gao. 2018. "Minireview of Potential Applications of Hydrochar Derived from Hydrothermal Carbonization of Biomass." *Journal of Industrial and Engineering Chemistry* 57 (January): 15–21. https://doi.org/10.1016/j.jiec.2017.08.026.

Farghali, Mohamed, Atsushi Shimahata, Israa M. A. Mohamed, et al. 2022. "Integrating Anaerobic Digestion with Hydrothermal Pretreatment for Bioenergy Production: Waste Valorization of Plastic Containing Food Waste and Rice Husk." *Biochemical Engineering Journal* 186 (August): 108546. https://doi.org/10.1016/j.bej.2022.108546.

Feng, Rui Zhe, Asad A. Zaidi, Kun Zhang, and Yue Shi. 2019. "Optimisation of Microwave Pretreatment for Biogas Enhancement through Anaerobic Digestion of Microalgal Biomass." *Periodica Polytechnica Chemical Engineering* 63 (1): 65–72. https://doi.org/10.3311/PPch.12334.

Foti, Paola, Flora V. Romeo, Nunziatina Russo, et al. 2021. "Olive Mill Wastewater as Renewable Raw Materials to Generate High Added-Value Ingredients for Agro-Food Industries." *Applied Sciences* 11 (16): 7511. https://doi.org/10.3390/app11167511.

Freitas, Emanuelle Neiverth de, Robson Carlos Alnoch, Alex Graça Contato, et al. 2021. "Enzymatic Pretreatment with Laccases from Lentinus Sajor-caju Induces Structural Modification in Lignin and Enhances the Digestibility of Tropical Forage Grass (Panicum Maximum) Grown under Future Climate Conditions." *International Journal of Molecular Sciences* 22 (17). https://doi.org/10.3390/ijms22179445.

Frowijn, Laurens S. F., and Wilfried G. J. H. M. van Sark. 2021. "Analysis of Photon-Driven Solar-to-Hydrogen Production Methods in the Netherlands." *Sustainable Energy Technologies and Assessments* 48 (December). https://doi.org/10.1016/j.seta.2021.101631.

Fuertes, A. B., M. Camps Arbestain, M. Sevilla, et al. 2010. "Chemical and Structural Properties of Carbonaceous Products Obtained by Pyrolysis and Hydrothermal Carbonisation of Corn Stover." *Australian Journal of Soil Research* 48 (6–7): 618–26. https://doi.org/10.1071/SR10010.

Gaitán-Hernández, R., and G. Mata. 2004. "Cultivation of the Edible Mushroom Lentinula Edodes (Shiitake) in Pasteurized Wheat Straw - Alternative Use of Geothermal Energy in Mexico." *Engineering in Life Sciences* 4 (4): 363–67. https://doi.org/10.1002/elsc.200420042.

Gebreeyessus, Getachew D., and Pavel Jenicek. 2016. “Thermophilic versus Mesophilic Anaerobic Digestion of Sewage Sludge: A Comparative Review.” *Bioengineering* 3 (2). https://doi.org/10.3390/bioengineering3020015.

Geisendorf, Sylvie, and Felicitas Pietrulla. 2018. “The Circular Economy and Circular Economic Concepts—a Literature Analysis and Redefinition.” *Thunderbird International Business Review* 60 (5): 771–82. https://doi.org/10.1002/tie.21924.

Gienau, T., U. Brüß, M. Kraume, and S. Rosenberger. 2018. “Nutrient Recovery from Biogas Digestate by Optimised Membrane Treatment.” *Waste and Biomass Valorization* 9 (12): 2337–47. https://doi.org/10.1007/s12649-018-0231-z.

Gil, Aida, Jose A. Siles, Antonio Serrano, Arturo F. Chica, and M. Angeles Martín. 2019. “Effect of Variation in the C/[N+P] Ratio on Anaerobic Digestion.” *Environmental Progress and Sustainable Energy* 38 (1): 228–36. https://doi.org/10.1002/ep.12922.

Golroudbary, Saeed Rahimpour, Mohammad El Wali, and Andrzej Kraslawski. 2019. “Environmental Sustainability of Phosphorus Recycling from Wastewater, Manure and Solid Wastes.” *Science of the Total Environment* 672 (July): 515–24. https://doi.org/10.1016/j.scitotenv.2019.03.439.

Gomec, Cigdem Y., Esra Erdim, Ilknur Turan, Ali F. Aydin, and Izzet Ozturk. 2007. “Advanced Oxidation Treatment of Physico-Chemically Pre-Treated Olive Mill Industry Effluent.” *Journal of Environmental Science and Health - Part B Pesticides, Food Contaminants, and Agricultural Wastes* 42 (6): 741–47. https://doi.org/10.1080/03601230701466021.

Gómez Camacho, Carlos Enrique, Bernardo Ruggeri, Lorenzo Mangialardi, Marco Persico, and Andrea Cristina Luongo Malavé. 2019. “Continuous Two-Step Anaerobic Digestion (TSAD) of Organic Market Waste: Rationalising Process Parameters.” *International Journal of Energy and Environmental Engineering* 10 (4): 413–27. https://doi.org/10.1007/s40095-019-0312-1.

González, Lisbet Mailin López, and Monika Heiermann. 2021. “Effect of Liquid Hot Water Pretreatment on Hydrolysates Composition and Methane Yield of Rice Processing Residue.” *Energies* 14 (11). https://doi.org/10.3390/en14113254.

González-García, Isabel, Berta Riaño, Beatriz Molinuevo-Salces, and María Cruz García-González. 2023. “Effect of Alkali and Membrane Area on the Simultaneous Recovery of Nitrogen and Phosphorous from Digestate by Membrane Technology and Chemical Precipitation.” *Sustainability (Switzerland)* 15 (5). https://doi.org/10.3390/su15053909.

Govasmark, Espen, Jessica Stäb, Børge Holen, Douwe Hoornstra, Tommy Nesbakk, and Mirja Salkinoja-Salonen. 2011. “Chemical and Microbiological Hazards Associated with Recycling of Anaerobic Digested Residue Intended for Agricultural Use.” *Waste Management* 31 (12): 2577–83. https://doi.org/10.1016/j.wasman.2011.07.025.

Gu, Tingyue, Michael A. Held, and Ahmed Faik. 2013. “Supercritical CO2 and Ionic Liquids for the Pretreatment of Lignocellulosic Biomass in Bioethanol Production.” *Environmental Technology (United Kingdom)* 34 (13–14): 1735–49. https://doi.org/10.1080/09593330.2013.809777.

Habashy, Mahmoud M., Ee Shen Ong, Omar M. Abdeldayem, Eslam G. Al-Sakkari, and Eldon R. Rene. 2021. “Food Waste: A Promising Source of Sustainable Biohydrogen Fuel.” *Trends in Biotechnology* 39 (12): 1274–88. https://doi.org/10.1016/j.tibtech.2021.04.001.

Haque, Md Ariful, Vasiliki Kachrimanidou, Apostolis Koutinas, and Carol Sze Ki Lin. 2016. “Valorization of Bakery Waste for Biocolorant and Enzyme Production by Monascus Purpureus.” *Journal of Biotechnology* 231 (August): 55–64. https://doi.org/10.1016/j.jbiotec.2016.05.003.

Hidalgo, Dolores, Enrique Pérez-Zapatero, and Jesús M. Martín-Marroquín. 2023. “Comparative Effect of Acid and Heat Inoculum Pretreatment on Dark Fermentative Biohydrogen Production.” *Environmental Research* 239 (December). https://doi.org/10.1016/j.envres.2023.117433.

Hosseini Koupaie, E., S. Dahadha, A. A. Bazyar Lakeh, A. Azizi, and E. Elbeshbishy. 2019. “Enzymatic Pretreatment of Lignocellulosic Biomass for Enhanced Biomethane Production-A Review.” *Journal of Environmental Management* 233 (March): 774–84. https://doi.org/10.1016/j.jenvman.2018.09.106.

Hussain, Athar, Pradeep Kumar, and Indu Mehrotra. 2015. “Nitrogen and Phosphorus Requirement in Anaerobic Process: A Review.” *Environmental Engineering and Management Journal* 14 (4): 769–80. https://doi.org/10.30638/eemj.2015.086.

“ISTAT Official Statistic Data on the Italian Agricoltural Sector 2021.” n.d. Accessed April 3, 2023. http://dati.istat.it/Index.aspx?DataSetCode=DCSP_LATTE#.

“Italia Domani, Il Piano Nazionale Di Ripresa e Resilienza.” 2021. https://www.italiadomani.gov.it/content/sogei-ng/it/it/home.html.

Izzatie, N. I., M. H. Basha, Y. Uemura, et al. 2016. "Co-Pyrolysis of Rice Straw and Polypropylene Using Fixed-Bed Pyrolyzer." *IOP Conference Series: Materials Science and Engineering* 160 (1). https://doi.org/10.1088/1757-899X/160/1/012033.

Jahirul, Mohammad I., Mohammad G. Rasul, Ashfaque Ahmed Chowdhury, and Nanjappa Ashwath. 2012. "Biofuels Production through Biomass Pyrolysis- A Technological Review." *Energies* 5 (12): 4952–5001. https://doi.org/10.3390/en5124952.

Jeon, Yong Woo, Jong Woo Kang, Ho Kim, Young Man Yoon, and Dong Hoon Lee. 2013. "Unit Mass Estimation and Characterization of Litter Generated in the Broiler House and Slaughter House." *International Biodeterioration and Biodegradation* 85 (November): 592–97. https://doi.org/10.1016/j.ibiod.2013.03.030.

Jin, Hongmei, and Zhizhou Chang. 2011. "Distribution of Heavy Metal Contents and Chemical Fractions in Anaerobically Digested Manure Slurry." *Applied Biochemistry and Biotechnology* 164 (3): 268–82. https://doi.org/10.1007/s12010-010-9133-7.

Jin, Keda, Andrea Pezzuolo, Shaban G. Gouda, et al. 2022. "Valorization of Bio-Fertilizer from Anaerobic Digestate through Ammonia Stripping Process: A Practical and Sustainable Approach towards Circular Economy." *Environmental Technology and Innovation* 27 (August). https://doi.org/10.1016/j.eti.2022.102414.

Kanwal, Fariha, and Angel A. J. Torriero. 2022. "Biohydrogen—A Green Fuel for Sustainable Energy Solutions." *Energies* 15 (20). https://doi.org/10.3390/en15207783.

Kapdan, Ilgi Karapinar, and Fikret Kargi. 2006. "Bio-Hydrogen Production from Waste Materials." *Enzyme and Microbial Technology* 38 (5): 569–82. https://doi.org/10.1016/j.enzmictec.2005.09.015.

Karanasiou, Anthoula, Kleio Angistali, Konstantinos V. Plakas, Margaritis Kostoglou, and Anastasios J. Karabelas. 2023. "Ammonia Recovery from Anaerobic-Fermentation Liquid Digestate with Vacuum Membrane Distillation." *Separation and Purification Technology*, June, 123602. https://doi.org/10.1016/j.seppur.2023.123602.

Khan, Ershad Ullah, and Åke Nordberg. 2018. "Membrane Distillation Process for Concentration of Nutrients and Water Recovery from Digestate Reject Water." *Separation and Purification Technology* 206 (November): 90–98. https://doi.org/10.1016/j.seppur.2018.05.058.

Kobayashi, Takuro, Kai Qin Xu, Yu You Li, and Yuhei Inamori. 2012. "Effect of Sludge Recirculation on Characteristics of Hydrogen Production in a Two-Stage Hydrogen-Methane Fermentation Process Treating Food Wastes." *International Journal of Hydrogen Energy* 37 (7): 5602–11. https://doi.org/10.1016/j.ijhydene.2011.12.123.

Kocher, Gurvinder Singh, Pardeep Kaur, and Monica Sachdeva Taggar. 2017. "An Overview of Pretreatment Processes with Special Reference to Biological Pretreatment for Rice Straw Delignification." *Current Biochemical Engineering* 4.

Köninger, Julia, Emanuele Lugato, Panos Panagos, Mrinalini Kochupillai, Alberto Orgiazzi, and Maria J. I. Briones. 2021. "Manure Management and Soil Biodiversity: Towards More Sustainable Food Systems in the EU." *Agricultural Systems* 194 (December). https://doi.org/10.1016/j.agsy.2021.103251.

Krishnan, Santhana, Lakhveer Singh, Mimi Sakinah, Sveta Thakur, Zularisam A. Wahid, and Johan Sohaili. 2016. "Effect of Organic Loading Rate on Hydrogen (H2) and Methane (CH4) Production in Two-Stage Fermentation under Thermophilic Conditions Using Palm Oil Mill Effluent (POME)." *Energy for Sustainable Development* 34 (October): 130–38. https://doi.org/10.1016/j.esd.2016.07.002.

La, Joohee, Taeyoung Kim, Jae Kyung Jang, and In Seop Chang. 2014. "Ammonia Nitrogen Removal and Recovery from Swine Wastewater by Microwave Radiation." *Environmental Engineering Research* 19 (4): 381–85. https://doi.org/10.4491/eer.2014.064.

Lan, Yibo, Shuang Gai, Kui Cheng, and Fan Yang. 2022. "Advances in Biomass Thermochemical Conversion on Phosphorus Recovery: Water Eutrophication Prevention and Remediation." *Environmental Science: Water Research and Technology* 8 (6): 1173–87. https://doi.org/10.1039/d2ew00169a.

Lee, Myoung Joo, Ji Hyeon Song, and Sun Jin Hwang. 2009. "Effects of Acid Pre-Treatment on Bio-Hydrogen Production and Microbial Communities during Dark Fermentation." *Bioresource Technology* 100 (3): 1491–93. https://doi.org/10.1016/j.biortech.2008.08.019.

Lee, Wonbae, Kyung Mo, Chul Park, et al. 2023. "Co-Digestion of Food Waste and Sewage Sludge Using the Combination of a Thermal Alkali Pre-Treatment and a Two-Stage Anaerobic Digestion System." *Journal of Chemical Technology and Biotechnology* 98 (3): 591–601. https://doi.org/10.1002/jctb.7133.

Lei, Yang, Bingnan Song, Renata D. Van Der Weijden, Michel Saakes, and Cees J. N. Buisman. 2017. "Electrochemical Induced Calcium Phosphate Precipitation: Importance of Local

pH." *Environmental Science and Technology* 51 (19): 11156–64. https://doi.org/10.1021/acs.est.7b03909.

Lembo, Giuseppe, Antonella Signorini, Antonella Marone, Claudio Carbone, and Alessandro Agostini. 2022. "Hydrogen and Methane Production by Single- and Two-Stage Anaerobic Digestion of Second Cheese Whey: Economic Performances and GHG Emissions Evaluation." *Energies* 15 (21). https://doi.org/10.3390/en15217869.

Li, Chunxing, Jie Li, Lanjia Pan, et al. 2020. "Treatment of Digestate Residues for Energy Recovery and Biochar Production: From Lab to Pilot-Scale Verification." *Journal of Cleaner Production* 265 (August). https://doi.org/10.1016/j.jclepro.2020.121852.

Li, Huan, Youkang Li, Shuxin Zou, and Chenchen Li. 2014. "Extracting Humic Acids from Digested Sludge by Alkaline Treatment and Ultrafiltration." *Journal of Material Cycles and Waste Management* 16 (1): 93–100. https://doi.org/10.1007/s10163-013-0153-6.

Li, Mi, Shilin Cao, Xianzhi Meng, et al. 2017. "The Effect of Liquid Hot Water Pretreatment on the Chemical-Structural Alteration and the Reduced Recalcitrance in Poplar." *Biotechnology for Biofuels* 10 (1). https://doi.org/10.1186/s13068-017-0926-6.

Lin, Carol Sze Ki, Lucie A. Pfaltzgraff, Lorenzo Herrero-Davila, et al. 2013. "Food Waste as a Valuable Resource for the Production of Chemicals, Materials and Fuels. Current Situation and Global Perspective." *Energy and Environmental Science* 6 (2): 426–64. https://doi.org/10.1039/c2ee23440h.

Link, Siim, Stelios Arvelakis, Aadu Paist, Truls Liliedahl, and Christer Rosén. 2018. "Effect of Leaching Pretreatment on the Gasification of Wine and Vine (Residue) Biomass." *Renewable Energy* 115: 1–5. https://doi.org/10.1016/j.renene.2017.08.028.

Liu, Baojie, Lu Liu, Baojuan Deng, et al. 2022. "Application and Prospect of Organic Acid Pretreatment in Lignocellulosic Biomass Separation: A Review." *International Journal of Biological Macromolecules* 222 (December): 1400–1413. https://doi.org/10.1016/j.ijbiomac.2022.09.270.

Liu, Dawei, Dapeng Liu, Raymond J. Zeng, and Irini Angelidaki. 2006. "Hydrogen and Methane Production from Household Solid Waste in the Two-Stage Fermentation Process." *Water Research* 40 (11): 2230–36. https://doi.org/10.1016/j.watres.2006.03.029.

Liu, Jianwei, Mengfei Zhao, Chen Lv, and Peng Yue. 2020. "The Effect of Microwave Pretreatment on Anaerobic Co-Digestion of Sludge and Food Waste: Performance, Kinetics and Energy Recovery." *Environmental Research* 189 (October). https://doi.org/10.1016/j.envres.2020.109856.

Liu, Jingxin, Simian Huang, Kai Chen, Teng Wang, Meng Mei, and Jinping Li. 2020. "Preparation of Biochar from Food Waste Digestate: Pyrolysis Behavior and Product Properties." *Bioresource Technology* 302 (April). https://doi.org/10.1016/j.biortech.2020.122841.

Liu, Xinyuan, Ruying Li, Min Ji, and Li Han. 2013. "Hydrogen and Methane Production by Co-Digestion of Waste Activated Sludge and Food Waste in the Two-Stage Fermentation Process: Substrate Conversion and Energy Yield." *Bioresource Technology* 146: 317–23. https://doi.org/10.1016/j.biortech.2013.07.096.

Liu, Xuran, Qiuxiang Xu, Dongbo Wang, et al. 2019. "Microwave Pretreatment of Polyacrylamide Flocculated Waste Activated Sludge: Effect on Anaerobic Digestion and Polyacrylamide Degradation." *Bioresource Technology* 290 (October). https://doi.org/10.1016/j.biortech.2019.121776.

Liu, Zhengang, Fu Shen Zhang, and Jianzhi Wu. 2010. "Characterization and Application of Chars Produced from Pinewood Pyrolysis and Hydrothermal Treatment." *Fuel* 89 (2): 510–14. https://doi.org/10.1016/j.fuel.2009.08.042.

Logan, Mohanakrishnan, and Chettiyappan Visvanathan. 2019. "Management Strategies for Anaerobic Digestate of Organic Fraction of Municipal Solid Waste: Current Status and Future Prospects." *Waste Management and Research* 37 (1_suppl): 27–39. https://doi.org/10.1177/0734242X18816793.

Loow, Yu Loong, Ta Yeong Wu, Jamaliah Md Jahim, Abdul Wahab Mohammad, and Wen Hui Teoh. 2016. "Typical Conversion of Lignocellulosic Biomass into Reducing Sugars Using Dilute Acid Hydrolysis and Alkaline Pretreatment." *Cellulose* 23 (3): 1491–520. https://doi.org/10.1007/s10570-016-0936-8.

Lorenci Woiciechowski, Adenise, Carlos José Dalmas Neto, Luciana Porto de Souza Vandenberghe, et al. 2020. "Lignocellulosic Biomass: Acid and Alkaline Pretreatments and Their Effects on Biomass Recalcitrance – Conventional Processing and Recent Advances." *Bioresource Technology* 304 (May). https://doi.org/10.1016/j.biortech.2020.122848.

Lorick, Dag, Biljana Macura, Marcus Ahlström, Anders Grimvall, and Robin Harder. 2020. "Effectiveness of Struvite Precipitation and Ammonia Stripping for Recovery of Phosphorus and

Nitrogen from Anaerobic Digestate: A Systematic Review." *Environmental Evidence* 9 (1). https://doi.org/10.1186/s13750-020-00211-x.

Lu, Jin, and Suyun Xu. 2021. "Post-Treatment of Food Waste Digestate towards Land Application: A Review." *Journal of Cleaner Production* 303 (June). https://doi.org/10.1016/j.jclepro.2021.127033.

Lukitawesa, Rachma Wikandari, Ria Millati, Mohammad J. Taherzadeh, and Claes Niklasson. 2018. "Effect of Effluent Recirculation on Biogas Production Using Two-Stage Anaerobic Digestion of Citrus Waste." *Molecules* 23 (12): 3380. https://doi.org/10.3390/molecules23123380.

Makádi, Marianna, Attila Tomócsik, and Viktória Orosz. 2012. "Digestate: A New Nutrient Source-Review." In *Biogas*. www.intechopen.com.

Marteel-Parrish, Anne E., and Martin A. Abraham. 2013. "Principles of Green Chemistry and Green Engineering." In *Green Chemistry and Engineering: A Pathway to Sustainability*. Wiley.

Martín-Hernándaez, Edgar, Mariano Martín, and Gerardo J. Ruiz-Mercado. 2021. "A Geospatial Environmental and Techno-Economic Framework for Sustainable Phosphorus Management at Livestock Facilities." *Resources, Conservation and Recycling* 175 (December). https://doi.org/10.1016/j.resconrec.2021.105843.

Maspolim, Yogananda, Yan Zhou, Chenghong Guo, Keke Xiao, and Wun Jern Ng. 2015. "Comparison of Single-Stage and Two-Phase Anaerobic Sludge Digestion Systems - Performance and Microbial Community Dynamics." *Chemosphere* 140 (December): 54–62. https://doi.org/10.1016/j.chemosphere.2014.07.028.

Melitos, George, Xenofon Voulkopoulos, and Anastasia Zabaniotou. 2021. "Waste to Sustainable Biohydrogen Production Via Photo-Fermentation and Biophotolysis − A Systematic Review." *Renewable Energy and Environmental Sustainability* 6: 45. https://doi.org/10.1051/rees/2021047.

Miklas, Václav, Michal Touš, Marta Miklasová, Vítězslav Máša, and David Horňák. 2022. "Winery Wastewater Treatment Technologies: Current Trends and Future Perspective." *Chemical Engineering Transactions* 94: 847–52. https://doi.org/10.3303/CET2294141.

Möller, Kurt, and Torsten Müller. 2012. "Effects of Anaerobic Digestion on Digestate Nutrient Availability and Crop Growth: A Review." *Engineering in Life Sciences* 12 (3): 242–57. https://doi.org/10.1002/elsc.201100085.

Monlau, F., C. Sambusiti, E. Ficara, A. Aboulkas, A. Barakat, and H. Carrère. 2015. "New Opportunities for Agricultural Digestate Valorization: Current Situation and Perspectives." *Energy and Environmental Science* 8 (9): 2600–2621. https://doi.org/10.1039/c5ee01633a.

Monlau, Florian, Cecilia Sambusiti, and Abdellatif Barakat. 2019. "Comparison of Dry versus Wet Milling to Improve Bioethanol or Methane Recovery from Solid Anaerobic Digestate." *Bioengineering* 6 (3). https://doi.org/10.3390/bioengineering6030080.

Mudhoo, Ackmez. 2012. *Biogas Production : Pretreatment Methods in Anaerobic Digestion*. John Wiley & Sons, Incorporated.

Mumme, Jan, Lion Eckervogt, Judith Pielert, Mamadou Diakité, Fabian Rupp, and Jürgen Kern. 2011. "Hydrothermal Carbonization of Anaerobically Digested Maize Silage." *Bioresource Technology* 102 (19): 9255–60. https://doi.org/10.1016/j.biortech.2011.06.099.

Nabaterega, Resty, Vikas Kumar, Shiva Khoei, and Cigdem Eskicioglu. 2021. "A Review on Two-Stage Anaerobic Digestion Options for Optimizing Municipal Wastewater Sludge Treatment Process." *Journal of Environmental Chemical Engineering* 9 (4). https://doi.org/10.1016/j.jece.2021.105502.

Nanda, Sonil, Ramin Azargohar, Janusz A. Kozinski, and Ajay K. Dalai. 2014. "Characteristic Studies on the Pyrolysis Products from Hydrolyzed Canadian Lignocellulosic Feedstocks." *Bioenergy Research* 7 (1): 174–91. https://doi.org/10.1007/s12155-013-9359-7.

Nathao, Chananchida, Ubonrat Sirisukpoka, and Nipon Pisutpaisal. 2013. "Production of Hydrogen and Methane by One and Two Stage Fermentation of Food Waste." *International Journal of Hydrogen Energy* 38 (35): 15764–69. https://doi.org/10.1016/j.ijhydene.2013.05.047.

Navarro, Armando, Carmina Montiel, Jesús Gracia-Fadrique, Alberto Tecante, and Eduardo Bárzana. 2021. "Supercritical Carbon Dioxide 'Explosion' on Blue Agave Bagasse to Enhance Enzymatic Digestibility." *Biomass Conversion and Biorefinery*, ahead of print. https://doi.org/10.1007/s13399-021-01557-z.

Nečemer, Marijan, Doris Potočnik, and Nives Ogrinc. 2016. "Discrimination between Slovenian Cow, Goat and Sheep Milk and Cheese According to Geographical Origin Using a Combination of Elemental Content and Stable Isotope Data." *Journal of Food Composition and Analysis* 52 (September): 16–23. https://doi.org/10.1016/j.jfca.2016.07.002.

Nielsen, H. B., Z. Mladenovska, P. Westermann, and B. K. Ahring. 2004. "Comparison of Two-Stage Thermophilic (68°C/55°C) Anaerobic Digestion with One-Stage Thermophilic (55°C)

Digestion of Cattle Manure." *Biotechnology and Bioengineering* 86 (3): 291–300. https://doi.org/10.1002/bit.20037.

Nkemka, Valentine Nkongndem, Jorge Arenales-Rivera, and Marika Murto. 2014. "Two-Stage Dry Anaerobic Digestion of Beach Cast Seaweed and Its Codigestion with Cow Manure." *Journal of Waste Management* 2014 (July): 1–9. https://doi.org/10.1155/2014/325341.

Norrrahim, Mohd Nor Faiz, Rushdan Ahmad Ilyas, Norizan Mohd Nurazzi, Mohd Saiful Asmal Rani, Mahamud Siti Nur Atikah, and Siti Shazra Shazleen. 2021. "Chemical Pretreatment of Lignocellulosic Biomass for the Production of Bioproducts: An Overview." *Applied Science and Engineering Progress* 14 (4): 588–605. https://doi.org/10.14416/j.asep.2021.07.004.

Okolie, Jude A., Emmanuel I. Epelle, Meshach E. Tabat, et al. 2022. "Waste Biomass Valorization for the Production of Biofuels and Value-Added Products: A Comprehensive Review of Thermochemical, Biological and Integrated Processes." *Process Safety and Environmental Protection* 159 (March): 323–44. https://doi.org/10.1016/j.psep.2021.12.049.

Okoro, Oseweuba Valentine, and Zhifa Sun. 2021. *The Characterisation of Biochar and Biocrude Products of the Hydrothermal Liquefaction of Raw Digestate Biomass*. https://doi.org/10.1007/s13399-020-00672-7/Published.

"Organic Rankine Cycle Cogeneration Plant of One-Farm Size Using Rice Straw as Single Fuel." n.d. Accessed June 19, 2024. https://cordis.europa.eu/project/id/745062.

Osman, Ahmed I., Tanmay J. Deka, Debendra C. Baruah, and David W. Rooney. 2023. "Critical Challenges in Biohydrogen Production Processes from the Organic Feedstocks." *Biomass Conversion and Biorefinery* 13: 8383–401. https://doi.org/10.1007/s13399-020-00965-x/Published.

O-Thong, Sompong, Wantanasak Suksong, Kanathip Promnuan, Mathavee Thipmunee, Chonticha Mamimin, and Poonsuk Prasertsan. 2016. "Two-Stage Thermophilic Fermentation and Mesophilic Methanogenic Process for Biohythane Production from Palm Oil Mill Effluent with Methanogenic Effluent Recirculation for pH Control." *International Journal of Hydrogen Energy* 41 (46): 21702–12. https://doi.org/10.1016/j.ijhydene.2016.07.095.

Panigrahi, Sagarika, and Brajesh K. Dubey. 2019. "A Critical Review on Operating Parameters and Strategies to Improve the Biogas Yield from Anaerobic Digestion of Organic Fraction of Municipal Solid Waste." *Renewable Energy* 143 (December): 779–97. https://doi.org/10.1016/j.renene.2019.05.040.

Parmar, Kiran R., and Andrew B. Ross. 2019. "Integration of Hydrothermal Carbonisation with Anaerobic Digestion; Opportunities for Valorisation of Digestate." *Energies* 12 (9). https://doi.org/10.3390/en12091586.

Parmar, Nagina, Ajay Singh, and Owen P. Ward. 2001. "Characterization of the Combined Effects of Enzyme, pH and Temperature Treatments for Removal of Pathogens from Sewage Sludge." *World Journal of Microbiology and Biotechnology* 17 (2): 169–72. https://doi.org/10.1023/A:1016606020993.

Pattarapisitporn, Alisa, Nonglak Thiangthong, Pakorn Inthajak, Pannapapol Jaichakan, Wantana Panpa, and Wannaporn Klangpetch. 2021. "Production of Xyloligosaccharides from Rice Straw by Microwave-Assisted Enzymatic Hydrolysis and Evaluation of Their Prebiotic Properties." *Chiang Mai University Journal of Natural Sciences* 20 (2): 1–10. https://doi.org/10.12982/CMUJNS.2021.037.

Paudel, Shukra Raj, Sushant Prasad Banjara, Oh Kyung Choi, Ki Young Park, Young Mo Kim, and Jae Woo Lee. 2017. "Pretreatment of Agricultural Biomass for Anaerobic Digestion: Current State and Challenges." *Bioresource Technology* 245: 1194–205. https://doi.org/10.1016/j.biortech.2017.08.182.

Pecchi, Matteo, and Marco Baratieri. 2019. "Coupling Anaerobic Digestion with Gasification, Pyrolysis or Hydrothermal Carbonization: A Review." *Renewable and Sustainable Energy Reviews* 105 (May): 462–75. https://doi.org/10.1016/j.rser.2019.02.003.

Pellegrini, Marco, Cesare Saccani, Augusto Bianchini, and Luca Bonfiglioli. 2016. "Sewage Sludge Management in Europe: A Critical Analysis of Data Quality." *International Journal of Environment and Waste Management* 18 (3): 226. https://doi.org/10.1504/ijewm.2016.10001645.

Petta, Luigi, Sabino De Gisi, Patrizia Casella, Roberto Farina, and Michele Notarnicola. 2017. "Evaluation of the Treatability of a Winery Distillery (Vinasse) Wastewater by UASB, Anoxic-Aerobic UF-MBR and Chemical Precipitation/Adsorption." *Journal of Environmental Management* 201 (October): 177–89. https://doi.org/10.1016/j.jenvman.2017.06.042.

Piash, Km Prottoy Shariar, Rifat Anwar, Carley Shingleton, Rebecca Erwin, Lian Shin Lin, and Oishi Sanyal. 2022. "Integrating Chemical Precipitation and Membrane Separation for Phosphorus and Ammonia Recovery from Anaerobic Digestate." *AIChE Journal* 68 (12). https://doi.org/10.1002/aic.17869.

Pituello, Chiara, Ornella Francioso, Gianluca Simonetti, et al. 2015. "Characterization of Chemical–Physical, Structural and Morphological Properties of Biochars from Biowastes Produced at Different Temperatures." *Journal of Soils and Sediments* 15 (4): 792–804. https://doi.org/10.1007/s11368-014-0964-7.

Ramos, Lucas Rodrigues, Giovanna Lovato, José Alberto Domingues Rodrigues, and Edson Luiz Silva. 2021. "Anaerobic Digestion of Vinasse in Fluidized Bed Reactors: Process Robustness between Two-Stage Thermophilic-Thermophilic and Thermophilic-Mesophilic Systems." *Journal of Cleaner Production* 314 (September). https://doi.org/10.1016/j.jclepro.2021.128066.

Rasit, Nazaitulshila, Azni Idris, Razif Harun, and Wan Azlina Wan Ab Karim Ghani. 2015. "Effects of Lipid Inhibition on Biogas Production of Anaerobic Digestion from Oily Effluents and Sludges: An Overview." *Renewable and Sustainable Energy Reviews* 45: 351–58. https://doi.org/10.1016/j.rser.2015.01.066.

Ravindran, Anita, Sunil Adav, and Shang Shyng Yang. 2010. "Effect of Heat Pre-Treatment Temperature on Isolation of Hydrogen Producing Functional Consortium from Soil." *Renewable Energy* 35 (12): 2649–55. https://doi.org/10.1016/j.renene.2010.04.010.

Risberg, Kajsa, Harald Cederlund, Mikael Pell, Veronica Arthurson, and Anna Schnürer. 2017. "Comparative Characterization of Digestate versus Pig Slurry and Cow Manure – Chemical Composition and Effects on Soil Microbial Activity." *Waste Management* 61 (March): 529–38. https://doi.org/10.1016/j.wasman.2016.12.016.

Rivera, Fanny, Raúl Muñoz, Pedro Prádanos, Antonio Hernández, and Laura Palacio. 2022. "A Systematic Study of Ammonia Recovery from Anaerobic Digestate Using Membrane-Based Separation." *Membranes* 12 (1). https://doi.org/10.3390/membranes12010019.

Rizzioli, Fabio, Davide Bertasini, David Bolzonella, Nicola Frison, and Federico Battista. 2023. "A Critical Review on the Techno-Economic Feasibility of Nutrients Recovery from Anaerobic Digestate in the Agricultural Sector." *Separation and Purification Technology* 306 (February). https://doi.org/10.1016/j.seppur.2022.122690.

Rodriguez Correa, Catalina, Maria Bernardo, Rui P. P. L. Ribeiro, Isabel A. A. C. Esteves, and Andrea Kruse. 2017. "Evaluation of Hydrothermal Carbonization as a Preliminary Step for the Production of Functional Materials from Biogas Digestate." *Journal of Analytical and Applied Pyrolysis* 124 (March): 461–74. https://doi.org/10.1016/j.jaap.2017.02.014.

Rousseau, Raphaël, Luc Etcheverry, Emma Roubaud, Régine Basséguy, Marie Line Délia, and Alain Bergel. 2020. "Microbial Electrolysis Cell (MEC): Strengths, Weaknesses and Research Needs from Electrochemical Engineering Standpoint." *Applied Energy* 257 (January). https://doi.org/10.1016/j.apenergy.2019.113938.

Roy, Moumita, Nabin Aryal, Yifeng Zhang, Sunil A. Patil, and Deepak Pant. 2022. "Technological Progress and Readiness Level of Microbial Electrosynthesis and Electrofermentation for Carbon Dioxide and Organic Wastes Valorization." *Current Opinion in Green and Sustainable Chemistry* 35 (June). https://doi.org/10.1016/j.cogsc.2022.100605.

Ruffino, Barbara, and Maria Chiara Zanetti. 2012. "Experimental Study on the Abatement of Ammonia and Organic Carbon with Ozone." *Desalination and Water Treatment* 37 (1–3): 130–38. https://doi.org/10.1080/19443994.2012.661264.

Ruggeri, Bernardo, Tonia Tommasi, and Sara Sanfilippo. 2015. *BioH2 & BioCH4 Through Anaerobic Digestion From Research to Full-Scale Applications*. http://www.springer.com/series/8059.

Ruiz-Aguilar, Graciela M. L., Hector G. Nuñez-Palenius, Nanh Lovanh, and Sarai Camarena-Martínez. 2022. "Comparative Study of Methane Production in a One-Stage vs. Two-Stage Anaerobic Digestion Process from Raw Tomato Plant Waste." *Energies* 15 (23). https://doi.org/10.3390/en15239137.

Saerens, Bart, Sam Geerts, and Marjoleine Weemaes. 2021. "Phosphorus Recovery as Struvite from Digested Sludge – Experience from the Full Scale." *Journal of Environmental Management* 280 (February). https://doi.org/10.1016/j.jenvman.2020.111743.

Sajjadi, Baharak, Wei Yin Chen, and Nosa O. Egiebor. 2019. "A Comprehensive Review on Physical Activation of Biochar for Energy and Environmental Applications." *Reviews in Chemical Engineering* 35 (6): 735–76. https://doi.org/10.1515/revce-2017-0113.

Sajjadi, Baharak, Tetiana Zubatiuk, Danuta Leszczynska, Jerzy Leszczynski, and Wei Yin Chen. 2019. "Chemical Activation of Biochar for Energy and Environmental Applications: A Comprehensive Review." *Reviews in Chemical Engineering* 35 (7): 777–815. https://doi.org/10.1515/revce-2018-0003.

Samarina, Tatiana, Luca Guagneli, Esther Takaluoma, Sari Tuomikoski, Janne Pesonen, and Outi Laatikainen. 2022. "Ammonium Removal by Metakaolin-Based Geopolymers from Municipal and Industrial Wastewaters and Its Sequential Recovery by Stripping Techniques." *Frontiers in Environmental Science* 10 (November). https://doi.org/10.3389/fenvs.2022.1033677.

Sambusiti, C., F. Monlau, and A. Barakat. 2016. “Bioethanol Fermentation as Alternative Valorization Route of Agricultural Digestate According to a Biorefinery Approach.” *Bioresource Technology* 212 (July): 289–95. https://doi.org/10.1016/j.biortech.2016.04.056.

Sambusiti, C., F. Monlau, E. Ficara, et al. 2015. “Comparison of Various Post-Treatments for Recovering Methane from Agricultural Digestate.” *Fuel Processing Technology* 137 (May): 359–65. https://doi.org/10.1016/j.fuproc.2015.04.028.

Saracco, Guido. 2017. *Chimica Verde 2.0*. Zanichelli.

Sarlaki, E., Ali Sharif Paghaleh, Mohammad Hossein Kianmehr, and Keyvan Asefpour Vakilian. 2019. “Extraction and Purification of Humic Acids from Lignite Wastes Using Alkaline Treatment and Membrane Ultrafiltration.” *Journal of Cleaner Production* 235 (October): 712–23. https://doi.org/10.1016/j.jclepro.2019.07.028.

Schlömer, Steffen, Thomas Bruckner, Lew Fulton, et al. 2014. *III ANNEX Technology-Specific Cost and Performance Parameters Editor: Lead Authors: Contributing Authors: To the Fifth Assessment Report of the Intergovernmental Panel on Climate Change [Edenhofer Technology-Specific Cost and Performance Parameters Annex III AIII Contents*. Intergovernmental Panel on Climate Change (IPCC).

Selim, khaled, Waleed Badawy, and Iryna Smetanska. 2020. “Utilization of Olive Pomace as a Source of Bioactive Compounds in Quality Improving of Toast Bread.” *Egyptian Journal of Food Science* 0 (0): 0–0. https://doi.org/10.21608/ejfs.2020.22871.1038.

Senthil Rathi, B., P. Senthil Kumar, Gayathri Rangasamy, and Saravanan Rajendran. 2022. “A Critical Review on Biohydrogen Generation from Biomass.” *International Journal of Hydrogen Energy*, ahead of print. https://doi.org/10.1016/j.ijhydene.2022.10.182.

Sert, Murat, Dilek Selvi Gökkaya, Nihal Cengiz, Levent Ballice, Mithat Yüksel, and Mehmet Sağlam. 2018. “Hydrogen Production from Olive-Pomace by Catalytic Hydrothermal Gasification.” *Journal of the Taiwan Institute of Chemical Engineers* 83 (February): 90–98. https://doi.org/10.1016/j.jtice.2017.11.026.

Setyobudi, Roy Hendroko, Ahmad Wahyudi, and Zane Vincēviča-Gaile. 2017. *Study of Biorefinery Capsule Husk from Jatropha Curcas L. Waste Crude Jatropha Oil as Source for Biogas*. 1 (1).

Shang, Gaoyuan, Congguang Zhang, Fei Wang, Ling Qiu, Xiaohui Guo, and Fuqing Xu. 2019. “Liquid Hot Water Pretreatment to Enhance the Anaerobic Digestion of Wheat Straw—Effects of Temperature and Retention Time.” *Environmental Science and Pollution Research* 26 (28): 29424–34. https://doi.org/10.1007/s11356-019-06111-z.

Shanmugam, Sabarathinam, Thangavel Mathimani, Eldon R. Rene, et al. 2021. “Biohythane Production from Organic Waste: Recent Advancements, Technical Bottlenecks and Prospects.” *International Journal of Hydrogen Energy* 46 (20): 11201–16. https://doi.org/10.1016/j.ijhydene.2020.10.132.

Sharma, Abhishek, Vishnu Pareek, and Dongke Zhang. 2015. “Biomass Pyrolysis - A Review of Modelling, Process Parameters and Catalytic Studies.” *Renewable and Sustainable Energy Reviews* 50 (June): 1081–96. https://doi.org/10.1016/j.rser.2015.04.193.

Shin, Dong Chul, I. Tae Kim, Jinhong Jung, Yoonah Jeong, Ye Eun Lee, and Kwang Ho Ahn. 2022. “Increasing Anaerobic Digestion Efficiency Using Food-WasteBased Biochar.” *Fermentation* 8 (6). https://doi.org/10.3390/fermentation8060282.

Shu, Chin Hang, Rajan Jaiswal, Mu Do Kuo, and Bing Hung Yu. 2022. “Enhancing Methane Production in a Two-Stage Anaerobic Digestion of Spent Mushroom Substrate and Chicken Manure via Activation of Sludge, Optimization of Temperature, and C/N Ratio.” *Frontiers in Environmental Science* 9 (February). https://doi.org/10.3389/fenvs.2021.810678.

Shukla, Akanksha, Deepak Kumar, Madhuri Girdhar, et al. 2023. “Strategies of Pretreatment of Feedstocks for Optimized Bioethanol Production: Distinct and Integrated Approaches.” *Biotechnology for Biofuels and Bioproducts* 16 (1). https://doi.org/10.1186/s13068-023-02295-2.

Siciliano, A., and S. De Rosa. 2014. “Recovery of Ammonia in Digestates of Calf Manure through a Struvite Precipitation Process Using Unconventional Reagents.” *Environmental Technology (United Kingdom)* 35 (7): 841–50. https://doi.org/10.1080/09593330.2013.853088.

Simonič, Tajda, and Marjana Simonič. 2018. “Vacuum Evaporation of Liquid Fraction of Digestate.” *KEMIJA U INDUSTRIJI*.

Slepetiene, Alvyra, Jonas Volungevicius, Linas Jurgutis, et al. 2020. “The Potential of Digestate as a Biofertilizer in Eroded Soils of Lithuania.” *Waste Management* 102 (February): 441–51. https://doi.org/10.1016/j.wasman.2019.11.008.

Solomakou, Nikoletta, and Athanasia M. Goula. 2020. “Novel Low-Cost Biosorbents of Phenolic Compounds from Olive Mill Wastewaters.” December 23, 1. https://doi.org/10.3390/asec2020-07544.

Sołowski, Gawel. 2018. “Biohydrogen Production-Sources and Methods: A Review.” *International Journal of Bioprocessing and Biotechniques* 2018 (01). https://doi.org/10.20911/IJBBT-101.

Sołowski, Gaweł, Izabela Konkol, and Adam Cenian. 2020. “Production of Hydrogen and Methane from Lignocellulose Waste by Fermentation. A Review of Chemical Pretreatment for Enhancing the Efficiency of the Digestion Process.” In *Journal of Cleaner Production*, vol. 267. Elsevier Ltd. https://doi.org/10.1016/j.jclepro.2020.121721.

Stasinakis, Athanasios S., Panagiotis Charalambous, and Ioannis Vyrides. 2022. “Dairy Wastewater Management in EU: Produced Amounts, Existing Legislation, Applied Treatment Processes and Future Challenges.” *Journal of Environmental Management* 303 (February). https://doi.org/10.1016/j.jenvman.2021.114152.

Stoumpou, Vasileia, Jelica Novakovic, Nikoleta Kontogianni, et al. 2020. “Assessing Straw Digestate as Feedstock for Bioethanol Production.” *Renewable Energy* 153 (June): 261–69. https://doi.org/10.1016/j.renene.2020.02.021.

Sun, Cheng, Liang Guo, Yongkang Zheng, et al. 2022. “Effect of Mixed Primary and Secondary Sludge for Two-Stage Anaerobic Digestion (AD).” *Bioresource Technology* 343 (January). https://doi.org/10.1016/j.biortech.2021.126160.

Tan, H., C. T. Lee, P. Y. Ong, et al. 2021. “A Review On The Comparison Between Slow Pyrolysis And Fast Pyrolysis On The Quality Of Lignocellulosic And Lignin-Based Biochar.” *IOP Conference Series: Materials Science and Engineering* 1051 (1): 012075. https://doi.org/10.1088/1757-899x/1051/1/012075.

Tang, Jingchun, Wenying Zhu, Rai Kookana, and Arata Katayama. 2013. “Characteristics of Biochar and Its Application in Remediation of Contaminated Soil.” *Journal of Bioscience and Bioengineering* 116 (6): 653–59. https://doi.org/10.1016/j.jbiosc.2013.05.035.

Tena, Miriam, Montserrat Perez, and Rosario Solera. 2021. “Effect of Hydraulic Retention Time on the Methanogenic Step of a Two-Stage Anaerobic Digestion System from Sewage Sludge and Wine Vinasse: Microbial and Kinetic Evaluation.” *Fuel* 296 (July). https://doi.org/10.1016/j.fuel.2021.120674.

Terasawat, Ariyah, and Sivawan Phoolphundh. 2021. “Simultaneous Biological Pretreatment and Saccharification of Rice Straw by Ligninolytic Enzymes from Panus Neostrigosus I9 and Commercial Cellulase.” *Journal of Fungi* 7 (10). https://doi.org/10.3390/jof7100853.

Thaemngoen, Amornpan, Kanyarat Saritpongteeraka, Shao Yuan Leu, Chettaphong Phuttaro, Chayanon Sawatdeenarunat, and Sumate Chaiprapat. 2020. “Anaerobic Digestion of Napier Grass (Pennisetum Purpureum) in Two-Phase Dry Digestion System Versus Wet Digestion System.” *Bioenergy Research* 13 (3): 853–65. https://doi.org/10.1007/s12155-020-10110-1.

Tsai, Wen Tien, Po Cheng Huang, and Yu Quan Lin. 2019. “Characterization of Biochars Produced from Dairy Manure at High Pyrolysis Temperatures.” *Agronomy* 9 (10). https://doi.org/10.3390/agronomy9100634.

Tufaner, F., and Y. Avşar. 2016. “Effects of Co-Substrate on Biogas Production from Cattle Manure: A Review.” *International Journal of Environmental Science and Technology* 13 (9): 2303–12. https://doi.org/10.1007/s13762-016-1069-1.

Ubando, Aristotle T., Wei Hsin Chen, Dennis A. Hurt, Ariel Conversion, Saravanan Rajendran, and Sheng Lun Lin. 2022. “Biohydrogen in a Circular Bioeconomy: A Critical Review.” *Bioresource Technology* 366 (December). https://doi.org/10.1016/j.biortech.2022.128168.

Uddin, Md Mosleh, and Mark Mba Wright. 2023. “Anaerobic Digestion Fundamentals, Challenges, and Technological Advances.” *Physical Sciences Reviews* 8 (9): 2819–37. https://doi.org/10.1515/psr-2021-0068.

Uzkurt Kaljunen, J., R. A. Al-Juboori, W. Khunjar, A. Mikola, and G. Wells. 2022. “Phosphorus Recovery Alternatives for Sludge from Chemical Phosphorus Removal Processes – Technology Comparison and System Limitations.” *Sustainable Materials and Technologies* 34 (December). https://doi.org/10.1016/j.susmat.2022.e00514.

Vanotti, M. B., P. J. Dube, A. A. Szogi, and M. C. García-González. 2017. “Recovery of Ammonia and Phosphate Minerals from Swine Wastewater Using Gas-Permeable Membranes.” *Water Research* 112: 137–46. https://doi.org/10.1016/j.watres.2017.01.045.

Vidal, G., A. Carvalho, R. M. Endez, and J. M. Lema. 2000. *In¯uence of the Content in Fats and Proteins on the Anaerobic Biodegradability of Dairy Wastewaters*.

Vidlarova, P., S. Heviankova, and M. Kyncl. 2017. “Contribution to the Study of Ammonia Removal from Digestate by Struvite Precipitation.” *IOP Conference Series: Earth and Environmental Science* 92 (1). https://doi.org/10.1088/1755-1315/92/1/012072.

Vlyssides, A. G., E. M. Barampouti, and S. Mai. 2005. "Wastewater Characteristics from Greek Wineries and Distilleries." *Water Science and Technology* 51 (1): 53–60. https://doi.org/10.2166/wst.2005.0007.

Wang, Dianlong, Jiang Xi, Ping Ai, et al. 2016. "Enhancing Ethanol Production from Thermophilic and Mesophilic Solid Digestate Using Ozone Combined with Aqueous Ammonia Pretreatment." *Bioresource Technology* 207 (May): 52–58. https://doi.org/10.1016/j.biortech.2016.01.119.

Wang, Ning, Qindong Chen, Chao Zhang, Zihang Dong, and Qiyong Xu. 2022. "Improvement in the Physicochemical Characteristics of Biochar Derived from Solid Digestate of Food Waste with Different Moisture Contents." *Science of the Total Environment* 819 (May). https://doi.org/10.1016/j.scitotenv.2022.153100.

Wang, Shiwei, Fang Ma, Weiwei Ma, Ping Wang, Guang Zhao, and Xiaofei Lu. 2019. "Influence of Temperature on Biogas Production Efficiency and Microbial Community in a Two-Phase Anaerobic Digestion System." *Water (Switzerland)* 11 (1). https://doi.org/10.3390/w11010133.

Wang, Wei, Jo Shu Chang, and Duu Jong Lee. 2023a. "Anaerobic Digestate Valorization beyond Agricultural Application: Current Status and Prospects." *Bioresource Technology* 373 (April). https://doi.org/10.1016/j.biortech.2023.128742.

Wang, Wei, Jo Shu Chang, and Duu Jong Lee. 2023b. "Digestate-Derived Carbonized Char and Activated Carbon: Application Perspective." *Bioresource Technology* 381 (August). https://doi.org/10.1016/j.biortech.2023.129135.

Wang, Xiqing, Tao Lyu, Renjie Dong, Hongtao Liu, and Shubiao Wu. 2021. "Dynamic Evolution of Humic Acids during Anaerobic Digestion: Exploring an Effective Auxiliary Agent for Heavy Metal Remediation." *Bioresource Technology* 320 (January). https://doi.org/10.1016/j.biortech.2020.124331.

"Wheat Straw Waste Could Be Basis for Greener Chemicals." 2017. https://projects.research-and-innovation.ec.europa.eu/en/horizon-magazine/wheat-straw-waste-could-be-basis-greener-chemicals.

Williams, Paul T., and Anton R. Reed. 2004. "High Grade Activated Carbon Matting Derived from the Chemical Activation and Pyrolysis of Natural Fibre Textile Waste." *Journal of Analytical and Applied Pyrolysis* 71 (2): 971–86. https://doi.org/10.1016/j.jaap.2003.12.007.

Wirth, Roland, Etelka Kovács, Gergely Maráti, Zoltán Bagi, Gábor Rákhely, and Kornél L. Kovács. 2012. "Characterization of a Biogas-Producing Microbial Community by Short-Read next Generation DNA Sequencing." *Biotechnology for Biofuels* 5. https://doi.org/10.1186/1754-6834-5-41.

Wiśniewski, Dariusz, Janusz Gołaszewski, and Andrzej Białowiec. 2015. "The Pyrolysis and Gasification of Digestate from Agricultural Biogas Plant." *Archives of Environmental Protection* 41 (3): 70–75. https://doi.org/10.1515/aep-2015-0032.

Xie, Xiaodi, Chao Peng, Xinyu Song, Nana Peng, and Chao Gai. 2022. "Pyrolysis Kinetics of the Hydrothermal Carbons Derived from Microwave-Assisted Hydrothermal Carbonization of Food Waste Digestate." *Energy* 245 (April). https://doi.org/10.1016/j.energy.2022.123269.

Yang, Yunpeng, and Hailong Liu. 2022. "The Mechanisms of Ozonation for Ammonia Nitrogen Removal: An Indirect Process." *Journal of Environmental Chemical Engineering* 10 (5). https://doi.org/10.1016/j.jece.2022.108525.

Yu, Qiong, Ronghou Liu, Kun Li, and Ruijie Ma. 2019. "A Review of Crop Straw Pretreatment Methods for Biogas Production by Anaerobic Digestion in China." *Renewable and Sustainable Energy Reviews* 107 (June): 51–58. https://doi.org/10.1016/j.rser.2019.02.020.

Zabihi, Samyar, Amir Sharafi, Hossein Motamedi, Feridun Esmaeilzadeh, and William O. S. Doherty. 2021. "Environmentally Friendly Acetic Acid/Steam Explosion/Supercritical Carbon Dioxide System for the Pre-Treatment of Wheat Straw." *Environmental Science and Pollution Research*, ahead of print. https://doi.org/10.1007/s11356-021-13410-x/Published.

Zamri, M. F. M. A., Saiful Hasmady, Afifi Akhiar, et al. 2021. "A Comprehensive Review on Anaerobic Digestion of Organic Fraction of Municipal Solid Waste." *Renewable and Sustainable Energy Reviews* 137 (March). https://doi.org/10.1016/j.rser.2020.110637.

Zhang, Jin Zhong. 2014. "Biohydrogen Generation and Other Methods." In *Hydrogen Generation, Storage, and Utilization*.

Zhao, X., G. C. Becker, N. Faweya, et al. 2018. "Fertilizer and Activated Carbon Production by Hydrothermal Carbonization of Digestate." *Biomass Conversion and Biorefinery* 8 (2): 423–36. https://doi.org/10.1007/s13399-017-0291-5.

Zheng, Yaping, Quanguo Zhang, Zhiping Zhang, et al. 2022. "A Review on Biological Recycling in Agricultural Waste-Based Biohydrogen Production: Recent Developments." *Bioresource Technology* 347 (March). https://doi.org/10.1016/j.biortech.2021.126595.

Zheng, Zehui, Yafan Cai, Yue Zhang, et al. 2021. “The Effects of C/N (10–25) on the Relationship of Substrates, Metabolites, and Microorganisms in ‘Inhibited Steady-State’ of Anaerobic Digestion.” *Water Research* 188 (January). https://doi.org/10.1016/j.watres.2020.116466.

Zhou, Man, Hongnan Yang, Dan Zheng, et al. 2019. “Methanogenic Activity and Microbial Communities Characteristics in Dry and Wet Anaerobic Digestion Sludges from Swine Manure.” *Biochemical Engineering Journal* 152 (December). https://doi.org/10.1016/j.bej.2019.107390.

Zhou, Ziyuan, Denghao Ouyang, Dehua Liu, and Xuebing Zhao. 2023. “Oxidative Pretreatment of Lignocellulosic Biomass for Enzymatic Hydrolysis: Progress and Challenges.” *Bioresource Technology* 367 (January). https://doi.org/10.1016/j.biortech.2022.128208.

Zhu, Xianpu, Dominic Yellezuome, Ronghou Liu, Zengzhen Wang, and Xin Liu. 2022. “Effects of Co-Digestion of Food Waste, Corn Straw and Chicken Manure in Two-Stage Anaerobic Digestion on Trace Element Bioavailability and Microbial Community Composition.” *Bioresource Technology* 346 (February). https://doi.org/10.1016/j.biortech.2021.126625.

Ziegler-Devin, Isabelle, Laurent Chrusciel, and Nicolas Brosse. 2021. “Steam Explosion Pretreatment of Lignocellulosic Biomass: A Mini-Review of Theorical and Experimental Approaches.” *Frontiers in Chemistry* 9 (November). https://doi.org/10.3389/fchem.2021.705358.

Chapter 2

2. Two-stage anaerobic digestion of fruit and vegetable waste: optimization of dark fermentation through thermal pretreatment and co-digestion with sugar-rich wastewater

The material presented in this chapter has been published in the article:
Gaia Mazzanti, Francesca Demichelis, Debora Fino, Tonia Tommasi,
"**Two-stage anaerobic digestion of fruit and vegetable waste: optimization of dark fermentation through thermal pretreatment and co-digestion with sugar-rich wastewater**"
Bioresource Technology, Volume 440, 2026, 133423, ISSN 0960-8524,
https://doi.org/10.1016/j.biortech.2025.133423.

2.1 Introduction

2.1.1 Fruit and vegetable waste management

The exponential population growth has led to an increase in biomass waste generation from anthropogenic activities. Food waste is a major contributor to biomass waste, driven by the need to meet the growing global demand for food. Each year, an estimated 59 million tons of food waste are generated across the EU, with 54% originating from households and 46% occurring within the food supply chain (Eurostat 2022). Notably, half of household food waste is linked to the consumption of fresh fruits and vegetables, while a significant portion also arises from agricultural and industrial sectors (Martínez-Mendoza et al. 2023; De Laurentiis et al. 2018). Fruit and vegetable waste (FVW) is typically managed

through landfilling or composting. Landfilling remains a common disposal method due to the biodegradability of FVW. However, its use has been increasingly restricted due to associated environmental issues, such as methane emissions and leachate formation. Leachate, resulting from water infiltration into the soil, contaminates it with organic matter, salts, pollutants, and heavy metals.

To address these concerns, composting has been proposed as a sustainable alternative for managing easily biodegradable waste like FVW. This process involves the aerobic degradation of organic matter into CO_2, NH_3, and N_2, with the production of a solid residue known as compost. Rich in humic substances, compost can be used as a soil amendment. On the other hand, composting can also lead to odors, leachate production and greenhouse gases emissions, posing an additional environmental challenge (García-Rández et al. 2025; Esparza et al. 2020; K. Brown et al. 2013).

Effective management of FVW is essential to mitigate health risks, odors, and environmental contamination from leachates and emissions. However, conventional disposal methods contribute to environmental pollution and are associated to an economic and resource loss. In this context, converting biomass residues into bioenergy and biochemicals offers a promising solution, aligning with circular economy principles by transforming waste into a renewable resource. This approach supports the Sustainable Development Goals 2030, which promote circularity in human activities (European Commission 2015).

FVW results particularly suitable for microbial process due to the high humidity and carbohydrates content of FWV as well as the presence of others compounds useful in microbial growth (Martínez-Mendoza et al. 2023). Moreover its utilization is convenient as FVW is easily available and affordable (Soltan et al. 2024). Two-stage anaerobic digestion (TSAD) has been proposed as biological process to exploit FVW.

2.1.2 Thermal pretreatments

The microbial community involved in dark fermentation must be free of methanogens, so inoculum pretreatment is required to remove them and promote the growth of hydrogen-producing bacteria.

As discussed earlier, thermal and acid pretreatments are the most commonly applied methods in dark fermentation processes. Although some studies report chemical pretreatment as the most effective approach, others show that heat-shock treatment is more efficient in suppressing methanogens and improving hydrogen production (Al-Haddad et al. 2023; Chen et al. 2021). Nevertheless, considering the goals of waste reduction and minimizing the use of non-renewable chemicals, thermal pretreatment appears to be the more sustainable and environmentally preferable option.

Thermal pretreatment can also be applied to substrates to solubilize the outer layers and enhance subsequent conversion (Agrawal et al. 2023). Ruggeri et al. (2013) investigated several pretreatment methods on market organic waste, including acid (HCl 2N to pH 3), alkaline (NaOH 2N to pH 12), thermal (120 °C

for 5 to 90 min), thermal-acid (HCl 2N at 120 °C for 15-30 min), and thermal-alkaline (NaOH 2N at 120 °C for 5-30 minutes). Their results demonstrated that thermal-acid pretreatment was the most effective, increasing energy production by 10 times. Similarly, Li et al. (2016) applied thermal pretreatment (55-160 °C for 15–120 min) to kitchen waste prior to anaerobic digestion. Their findings confirmed that thermal treatment, particularly at temperatures below 120 °C and durations of 15 min, improved CH_4 yield, reduced digestion time, and enhanced overall process efficiency.

2.1.3 Sugar source in dark fermentation

Glucose is commonly employed as a model sugar source in DF studies due to its high bioavailability. For example, Mizuno et al. (2000) conducted DF in a 2.3 L continuous stirred-tank reactor (CSTR) at 35 °C with pH maintained at 6. A culture medium containing 10 g/L of glucose was added to the inoculum, resulting in a H_2 content of 53 % in the biogas and a H_2 yield of 110 $mL/g_{carbohydrates}$. Similarly, Kumar e Das (2000) performed DF in 50 mL rubber-stoppered conical flasks at 36 °C over 10 h, using 1 % glucose. This setup achieved a H_2 yield of 270 $mL/g_{carbohydrates}$.

Beyond glucose, other sugars have also been explored for DF. Fang et al. (2002) investigated the use of sucrose in a 3 L fermenter at 26 °C, maintaining the pH at 5.5. Sucrose was initially provided at a concentration of 2 g/L and gradually increased to 12.15 g/L. The resulting biogas contained 63 % H_2, with a H_2 yield of 280 $mL/g_{carbohydrates}$, demonstrating the viability of sucrose as an effective sugar source for DF.

However, the use of commercial sugars such as glucose and sucrose poses economic challenges for large-scale biogas plants. To address this, alternative sugar sources have been considered. Zagrodnik (2022) evaluated lignocellulosic hydrolysates, which are rich in cellobiose, xylose, and arabinose. These sugars are typically released during lignocellulosic biomass pretreatment. The study was conducted in a 0.2 L CSTR operated at 32 °C, with pH adjusted using NaOH across a range of 4.0 to 7.5 to assess optimal conditions for DF. Cellobiose was completely converted under all conditions, while xylose and arabinose showed the highest conversion at pH 6 and 7, respectively. Overall, the most efficient sugar conversion occurred between pH 5.5 and 7.5, which aligns with the optimal pH range for DF. These findings also highlighted the lower degradability of pentoses, emphasizing that DF performance is strongly influenced by the type of sugar present in the substrate.

Among alternatives to commercial sugar sources, jam industry wastewater represents a novel and mostly underexplored waste. Mohan e Sunny (2008) investigated the biomethanation of wastewater from the jam industry, testing methane production in both batch and continuous systems using 2 L reactors. In batch experiments, a 90 % reduction in soluble COD was achieved within three days of operation. The continuous system demonstrated a COD removal efficiency of 83.6 %, confirming that anaerobic digestion can significantly reduce

the organic content of jam production wastewater while generating methane. Ruffino e Zanetti (2017) studied the anaerobic digestion of wastewater from a fruit processing plant, which included liquid waste from fruits and spent processing water used for sanitation and cleaning. Digestion was carried out in 6 L reactors at 38 °C, yielding 0.329 Nm^3 of methane per kg of volatile solids (VS). Based on experimental results, a new reactor was designed to integrate the anaerobic digestion process into the factory, demonstrating its potential to reduce disposal costs and lower CO_2 emissions.

2.1.4 Goal

To the best of the authors' knowledge, research on the use of jam wastewater (JWW) remains scarce, and no studies have specifically focused on TSAD.

The study first evaluates the activity of the inoculum to determine its suitability for DF with simple sugars. Thermal pretreatment is tested to evaluate its compatibility with the specific inoculum used. Subsequently, DF process is applied to a mixture of FVW and JWW to evaluate hydrogen production through co-digestion. Then, TSAD was tested to examine the influence of the substrate-to-inoculum (S:I) ratio and substrate pretreatment on H_2 and CH_4 yields. Finally, the effects of OLR and reactor scale were examined in order to gain a deeper understanding of key operational conditions and to assess the implications of scaling up the process.

To address the limited use of jam wastewater, this study investigates its integration with a common substrate such as FVW offering an alternative solution for managing biomass waste. This approach not only facilitates energy production but also reduces the reliance on fresh water, leveraging the water content present in JWW. Overall, this work supports circular economy goals and contributes to more environmentally friendly energy systems.

2.2 Materials and method

2.2.1 Substrates and inoculum characterization

The inoculum employed in DF and AD was the mesophilic digestate of cow-agricultural sludge (CAS) provided by "Cascina La Speranza" (Fossano, Cuneo, Italy). FVW was collected from household residue (mass composition of 75% vegetables and 25 % fruits) and chopped through a kitchen blender. JWW was supplied by a local agricultural cooperative (Piedmont, Italy) as the water employed to wash jam production equipment. Both FVW and JWW were frozen at -18 °C after their collection to avoid natural decomposition. Then they were defrosted before being fed into the fermentation system. JWW, FVW and inoculum characterization are presented in *Table 2.1*. All the experiments have been performed with the same lot of JWW, FVW and inoculum to ensure the reproducibility and comparability of the achieved results.

2.2.2 Inoculum thermal pretreatment

In the present study, inoculum was thermally pretreated at 60 °C for 30 min to eliminate H_2-consumers and favor sporulation of H_2-producers. Time and temperature were chosen in accordance with literature results (Ravindran et al. 2010; Hidalgo et al. 2023). Inoculum was heated in the oven covered by aluminum foils to avoid significant water evaporation from the samples.

2.2.3 Process setup and operative condition

DF and AD were performed in 250 mL Pyrex glass bottles (Duran, Germany) with a working volume of 80 % at 35°C. The heating was controlled by a 55 L thermostatic water-bath (Julabo-Corio-C, Merck, Germany). Reactors were operated in batch feeding mode with 6% of total solids and shaken manually to keep the mixture homogeneous inside the reactor. Each reactor was sealed with a two-port cap. Through one of the ports, anaerobic conditions were assured by purging N_2 directly inside the biomass to change the volume of the reactor three times and closing the port. The second port was connected to a 1 L Teddlar gas bag where biogas was collected. The duration of each assay depended on biogas or H_2 production: testing was stopped when daily H_2 (for DF tests) and biogas (for AD tests) production was less than 1 % of the overall production recorded during the period of preparation (VDI 4630 2006). The experimental campaign consists of three main experiments and all the campaigns were studied in replicates. The pH of each reactor was measured at the beginning and at the end of the experiments. In the first test, no pH adjustment was applied in order to monitor how the pretreated inoculum behaved in terms of natural pH variation during dark fermentation. In the second and third experiments, when necessary, HCl was added to the reactors to lower pH to around 6-7 in DF. AD pH was maintained between 7 and 8.

In the first experiment, eight configurations were tested to investigate the role of the inoculum in the DF. In detail, the utilization of the inoculum thermally pre-treated (to inhibit the methanogenic consortia), the addition or not of a medium culture, and the effect of the source of sugar employed (glucose or sucrose) were compared. The medium culture was prepared based on (H. H. P. Fang et al. 2006), then modified to avoid precipitation of metals. In each 250 mL bottle, 2 mL of metals solution, 2 mL of yeast solution, 2 mL of phosphates solution, 2 mL of calcium solution ($CaCl_2$) and 0.5 g of ammonium were added. Glucose and sucrose were added at a concentration of 50 g/L and 25 g/L, respectively. These concentrations were chosen to get the same number of monosaccharide units, since sucrose splits into two sugars (glucose and fructose). This keeps the total sugar units equal for the reactions.

In the second experiment, eight configurations were tested to explore: source and content of sugar employed (the commercial sugars among glucose and sucrose resulting most performing from experiment 1 and JWW) and the H_2 yield from the DF of FVW, employed as substrate. The mixture of FVW and JWW was tested in a ratio of 19:1 (95/5 %, marked with A) and 5.67:1 (85/15 %, marked with B), based on VS. These quantities were chosen to decrease as much as possible the utilization of clean water in order to have total solids at 6 %. Since JWW contained 7.7 g/L of glucose, sucrose was added to supply the system with the same amount of monosaccharides provided by JWW. The inoculum was thermally pretreated for each configuration. The ratio between substrate and inoculum was maintained equal to 1:1 based on VS.

In the third experiment, DF was tested on a mixture of FVW and JWW and TSAD was performed. Four configurations were tested: application or not of thermal treatment on FVW and S:I either 2 or 1. Thermal pretreatment was applied to FVW during the first stage of TSAD experiments to test its efficiency in improving the biodegradability of biomasses. A temperature of 60 °C was applied for 30 min as inoculum pretreatment to minimize the energy consumption of the process. FVW was heated in the oven covered by aluminum foil to avoid significant water evaporation from the samples. The ratio between FVW and JWW was chosen depending on the configuration which achieved the highest H_2 in the previous experiment. The second stage of the process, the AD, was performed on DF digestate which acted as a substrate. S:I was maintained at 1 and the inoculum was not pretreated. A summary of configurations characteristics is presented in *Table 2.2*. Single-stage AD was performed on the two configurations from the third experiment that showed the highest H_2 yields: one with a S:I ratio of 2:1 and another with a ratio of 1:1.

The effect of OLR during DF was evaluated using the configuration that had achieved the highest H_2 yield in the third experimental phase, without applying thermal pretreatment to the substrate.

Scale-up test of TSAD was carried out using the configuration that had produced the highest CH_4 yield in the TSAD experiments with FVW and JWW. For operation at a larger volume, a 5-L tank was used as reactor. A port was installed on the tank lid to allow the connection of a tube leading to a 5-L Tedlar

gas bag for biogas collection. All operational conditions matched those applied in the smaller-scale experiments, ensuring comparability between scales.

2.2.4 General design of anaerobic digestion

As mentioned, AD was designed depending on TS fed to the system and the relative ratio between substrates and inoculum VS (S_R:I_R). Accordingly, the required amounts of inoculum and substrates were determined using the equations below, where xi represents the fractional contribution of each substrate in the case of co-digestion.

$$\mathrm{TS_{fed}\,[g]} = \mathrm{V_W[mL]} \cdot \mathrm{TS_{fed}[\%]} \tag{2.1}$$

$$\mathrm{VS_{fed}\,[g]} = \frac{\mathrm{TS_{fed}\,[g]}}{\mathrm{S_R} \cdot \sum_i \frac{\mathrm{x_i}}{\mathrm{VS_{S,i}[\%]}} + \frac{\mathrm{I_R}}{\mathrm{VS_I[\%]}}} \tag{2.2}$$

$$\mathrm{VS_{S,i}[g]} = \mathrm{x_i} \cdot \frac{\mathrm{S_R}}{\mathrm{I_R}} \cdot \mathrm{VS_{fed}[g]} \qquad \mathrm{VS_I[g]} = \frac{\mathrm{I_R}}{\mathrm{S_R}} \cdot \sum_i \mathrm{VS_{S,i}[g]} \tag{2.3}$$

$$\mathrm{TS_{S,i}\,[g]} = \frac{\mathrm{VS_{S,i}[g]}}{\mathrm{VS_{S,i}[\%]}} \qquad \mathrm{TS_I\,[g]} = \frac{\mathrm{VS_I[g]}}{\mathrm{VS_I[\%]}} \tag{2.4}$$

$$\mathrm{S_i\,[g]} = \frac{\mathrm{TS_{S,i}\,[g]}}{\mathrm{TS_{S,i}[\%]}} \qquad \mathrm{I\,[g]} = \frac{\mathrm{TS_I\,[g]}}{\mathrm{TS_I[\%]}} \tag{2.5}$$

Finally, the eventual quantity of water to add or remove, to reach the set TS% content, was calculated according:

$$\mathrm{Water\,[g]} = \mathrm{V_W[mL]\text{-}S\,[g]\text{-}I\,[g]} \tag{2.6}$$

2.2.5 Analytical methods and data elaboration

Inoculum, FVW and JWW were characterized in terms of TS, VS, and elemental analysis (CHNS, O as difference). TS and VS were measured according to (EPA 2001). To assess the evolution of the AD process, digestate samples were collected at the end of the experiment and analyzed for TS, VS, and CHNS.

Results of these analyses will be reported in Appendix A. Humidity and TS were measured by drying the samples overnight at 105 °C using a U110 oven (Memmert, Germany). VS were quantified on a dry-matter basis by igniting the dried samples at 550 °C for 6 hours with a heating rate of 10 °C/min in a Carbolite-Gero CWF 12/13 furnace (UK). The parameters were determined as shown below:

$$\text{Total Solids (TS)} = \frac{W_1}{W_0}\ \% \tag{2.7}$$

$$\text{Humidity} = \frac{W_0\text{-}W_1}{W_0}\ \% \tag{2.8}$$

$$\text{Volatile Solids (VS)} = \frac{W_1\text{-}W_2}{W_0}\ \% \tag{2.9}$$

$$\text{Ashes} = \frac{W_2}{W_1}\ \% \tag{2.10}$$

where W_0 is the initial fresh weight of the sample; W_1 is the dry weight of the sample after drying at 105 °C; W_2 is the weight of the sample after combustion to ash at 550 °C.

pH was measured with PC 80+ DHS® (XS Instruments, Italy).

Elemental composition was determined on dry basis through an elemental analyzer (Elementar vario Macro Cube) where solid dried samples of 20 mg were investigated to obtain carbon (C), hydrogen (H), nitrogen (N), sulfur (S) and oxygen (O) percentages. For quantifying sugars content in JWW, HPLC (Prominence Shimadzu, Kyoto, Japan) was employed. It was equipped with a refractive index detector (RID-10A Shimadzu, Kyoto, Japan) and a 300 mm x 7.8 mm ROA-Organic Acid H^+ (8%) column (Phenomenex, Torrance, USA).

Biogas composition was evaluated through Micro-GC (SRA) equipped with Molsieve 5A (using argon as carrier) and PoraPlot U (using helium as carrier) columns, along with a TCD detector. The composition was analyzed daily along with the biogas volume produced by emptying each gas bag with a 60 mL syringe. To quantify the net biogas and biomethane production attributable to the substrate, daily and cumulative values were calculated after correcting for inoculum-derived gas, according to:

$$\text{Net Biogas Production of Substrate } [\text{NmL}/g_{\text{VS Substrate}}] = \frac{\text{Biogas Production of I\&S [N mL]-Biogas Production of I [N mL}/g_{\text{VS Inoculum}}] \cdot g_{\text{VS Inoculum}}}{g_{\text{VS Substrate}}} \quad (2.11)$$

For quantifying VFAs, HPLC (model LC40DXR, Shimadzu, Kyoto, Japan) was employed with a KINETEX 5 μm EVO C18 column, measuring 150 x 4.6 mm (Phenomenex, Torrance, USA). HPLC analysis was performed on the liquid fraction of digestate, obtained through centrifugation at 13000 rom for 10 minutes.

The experimental data of biogas productions were subjected to one-way ANOVA to compare the mean results of process conditions on DF and TSAD performances. After the ANOVA, Duncan's post-hoc test ($p < 0.05$) was performed.

2.3 Results

2.3.1 Characterization of inoculum and substrates

The inoculum and substrates were characterized based on TS, VS, and elemental composition using a CHNS analyzer. The results of this analysis are presented in *Table 2.1*. The TS content of the inoculum and FVW were comparable, whereas the JWW exhibited a significantly lower TS content, not even reaching 1%, due to its highly diluted nature.

As expected, the inoculum had a lower VS percentage, reflecting its higher inorganic content. This inoculum derived from the digestate of an AD process treating agricultural waste contains the residual compounds that were not degraded during digestion, along with a fraction of organic matter indicated by the VS/TS (Niya et al. 2023). In contrast, both FVW and JWW exhibited a high proportion of volatile solids, consistent with their composition being primarily made up of easily biodegradable organic compounds (Martínez-Mendoza et al. 2023).

While literature reports a wide variability in TS and VS/TS values of FVW, the average TS content tends to be slightly higher than that observed in this study, typically around 11 % (Magama and Chiyanzu 2021; Scotto di Perta et al. 2022; Soltan et al. 2024). However, the VS/TS ratio in our samples aligns with the findings of (de Quadros et al. 2023), indicating a high content of biodegradable material, making these substrates suitable for biological conversion processes.

Regarding elemental composition, carbon and nitrogen are critical parameters. The optimal carbon-to-nitrogen (C/N) ratio for microbial activity generally ranges from 15 to 30 (Mazzanti et al. 2025), ensuring sufficient organic carbon for energy and adequate nitrogen for microbial growth and metabolism. In this study, the combined use of FVW and JWW resulted in a C/N ratio of approximately 15, eliminating the need for additional chemical supplementation.

Table 2.1 Chemical and physical characterization of inoculum, fruit and vegetable waste (FVW) and jam wastewater (JWW).

	Inoculum	**FVW**	**JWW**
TS (%)	7.00 ± 0.00	7.50 ± 0.01	0.94 ± 0.00
VS/TS (%)	72.73 ± 0.02	92.95 ± 0.02	95.67 ± 0.03
N (%)	3.18 ± 0.35	2.60 ± 0.29	0.96 ± 0.02
C (%)	37.43 ± 1.26	39.41 ± 4.33	52.86 ± 3.98
H (%)	5.17 ± 1.28	5.54 ± 0.44	6.75 ± 0.28
S (%)	0.44 ± 0.16	0.50 ± 0.04	0.31 ± 0.04
O (%)	53.78 ± 2.72	51.96 ± 5.03	39.14 ± 4.23
C/N	11.77 ± 1.35	15.18 ± 2.37	55.35 ± 4.30

Table 2.2 Configurations tested across three experiments: (i) first, varying inoculum thermal pretreatment, culture medium addition, and sugar source; (ii) second, varying sugar source and adding FVW with A = FVW:JWW 19:1 (VS basis) and B = FVW:JWW 5.67:1 (VS basis); (iii) third, varying FVW thermal pretreatment and the S:I ratio.

FIRST EXPERIMENT			
Configuration	**Inoculum Thermal Pretreatment**	**Sugar source**	**Culture medium**
G	NO	Glucose	NO
S	NO	Sucrose	NO
G_M	NO	Glucose	YES
S_M	NO	Sucrose	YES
G_T	YES	Glucose	NO
S_T	YES	Sucrose	NO
G_M_T	YES	Glucose	YES
S_M_T	YES	Sucrose	YES
SECOND EXPERIMENT			
Configuration	**Sugar source**	**FVW**	
SUCR_A	Sucrose (A)	NO	
SUCR_B	Sucrose (B)	NO	
JWW_A	Jam wastewater (A)	NO	
JWW_B	Jam wastewater (B)	NO	
SUCR_FVW_A	Sucrose (A)	YES	
SUCR_FVW_B	Sucrose (B)	YES	
JWW_FVW_A	Jam wastewater (A)	YES	
JWW_FVW_B	Jam wastewater (B)	YES	
THIRD EXPERIMENT			
Configuration	**FVW thermal pretreatment**	**S:I**	
JWW_FVW_1:1	no	1-1	
JWW_FVW_2:1	no	2-1	
JWW_FVW_T_1:1	yes	1-1	
JWW_FVW_T_2:1	yes	2-1	

2.3.2 Role of the inoculum in dark fermentation

This experimental campaign investigated the role of the mesophilic digestate of CAS used as inoculum in the DF of commercial and pure sugars. Specifically, the study examined and compared the use of thermally pre-treated CAS inoculum (to inhibit methanogenic consortia), the presence or absence of a culture medium, and the impact of the type of sugar used (glucose or sucrose). The study investigated eight configurations. A detailed summary of them is provided in *Table 2.2*.

2.3.2.1 Effect of sugar source

Figure 2.1-a presents the biogas production (expressed as mean plus standard deviation) over nine days for DF using glucose or sucrose as sugar source. There is no lag phase since biogas production commenced from day 1 in all configurations, demonstrating the effective activation of the inoculum in degrading the respective sugar. However, a stationary phase was observed in most configurations beginning around day 5.

A significant difference in DF performance was observed between configurations fed with glucose (G, G_M, G_T, G_M_T) and those fed with sucrose (S, S_M, S_T, S_M_T). Systems supplied with glucose exhibited significantly lower biogas yields, reaching a maximum of 106 N mL/g_{VS} for G_M configuration, approximately one third the biogas production achieved in sucrose-fed setups. A similar trend was observed for H_2 in *Figure 2.1-b*, with sucrose-fed systems outperforming their glucose-fed counterparts, achieving higher yields of both biogas and H_2. Glucose-fed setups experienced a marked reduction in both biogas and H_2 production after the first day, which correlated with a significant drop in pH, visible in *Figure 2.1-f*. Although the initial pH was approximately 8 due to the inherent alkalinity of the inoculum, DF process probably led to the production VFAs, resulting in a pH decline across all configurations. In setups using sucrose as the substrate, the pH drop was more moderate, with final values around 6, which is an optimal range for DF activity. In contrast, configurations G, G_M, and G_T exhibited a final pH of approximately 4, a level commonly associated with microbial inhibition and reduced process efficiency (Elbeshbishy et al. 2017). VFAs are toxic to cells because, in their undissociated form, they can cross the cell membrane and disrupt cellular function, potentially leading to the collapse of the microbial community (Chen et al. 2021). Moreover, a decrease in pH can alter microbial metabolism and suppress H_2 generation (Chen et al. 2021). The same trend can be observed for CH_4 and CO_2 production with sucrose-fed system presenting higher quantity of both gases compared to glucose-fed systems. Regarding CH_4, maximum yield was reached in S_M_T configuration with 29.8 N mL/g_{VS}, as showed in *Figure 2.1-c* and *-d*. However, more visible differences could be noted in CO_2 yield since sucrose-fed configurations produced more than double the glucose-fed reactors, which is in accordance with biogas yield. Statistical analysis revealed significant differences in the performance of glucose- and sucrose-fed configurations. Specifically, sucrose-fed reactors showed

significantly higher performance, highlighting the inoculum's ability to effectively hydrolyze disaccharides and convert them into H_2 and CO_2.

2.3.2.2 Effect of thermal pretreatment and culture medium

Regarding the effect of thermal pretreatment, no substantial differences in biogas production were observed between untreated and thermally treated inoculum. In sucrose-fed configurations without a culture medium (S and S_T), the treated and untreated inoculum produced 325 and 320 N mL/g_{VS} of biogas, respectively. However, thermal pretreatment did accelerate the onset of maximum H_2 production. Specifically, in thermally treated setups, maximum H_2 production was achieved on day 4, reaching a maximum yield of 45.8 N mL/g_{VS} for S_T, while in untreated inoculum, H_2 production was delayed until day 7, ultimately reaching 42.1 N mL/g_{VS}. Among the glucose-fed setups, only G_M_T produced H_2 (6.5 N mL/g_{VS}), though the yield remained considerably lower compared to that of sucrose-fed configurations. Although final H_2 yields were similar, thermal pretreatment clearly facilitated a faster process startup which is an important advantage for the potential scale-up of DF processes.

Concerning the contribution of the culture medium, its addition enhanced biogas and H_2 production in glucose-fed setups, but the improvements were limited due to the strong inhibitory effects observed after day 1. In sucrose-fed configurations, the addition of a culture medium improved the rate of biogas and H_2 production. When the culture medium was present, H_2 production became visible from day 3, compared to day 4 in setups without the medium. However, the maximum H_2 yield (45.8 N mL/g_{VS}) was achieved in the sucrose-fed configuration without the culture medium (S_T). This finding suggests that mixed cultures are well-suited for dark fermentation due to their resilience and ability to withstand harsh conditions and a culture medium is not strictly necessary (Mohanakrishna and Pengadeth 2024). No clear effect of thermal pretreatment and culture medium was noted in CH_4 and CO_2 production.

2.3.2.3 Biogas composition and discussion

Figure 2.1-e illustrates the composition of biogas, including H_2, CH_4 and CO_2. In DF processes, the H_2 content in biogas typically ranges between 10 % and 60%, depending on factors such as temperature and substrate composition (Ghimire et al. 2015). In this study, the H_2 percentage in biogas remained below 15% in each configuration, reaching a maximum of 14.5 % in S_T. This result was primarily attributed to the premature inhibition of the process, likely caused by the decrease in pH due to the possible accumulation of VFAs alongside biogas production (Chen et al. 2021). This effect was particularly visible in glucose-fed configurations, where biogas and H_2 production sharply declined after day 1. In all configurations the main component of biogas is CO_2, ranging between 78-92 %. The bars also show a portion corresponding to CH_4 production, ranging from 4 % to 11 %, likely due to the survival of some methanogens after thermal pretreatment. H_2 yields in this study can be compared to those reported by (J.

Wang and Wan 2008), who investigated the effects of five different pretreatment methods on digested sludge: thermal (100 °C for 15 min), acid (HCl), alkaline (NaOH), aeration, and chemical (chloroform). All pretreatments enhanced H_2 production from glucose compared to the untreated control, with yields ranging from 85 to 220 mL/g_{VS}. Among these, thermal pretreatment yielded the highest H_2 production, outperforming the results observed in the present study.

Similarly, (De Amorim et al. 2012) utilized an anaerobic fluidized bed reactor to produce H_2 from thermally pretreated sludge (90 °C for 10 min), derived from swine wastewater effluent. They achieved a maximum H_2 yield of approximately 130 mL/g_{VS} from glucose, using a HRT of 2 h and an initial glucose concentration of 2 g/L. The study also found that increasing HRT and glucose concentration led to decreased H_2 production.

Hu and Chen (2007) examined three pretreatment strategies: acidic (HCl), thermal (boiling water for 10 -30 min), and chemical (chloroform). They were applied to two inoculum types: anaerobic sewage sludge and methanogenic granules. The culture medium contained 18.75 g/L of glucose. Acid pretreatment had little positive effect on H_2 production for either inoculum. However, chloroform addition at concentrations below 1% significantly enhanced H_2 production in methanogenic granules, reaching a maximum of 135 mL/g_{VS} at 0.05% concentration. Thermal pretreatment showed similar benefits, particularly when the granules were boiled for 30 minutes, resulting in a yield of 118 mL/g_{VS}.

Overall, this experiment demonstrated the viability of CAS inoculum in DF by effectively degrading both monosaccharides, such as glucose, and more complex sugars, such as sucrose. The impact of thermal pretreatment was also evaluated, and while its effect on enhancing total biogas and H_2 production was not particularly visible, it was evident that pretreatment influenced the rate of production by facilitating a faster startup of the process. The role of a culture medium was also investigated, revealing that its presence is not essential for improving process yield. This is an important consideration for scaling up DF, as avoiding the use of a culture medium can lead to reduced operational costs. Furthermore, this study underscored the critical role of pH in DF. Although the initial pH was adjusted to 6 to promote fermentation, the rapid production of VFAs led to a significant decline in pH, ultimately hindering the process.

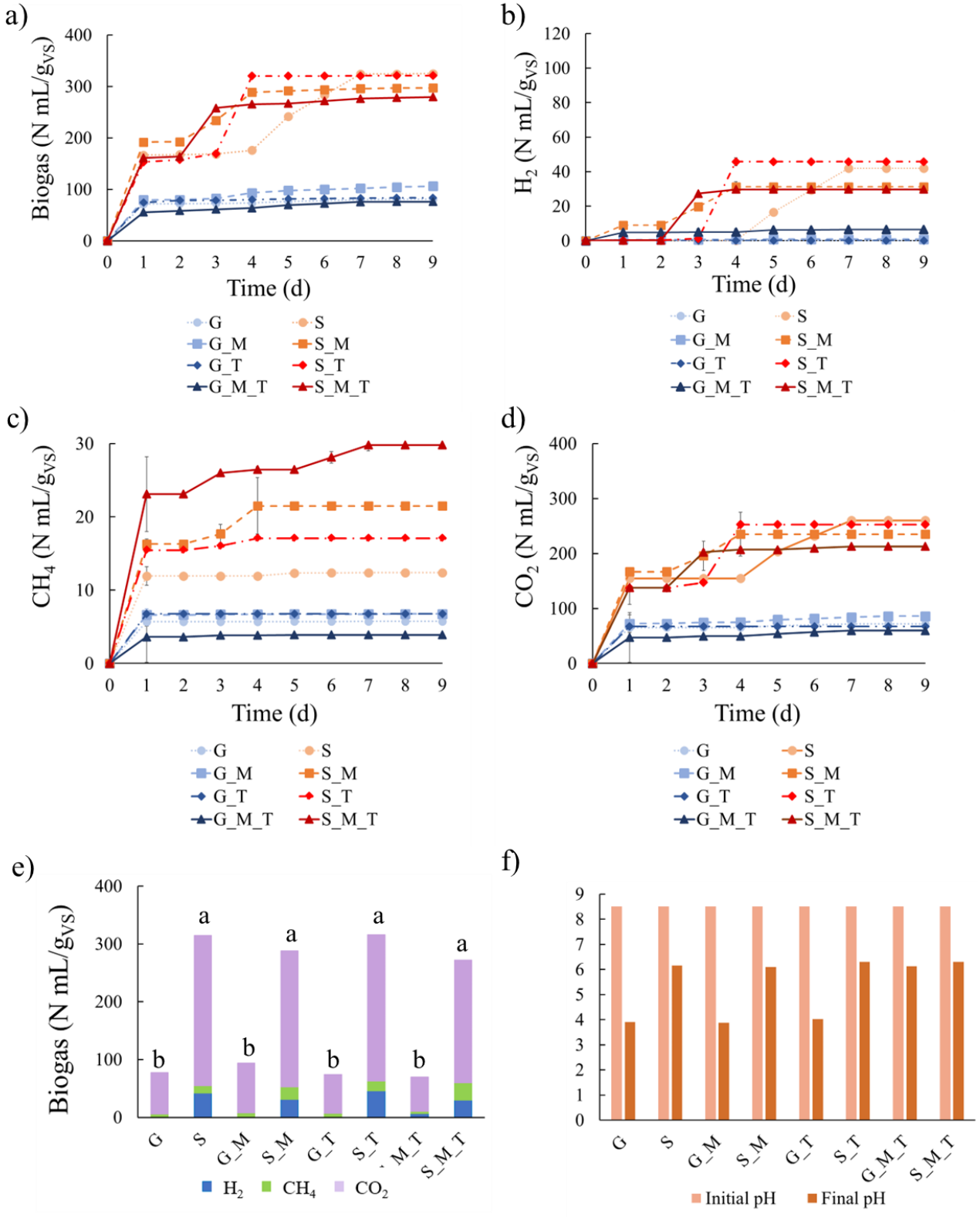

Figure 2.1 Results from the first experiment: a) biogas yield, b) H_2 yield, c) CH_4 yield, d) CO_2 yield, e) composition of total biogas produced during dark fermentation considering H_2, CH_4 and CO_2, f) pH value at day 0 and day 9.

2.3.3 Dark fermentation of fruit and vegetable wastes with jam wastewater

The second experimental campaign evaluated the technical feasibility of using alternative sugar sources for H_2 production through DF. To reduce reliance on commercial sugars, which could be cost-prohibitive at larger scales, sugar-rich biomass wastes were considered potential alternatives. JWW, generated during the cleaning of equipment in a blueberry jam production facility, could be an option. This wastewater contains a monosaccharide concentration of approximately 7.7 g/L. In this study, the performance of JWW as a sugar source for DF was compared to that of commercial sucrose. Both sugar sources were also used in the DF of real biomass waste, specifically FVW, to assess their biocompatibility and effectiveness in H_2 production.
The experiment was conducted considering eight configurations, with half utilizing sucrose as the sugar source (since it was considered the most suitable sugar source according to the main findings of paragraph 3.2) and the other half employing JWW. A detailed summary of them is provided in *Table 2.2*.

2.3.3.1 Effect of sugar source

Figure 2.2-a and *-b* illustrate biogas and H_2 production across the configurations over a 7-day period. In the reactors containing only sugar sources (SUCR_A, SUCR_B, JWW_A, and JWW_B), the trends in H_2 and biogas production differed noticeably. These configurations produced very low levels of H_2, with yields close to 0 mL/g_{VS}, indicating that the systems failed to initiate effective H_2 fermentation. In contrast, biogas production was relatively high, likely due to CO_2 released from carbon degradation and the presence of methane. No clear difference was observed regarding the use of sucrose or JWW as the sugar source. The low H_2 output may be attributed to the diluted concentration of sugars and the limited availability of nutrients essential for microbial activity and system startup.

On the other hand, when sugar sources were used together with FVW, H_2 production improved across all other configurations. The highest H_2 yields were achieved in JWW_FVW_A and JWW_FVW_B, reaching 67.1 N mL/g_{VS}. These values were higher than those obtained in SUCR_FVW_A and SUCR_FVW_B, which yielded 50 and 37.6 N mL/g_{VS}, respectively. These findings suggest that JWW helped increase H_2 production at both tested concentrations, likely due to its content of easily fermentable sugars. The presence of JWW also appeared to enhance the H_2 production rate. Most setups reached a stationary phase by day 4, which is consistent with commonly reported HRT for DF (de Menezes et al. 2024; Scotto di Perta et al. 2022). No significant differences ($p > 0.05$) were revealed in biogas production since it remained similar between the setups using sucrose and

those using JWW. This suggests that JWW can effectively replace commercial sugars sources in DF, as its performance is comparable to that of sucrose.

2.3.3.2 Biogas composition and discussion

Figure 2.2-e depicts the composition of biogas for all the configurations. H_2 only appears in the configurations with FVW and its maximum concentration in biogas reached 32 % for JWW_FVW_B, 30 % in JWW_FVW_A, 24 % in SUCR_FVW_A and 29 % in SUCR_FVW_B. In these configurations, CO_2 percentage in biogas resulted lower than previous experiment ranging between 48-76 % while CH_4 content was nearly negligible. However, CH_4 was present when only the sugar source was added to the reactors over 25 %. It is not clear why thermal pretreatment was less effective in some cases while it enhanced H_2-producing microbial activity in others. It is possible that when only the sugar source was present in the reactor, the carbohydrate supply was insufficient to support all microbial groups. This may have allowed the surviving methanogens, even though weakened by thermal pretreatment, to dominate and outcompete the H_2-producers.

The initial pH of all configurations (*Figure 2.2-f*) was adjusted to between 5.5 and 6, the optimal range for DF. Following the process, SUCR_A, SUCR_B, JWW_A, and JWW_B exhibited elevated final pH values between 7- 8, consistent with their low H_2 and likely low VFAs production. In contrast, the pH in SUCR_FVW_A, SUCR_FVW_B, JWW_FVW_A, and JWW_FVW_B remained relatively stable, ranging from 5 to 6. This stability aligns with higher H_2 yields observed in these reactors, likely supported by favorable pH conditions for microbial activity. The results of this study can be compared to those reported by (Martínez-Mendoza et al. 2022), who investigated H_2 production from FVW using 0.7 L reactors operated at 37 °C. Their experiment employed an inoculum that underwent thermal pretreatment at 90 °C for 20 min, resulting in a H_2 yield of 73.2 mL/g_{VS}. This slightly higher yield, relative to the present study, may be attributed to the more intense heat shock applied to the inoculum. Additionally, the use of pH control through the addition of 6 M NaOH to maintain a neutral pH of 7, may have contributed to improved system performance.

Even higher H_2 production was reported by (Magama and Chiyanzu 2021), who also fermented FVW in 0.4 L reactors at 35 °C. In their case, the inoculum was pretreated with H_2SO_4 to reach a pH of 4 and maintained under these conditions for 24 hours. This approach resulted in an H_2 yield of 140 N mL/g_{VS}, suggesting that acid pretreatment can be highly effective in enhancing microbial activity and H_2 output.

(Scotto di Perta et al. 2022) applied thermal pretreatment by heating the inoculum to 105 °C for several hours and carried out DF in 0.25 L reactors at 30–34 °C. This setup achieved a H_2 yield of 193 N mL/g_{VS}, further confirming the effectiveness of thermal pretreatment in optimizing H_2 production from FVW under mesophilic conditions. Overall, this experiment successfully demonstrated the capability of CAS inoculum in converting real waste materials into H_2-rich biogas through DF. However, despite the positive outcomes, both H_2 yield, and

concentration were not as high as some values reported in the literature, indicating the necessity for process optimization. Future improvements could focus on refining operational conditions, such as pretreatment strategies and pH regulation, to enhance microbial activity and overall process efficiency. Nonetheless, these results provide a promising foundation for considering the implementation of a TSAD system for FVW and JWW, which could further optimize biomass utilization and improve energy recovery.

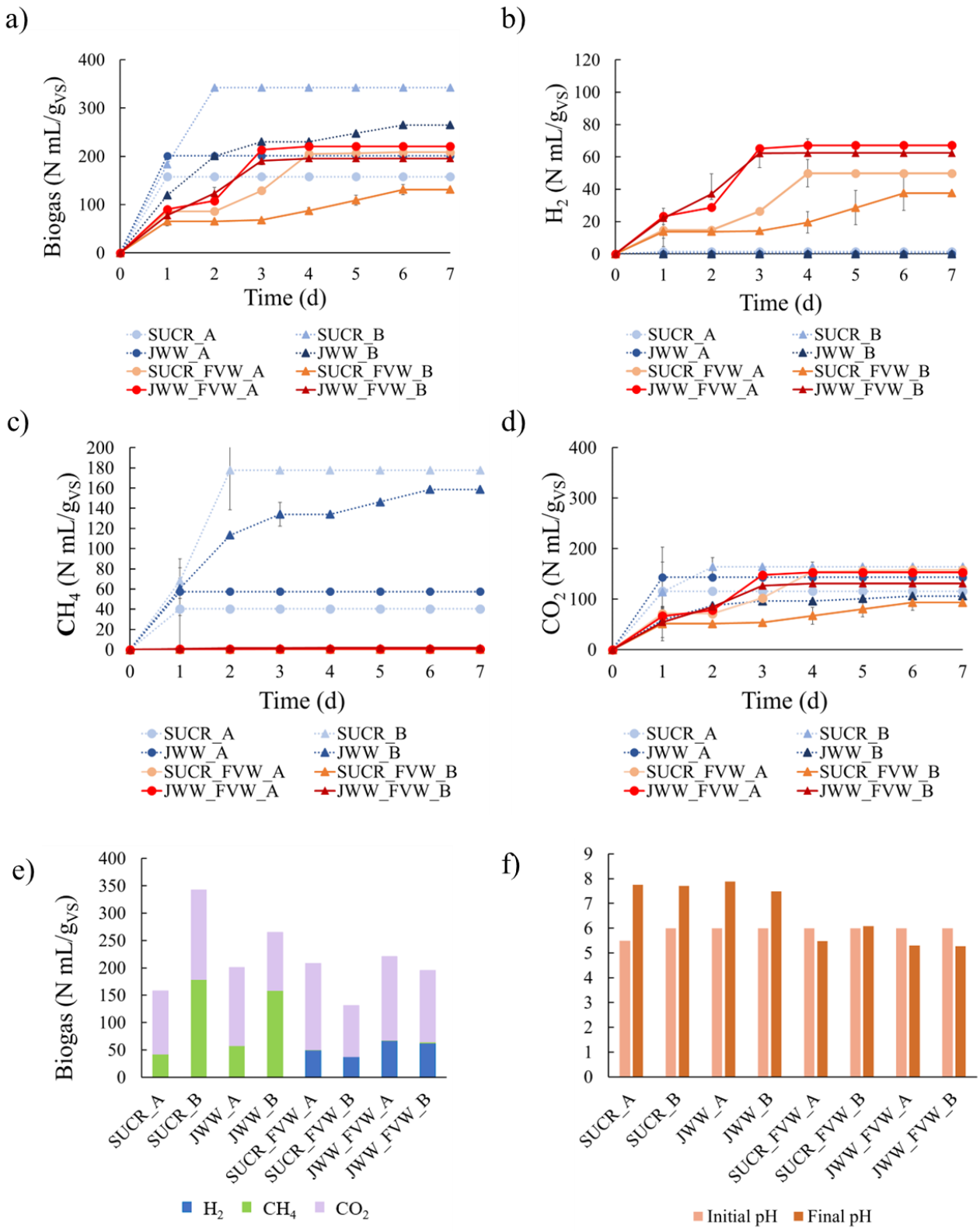

Figure 2.2 Results from the second experiment: a) biogas yield, b) H_2 yield, c) CH_4 yield, d) CO_2 yield, e) composition of total biogas produced during dark fermentation considering H_2, CH_4 and CO_2, f) pH value at day 0 and day 7.

2.3.4 Two-stage anaerobic digestion of fruit and vegetable waste and jam wastewater: dark fermentation

This experimental campaign evaluated the feasibility of integrating DF and AD in a sequential process, specifically applying a TSAD process to FVW and JWW. Four different configurations were tested in the first stage of TSAD, with variations in the S:I ratio and the application of thermal pretreatment to FVW. The ratio between FVW and JWW was 19:1 on VS basis, associated with the highest H_2 yield in the previous experiment as presented in paragraph 3.3.
In two configurations (JWW_FVW_1:1 and JWW_FVW_T_1:1), the S:I ratio was set to 1, while in the other two, it was increased to 2 (JWW_FVW_2:1 and JWW_FVW_T_2:1), based on VS. The S:I ratio is a critical parameter for maintaining a balanced system (Pan et al. 2008). An insufficient substrate supply can inhibit microbial activity and promote the development of alternative metabolic pathways that are not favorable for optimal energy recovery. Conversely, an excess substrate may lead to excessive sludge growth at the expense of valuable product formation (Cappai et al. 2018). Additionally, thermal pretreatment was applied to FVW at 60 °C for 30 min in two of the configurations (JWW_FVW_T_1:1 and JWW_FVW_T_2:1) to assess its effectiveness in enhancing microbial access to available carbon. Details of the configurations are provided in *Table 2.2*.

2.3.4.1 Effect of substrate-to-inoculum ratio

The effect of varying S:I can be evaluated through the biogas and H_2 yield presented in *Figure 2.3-a* and *-b*. Biogas production commenced from day 1 in all configurations; however, the trends varied significantly among them. The two configurations with an S:I ratio of 2 (JWW_FVW_2:1 and JWW_FVW_T_2:1), exhibited lower biogas production compared to other configurations, and they entered a stationary phase starting on day 1, which persisted throughout the DF period. In contrast, the configurations with an S:I ratio of 1 demonstrated substantially higher biogas yields. The highest production was observed in JWW_FVW_T_1:1, reaching a maximum of 261 mL/g_{VS}, whereas JWW_FVW_1:1 produced a maximum of 179 mL/g_{VS}.
While biogas was produced from day 1 in all cases, H_2 production followed a different pattern. In configurations with an S:I ratio of 2, H_2 production was negligible. JWW_FVW_1:1 presented a H_2 yield of 34.3 N mL/g_{VS}, and the process entered a stationary phase after just one day, preventing further substrate conversion in H_2. The highest H_2 yield recorded was 99.5 N mL/g_{VS} for JWW_FVW_T_1:1. The lower efficiency of DF in the high-S:I configurations could be attributed to excessive organic loading, which likely overwhelmed the microbial community and led to system inhibition, resulting in comparable outcomes in both cases. Conversely, the S:I ratio of 1 appeared to provide a more

manageable organic load, allowing microorganisms to efficiently perform DF and achieve higher biogas production.

2.3.4.2 Effect of substrate thermal pretreatment

The statistically significant difference in biogas and H_2 yield between thermally pretreated and untreated substrates can likely be explained by the effectiveness of thermal pretreatment in partially degrading the substrate, thereby increasing the availability of simple sugars for microbial metabolism. This trend was particularly evident in JWW_FVW_T_1:1, where the rate of production remained stable, further corroborating findings from the previous experiment, in which a distinct lag phase only became apparent from day 4 of DF. The highest H_2 yield recorded was 99.5 N mL/g_{VS} (JWW_FVW_T_1:1), which was also higher than the maximum yield observed in the previous experiment, highlighting the effectiveness of thermal pretreatment in improving substrate accessibility and enhancing conversion efficiency for H_2 production.

2.3.4.3 Biogas composition and discussion

The composition of the produced biogas is presented in *Figure 2.3-e*. The H_2 content was higher than the previous experiments (paragraph 3.3), reaching a maximum of 38% in JWW_FVW_T_1:1. The predominant gas was CO_2 in all the configuration with percentage between 61-99 % while CH_4 content was negligible suggesting the efficacy of the thermal pretreatment.

pH trends are presented in *Figure 2.3-f*. The initial pH across all configurations was approximately 7, but it decreased during the process in every case. In JWW_FVW_1:1 and JWW_FVW_T_1:1, the final pH ranged between 5.5 and 6.5 which is an optimal range for DF, and it is correlated with the highest H_2 yields observed. In contrast, JWW_FVW_2:1 and JWW_FVW_T_2:1 experienced a more visible pH drop, reaching values between 4.5 and 5, which likely contributed to the lower H_2 production in these setups.

Numerous studies have investigated the influence of the S:I ratio on H_2 production during DF. Pan et al. (2008) conducted food waste fermentation under mesophilic conditions in 1 L reactors and achieved a H_2 yield of 38.8 mL/g_{VS} at an S:I ratio of 6 (based on VS). Nathao et al. (2013) used a slightly higher ratio of 7.5 for the DF of food waste in 0.5 L reactors at 37 °C, resulting in a yield of 55 mL/g_{VS}. Ghimire et al. (2016), on the other hand, applied a low S:I ratio of 0.5 under thermophilic conditions and obtained 60.6 mL/g_{VS}. Their investigation also highlighted the role of initial pH, identifying 4.5 as optimal for DF which is a result that contrasts with our findings in Section 3.2, where pH values below 5 led to microbial inhibition. Cappai et al. (2018) reported the highest yield among the referenced studies, reaching 90 mL/g_{VS} using a 5 L reactor at 39 °C and an S:I ratio of 7.14, aligning with the conditions applied by Nathao et al. (2013). While several reports suggest that increasing the S:I ratio can enhance H_2 production, the present study observed a different trend, indicating that excessive substrate

loading may impair system performance. These findings emphasize the need for careful optimization of the S:I ratio to ensure efficient energy recovery.

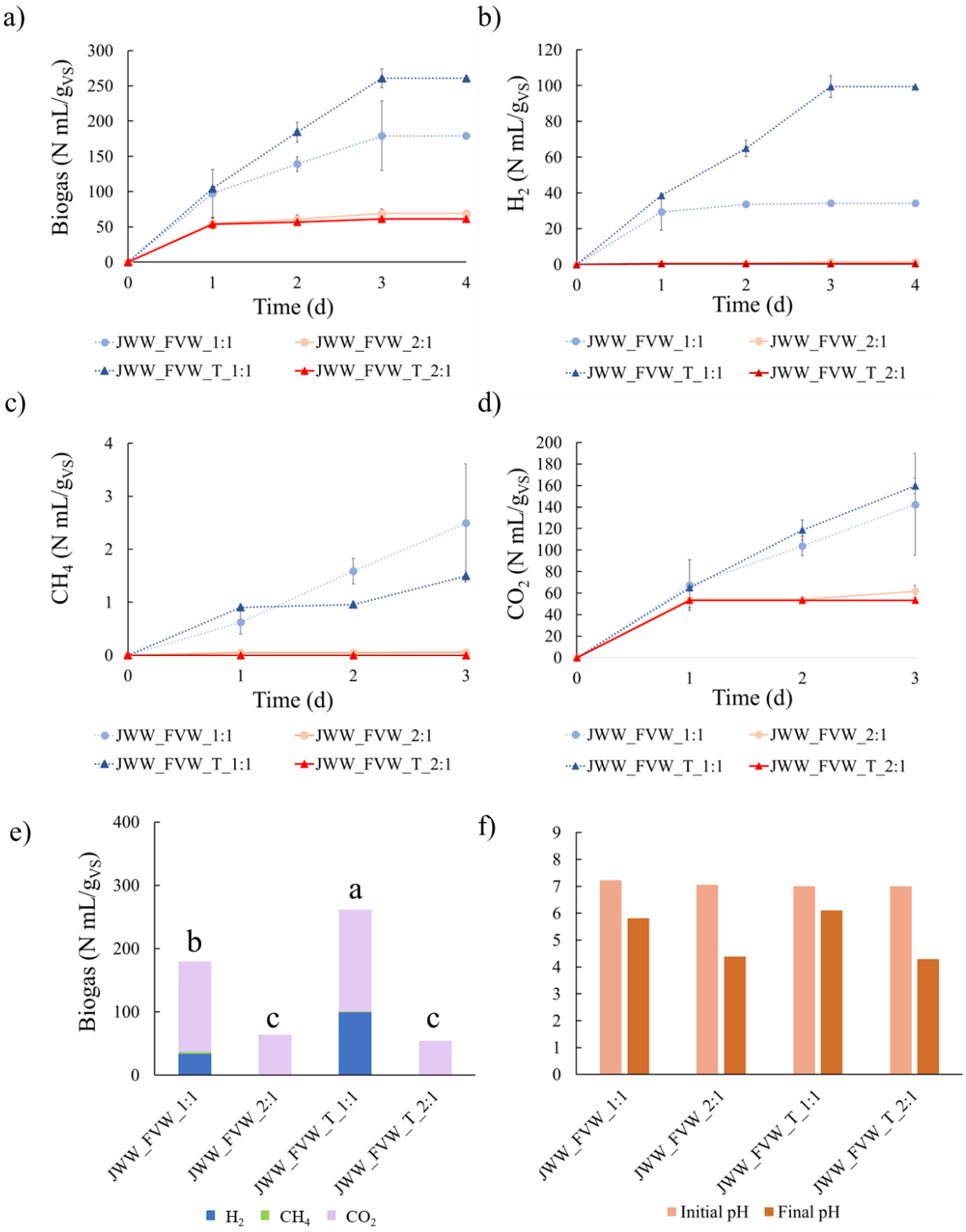

Figure 2.3 Results from the first stage of the third experiment: a) biogas yield, b) H_2 yield, c) CH_4 yield, d) CO_2 yield, e) composition of total biogas produced during dark fermentation considering H_2, CH_4 and CO_2, f) pH value at day 0 and day 3.

2.3.4.5 Volatile fatty acids analysis

The digestate from the first stage of DF was analyzed for VFAs, specifically acetic, propionic, and butyric acids, to assess the progression of the process. The results are presented in *Figure 2.4*. The distribution of VFAs was highly heterogeneous across the samples. Acetic acid was detected in all reactors (ranging from 1 to 2 g/L), while propionic acid appeared only in half of the cases. The configurations JWW_FVW_1:1 and JWW_FVW_T_1:1 exhibited similar VFAs profiles, with all three acids present in comparable concentrations. JWW_FVW_1:1 had the highest concentration of butyric acid (4.3 g/L), followed by JWW_FVW_T_1:1 (3.1 g/L), making butyric acid the most abundant acid in both cases. Acetic acid concentrations were 1.6 and 2.0 g/L, respectively, while propionic acid was present at 1.3 g/L in both configurations. The total VFAs concentrations were 7.2 g/L for JWW_FVW_1:1 and 6.4 g/L for JWW_FVW_T_1:1. These values exceed the peak of 5.7 g/L reported by Zuo et al. (2014) from the fermentation of vegetable waste but remain below the inhibitory threshold of 8 g/L, as indicated by Cremonez et al. (2021).

The presence of all three acids likely results from the availability of readily fermentable compounds in FVW, which are metabolized through acetyl-CoA and lactate pathways (Ungerfeld 2020). The predominance of acetic and butyric acids aligns with findings from Dinh and Fujiwara (2023), who reported a VFAs production of 370 mg_{VFAs}/g_{VS} from FVW fermentation which is comparable to the 367 and 326 mg_{VFAs}/g_{VS} observed in JWW_FVW_1:1 and JWW_FVW_T_1:1, respectively.

In contrast, the configurations JWW_FVW_2:1 and JWW_FVW_T_2:1 produced lower VFAs concentrations, with total contents of 2.0 and 0.9 g/L, respectively. While both acetic and butyric acids were detected in JWW_FVW_2:1 (1.2 and 0.7 g/L), only acetic acid was observed in JWW_FVW_T_2:1. The substantially higher VFAs production in the 1:1 S:I ratio configurations can be correlated with better system performance and higher H_2 yields. Conversely, the limited acid production in the 2:1 S:I configurations likely reflect system failure or suboptimal metabolic activity.

The results of this experiment confirm the viability of using a mixture of FVW as a substrate for DF and combining it with JWW as a sugar source. The utilization of a S:1 = 1 on VS basis and a thermal pretreatment of FVW can further enhance the yield of the process, supporting the potential implementation of a TSAD process to further exploit the energy potential of the remaining biomass.

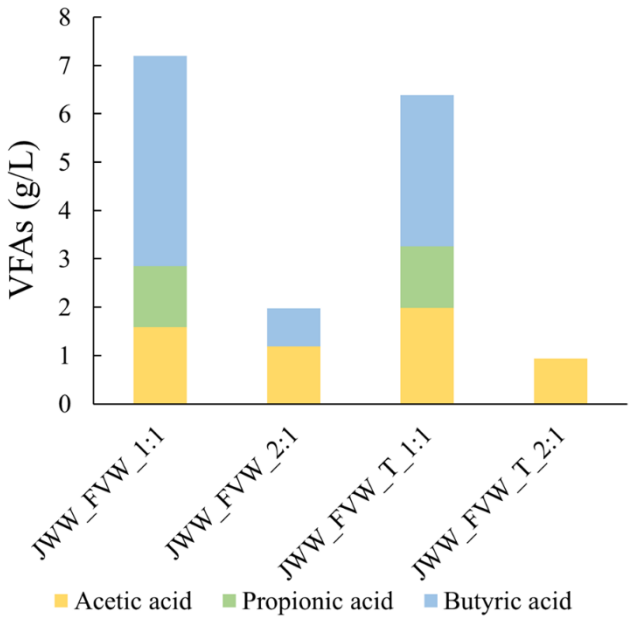

Figure 2.4 Volatile fatty acids (VFAs) content in g/L in the four configurations.

2.3.5 Two-stage anaerobic digestion of fruit and vegetable waste and jam wastewater: anaerobic digestion

The second stage of the process (AD) utilized the digestate from the DF stage as the primary substrate. This digestate was combined with non-pretreated CAS inoculum at a 1:1 ratio while maintaining a TS content of 6%.

2.3.5.1 Effect of substrate-to-inoculum ratio

The impact of the S:I ratio in the second stage can be evaluated through biogas and CH_4 production results over 22 days, presented in *Figure 2.5-a* and *-b*. All configurations exhibited biogas production even at different rates. JWW_FVW_1:1 and JWW_FVW_T_1:1 exhibited a slower initial biogas production, with negligible gas output during this period. However, between days 7 and 11, they began producing biogas at a higher rate than the other two configurations. In the final phase of the experiment, these two configurations experienced a gradual deceleration in biogas production, reaching a plateau around day 21, with a maximum biogas yield of 207 N mL/g_{VS}. CH_4 production remained relatively low across all four configurations during the first 5 days. JWW_FVW_1:1 and JWW_FVW_T_1:1 presented an increase in CH_4 production rate from day 6 to day 11. From day 12, the production rate decelerated, reaching a maximum CH_4 yield of 155 and 146 N mL/g_{VS}, respectively.
JWW_FVW_2:1 and JWW_FVW_T_2:1 exhibited a more rapid start-up phase within the first 6 days in biogas production compared to JWW_FVW_1:1 and JWW_FVW_T_1:1. Configurations with 2:1 ratio presented a continuous increase in biogas production, achieving maximum yields of 279 and 297 N mL/g_{VS}, respectively. These two configurations did not experience a distinct stationary

phase, instead maintaining a steady upward trajectory in biogas production throughout the entire experimental period.
Regarding CH_4 yield, JWW_FVW_2:1 and JWW_FVW_T_2:1 exhibited a delayed production phase during the first 7 days. From day 8, an increase in CH_4 production rate was detectable. After day 13, a slowdown in production was observed, while no distinct stationary phase throughout the 22-day period was visible. The highest CH_4 yield (184 N mL/g_{VS}) was achieved by both JWW_FVW_2:1 and JWW_FVW_T_2:1.

2.3.5.2 Effect of substrate thermal pretreatment

Thermal pretreatment of the substrate led to the highest overall biogas yield in the JWW_FVW_T_2:1 configuration. However, statistical analysis showed no significant differences in biogas production during the second stage of TSAD ($p > 0.05$). Although thermal treatment enhanced hydrogen production in the DF, its impact on biogas and CH_4 generation in the subsequent AD phase was limited, indicating that the effect of pretreatment may be specific to the first stage. Similarly, variations in S:I ratio did not significantly influence biogas output in the AD stage, as no statistical differences were observed among the tested configurations.

2.3.5.3 Biogas composition and discussion

Figure 2.5-e shows the biogas composition of all configurations. The main component in all cases is CH_4 which reaches 81 % in JWW_FVW_1:1, 65 % in JWW_FVW_T_2:1, 73 % in JWW_FVW_T_1:1 and 61 % in JWW_FVW_T_2:1. CO_2 levels were lower with percentage ranging between 19 and 37 %. Interestingly, even if JWW_FVW_1:1 and JWW_FVW_T_1:1 presented a lower CH_4 yield, the relative CH_4 percentages were higher compared to JWW_FVW_2:1 and JWW_FVW_T_2:1.

The pH trends of the four configurations are shown in *Figure 2.5-f*. Both initial and final pH values ranged between 7 and 8, which is considered optimal for AD. These results suggest that pH was not a limiting factor for the suboptimal CH_4 yields observed.

The performance of the TSAD system in this study can be compared with previous research. Dinh and Fujiwara (2023) investigated TSAD of FVW using sequential acidogenic and methanogenic reactors. The first stage operated at 35 °C, while the second was tested under both mesophilic and thermophilic conditions, obtaining a CH_4 yield of 306 mL/g_{VS} and 346 mL/g_{VS}, respectively. These higher values, compared to those reported in the present study, may be attributed to the feeding strategy: only the liquid fraction of the digestate, rich in VFAs, was used in the methanogenic reactor, whereas the full digestate was fed in this work.

Similarly, Dinh et al. (2019) applied TSAD to vegetable waste using a CSTR for DF and an upflow anaerobic sludge blanket (UASB) reactor for methanogenesis at 36 °C. Although little to no H_2 was detected during the first stage (with biogas primarily composed of CO_2), the second stage produced 274 mL/g_{VS} of CH_4. Wu et al. (2016) also reported comparable outcomes, applying TSAD to FVW using a 1.2 L CSTR for DF and a mesophilic 1 L UASB reactor for AD. In this case, H_2 production was again negligible in the first stage, while CH_4 yield reached 244 mL/g_{VS}.

Zuo et al. (2014) conducted TSAD using a 3 L CSTR for DF and a 4 L fixed-bed biofilm reactor for methanogenesis, both under mesophilic conditions. Although no H_2 data was provided, the CH_4 yield was approximately 300 mL/g_{VS}.

The results obtained in this study fall between those previously reported and those achieved by Nathao et al. (2013), who applied TSAD to food waste. H_2 production reached 55 mL/g_{VS}, and CH_4 yield was 94.8 mL/g_{VS}, obtained from batch reactors operating at 37 °C. The lower CH_4 production compared to this study could be due to the composition of the substrate, which likely contained a broader range of organic matter, including proteins and fats in addition to carbohydrates. Gómez Camacho et al. (2019) also investigated TSAD using organic market waste. DF and AD were conducted in 2 L and 14 L bioreactors, respectively, both at 35 °C. The H_2 yield was 50 mL/g_{VS}, while CH_4 production reached 179 mL/g_{VS}. Although H_2 yields were slightly lower than those reported in the present study, the CH_4 aligns with the results of this study.

These findings emphasize that the effects of thermal pretreatment and the substrate-to-inoculum ratio are stage-specific within TSAD process. Although the CH_4 yield was satisfactory, it remains lower than that reported in similar studies, indicating that process optimization may be necessary.

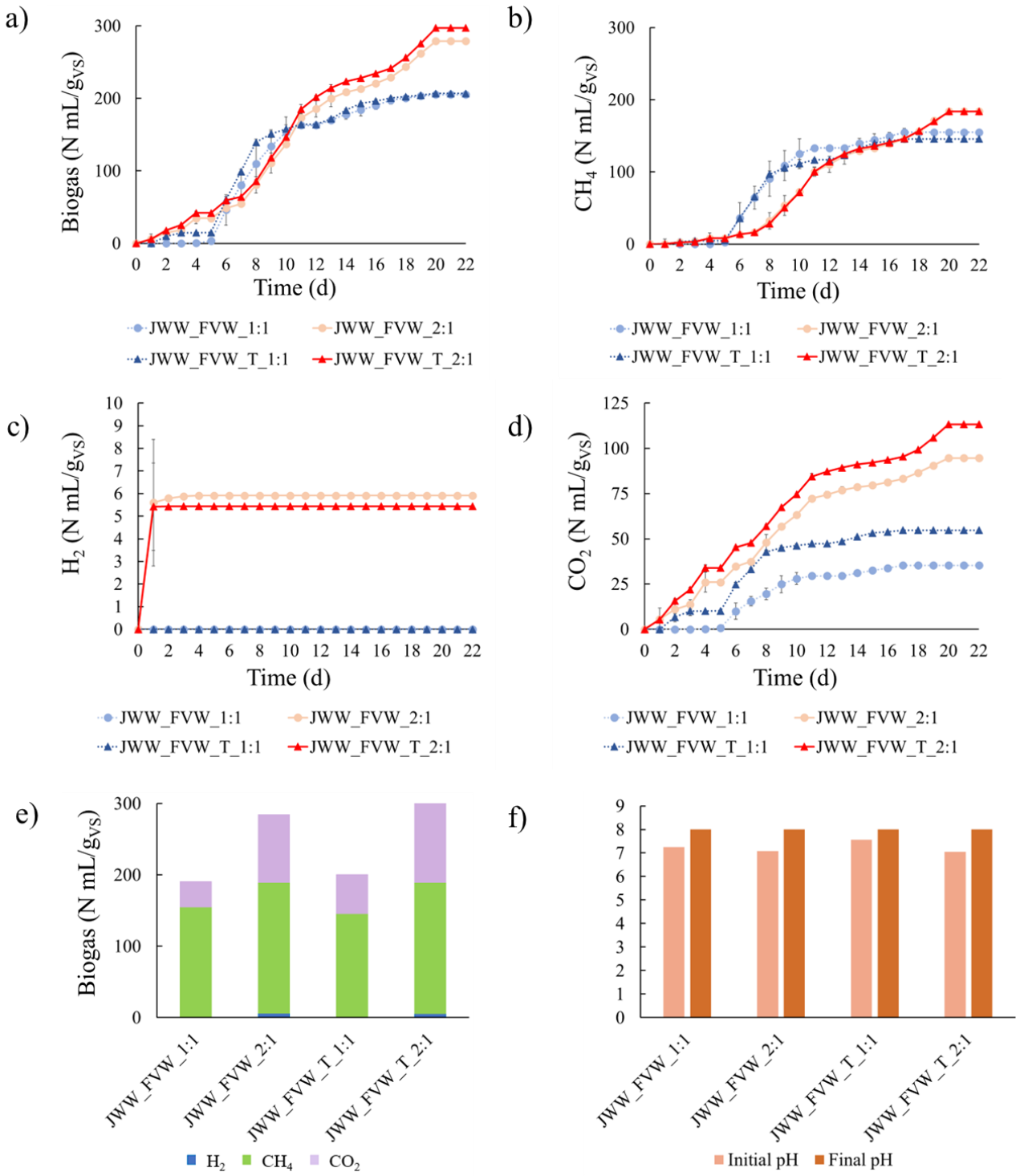

Figure 2.5 Results from the second stage of the third experiment: a) biogas yield, b) CH_4 yield, c) H_2 yield, d) CO_2 yield, e) composition of total biogas produced during AD considering H_2, CH_4 and CO_2, f) pH value at day 0 and day 22.

2.3.6 Comparison between single and two-stage anaerobic digestion of fruit and vegetable waste

As previously mentioned in paragraphs 3.4 and 3.5, the implementation of TSAD rather than single stage AD, is expected to enhance CH_4 production. To evaluate this hypothesis within the scope of this study, AD was applied to the configurations JWW_FVW_2:1 and JWW_FVW_T_1:1, following the criteria stated in paragraph 2.3.

Biogas and CH_4 yields are presented in *Figure 2.6-a* and *-b*. Among all configurations, AD of JWW_FVW_T_1:1 yielded the highest biogas output at 416 N mL/g_{VS}, significantly outperforming the others, which ranged between 206 and 279 N mL/g_{VS}. However, the trend for CH_4 production was visibly different. The highest CH_4 yield (183 N mL/g_{VS}) was achieved by TSAD JWW_FVW_2:1, which was substantially higher than the corresponding AD configuration, which produced only 7.5 N mL/g_{VS}. This highlights the positive impact of the DF stage in enhancing the overall digestion performance, likely due to the initial hydrolysis and breakdown of complex organic matter. In contrast, applying AD directly to JWW_FVW_2:1 is suboptimal, possibly due to an excessive organic load that exceeded the inoculum metabolic capacity. Both TSAD and AD applied to JWW_FVW_T_1:1 resulted in similar CH_4 yields of approximately 146 N mL/g_{VS}.

Variations in specific methane production rates can be observed and assessed based on the slope of the cumulative yield curves. TSAD configurations showed a clear onset of CH_4 production around days 6 and 8, respectively. Conversely, AD JWW_FVW_2:1 showed an almost flat production curve, while AD JWW_FVW_T_1:1 exhibited a delayed but sharp increase starting at day 14, which was nearly double the stationary phase compared to its TSAD counterpart. These findings indicate that TSAD not only enhances CH_4 yield but also accelerates the production rate, enabling faster reaching of peak yields which is an advantage of considerable relevance for industrial-scale applications where time efficiency is critical. Previous studies also supported the benefits of TSAD for improving CH_4 recovery. Nathao et al. (2013) compared TSAD and AD of food waste in batch reactors at 37 °C and reported an 18% increase in energy recovery with TSAD. Similarly, Liu et al. (2006) evaluated TSAD and AD of household solid waste under mesophilic conditions and observed a 21% increase in CH_4 yield from the TSAD process. These studies further reinforce the advantages of TSAD for maximizing energy recovery from biomass waste.

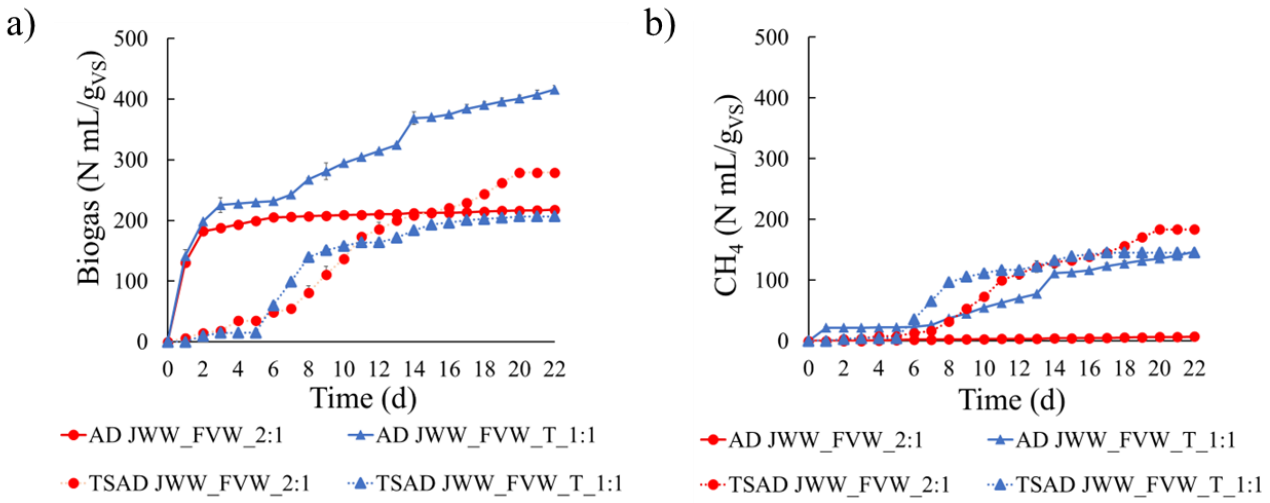

Figure 2.6 a) Biogas yield between the application of TSAD or AD to JWW_FVW_2:1 and JWW_FVW_T_1:1, b) CH_4 yield between the application of TSAD or AD to JWW_FVW_2:1 and JWW_FVW_T_1:1.

2.3.7 Influence of organic loading rate in the dark fermentation of fruit and vegetable waste and jam wastewater

As previously discussed in Sections 3.4 and 3.5, the effect of OLR was investigated by carrying out DF of FVW and JWW at three different loading conditions. The selected OLR values fell within the commonly recommended range for anaerobic digestion (1.2-12 kg_{VS}/m^3 d) and were approximately doubled from one experimental run to the next. The substrate ratio and the substrate-to-inoculum (S:I) ratio were maintained according to the best-performing configuration identified in the earlier phase of the study, namely JWW_FVW_1:1. Biogas and hydrogen production trends are reported in *Figure 2.7-a* and *-b*. In all configurations, biogas generation began immediately on day 1. The reactors operated at OLR equal to 1.8 and 7.9 kg_{VS}/m^3 d exhibited similar production patterns, whereas OLR 3.6 showed a substantially reduced biogas output, reaching a plateau as early as day 2. Among the three conditions, OLR 7.9 achieved the highest biogas yield, with a maximum of 132 N mL/g_{VS}, followed by OLR 1.8 with 116 N mL/g_{VS}. Hydrogen production, however, displayed a markedly different behavior: the highest H_2 yield was observed in OLR 1.8, reaching 44.4 N mL/g_{VS}, while OLR 7.9 produced 40.9 N mL/g_{VS}. Consistent with its lower biogas output, OLR 3.6 also resulted in the lowest H_2 yield, reaching only 14.7 N mL/g_{VS}. All systems reached a production plateau by day 2, which is typical for DF processes.

Regarding methane (*Figure 2.7-c*), only OLR 1.8 generated an appreciable amount, attaining a maximum of 11 N mL/g_{VS}, whereas CH_4 production in OLR 3.6 and OLR 7.9 was negligible. CO_2 (*Figure 2.7-d*) followed a trend similar to that of biogas, with the highest yield recorded in OLR 7.9 (91 N mL/g_{VS}), followed by OLR 1.8 (47 N mL/g_{VS}) and OLR 3.6 (34 N mL/g_{VS}).

The relative abundances of the gas components, also illustrated in *Figure 2.7-e*, show that CO_2 was the predominant constituent under all tested conditions, reaching 46 % at OLR 1.8 and approximately 69 % at OLR 3.6 and OLR 7.9. Hydrogen displayed an opposite behavior, achieving its highest proportion at OLR 1.8 (44 %), while decreasing to 30 % and 31 % for OLR 3.6 and OLR 7.9, respectively. As noted earlier, CH_4 was detectable only at OLR 1.8, where it accounted for about 10 % of the biogas

The digestate was analyzed for VFAs, with particular attention to acetic, propionic, and butyric acids, in order to monitor process evolution and metabolic pathways. The results are reported in *Figure 2.7-f*. Overall, a similar VFAs distribution was observed for all three configurations, with acetic acid representing the dominant fraction, followed by butyric acid, whereas propionic acid was detected only in negligible amounts throughout the experiment.

The highest total VFAs concentration was measured under OLR 7.9, reaching a maximum value of approximately 9 g/L, followed by OLR 3.6 with 5 g/L and OLR 1.8 with around 3.5 g/L. As previously discussed, VFAs concentrations above 8 g/L are generally considered inhibitory for AD processes; therefore, the elevated acid levels observed at OLR 7.9 suggest a greater tolerance of acidogenic and acetogenic populations to high VFAs concentrations. Nevertheless, biogas production ceased after day 3, likely due to VFAs accumulation.

In terms of individual acid composition, acetic acid accounted for the largest share of total VFAs, with relative abundances of 70.5 %, 68.1 %, and 65.6 % for OLR 1.8, OLR 3.6, and OLR 7.9, respectively. Propionic acid remained below 1.6 % in all configurations, indicating limited formation of this intermediate, while butyric acid represented between 27.9 % and 34.2 % of the total VFAs content.

The effect of OLR on dark fermentation has been widely explored in the literature. Krishnan et al. (2016) investigated this parameter during thermophilic TSAD of palm oil mill effluent (POME). In their study, the DF inoculum was heat-treated at 90 °C for 60 minutes and mixed with the substrate in a 4 L UASB reactor operated at 55 °C. OLR was varied from 25 to 125 kg_{COD}/m^3 d, corresponding to a reduction in HRT from 12 to 3 h. H_2 yield increased steadily with OLR up to 75 kg_{COD}/m^3 d, reaching a maximum of 49 mL/g_{COD}, but subsequently declined when OLR was reduced to 30 kg_{COD}/m^3 d, reaching 150 mL/g_{COD} even though the lowest value was obtained at 25 kg_{COD}/m^3 d. Conversely, VFAs concentrations rose continuously with increasing OLR, reaching 8.8 g/L at the highest loading. The authors concluded that OLR strongly affected system performance: excessively low OLR led to insufficient substrate availability and, consequently, reduced H_2 production, whereas excessively high OLR resulted in VFAs accumulation and potential process inhibition. A similar trend was observed by Martins et al. (2022), who examined the influence of OLR during thermophilic TSAD of the organic fraction of municipal solid waste (OFMSW). DF was conducted in a 2.1 L CSTR under mesophilic conditions at three OLR values: 10.6, 18.0, and 23.6 g_{VS}/L d, yielding 8.5, 18.2, and 1.64 L/kg_{VS} of H_2, respectively. As in the previous study, VFAs levels increased with OLR, reaching 10.8 g/L at the highest loading. These results again confirmed that

moderate OLR values help maintain system stability by preventing excessive VFAs accumulation and avoiding overloading while still ensuring adequate substrate availability.

The role of OLR was also addressed by Paudel et al. (2017), who studied DF of food waste and brown water in a 10 L reactor at 35 °C. In their work, OLR was progressively increased from 17.7 to 34.8, 70.8, and 106 g_{VS}/L d while HRT was reduced from 48 to 8 h. H_2 production increased correspondingly, rising from 68.5 to a maximum of 99.8 mL/g_{VS}. These findings further support the notion that appropriate substrate loading is essential to ensure efficient fermentation performance. It is worth noting that the OLR values used in this experiment were far above the typical range recommended in the literature, and significantly higher than those applied in the present study, yet H_2 yields were comparable. This outcome may be attributed to the characteristics of the substrates used, particularly brown water, which contains substantial nitrogen levels that may help mitigate inhibition caused by VFAs accumulation or overfeeding.

The fermentation of high-strength wastewater was also investigated using a configuration different from the conventional CSTR, namely the Upflow Anaerobic Sludge Blanket (UASB) reactor. In this configuration, the substrate enters from the bottom of the reactor and passes through a granular sludge bed, where microorganisms are retained and attached to the granules. This configuration requires lower energy consumption and is effective for the treatment of high COD loads. Organic matter is converted into biogas through a stable and efficient process, which is also suitable for diluted waste streams (Mainardis et al. 2020). For instance, municipal solid waste leachate has been successfully treated in a 4.2 L UASB operated at 35 °C. The system was run at OLR ranging from 1.6 to 7.43 g COD/L d, with HRT between 1.3 and 3 days. Under these conditions, COD removal efficiencies reached 97.5-99.5 %, demonstrating very high treatment performance. These results highlight the strong potential of UASB reactors for efficiently treating complex wastewater with high organic loads, particularly when stable granular sludge is maintained and operating conditions are properly controlled (J. Li et al. 2020). However, this configuration was not considered in this thesis due to technical limitations related to the laboratory equipment available for the experiments. In particular, the required setup and operational conditions could not be properly reproduced at the lab scale, which prevented its implementation within the scope of this work.

Taken together, the studies reviewed illustrate that OLR has a decisive influence on biological H_2 production. In DF maintaining an appropriate OLR is essential to avoid both insufficient substrate supply, which limits microbial activity, and excessive loading, which leads to VFAs accumulation and inhibition. In this work, the OLR range tested was relatively narrow compared to previous studies, which may explain the limited differences observed among configurations. From a sustainability perspective, higher OLRs are generally preferable, as they enable greater waste treatment capacity and increased renewable energy production, improving both process efficiency and economic feasibility.

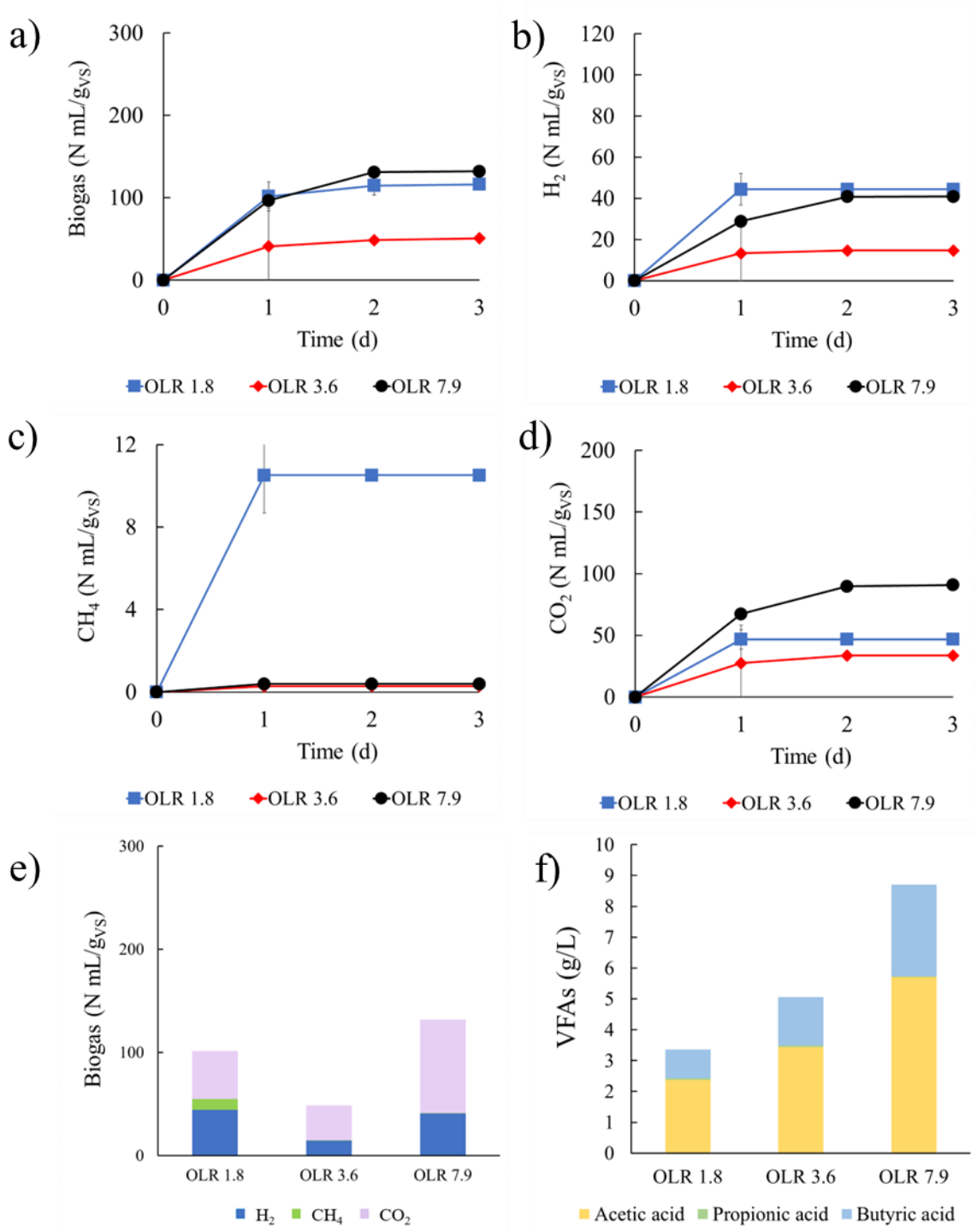

Figure 2.7 Results from the OLR investigation: a) biogas yield, b) H_2 yield, c) CH_4 yield, d) CO_2 yield, e) composition of total biogas produced during dark fermentation considering H_2, CH_4 and CO_2, f) VFAs concentration in the three configurations as g/L.

2.3.8 TSAD scale-up of fruit and vegetable waste and jam wastewater

All the experiments discussed in the previous sections were conducted using 250 mL reactors, a typical small-scale laboratory volume. However, scaling up AD processes often leads to a reduction in overall performance, as larger systems may experience additional operational constraints such as reduced mixing efficiency, temperature gradients, or mass-transfer limitations. For this reason, the present experiment aimed to evaluate the performance of TSAD of FVW and JWW in a 5 L digester operated under the same conditions applied to the 250 mL tests. The selected configuration was JWW_FVW_2:1, previously identified in paragraph 2.3.6 as the only ratio that remained functional when the working volume was increased. Both DF and AD were carried out to compare H_2 and CH_4 production at the two scales.

Biogas production profiles are shown in *Figure 2.8-a*. In both reactor sizes, biogas generation started on the first day; however, substantial differences emerged as the process advanced. The 250 mL configuration produced more than double the biogas obtained from the 5 L digester, reaching 69 N mL/g_{VS} compared to 33.7 N mL/g_{VS}. Interestingly, an opposite trend was observed for hydrogen production (*Figure 2.8-b*): although the 250 mL reactor exhibited a faster start-up phase, the 5 L digester eventually exceeded its performance, achieving a maximum H_2 yield of 4.5 N mL/g_{VS} versus only 1.6 N mL/g_{VS} in the smaller system. Nevertheless, this H_2 yield remains significantly lower than typical values reported in the literature for DF of FVW, suggesting that the overfeeding-related inhibition observed in the 250 mL experiments was likely still present in the 5 L system. As expected for DF, CH_4 production was negligible in both reactors (*Figure 2.8-c*). Consistent with biogas trends, CO_2 production was also higher in the 250 mL configuration *(Figure 2.8-d)*.

A similar pattern emerged during the second stage of TSAD (*Figure 2.9*). For biogas, H_2, CH_4 and CO_2, the 250 mL reactors again outperformed the 5 L system. Total biogas production reached 279 N mL/g_{VS} in the small reactors, compared with 201 N mL/g_{VS} in the 5 L digester. CH_4 yield followed the same tendency, with 183 N mL/g_{VS} and 132 N mL/g_{VS} for the 250 mL and 5 L reactors, respectively. H_2 production remained negligible in both cases, while CO_2 evolution mirrored biogas dynamics. It is also worth noting that the 250 mL systems exhibited faster kinetics, as indicated by higher slope of the curves and by the earlier achievement of maximum yields, approximately on day 20.

The presence of a scale effect in anaerobic digestion has also been highlighted by other authors. For instance, Ruffino et al. (2015) investigated the AD of vegetable and oil waste using both 6 L laboratory-scale digesters and a 300 L pilot-scale reactor operated under mesophilic conditions. Under comparable VS loads, the pilot-scale system achieved only 80% of the biogas yield obtained at the laboratory scale, clearly confirming a scale-dependent reduction in performance. Conversely, Kowalczyk et al. (2011), who studied the AD of a mixture of corn-cob mix (CCM) and cow manure (CM), observed slightly improved performance

in a 390 L digester compared with a 22 L one, despite operating both systems at 38 °C under identical conditions. Although the differences were modest, the authors concluded that scale-up is feasible, while emphasizing the necessity of further validation at industrial scale.

As these studies illustrate, the literature does not provide a universal consensus regarding the magnitude or even the direction of scale effects in anaerobic digestion. The results of the present work suggest a clear decline in performance when reactor volume was increased from 0.25 L to 5 L. In the specific context of this study, this decrease may be attributed to difficulties in maintaining uniform temperature distribution throughout the larger digester and, more critically, to inadequate mixing. Since no mechanical system was available, the reactors used here relied solely on manual shaking, which is less effective at larger volumes and may have contributed to mass-transfer limitations and localized inhibition. Since scale effects play a fundamental role in the design of full-scale AD plants, appropriate correction factors should be applied with care, as recommended by Demichelis et al. (2024).

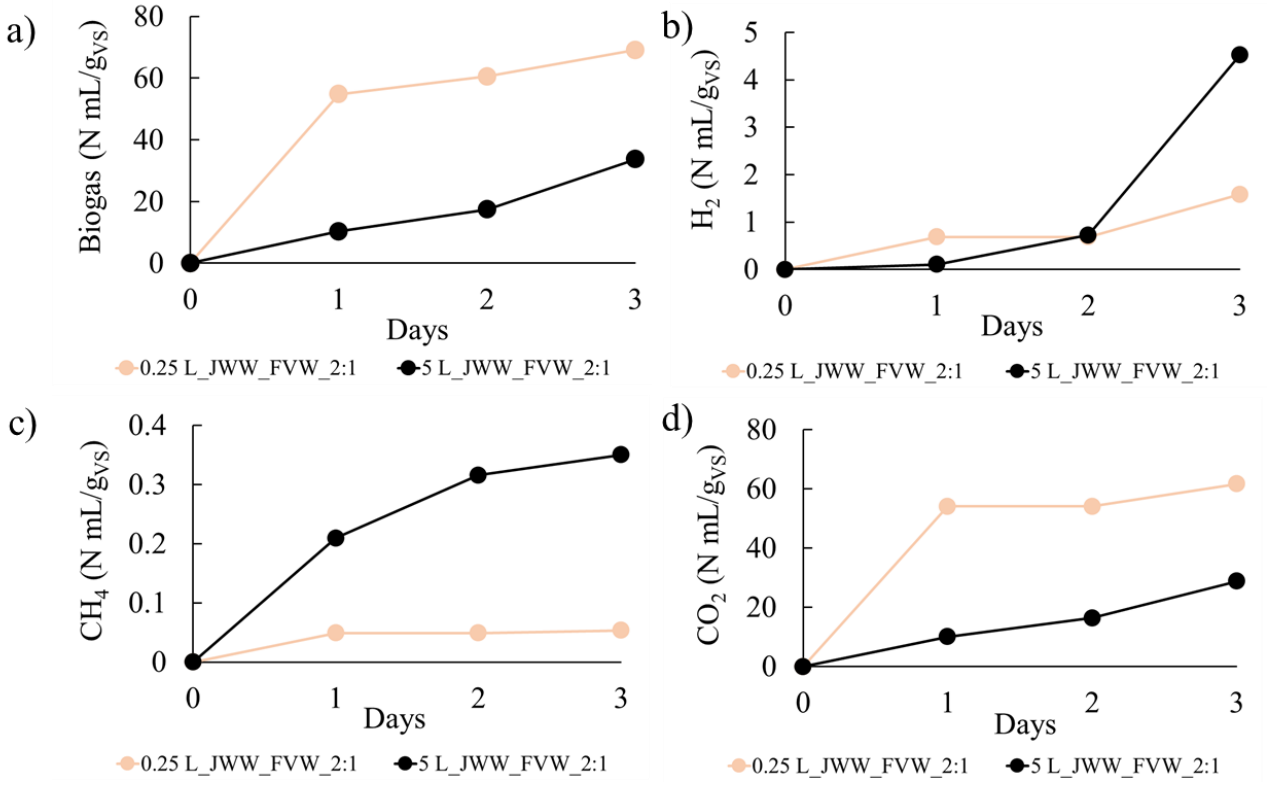

Figure 2.8 Results from the first stage of the scale up investigation: a) biogas yield, b) H_2 yield, c) CH_4 yield and d) CO_2 yield.

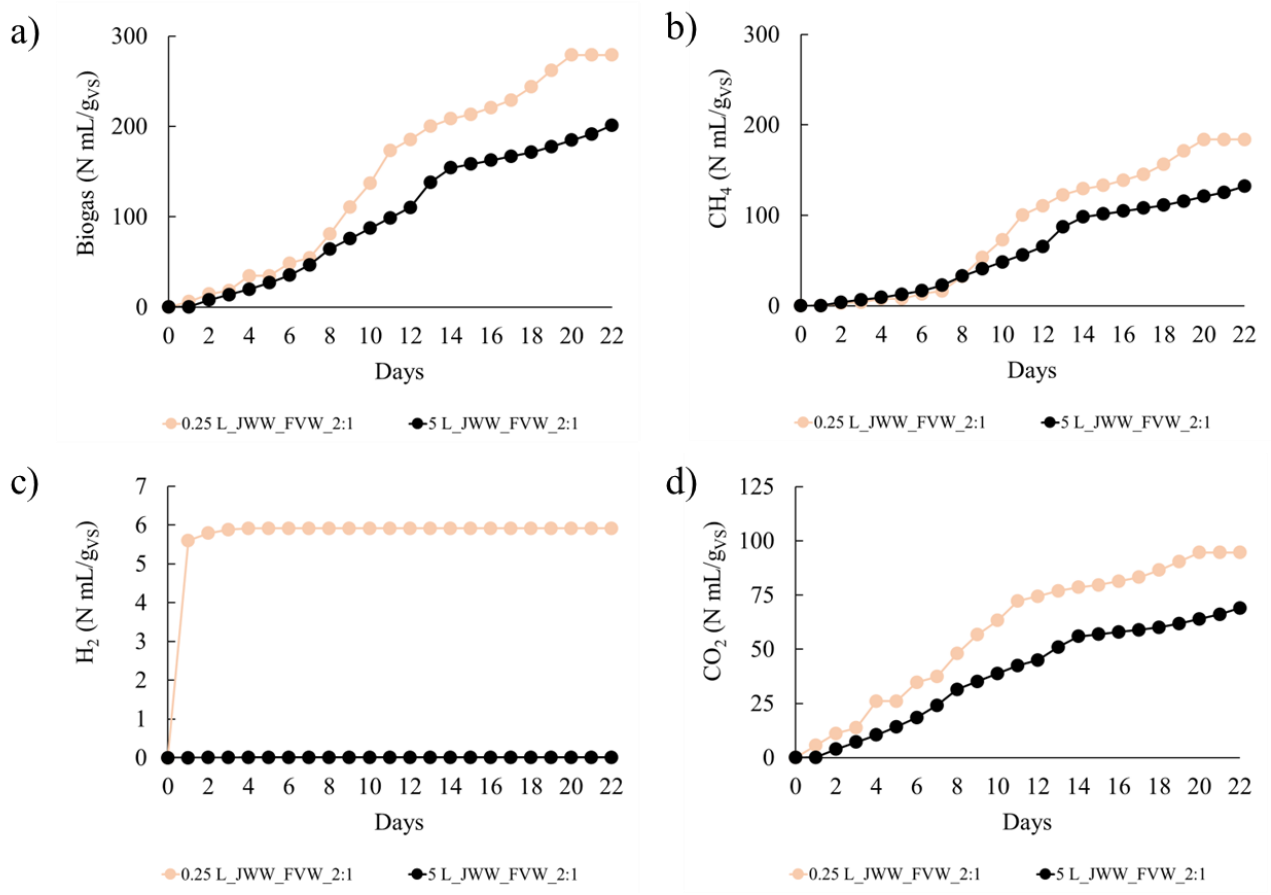

Figure 2.9 Results from the second stage of the scale up investigation: a) biogas yield, b)CH_4 yield, c) H_2 yield and d) CO_2 yield.

References

Agrawal, Akanksha, Parmesh Kumar Chaudhari, and Prabir Ghosh. 2023. "Anaerobic Digestion of Fruit and Vegetable Waste: A Critical Review of Associated Challenges." *Environmental Science and Pollution Research* 30 (10): 24987–5012. https://doi.org/10.1007/s11356-022-21643-7.

Al-Haddad, Saleh, Cynthia Kusin Okoro-Shekwaga, Louise Fletcher, Andrew Ross, and Miller Alonso Camargo-Valero. 2023. "Assessing Different Inoculum Treatments for Improved Production of Hydrogen through Dark Fermentation." *Energies* 16 (3). https://doi.org/10.3390/en16031233.

Brown, Kayleigh, Avik J. Ghoshdastidar, Jillian Hanmore, James Frazee, and Anthony Z. Tong. 2013. "Membrane Bioreactor Technology: A Novel Approach to the Treatment of Compost Leachate." *Waste Management* 33 (11): 2188–94. https://doi.org/10.1016/j.wasman.2013.04.006.

Bundhoo, M. A. Zumar, Romeela Mohee, and M. Ali Hassan. 2015. "Effects of Pre-Treatment Technologies on Dark Fermentative Biohydrogen Production: A Review." *Journal of Environmental Management* 157 (July): 20–48. https://doi.org/10.1016/j.jenvman.2015.04.006.

Chen, Yang, Yanan Yin, and Jianlong Wang. 2021. "Recent Advance in Inhibition of Dark Fermentative Hydrogen Production." *International Journal of Hydrogen Energy* 46 (7): 5053–73. https://doi.org/10.1016/j.ijhydene.2020.11.096.

De Laurentiis, Valeria, Sara Corrado, and Serenella Sala. 2018. "Quantifying Household Waste of Fresh Fruit and Vegetables in the EU." *Waste Management* 77 (July): 238–51. https://doi.org/10.1016/j.wasman.2018.04.001.

Demichelis, Francesca, Robotti Elisa, Deorsola Fabio Alessandro, Marengo Emilio, Tommasi Tonia, and Fino Debora. 2024. "Modelling of Technical, Environmental, and Economic Evaluations of the Effect of the Organic Loading Rate in Semi-Continuous Anaerobic Digestion of Pre-Treated Organic Fraction Municipal Solid Waste." *Environmental Pollution* 344 (March): 123417. https://doi.org/10.1016/j.envpol.2024.123417.

Esparza, Irene, Nerea Jiménez-Moreno, Fernando Bimbela, Carmen Ancín-Azpilicueta, and Luis M. Gandía. 2020. "Fruit and Vegetable Waste Management: Conventional and Emerging Approaches." *Journal of Environmental Management* 265 (July). https://doi.org/10.1016/j.jenvman.2020.110510.

European Commission. 2015. "Transforming Our World: The 2030 Agenda for Sustainable Development." https://sdgs.un.org/2030agenda.

Eurostat. 2022. "Food Waste and Food Waste Prevention - Estimates." https://ec.europa.eu/eurostat/.

Fang, Herbert H. P., Hong Liu, and Tong Zhang. 2002. "Characterization of a Hydrogen-Producing Granular Sludge." *Biotechnology and Bioengineering* 78 (1): 44–52. https://doi.org/10.1002/bit.10174.

García-Rández, Ana, Luciano Orden, Evan A. N. Marks, et al. 2025. "Monitoring of Greenhouse Gas Emissions and Compost Quality during Olive Mill Waste Co-Composting at Industrial Scale: The Effect of N and C Sources." *Waste Management* 193 (October 2024): 33–43. https://doi.org/10.1016/j.wasman.2024.11.039.

Hidalgo, Dolores, Enrique Pérez-Zapatero, and Jesús M. Martín-Marroquín. 2023. "Comparative Effect of Acid and Heat Inoculum Pretreatment on Dark Fermentative Biohydrogen Production." *Environmental Research* 239 (December). https://doi.org/10.1016/j.envres.2023.117433.

Kowalczyk, Alexandra, Sebastian Schwede, Mandy Gerber, and Roland Span. 2011. "Scale Up of Laboratory Scale to Industrial Scale Biogas Plants." November 3, 48–55. https://doi.org/10.3384/ecp1105748.

Krishnan, Santhana, Lakhveer Singh, Mimi Sakinah, Sveta Thakur, Zularisam A. Wahid, and Johan Sohaili. 2016. "Effect of Organic Loading Rate on Hydrogen (H2) and Methane (CH4) Production in Two-Stage Fermentation under Thermophilic Conditions Using Palm Oil Mill

Effluent (POME)." *Energy for Sustainable Development* 34 (October): 130–38. https://doi.org/10.1016/j.esd.2016.07.002.

Kumar, Narendra, and Debabrata Das. 2000. "Enhancement of Hydrogen Production by Enterobacter Cloacae IIT-BT 08." In *Process Biochemistry*, vol. 35. www.elsevier.com/locate/procbio.

Lee, Myoung Joo, Ji Hyeon Song, and Sun Jin Hwang. 2009. "Effects of Acid Pre-Treatment on Bio-Hydrogen Production and Microbial Communities during Dark Fermentation." *Bioresource Technology* 100 (3): 1491–93. https://doi.org/10.1016/j.biortech.2008.08.019.

Li, Jin, Chao He, Tian Tian, et al. 2020. "UASB-Modified Bardenpho Process for Enhancing Bio-Treatment Efficiency of Leachate from a Municipal Solid Waste Incineration Plant." *Waste Management* 102 (February): 97–105. https://doi.org/10.1016/j.wasman.2019.10.028.

Li, Yangyang, Yiying Jin, Jinhui Li, Hailong Li, and Zhixin Yu. 2016. "Effects of Thermal Pretreatment on the Biomethane Yield and Hydrolysis Rate of Kitchen Waste." *Applied Energy* 172 (June): 47–58. https://doi.org/10.1016/j.apenergy.2016.03.080.

Magama, Primrose, and Idan Chiyanzu. 2021. "Investigating Dark Fermentation as a Sustainable Organic Waste Management Technology for Producing Biohydrogen From Fruit and Vegetable Waste." Research Square, October 18. https://doi.org/10.21203/rs.3.rs-955255/v1.

Mainardis, Matia, Marco Buttazzoni, and Daniele Goi. 2020. "Up-Flow Anaerobic Sludge Blanket (UASB) Technology for Energy Recovery: A Review on State-of-the-Art and Recent Technological Advances." *Bioengineering* 7 (2): 43. https://doi.org/10.3390/bioengineering7020043.

Martínez-Mendoza, Leonardo J., Octavio García-Depraect, and Raúl Muñoz. 2023. "Unlocking the High-Rate Continuous Performance of Fermentative Hydrogen Bioproduction from Fruit and Vegetable Residues by Modulating Hydraulic Retention Time." *Bioresource Technology* 373 (April). https://doi.org/10.1016/j.biortech.2023.128716.

Mazzanti, Gaia, Francesca Demichelis, Debora Fino, and Tonia Tommasi. 2025. "A Closed-Loop Valorization of the Waste Biomass through Two-Stage Anaerobic Digestion and Digestate Exploitation." *Renewable and Sustainable Energy Reviews* 207 (September 2024): 114938. https://doi.org/10.1016/j.rser.2024.114938.

Mizuno, Osamu, Richard Dinsdale, Freda R. Hawkes, Dennis L. Hawkes, and Tatsuya Noike. 2000. *Enhancement of Hydrogen Production from Glucose by Nitrogen Gas Sparging*.

Mohan, S., and Neena Sunny. 2008. "Study on Biomethonization of Waste Water from Jam Industries." *Bioresource Technology* 99 (1): 210–13. https://doi.org/10.1016/j.biortech.2006.11.044.

Niya, Btissam, Kaoutar Yaakoubi, Salah Eddine Azaroual, Fatima Zahra Beraich, Moha Arouch, and Issam Meftah Kadmiri. 2023. "Anaerobic Digestion of Agricultural Waste Using Microbial Inocula: Performance and Characterization of Bacterial Communities Using 16S rRNA Sequencing Approach." *Energies* 16 (8). https://doi.org/10.3390/en16083300.

Paudel, Sachin, Youngjun Kang, Yeong Seok Yoo, and Gyu Tae Seo. 2017. "Effect of Volumetric Organic Loading Rate (OLR) on H2 and CH4 Production by Two-Stage Anaerobic Co-Digestion of Food Waste and Brown Water." *Waste Management* 61 (March): 484–93. https://doi.org/10.1016/j.wasman.2016.12.013.

Quadros, Thainara Camila Fernandes de, Isabela Mangerino Sicchieri, Jessica Klarosk Helenas Perin, et al. 2023. "Valorization of Fruit and Vegetable Waste by Anaerobic Digestion: Definition of Co-Substrates and Inoculum." *Waste and Biomass Valorization* 14 (2): 407–19. https://doi.org/10.1007/s12649-022-01887-7.

Ravindran, Anita, Sunil Adav, and Shang Shyng Yang. 2010. "Effect of Heat Pre-Treatment Temperature on Isolation of Hydrogen Producing Functional Consortium from Soil." *Renewable Energy* 35 (12): 2649–55. https://doi.org/10.1016/j.renene.2010.04.010.

Ruffino, Barbara, Silvia Fiore, Chiara Roati, Giuseppe Campo, Daniel Novarino, and Mariachiara Zanetti. 2015. "Scale Effect of Anaerobic Digestion Tests in Fed-Batch and Semi-Continuous Mode for the Technical and Economic Feasibility of a Full Scale Digester." *Bioresource Technology* 182 (April): 302–13. https://doi.org/10.1016/j.biortech.2015.02.021.

Ruffino, Barbara, and Mariachiara Zanetti. 2017. “Present and Future Solutions of Waste Management in a Candied Fruit – Jam Factory: Optimized Anaerobic Digestion for on Site Energy Production.” *Journal of Cleaner Production* 159 (August): 26–37. https://doi.org/10.1016/j.jclepro.2017.05.048.

Ruggeri, Bernardo, Andrea C. Luongo Malave, Milena Bernardi, and Debora Fino. 2013. “Energy Efficacy Used to Score Organic Refuse Pretreatment Processes for Hydrogen Anaerobic Production.” *Waste Management* 33 (11): 2225–33. https://doi.org/10.1016/j.wasman.2013.06.024.

Scotto di Perta, Ester, Alessandra Cesaro, Stefania Pindozzi, Luigi Frunzo, Giovanni Esposito, and Stefano Papirio. 2022. “Assessment of Hydrogen and Volatile Fatty Acid Production from Fruit and Vegetable Waste: A Case Study of Mediterranean Markets.” *Energies* 15 (14). https://doi.org/10.3390/en15145032.

Soltan, Mohamed, Mahmoud Elsayed, M. Mahmoud, and Amr M. Wahaballa. 2024. “Comparative Analysis of Organic Substrate Efficiency in Bio-Hydrogen Production through Dark Fermentation.” *Aswan University Journal of Science and Technology* 4 (4). https://journals.aswu.edu.eg/stjournal.

VDI 4630. 2006. *Fermentation of Organic Materials - Characterization of the Substrate, Sampling, Collection of Material Data, Fermentation Tests*. Engl. VDI-Gesellschaft Energie und Umwelt.

Zagrodnik, Roman. 2022. “Continuous H2 Production during Fermentation of the Carbon Components of Lignocellulose Hydrolysates: Insight into the Influence of pH Conditions on the Conversion Efficiency of Individual Sugars.” *International Journal of Hydrogen Energy* 47 (84): 35635–40. https://doi.org/10.1016/j.ijhydene.2022.08.165.

Chapter 3

3. Two-stage anaerobic digestion of starch wastewaters

3.1 Introduction

In the previous chapter, the two-stage anaerobic digestion (TSAD) of fruit and vegetable waste (FVW) and jam wastewater (JWW) was investigated to evaluate their potential for H_2 and CH_4 production. JWW proved to be particularly suitable for dark fermentation (DF), mainly due to its high content of readily biodegradable sugars as glucose and fructose. Glucose is the fundamental building block of starch, a high-molecular-weight compound that represents a major component of staple foods and cereals. Owing to its widespread use in food products, starch-based wastes are commonly generated as a result of supply chain inefficiencies and processing losses (Das and Basak 2021).

Due to the complex structure of starch, a hydrolysis step is required to convert it into a starch hydrolysate mainly composed of glucose and maltose, as occurs in the production of glucose syrup. This conversion increases sugar accessibility for microorganisms, thereby facilitating the production of H_2 and VFAs. Although several operational parameters influence DF, acetic and butyric acids are generally reported as the dominant VFAs in the effluent (Das and Basak 2021). Numerous studies have investigated the application of DF to starch-based wastes. Domińska et al. (2025) evaluated the DF of starch wastewater from the textile industry. The inoculum was thermally pretreated at 70 °C for 30 min and then applied to both natural and modified starch wastewater, either thermally treated or untreated. Experiments were conducted in 0.5 L glass bioreactors at 37 °C. The highest H_2 yield was obtained from untreated natural starch (214 mL/g_{VS}), whereas the lowest yield was observed for modified unheated starch (99 mL/g_{VS}). These results suggest that chemical or structural modifications of starch may shift microbial metabolism toward less efficient hydrogen-producing pathways. Nevertheless, the overall H_2 yields were relatively high, confirming the suitability

of starch-rich substrates for hydrogen production. VFAs concentrations ranged between 5 and 10 g/L across all configurations, with acetic and butyric acids as the predominant components, in agreement with previous findings.

Starch processing wastewater was also investigated by Sutthipattanasomboon and Wongthanate (2017). In this study, seed sludge was thermally pretreated at 90 °C for 10 min and incubated with the substrate in 180 mL batch reactors under both mesophilic and thermophilic conditions. Maximum H_2 yields of 13.84 and 37.59 mL/g_{COD} were obtained at mesophilic and thermophilic temperatures, respectively, with an initial pH between 7 and 8. As reported in other studies, acetic and butyric acids were the dominant VFAs. The relatively low H_2 yields suggest that insufficient hydrolysis limited sugar availability, highlighting the importance of effective pretreatment to enhance glucose release.

Taherdanak et al. (2015) further investigated starch DF in 118 mL reactors at 37 °C using inoculum pretreated at 90 °C for 45 min. The study also examined the effect of iron and nickel supplementation on microbial activity. The addition of both metals significantly improved system performance, with the optimal concentration identified at 37.5 mg/L for each metal. Under these conditions and with a starch concentration of 5 g/L, an H_2 yield of 147.3 mL/g_{VS} was achieved. These results indicate that, while trace metal addition can enhance H_2 production by supporting enzymatic activity, substrate concentration and carbohydrate accessibility remain critical factors. Similarly, Sinbuathong and Sillapacharoenkul (2021) studied the DF of starch factory wastewater in 120 mL reactors at 35 °C. The inoculum was pretreated using either acid (HCl 10 M) or alkaline (NaOH 10 M) conditions. Maximum H_2 yields of 138 and 182 mL/g_{COD} were obtained with acid and alkaline pretreatment, respectively. These values are higher than those reported in previous studies, likely because starch factory wastewater already contained readily available sugars, reducing the need for extensive hydrolysis before fermentation.

Starch wastewater can originate from different industrial processes, such as glucose syrup production, which generates multiple wastewater streams that remain rich in simple sugars.

During glucose syrup production, starch is first extracted from wheat flour using steam at temperatures above 100 °C. Enzymatic hydrolysis is then performed using enzymes such as alpha-amylase to produce a raw syrup containing polysaccharides along with impurities, including fats, mineral salts, proteins, and trace organic compounds. This raw syrup subsequently undergoes a saccharification step, tailored to the desired final product, followed by separation through ceramic membrane filtration. While the permeate proceeds to further refinement processes, the retentate is combined with waste streams from other production lines and subjected to a second filtration stage.

The retentate obtained from this second filtration step is referred to hereafter as *aliment* and represents one of the substrates investigated in this chapter for TSAD. This wastewater stream contains approximately 90-95 % glucose, along with impurities accumulated throughout the production process. Aliment can undergo further filtration, yielding a permeate that is sent to demineralization and a

retentate used as feedstock for alcoholic fermentation. Aliment, permeate, and retentate therefore represent three relevant waste streams from glucose syrup production that retain a high concentration of readily degradable sugars, making them promising substrates for fermentative H_2 production.

3.1.1 Goal

To the best of the authors' knowledge, DF and TSAD have not yet been specifically applied to permeate, retentate, and aliment as individual substrates.

To address the limited knowledge on glucose-rich residues from syrup production, TSAD is initially performed on each stream separately to assess their potential for H_2 and CH_4 generation. The process is then extended to evaluate the effect of co-digestion with FVW at two different mixing ratios.

By focusing on rarely studied substrates, this work explores their potential integration into existing bioenergy pathways. Overall, the results support TSAD as a promising approach for the valorization of underutilized biomass within a circular economy framework.

3.2 Materials and method

3.2.1 Substrates and inoculum characterization

The inoculum employed in DF and AD was the mesophilic digestate of CAS provided by "Cascina La Speranza" (Fossano, Cuneo, Italy). FVW was collected from household residue (mass composition of 75% vegetables and 25 % fruits) and chopped through a kitchen blender. Aliment, retentate, and permeate were supplied by a glucose syrup factory (Piedmont, Italy) as the wastewaters from filtration units. Both FVW and the starch wastewaters were frozen at -18 °C after their collection to avoid natural decomposition. Then they were defrosted before being fed into the fermentation system. The starch wastewaters, FVW, and inoculum characterization are presented in *Table 3.1*. All the experiments have been performed with the same lot of starch wastewaters, FVW, and inoculum to ensure the reproducibility and comparability of the achieved results.

3.2.2 Inoculum thermal pretreatment

In the present study, the inoculum was thermally pretreated at 80 °C for 1 h to eliminate H_2-consumers and favor sporulation of H_2-producers. The inoculum was heated in an oven and covered with aluminum foil to minimize water evaporation during treatment.

3.2.3 Process setup and operative condition

DF and AD were performed in 250 mL Pyrex glass bottles (Duran, Germany) with a working volume of 80 % at 35 °C. The heating was controlled by a 55 L thermostatic water-bath (Julabo-Corio-C, Merck, Germany). Reactors were operated in batch feeding mode and shaken manually to keep the mixture homogeneous inside the reactor. Each reactor was sealed with a two-port cap. Through one of the ports, anaerobic conditions were assured by purging N_2 directly inside the biomass to change the volume of the reactor three times and closing the port. The second port was connected to a 1 L Teddlar gas bag where biogas was collected. The duration of each assay depended on biogas or H_2 production: testing was stopped when daily H_2 (for DF tests) and biogas (for AD tests) production was less than 1 % of the overall production recorded during the period of preparation (VDI 4630 2006). The experimental campaign consists of two main experiments, and all the campaigns were studied in replicates. The pH of each reactor was measured at the beginning and at the end of the experiments. In the experiments, when necessary, HCl was added to the reactors to lower pH to around 6-7 in DF. AD pH was maintained between 7 and 8.

In the first experimental set, DF was carried out separately on the three substrates, followed by TSAD. All reactors were operated at a total solids content of 6 %. For each configuration, the inoculum was thermally pretreated, and the substrate-to-inoculum ratio was fixed at 1:1 on a VS basis. Aliment, retentate and

permeate were added accordingly to meet this condition. The digestates obtained from DF were subsequently used as feedstock for the AD stage, which was conducted at the same S:I ratio and total solids content, without inoculum pretreatment.

In the second experimental set, six configurations were tested to investigate the co-digestion of starch wastewaters with FVW. Each starch wastewater was combined with FVW at a ratio of 70/30 % on VS basis and evaluated under batch conditions at two total solids levels (3 % and 6 %). The inoculum was thermally pretreated for all DF tests, and the S:I ratio was again maintained at 1:1 on a VS basis. Only the digestate from the best-performing DF configuration for each starch wastewater was further processed in the AD stage, which was carried out without inoculum pretreatment and with an S:I ratio of 1:1. A summary of configuration characteristics is presented in *Table 3.2*.

DF design, analytical methods, and data processing were carried out in accordance with the procedures described in Sections 2.2.4 and 2.2.5 of this thesis.

3.3 Results

3.3.1 Characterization of inoculum and substrates

The inoculum and substrates were characterized in terms of TS, VS, and elemental composition using a CHNS analyzer, and the results are reported in *Table 3.1*. The starch-based wastewaters exhibited markedly high TS contents, exceeding 30%, which reflects their high carbohydrate concentration. In all cases, nearly the entire solid fraction was volatile, as indicated by VS/TS ratios above 99%, confirming that these substrates are predominantly composed of easily degradable organic matter. The TS content of starch wastewaters can vary considerably depending on the specific industrial process from which they are produced and the degree of dilution applied along the production line. In contrast, the VS fraction tends to remain relatively consistent across different starch-derived wastes, owing to the inherently volatile nature of starch and its hydrolysis products. This observation is supported by Sinbuathong and Sillapacharoenkul (2021), who reported a VS/TS ratio of 97 %, very close to the one of the substrates analyzed in this chapter. As expected, the C:N ratio was markedly unbalanced, mainly because of the very low nitrogen content of the substrates. This imbalance was particularly evident for the permeate, which exhibited a C:N ratio of 317.03:1. Such a high value reflects the origin of this stream, as it derives from a filtration step in which most impurities are retained in the retentate. This interpretation is supported by the significantly lower C:N ratio measured for the retentate (40.73:1), indicating a nitrogen content almost ten times higher than that of the permeate. The aliment showed an intermediate C:N ratio of 96.98:1, consistent with its mixed composition and processing history. From a process perspective, these results suggest that the starch-derived wastewaters are strongly carbon-rich and may therefore require nutrient supplementation through nitrogen-rich compounds to support stable microbial activity during DF and TSAD.

Table 3.1 Chemical and physical characterization of inoculum, fruit and vegetable waste (FVW) and starch wastewaters (permeate, retentate and aliment).

	Inoculum	**FVW**	**Permeate**	**Retentate**	**Aliment**
TS (%)	4.30 ± 0.11	10.89 ± 0.36	32.12 ± 0.04	36.73 ± 0.14	32.95 ± 0.02
VS/TS (%)	73.24 ± 0.45	85.04 ± 0.31	99.98 ± 0.02	99.96 ± 0.01	99.97 ± 0.03
N (%)	3.01 ± 0.22	1.52 ± 0.13	0.12 ± 0.02	1.09 ± 0.04	0.42 ± 0.02
C (%)	34.58± 0.98	41.65 ± 0.74	39.10 ± 1.72	44.51 ± 0.85	40.73 ± 0.40
H (%)	4.42 ± 0.13	6.35 ± 0.18	7.29 ± 0.46	7.58 ± 0.36	7.03 ± 0.17
S (%)	0.34 ± 0.07	0.21 ± 0.01	0.07 ± 0.02	0.07 ± 0.01	0.19 ± 0.08
O (%)	57.65 ± 1.15	50.27 ± 0.99	53.41 ± 2.14	46.74 ± 1.26	51.63 ± 0.50
C/N	11.49 ± 0.42	27.49 ± 2.14	317.03 ±25.11	40.73 ± 0.72	96.98 ± 3.13

Table 3.2 Configurations tested across two experiments: i) TSAD of the three starch wastewaters and ii) TSAD of starch wastewater with FVW.

Configuration	Substrate	TS content
	First experiment - DF	
Permeate	Permeate	6 %
Retentate	Retentate	6 %
Aliment	Aliment	6 %
	First experiment - AD	
Permeate	Digestate from Permeate DF	6 %
Retentate	Digestate from Retentate DF	6 %
Aliment	Digestate from Aliment DF	6 %
	Second experiment - DF	
Permeate 6%	Permeate + FVW	6 %
Permeate 3%	Permeate + FVW	3 %
Retentate 6%	Retentate + FVW	6 %
Retentate 3%	Retentate + FVW	3 %
Aliment 6%	Aliment + FVW	6 %
Aliment 6%	Aliment + FVW	3 %
	Second experiment - AD	
Permeate	Digestate from Permeate 6% DF	6 %
Retentate	Digestate from Retentate 6% DF	6 %
Aliment	Digestate from Aliment 6% DF	6 %

3.3.2 Two-stage anaerobic digestion of starch wastewaters: dark fermentation

This experimental campaign evaluated the feasibility of integrating DF and AD in a sequential process, specifically applying a TSAD process to aliment, permeate and retentate. Three different configurations were tested in the first stage of TSAD, with variations in the substrate employed.

Biogas production commenced on day 1 in all configurations, showing a comparable overall trend across the three substrates, as shown in *Figure 3.1-a*. In each case, the highest production rate was observed during the first day of operation, as indicated by the steep initial slope of the cumulative production curves. From day 2 onward, the production rate decreased markedly, and the curves progressively flattened, indicating a slowdown in microbial activity. Among the tested substrates, permeate achieved the highest cumulative biogas production, reaching 237 N mL/g_{VS}, followed closely by retentate and aliment, which yielded 233 and 226 N mL/g_{VS}, respectively. H_2 production *Figure 3.1-b* exhibited a similar temporal pattern, with the maximum production rate occurring within the first day and accounting for approximately 70-85 % of the total H_2 generated. After this initial phase, permeate and retentate displayed a slower but more sustained H_2 production compared to aliment, until day 4, when both substrates surpassed the H_2 yield obtained from aliment. Permeate and retentate reached a production plateau on day 6, whereas aliment stabilized earlier, on day 4. Overall, the highest H_2 yield was obtained in permeate-fed reactors, with a maximum of 60 N mL/g_{VS}, followed by retentate and aliment, which reached 56 and 51 N mL/g_{VS}, respectively.

CH_4 production exhibited a distinct pattern compared to H_2 and total biogas, as illustrated in *Figure 3.1-c*. Following a sharp increase during the first day, CH_4 production rapidly reached a plateau in all configurations and remained nearly constant until day 6, with cumulative CH_4 yields remaining below 6 N mL/g_{VS} in all cases. From day 7 onward, however, a renewed increase in CH_4 production was observed in the retentate- and aliment-fed reactors. This increase became particularly pronounced after day 9, as indicated by the steep slope of the curves, and culminated in maximum CH_4 yields of approximately 9 and 10 N mL/g_{VS} on day 11 for retentate and aliment, respectively.

In contrast, the permeate-fed configuration did not exhibit any further increase in methane production after day 2, instead maintaining a stable plateau throughout the remainder of the experimental period. The delayed CH_4 production observed in the retentate and aliment reactors may be attributed to the activation of methanogenic microorganisms that were not completely eliminated during inoculum pretreatment. These H_2-consuming microorganisms likely became active after the H_2-producing phase had declined, leading to the onset of methanogenesis. This phenomenon appears to be less pronounced in the permeate configuration, suggesting a more effective suppression of methanogens under these conditions.

CO_2 production, reported in *Figure 3.1-d*, followed a trend closely resembling that of total biogas production. As observed for biogas, the highest CO_2 production rate occurred during the first day of operation, followed by a slower and more gradual increase from day 2 until the end of the experiment. The highest cumulative CO_2 yield was obtained in the permeate-fed reactors, reaching 172 N mL/g_{VS}, while retentate and aliment achieved slightly lower values of 166 and 156 N mL/g_{VS}, respectively.

The composition of the produced biogas is presented in *Figure 3.1-e*. H_2 reached maximum concentrations of 25 % in the permeate-fed reactors and 24 % in both the retentate- and aliment-fed configurations. In all cases, CO_2 was the dominant component of the biogas, accounting for approximately 71-72 % of the total volume. CH_4 was detected in all configurations, although at relatively low concentrations, with a maximum of 5 % in the aliment-fed reactors, followed by 4 % in the retentate and 2 % in the permeate configurations. The variable effectiveness of thermal pretreatment across the different configurations is not entirely clear. One possible explanation is the inherent variability of the inoculum, which may have influenced the consistency of the pretreatment outcome. Under such conditions, methanogens that survived thermal pretreatment, although partially weakened, may have recovered and competed with H_2-producing microorganisms, thereby contributing to CH_4 formation.

No significant differences in overall biogas production were observed among the three substrates, indicating comparable fermentability under the tested conditions ($p > 0.05$). This finding suggests that permeate, retentate, and aliment can be interchangeably employed as sugar-rich substrates for dark fermentation.

Digestates from the dark fermentation stage were further analyzed for VFAs, specifically acetic, propionic, and butyric acids, to evaluate the metabolic

pathways involved in the process. The results are shown in *Figure 3.1-f*. Overall, the VFAs profiles were relatively homogeneous across the different configurations. The presence of all three acids likely results from the availability of readily fermentable compounds in the starch wastewaters. Acetic acid was detected in all reactors, with concentrations ranging from 2.23 to 3.42 g/L, while propionic acid was also present in all samples, although at lower and more variable concentrations. The highest propionic acid concentration was observed in the aliment-fed reactor (1.0 g/L), followed by the permeate- and retentate-fed reactors with 0.20 and 0.12 g/L, respectively. Butyric acid was the predominant acid in all configurations, reaching concentrations of 6.7 g/L in the aliment-fed reactor, 6.6 g/L in the retentate-fed reactor, and 3.9 g/L in the permeate-fed reactor. Consequently, total VFAs concentrations amounted to 6.4 g/L for permeate, 10.1 g/L for retentate, and 11.1 g/L for aliment. Two of these values exceeded the inhibitory threshold of 8 g/L reported by Cremonez et al. (2021) while in the permeate-fed configuration, acid concentrations were lower than in the other cases, although they remained relatively high. The accumulation of these acids may have contributed to process inhibition, as indicated by the marked decrease in production rate observed from day 2 onward, likely due to the inhibitory effects associated with elevated VFAs levels. The predominance of acetic and butyric acids aligns with what was stated by Das and Basak (2021).

DF of starch wastewater was also investigated by Nasr et al. (2013) using a 28 L up-flow anaerobic staged reactor (UASR) operated under mesophilic conditions. The effects of different OLR (ranging from 18 to 108 g_{COD}/L d) and S:I ratios (0.5-2.8 g_{COD}/g_{VSS} d) were evaluated. The maximum H_2 yield, 233 N mL/g_{VS}, was achieved at an OLR of 54 g_{COD}/L d and an S:I ratio of 1.4 g_{COD}/g_{VSS} d. This value is higher than that obtained in the present study, which may be attributed to improved process control associated with the reactor design, such as optimized mixing, HRT, and initial pH conditions.

Starch fermentation was also examined by Bao et al. (2012). who investigated hydrogen production using pure cultures of *Bacillus* and *Brevundimonas* strains. The experiments were conducted in 1 L batch reactors at 35 °C, testing each strain individually and in mixed cultures at different ratios. The highest H_2 yield (129 N mL/g_{VS}), along with the highest H_2 content in biogas (60 %), was obtained when the two strains were mixed at an equal ratio. The yields reported in this study were higher than those achieved in the present work, likely due to the use of selected H_2-producing strains rather than a mixed microbial community derived from an anaerobic digestion plant. The authors also investigated VFAs production and reported acetic and butyric acids as the predominant metabolites formed by the mixed cultures. However, VFAs concentrations remained below 2 g/L in all cases, indicating a metabolic shift compared to the present study, where higher acid accumulation was observed.

As discussed in Section 2.3.7, Upflow Anaerobic Sludge Blanket (UASB) reactors are widely used for treating high-COD wastewaters, such as starch-based effluents investigated in this chapter (Mainardis et al. 2020). Several studies have evaluated their performance with this type of substrate.

C. Fang et al. (2011) investigated the anaerobic digestion of potato starch wastewater using both a UASB reactor and an expanded granular sludge bed (EGSB) system, which operates at higher superficial up-flow velocities. The reactors had volumes of 1.2 L (UASB) and 1.0 L (EGSB) and were operated at 37 °C. The UASB achieved a maximum methane yield of 240 mL/g_{VS} at an OLR of 5.1 g_{COD}/L d, while the EGSB reached 380 mL/g_{VS} at an OLR of 3.2 g_{COD}/L d. These results confirm the suitability of both configurations for treating starch-rich wastewater. Although UASB systems can tolerate higher OLR and VFAs accumulation, the EGSB showed higher methane production under stable conditions, highlighting the advantages of enhanced mass transfer in this configuration.

X. Lu et al. (2015) further studied synthetic starch wastewater in a 6 L UASB reactor operated at 35 °C, varying the HRT from 24 to 3 hours. The best performance was observed at an HRT of 6 hours, with COD removal reaching 98.7 %. At shorter HRTs, VFAs accumulation led to process instability, highlighting the importance of optimizing operating conditions to maintain stable performance.

Despite its potential in starch wastewaters AD, UASB configuration was not considered in the present thesis due to technical limitations of the available laboratory equipment, which prevented its proper implementation at the required scale and operating conditions.

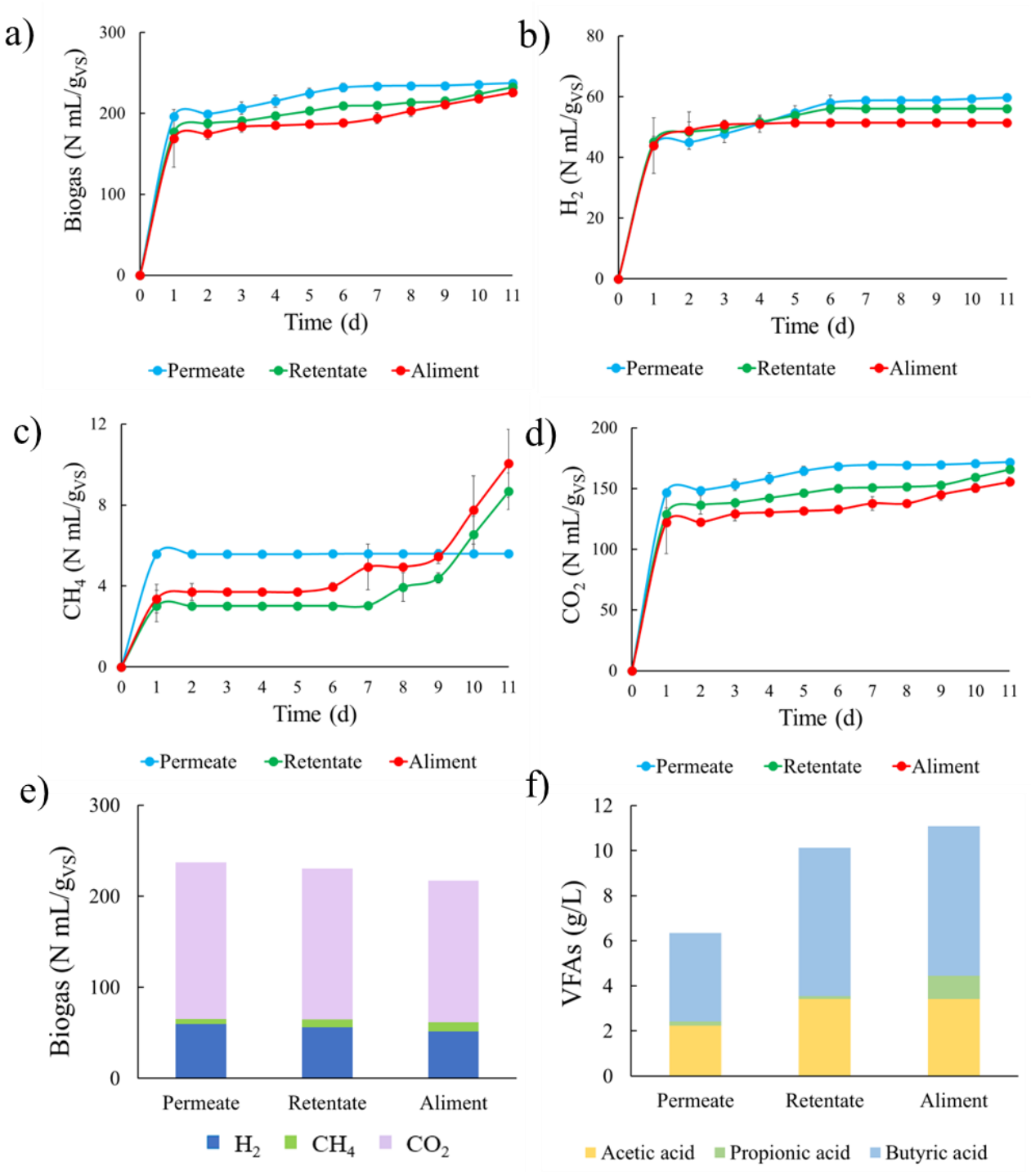

Figure 3.1 Results from the DF of the first experiment: a) biogas yield, b) H_2 yield, c) CH_4 yield, d) CO_2 yield, e) composition of total biogas produced during dark fermentation considering H_2, CH_4 and CO_2, f) VFAs concentration in the three configurations as g/L.

3.3.3 Two-stage anaerobic digestion of starch wastewaters: anaerobic digestion

The second stage of the process (AD) utilized the digestate from the DF stage as the primary substrate. This digestate was combined with non-pretreated CAS inoculum at a 1:1 ratio while maintaining a TS content of 6 %.

Biogas and CH_4 production over the 21-day experimental period are shown in *Figure 3.2-a* and *-b*. All configurations exhibited biogas generation, with comparable overall trends. During the initial phase (days 0–3), biogas production rates were relatively low, as indicated by the gentle slope of the curves. Between days 4 and 11, biogas production accelerated markedly in all reactors, resulting in steeper curves. In the final phase, production rates progressively declined, and a plateau was reached around day 13 for the permeate- and retentate-fed reactors, with cumulative biogas yields of 140 and 159 N mL/g_{VS}, respectively. In contrast, the aliment-fed configuration showed a more gradual increase, reaching the highest final biogas yield of 176 N mL/g_{VS} toward the end of the experiment.

CH_4 production followed trends like those observed for total biogas. An initial phase characterized by slow CH_4 accumulation was followed by a period of rapid production up to day 11, after which CH_4 generation rates decreased sharply in all configurations. The permeate-fed reactors exhibited the lowest CH_4 production, achieving a maximum of 99 N mL/g_{VS}, whereas both retentate- and aliment-fed reactors reached higher values of approximately 125 N mL/g_{VS}.

CO_2 production (*Figure 3.2-c*) also showed a consistent pattern among the substrates. The highest CO_2 production rates were observed during the first 11 days, followed by a more gradual increase toward the end of the experiment. The aliment-fed reactors reached the highest cumulative CO_2 yield (51 N mL/g_{VS}), while retentate- and permeate-fed configurations attained slightly lower values of 41 and 37 N mL/g_{VS}, respectively.

Statistical analysis indicated no significant differences in cumulative biogas production among the three substrates during the second stage of TSAD ($p > 0.05$). Similar to the results observed during the DF stage, the influence of substrate type on biogas and CH_4 production during the subsequent AD phase was limited. These findings suggest that permeate, retentate, and aliment can be used interchangeably as feedstocks for producing a digestate suitable for the second stage of the process.

The biogas composition for all configurations is presented in *Figure 3.2-d*. CH_4 was the dominant component in all cases, accounting for 71 % in permeate-fed reactors, 77 % in retentate-fed reactors, and 71 % in aliment-fed reactors. CO_2 concentrations ranged between 23 % and 28 %. Notably, although retentate-fed reactors exhibited slightly lower cumulative CH_4 yields than aliment-fed reactors, their relative CH_4 content in biogas was higher. Conversely, despite aliment-fed reactors achieving the highest absolute CH_4 yield, their CH_4 percentage was comparable to that of permeate-fed reactors. No H_2 was detected during the AD stage.

The performance of the proposed system can be compared with that reported by Zhang et al. (2020) who investigated a two-stage process consisting of photofermentation followed by AD of enzymatic hydrolysates obtained from corncob powder. In their study, photofermentation was carried out in 250 mL conical flasks at 30 °C, while anaerobic digestion of photofermentation effluent was performed at 35 °C. H_2 production in the first stage reached 22 mL/g_{VS}, whereas CH_4 production during the second stage amounted to 141 mL/g_{VS}. As discussed previously, the H_2 yields obtained in the present study were higher, likely due to the greater availability of readily fermentable sugars in starch-based wastewaters compared with corncob hydrolysates. In contrast, CH_4 yields were comparable to those achieved during the second stage of the present system. Cremonez et al. (2020) investigated TSAD applied to a polymer derived from cassava starch. Following thermal pretreatment of the inoculum at 100 °C for 30 min, DF was carried out in a 5 L acidogenic reactor operated in semi-continuous mode at 37 °C with HRT of 5 days. The second stage consisted of a 12 L methanogenic reactor operated under mesophilic conditions with an HRT of 20 days. H_2 yield in the first stage reached 20 mL/g_{VS}, while CH_4 production in the second stage reached 249 mL/g_{VS}. H_2 yields were lower than those obtained in the present study, likely due to the more complex nature of the substrate. Conversely, CH_4 yields were approximately twice those observed here. This difference may be attributed to the high concentration of fermentable carbohydrates remaining in the DF effluent, as suggested by the relatively low biogas production during the first stage, which likely preserved substantial substrate availability for CH_4 generation.

Overall, although the CH_4 yields obtained in this study can be considered satisfactory, they remain lower than those reported in comparable studies. This suggests that further optimization of operating conditions and process configuration may be required to enhance methane recovery.

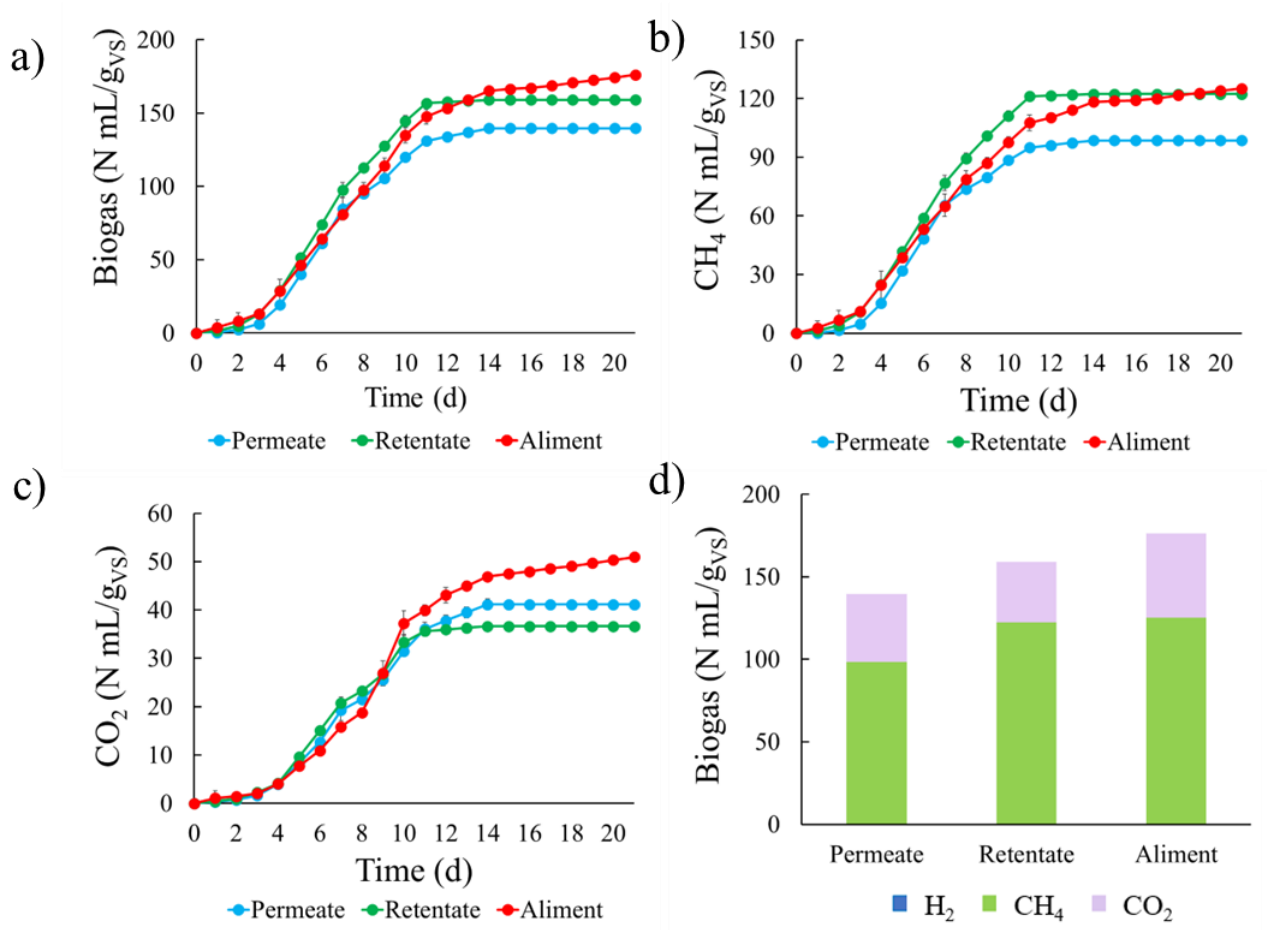

Figure 3.2 Results from the second stage of the first experiment: a) biogas yield, b) CH_4 yield, c) CO_2 yield and d) composition of total biogas produced during AD considering H_2, CH_4 and CO_2.

3.3.4 Two-stage anaerobic digestion of fruit and vegetable waste and starch wastewaters: dark fermentation

This experimental campaign evaluated the feasibility of integrating DF and AD in a sequential process, applying a TSAD process to three glucose-rich substrates (aliment, permeate, and retentate) co-digested with FVW. Six different configurations were investigated by varying both the substrate type and the TS content in the reactors. Each starch-derived wastewater (aliment, permeate, or retentate) was mixed with FVW at a ratio of 70/30 % on a VS basis and tested under batch conditions at two TS levels, namely 3 % and 6 %.

Biogas production began on day 1 in all configurations; however, the production profiles differed among the six setups over the course of the experiment, as shown in *Figure 3.3-a*. In all cases, the highest biogas production rate occurred during the first day of operation, as indicated by the steep initial slopes of the cumulative production curves. From day 2 onward, biogas generation markedly decreased in most configurations, with progressively flatter curves suggesting reduced microbial activity. Two notable exceptions were observed in the reactors co-digesting FVW with permeate and retentate at 3% TS (Permeate 3% and Retentate 3%), which exhibited a renewed increase in biogas production rate from approximately day 6 until day 8. Among all configurations, Retentate 3% achieved the highest cumulative biogas yield, reaching 225 N mL/g_{VS}, followed by Retentate 6% and Aliment 6%, which produced 173 and 176 N mL/g_{VS}, respectively. The remaining configurations exhibited lower biogas production, with Permeate 3% reaching 142 N mL/g_{VS}, followed by Aliment 3% and Permeate 6%, which achieved 112 and 108 N mL/g_{VS}, respectively.

H_2 production *Figure 3.3-b* displayed a markedly different trend compared to total biogas. In all configurations, the maximum H_2 production rate occurred within the first two days of operation, accounting for approximately 95 % of the total H_2 produced. After this initial phase, H_2 generation declined sharply in all reactors, as reflected by the very low slopes of the cumulative curves. Retentate 3% again represented a partial exception, showing a slight increase in H_2 production from day 6 until day 8. Overall, the highest H_2 yield was obtained in Retentate 6%, reaching 39 N mL/g_{VS}, followed by Aliment 6% and Permeate 6%, with yields of 28 and 27 N mL/g_{VS}, respectively. Among the configurations operated at 3 % TS, Permeate 3% achieved 26 N mL/g_{VS}, while Retentate 3% and Aliment 3% yielded 20 and 17 N mL/g_{VS}, respectively.

CH_4 production exhibited a distinct behavior compared to both H_2 and total biogas, as illustrated in *Figure 3.3-c*. In most configurations, CH_4 generation started slowly and reached a plateau between days 2 and 3, with cumulative CH_4 yields remaining below 3 N mL/g_{VS}. The only exception was Retentate 3%, which showed an increase in CH_4 production from day 4 to day 6, reaching a maximum of 7 N mL/g_{VS}. Compared to the results discussed previously, the survival and activity of methanogens appeared less pronounced in this experimental campaign, as CH_4 production ceased in all configurations after day 6.

CO_2 production *Figure 3.3-d* closely followed the trend observed for total biogas. As with biogas, the highest CO_2 production rates were recorded during the first day of operation, followed by a slower and more gradual increase from day 2 until the end of the experiment. Retentate 3% again showed the highest cumulative CO_2 yield, reaching 198 N mL/g_{VS}, followed by Retentate 6% and Aliment 6%, with yields of 136 and 144 N mL/g_{VS}, respectively. The remaining configurations produced lower amounts of CO_2, with Permeate 3% reaching 115 N mL/g_{VS}, followed by Aliment 3% and Permeate 6%, which yielded 94 and 79 N mL/g_{VS}, respectively.

The composition of the biogas produced during DF stage is presented in *Figure 3.3-e*. H_2 reached its highest concentrations in the configurations operated at 6% total solids, with maximum values of 25 % in Permeate 6% and 22 % in Retentate 6%. Lower H_2 fractions were observed in the remaining configurations, namely Permeate 3%, Aliment 6%, and Aliment 3%, which reached 18 %, 16 %, and 16 %, respectively. The lowest H_2 concentration was measured in Retentate 3%, where H_2 accounted for only 9 % of the biogas. This result is interesting, as Retentate 3% was also the configuration that achieved the highest cumulative biogas yield, indicating that elevated biogas production does not necessarily correspond to enhanced H_2 generation.

In all configurations, CO_2 was the dominant component of the biogas, representing between 73 % and 88 % of the total volume, depending on the substrate and total solids content. CH_4 was detected in all reactors, although at relatively low concentrations, with a maximum of 3 % in Retentate 3%, followed by 2 % in Permeate 6%. These low CH_4 fractions indicate a generally effective inhibition of methanogenic activity during the DF stage, although some residual activity cannot be excluded.

Statistically significant differences in cumulative biogas production were observed among the six configurations. In particular, Retentate 3% outperformed the other setups, followed by Retentate 6% and Aliment 6%. However, this comparison is based solely on total biogas production. In the context of DF, H_2 yield represents the primary performance indicator; therefore, configurations achieving higher H_2 production should be considered more favorable. In this respect, the results indicate that co-digestion of starch wastewaters with FVW at 6% TS led to higher H_2 yields compared to operation at 3% TS, suggesting that increased substrate availability positively influenced DF performance.

Digestates obtained from the DF stage were further analyzed for VFAs, specifically acetic, propionic, and butyric acids, in order to gain insight into the dominant metabolic pathways. The results are reported in *Figure 3.3-f*. Overall, the VFAs profiles showed similarities across configurations. Acetic acid was the most abundant acid in all reactors, followed by butyric acid, which represented the second most concentrated VFAs in nearly all cases. Propionic acid was also detected in all configurations, although at lower concentrations.

Acetic acid concentrations varied considerably among reactors, ranging from 1.23 to 7.89 g/L. Butyric acid reached a maximum concentration of 4.02 g/L in the Retentate 6% configuration, while its relative contribution varied between

approximately 9% and 39% of total VFAs. The highest propionic acid concentration was observed in Aliment 6% (1.44 g/L), followed by Retentate 6% and Permeate 6%, with concentrations of 1.41 and 1.25 g/L, respectively. Consequently, the highest total VFAs concentration was measured in Retentate 6% (13.3 g/L), followed by Permeate 6% (11.0 g/L) and Aliment 6% (9.1 g/L).

Notably, the highest VFAs concentrations were associated with the configurations that also achieved the highest H_2 yields. This observation is consistent with the metabolic activity of DF microorganisms, which simultaneously produce H_2 and VFAs. The relatively higher proportion of propionic acid observed in this experimental campaign compared to previous studies may indicate a partial shift in microbial metabolism, potentially induced by the co-digestion of starch wastewaters and FVW. A synergistic interaction between these substrates may have favored metabolic pathways leading to increased propionate formation.

DF of starch wastewater was also examined by Wadjeam et al. (2019) who investigated its co-digestion with buffalo dung in an 8 L CSTR operated at 30 °C. The system was run under HRT ranging from 48 to 72 h. The highest H_2 yield was achieved at an HRT of 60 h, reaching 16.9 $mL/g_{CODadded}$. In addition to hydrogen production, the authors analyzed VFAs formation. Butyric acid was the dominant fermentation product, with a concentration of 3.62 g/L, followed by propionic acid (0.57 g/L) and acetic acid (0.43 g/L). This VFAs distribution differs from that observed in the present study, suggesting that distinct microbial metabolic pathways were favored under the operating conditions adopted by Wadjeam et al. (2019). Such differences can reasonably be attributed to variations in inoculum origin, pretreatment strategy, and reactor operation, all of which are known to strongly influence microbial community structure and, consequently, process efficiency and fermentation pathway.

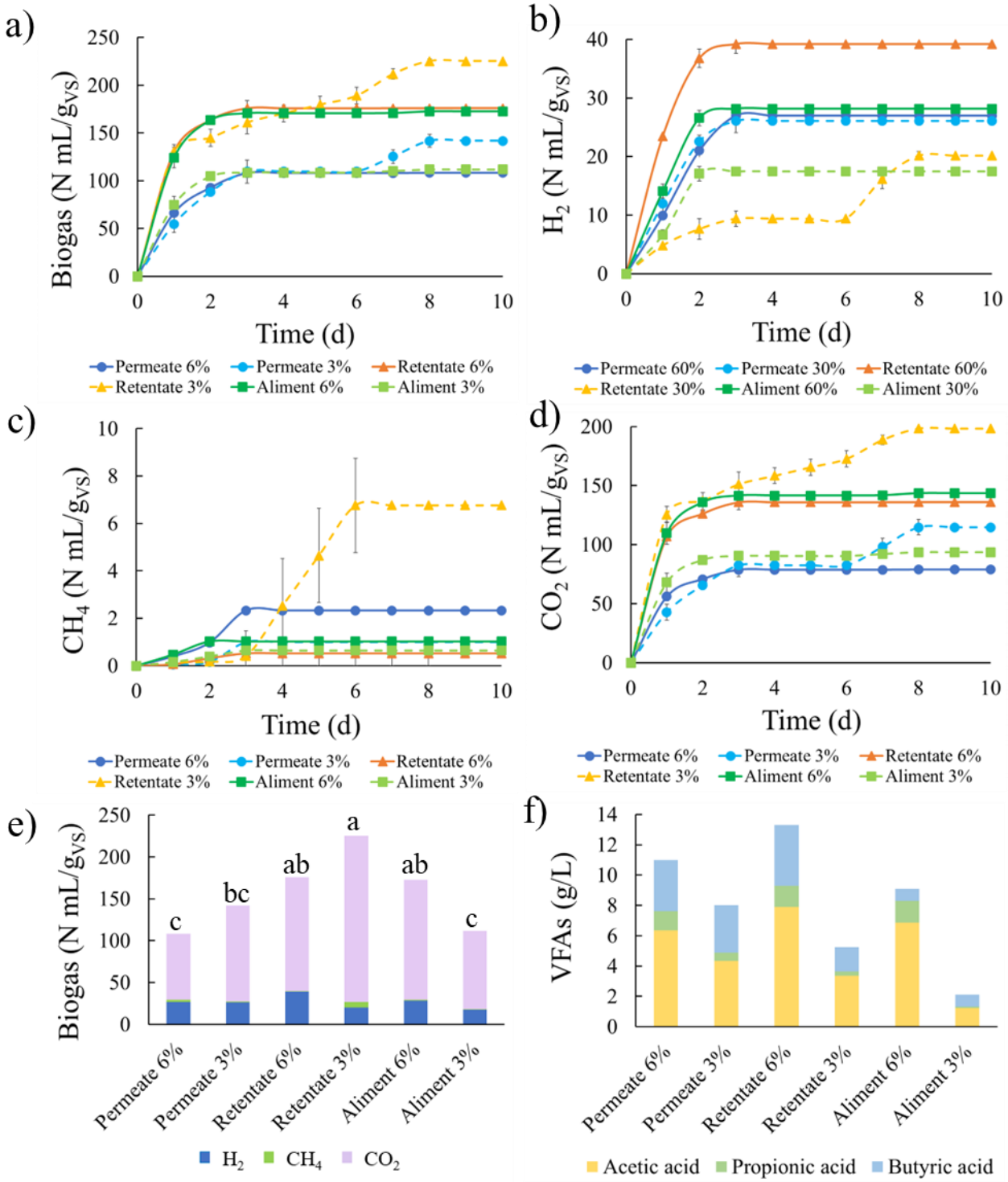

Figure 3.3 Results from the DF of the second experiment: a) biogas yield, b) H_2 yield, c) CH_4 yield, d) CO_2 yield, e) composition of total biogas produced during dark fermentation considering H_2, CH_4 and CO_2, f) VFAs concentration in the six configurations as g/L.

3.3.5 Two-stage anaerobic digestion of fruit and vegetable waste and starch wastewaters: anaerobic digestion

The second stage of the process (AD) employed the digestate obtained from the DF stage as the sole substrate. The digestate was mixed with non-pretreated CAS inoculum at a substrate-to-inoculum ratio of 1:1 on a VS basis, while maintaining a TS content of 6%. Only the three DF configurations that achieved the highest H_2 yields were selected for the AD stage. As the DF results indicated a better overall performance at 6% TS, only these conditions were further investigated. For simplicity, the three selected configurations are hereafter referred to as Permeate, Retentate, and Aliment.

Cumulative biogas and CH_4 production over the 21-day experimental period are presented in *Figure 3.4-a* and *-b*. All configurations produced biogas and exhibited comparable overall trends. During the initial phase of operation (days 0-3), biogas production rates were relatively low, as indicated by the gentle slopes of the curves. This was followed by a phase of accelerated biogas generation between days 4 and 11, during which all reactors showed a marked increase in production rates. In the final phase, biogas generation gradually slowed, and a plateau was reached at different times depending on the substrate. Retentate reached its maximum biogas yield around day 10, whereas permeate and aliment continued producing biogas until approximately day 16. The highest cumulative biogas yield was achieved by retentate (66 N mL/g_{VS}), followed by the aliment (57 N mL/g_{VS}) and permeate (54 N mL/g_{VS}), respectively. Notably, the retentate configuration was also the first to reach its maximum CH_4 yield, reflecting its higher production rate compared with permeate, which reached a plateau around day 15, and aliment, which continued producing CH_4 until day 21.

CH_4 production followed trends like those observed for total biogas. An initial phase characterized by slow CH_4 accumulation was followed by a period of rapid production, which lasted until approximately day 8 for both permeate and retentate. In contrast, the aliment exhibited a delayed plateau phase, reaching stable CH_4 production only after day 15. Permeate showed the lowest cumulative CH_4 yield (40 N mL/g_{VS}), while retentate and aliment reached slightly higher values of approximately 45 and 41 N mL/g_{VS}, respectively.

CO_2 production, shown in *Figure 3.4-c*, also displayed consistent trends across the three configurations. The highest CO_2 production rates were observed during the first 15 days in the aliment configuration, whereas permeate and retentate reached a plateau earlier, around day 11, followed by a slower increase until the end of the experiment. Retentate achieved the highest cumulative CO_2 yield (20 N mL/g_{VS}), while permeate and aliment reached slightly lower values of 14 and 16 N mL/g_{VS}, respectively.

Statistical analysis revealed significant differences in cumulative biogas production among the three configurations during the AD stage. In particular, the retentate-based digestate produced significantly higher amounts of biogas and CH_4, indicating a clearer influence of substrate type during the methanogenic phase. These findings suggest that retentate performs slightly better than the other

effluents under the tested conditions, although the overall yields remained lower than those reported in the previous chapter.

The biogas composition of all configurations is shown in *Figure 3.4-d*. CH_4 was the dominant component in all cases, accounting for 73 % in permeate, 69 % in retentate, and 73 % in aliment. CO_2 concentrations ranged between 27 % and 31 %. Although permeate and aliment achieved lower cumulative CH_4 yields than retentate, their relative methane content in the biogas was slightly higher. No hydrogen was detected during the AD stage.

The performance of the proposed system can be compared with that reported by Cremonez et al. (2024), who investigated TSAD applied to cassava starch-based polymer (CSP) and papaya waste at different mixing ratios. In their study, DF inoculum was thermally pretreated at 100 °C for 30 min, and both stages were carried out in 4 L reactors, with DF operating at 45 °C and AD at 37 °C. The maximum H_2 yield reached 100 mL/g_{VS} in the configuration containing 75 % CSP and 25 % papaya waste, while CH_4 production in the second stage reached 525 mL/g_{VS}. The H_2 yields obtained in the present study were lower, likely due to differences in process control and reactor configuration. Similarly, CH_4 yields were substantially higher in the cited study.

Comparable results were reported by Khongkliang et al. (2015), who investigated TSAD applied to cassava, rice, and corn starch wastewaters at concentrations of 5, 10, and 15 g/L. DF and AD were performed in 500 mL reactors under thermophilic conditions. Maximum H_2 was achieved for a concentration of 5 g/L and reached 81.5, 74.3, and 79.8 L/kg_{COD} for cassava, corn, and rice wastewaters, respectively, while methane production in the second stage ranged from 280.3 to 310.5 L/kg_{COD}. Both H_2 and CH_4 yields were considerably higher than those obtained in the present study, likely due to the simpler and more controlled nature of the synthetic starch substrates used.

Overall, H_2 and CH_4 yields obtained in this TSAD study remain lower than those reported in comparable studies. This outcome can likely be attributed to limitations in the experimental setup, particularly the absence of automatic mixing and pH control, which may have restricted optimal microbial activity. In addition, variability in the inoculum composition can significantly influence process performance, as differences in microbial communities may promote alternative metabolic pathways. These considerations indicate that further optimization of both operating conditions and reactor configuration is necessary to improve process stability and enhance energy recovery.

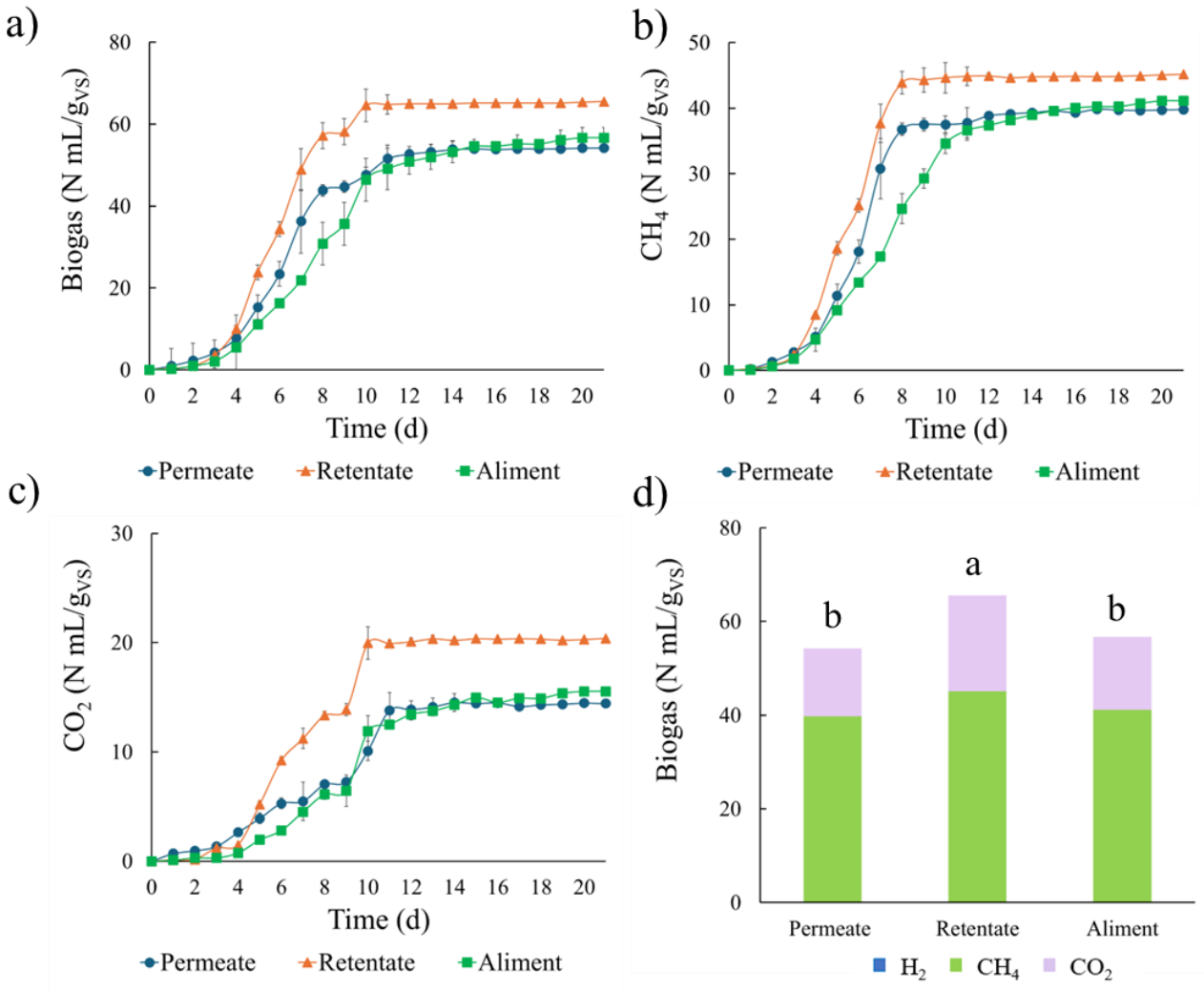

Figure 3.4 Results from the second stage of the second experiment: a) biogas yield, b) CH_4 yield, c) CO_2 yield and d) composition of total biogas produced during AD considering H_2, CH_4 and CO_2.

References

Bao, Meidan, Haijia Su, and Tianwei Tan. 2012. "Biohydrogen Production by Dark Fermentation of Starch Using Mixed Bacterial Cultures of Bacillus Sp and Brevumdimonas Sp." *Energy & Fuels* 26 (9): 5872–78. https://doi.org/10.1021/ef300666m.

Cremonez, Paulo André, Silvio Cesar Sampaio, Joel Gustavo Teleken, et al. 2020. "Effect of Substrate Concentrations on Methane and Hydrogen Biogas Production by Anaerobic Digestion of a Cassava Starch-Based Polymer." *Industrial Crops and Products* 151 (September): 112471. https://doi.org/10.1016/j.indcrop.2020.112471.

Cremonez, Paulo André, Joel Gustavo Teleken, Thompson Ricardo Weiser Meier, Helton José Alves, and Jhony Teleken. 2024. "Two-phase Anaerobic Codigestion of a Cassava Starch-based Biopolymer with Papaya Waste." *Environmental Progress & Sustainable Energy* 43 (4): e14368. https://doi.org/10.1002/ep.14368.

Cremonez, Paulo André, Joel Gustavo Teleken, Thompson Ricardo Weiser Meier, and Helton José Alves. 2021. "Two-Stage Anaerobic Digestion in Agroindustrial Waste Treatment: A Review." *Journal of Environmental Management* 281 (March). https://doi.org/10.1016/j.jenvman.2020.111854.

Das, Satya Ranjan, and Nitai Basak. 2021. "Molecular Biohydrogen Production by Dark and Photo Fermentation from Wastes Containing Starch: Recent Advancement and Future Perspective." *Bioprocess and Biosystems Engineering* 44 (1): 1–25. https://doi.org/10.1007/s00449-020-02422-5.

Domińska, Marlena, Martyna Gloc, Magdalena Olak-Kucharczyk, and Katarzyna Paździor. 2025. "Dark Fermentation of Sizing Process Waste: A Sustainable Solution for Hydrogen Production and Industrial Waste Management." *Water* 17 (11): 1716. https://doi.org/10.3390/w17111716.

Fang, Cheng, Kanokwan Boe, and Irini Angelidaki. 2011. "Biogas Production from Potato-Juice, a by-Product from Potato-Starch Processing, in Upflow Anaerobic Sludge Blanket (UASB) and Expanded Granular Sludge Bed (EGSB) Reactors." *Bioresource Technology* 102 (10): 5734–41. https://doi.org/10.1016/j.biortech.2011.03.013.

Khongkliang, Peerawat, Prawit Kongjan, and Sompong O-Thong. 2015. "Hydrogen and Methane Production from Starch Processing Wastewater by Thermophilic Two-Stage Anaerobic Digestion." *Energy Procedia* 79 (November): 827–32. https://doi.org/10.1016/j.egypro.2015.11.573.

Lu, Xueqin, Guangyin Zhen, Adriana Ledezma Estrada, et al. 2015. "Operation Performance and Granule Characterization of Upflow Anaerobic Sludge Blanket (UASB) Reactor Treating Wastewater with Starch as the Sole Carbon Source." *Bioresource Technology* 180 (March): 264–73. https://doi.org/10.1016/j.biortech.2015.01.010.

Mainardis, Matia, Marco Buttazzoni, and Daniele Goi. 2020. "Up-Flow Anaerobic Sludge Blanket (UASB) Technology for Energy Recovery: A Review on State-of-the-Art and Recent Technological Advances." *Bioengineering* 7 (2): 43. https://doi.org/10.3390/bioengineering7020043.

Nasr, Mahmoud, Ahmed Tawfik, Shinichi Ookawara, and Masaaki Suzuki. 2013. "Biological Hydrogen Production from Starch Wastewater Using a Novel Up-Flow Anaerobic Staged Reactor." *BioResources* 8 (4): 4951–68. https://doi.org/10.15376/biores.8.4.4951-4968.

Sutthipattanasomboon, Chonlapin, and Jaruwan Wongthanate. 2017. "Enhancement of Biohydrogen Production from Starch Processing Wastewater and Further inside Its Ecosystem Disclosed by 16S rDNA Sequencing and FISH." *Brazilian Archives of Biology and Technology* 60 (0). https://doi.org/10.1590/1678-4324-2017160260.

Taherdanak, Mohsen, Hamid Zilouei, and Keikhosro Karimi. 2015. "Investigating the Effects of Iron and Nickel Nanoparticles on Dark Hydrogen Fermentation from Starch Using Central Composite Design." *International Journal of Hydrogen Energy* 40 (38): 12956–63. https://doi.org/10.1016/j.ijhydene.2015.08.004.

Wadjeam, Parichat, Alissara Reungsang, Tsuyoshi Imai, and Pensri Plangklang. 2019. "Co-Digestion of Cassava Starch Wastewater with Buffalo Dung for Bio-Hydrogen Production." *International Journal of Hydrogen Energy* 44 (29): 14694–706. https://doi.org/10.1016/j.ijhydene.2019.04.138.

Zhang, Zhiping, Congcong Xu, Yue Zhang, et al. 2020. "Cohesive Strategy and Energy Conversion Efficiency Analysis of Bio-Hythane Production from Corncob Powder by Two-Stage Anaerobic Digestion Process." *Bioresource Technology* 300 (March): 122746. https://doi.org/10.1016/j.biortech.2020.122746.

Chapter 4

4. Dark fermentation and anaerobic digestion applied to animal-based biomasses

Paragraphs 4.2 and 4.3 of this chapter were developed in collaboration with the University of Western Ontario (London, Canada) under the supervision of Dr. George Nakhla and his research team. The direct contribution of the thesis author is limited to paragraph 4.2, which presents the results of the research conducted during her visiting period at Western University. Paragraph 4.3 reports the continuation of this research, which was carried out by Dr. Nakhla and his teams.

Part of this research will be part of a publication:
Basem Haroun, Mohamed El-Qelish, Hossein Naeimi, Gaia Mazzanti, Christopher Muller, Embrey Bronstad, Shubhashini Oza, Farokh Kakar, Katherine Y. Bell, Tonia Tommasi, Francesca Demichelis, George Nakhla.
*"***Integration of Microbial Hydrolysis by the Enriched Hyper-thermophilic Cellulose Degrading *Caldicellulosiruptor bescii* with Anaerobic Digestion***"**
(under review).

4.1 Dark fermentation of cow manure and milk wastewater

In the previous chapter, dark fermentation (DF) and anaerobic digestion (AD) were applied to plant-based biomasses, resulting in the production of relevant amounts of both H_2 and CH_4. However, agro-industrial residues also include animal-based biomasses, such as manure and dairy-related waste streams, which represent an important and widely available resource.

Cow manure (CM) is the dominant type of livestock waste, accounting for approximately 75 % of total manure production and reaching about 1.4 billion tons per year in the European Union. Its composition strongly depends on the manure management system. For instance, liquid manure is typically generated in facilities with slatted floors, whereas solid manure is produced when animals are housed on bedding materials such as straw or sawdust. Manure is commonly applied directly to agricultural land because of its high nutrient content, including N, P, K, S, and Mg. These elements contribute to soil fertility and help regulate soil pH (Köninger et al. 2021). However, direct land application is also associated with several environmental risks. Pathogens present in manure may contaminate soil and water bodies, while excess nutrients can lead to leaching and increased pollution.

Composting has been proposed as an alternative management option, but this practice is linked to greenhouse gas emissions due to carbon and nitrogen losses during the process (Font-Palma 2019). In addition, emissions may also occur during manure collection, storage, and treatment, mainly as a result of ammonia volatilization (Köninger et al. 2021).

Dairy industries are a relevant agri-food sector in Italy since 13 Mt of milk were gathered in 2021 (ISTAT Official Statistic Data on the Italian Agricultural Sector, 2021). Dairy product generation is associated with the production of cheese whey, which is characterized by a high BOD and COD. It mostly contains lipids, carbohydrates, soluble vitamins, minerals, and protein (Ahmad et al. 2019). Another by-product of dairy production is the wastewater generated in milking parlors. After fresh milk is collected from cows, the milking equipment and surrounding areas are rinsed with clean water, producing a wastewater stream that is chemically similar to diluted milk.

Numerous studies have investigated the application of DF and AD to CM and dairy industry wastes, either as standalone processes or within a two-stage anaerobic digestion (TSAD) configuration. Xing et al. (2010) studied DF of dairy manure using 250 mL serum bottles operated at 36 °C. In this work, H_2-producing microorganisms were obtained by heating the manure itself in an infrared oven for 2 h. Before DF, the substrate was subjected to different pretreatments to identify the most suitable strategy for H_2 production, including acidic pretreatment with HCl, alkaline pretreatment with NaOH, and infrared treatment. While untreated manure achieved an H_2 yield of 13 mL/g_{VS}, the highest yield (18 mL/g_{VS}) was obtained after acidic pretreatment. Shuang Liu et al. (2020) examined DF of cattle manure co-digested with food waste in 500 mL flasks at 35 °C, achieving an H_2 yield of 30.22 mL/g_{VS}. The higher yield compared to mono-digestion studies was attributed to improved nutrient balance resulting from co-digestion of the two substrates. Thermophilic DF of cow manure was investigated by Wang et al. (2013) using a 2 L semi-continuous CSTR operated at 50, 60, and 70 °C. H_2 yields of 5.73, 10.25, and 3.3 mL/g_{VS} were obtained, respectively. Although the highest production was observed at 60 °C, the overall yields remained relatively low. This behavior was likely caused by rapid accumulation of volatile fatty acids (VFAs), which led to microbial inhibition over a short operational period. Similar

results were reported by (Yokoyama et al. 2007) who tested dry DF of cow manure at 37, 47, 55, 60, 67 and 75 °C in 625 mL glass bottles. They reached a maximum H_2 yield of 0.09 mL/g_{VS} at 60 °C.

TSAD applied to cow manure has been investigated in several studies, often in combination with co-substrates to improve process performance. Bertin et al. (2013) evaluated the TSAD of a mixture of cow manure and cheese whey using different volumetric ratios, ranging from 0% to 100% with 10% incremental variations. DF was carried out in 100 mL glass bottles at 35 °C. The highest H_2 yield, equal to 84 mL/g_{VS}, was achieved with a 50:50 manure-to-whey ratio, while the subsequent AD stage produced 258 mL/g_{VS} of CH_4. Both results were considered satisfactory, with the H_2 yield being notably higher than those reported for mono-digestion of manure, further highlighting the advantages of co-digestion in TSAD systems.

Favorable outcomes were also reported for TSAD of cheese whey alone. Lembo et al. (2022) conducted TSAD using two continuously fed CSTR reactors, obtaining an H_2 yield of 120 mL/g_{VS} and a CH_4 yield of 340 mL/g_{VS}. These results confirm the high suitability of dairy industry residues, particularly cheese whey, as feedstocks for TSAD, due to their high biodegradability and favorable composition for both hydrogen and methane production.

4.1.1 Goal

To the best of the authors' knowledge, DF or AD applied to CM in combination with milk wastewater (MWW) has not been specifically addressed in the available literature.

To address the limited data on MWW, this study examines its behavior when combined with a widely used substrate such as cattle manure in DF. The use of MWW also allows partial replacement of fresh water by exploiting its intrinsic moisture content.

Overall, the results provide further insight into the applicability of DF and anaerobic digestion for mixed agro-industrial residues. They also support the evaluation of these systems within a circular economy framework.

4.1.2 Materials and method

4.1.2.1 Substrates and inoculum characterization

The inoculum employed in DF and AD was the mesophilic digestate of cow-agricultural sludge (CAS) provided by "Cascina La Speranza" (Fossano, Cuneo, Italy). CM and MWW were supplied by a local agricultural cooperative (Piedmont, Italy). Fruit and vegetable waste (FVW) was collected from household residue (mass composition of 75% vegetables and 25 % fruits) and chopped through a kitchen blender. MWW and FVW was frozen at -18 °C after its collection to avoid natural decomposition while CM was stored in laboratory fridge at 5 °C. MWW and FVW was defrosted before being fed into the

fermentation system. CM, MWW and inoculum characterization are presented in *Table 4.1*.

4.1.2.2 Inoculum and substrates pretreatment

In the present study, inoculum was thermally pretreated at 80 °C for 1 h to eliminate H_2-consumers and favor sporulation of H_2-producers. Similarly, MWW was subjected to thermal pretreatment at 80 °C for 1 h to suppress the activity of potential methanogens originating from the feedstock. Both the inoculum and MWW were heated in an oven and covered with aluminum foil to minimize water evaporation during treatment. For the same purpose, CM underwent acid pretreatment as suggested by Xing et al. (2010). The pH of the manure was adjusted to 4 by the gradual addition of 3 M HCl, monitored using a pH meter.

4.1.2.3 Process setup and operative condition

DF was performed in 250 mL Pyrex glass bottles (Duran, Germany) with a working volume of 80% at 35°C. The heating was controlled by a 55 L thermostatic water bath (Julabo-Corio-C, Merck, Germany). Reactors were operated in batch feeding mode with 6 % of total solids and shaken manually to keep the mixture homogeneous inside the reactor. Each reactor was sealed with a two-port cap. Through one of the ports, anaerobic conditions were assured by purging N_2 directly inside the biomass to change the volume of the reactor three times and closing the port. The second port was connected to a 1 L Tedlar gasbag, where biogas was collected. The duration of each assay depended on biogas or H_2 production: testing was stopped when daily H_2 (for DF tests) production was less than 1% of the overall production recorded during the period of preparation (VDI 4630 2006). The pH of each reactor was measured at the beginning and at the end of the experiments. HCl was added to the reactors to lower the pH to around 7 in DF. The experimental campaign consists of three configurations varying the substrate: manure alone, co-digestion of FVW and CM (in a ratio 50/50 %, based on VS), and co-digestion of MWW and CM (in a ratio 95/5 %, based on VS). The experiments were studied in replicates.

DF design, analytical methods, and data processing were carried out in accordance with the procedures described in Sections 2.2.4 and 2.2.5 of this thesis.

4.1.3 Results

The inoculum and substrates were characterized in terms of TS, VS and elemental composition using a CHNS analyzer. The results are reported in *Table 4.1*. The TS contents of the inoculum and FVW were comparable, whereas MWW showed a markedly lower TS content, below 1 %, reflecting its highly diluted nature. In contrast, CM exhibited more than twice the TS content of the other substrates. As the TS fraction exceeded 20 %, CM can be classified as a dry substrate according to Köninger et al. (2021b).

All substrates displayed a high VS fraction, indicating a predominance of organic matter that is readily biodegradable, in line with previous findings (Martínez-Mendoza et al. 2023).

The TS content of CM observed in this study is within the range commonly reported in the literature, typically between 20 % and 35 %. However, the VS/TS ratio of the CM samples was higher than values generally reported, which usually range between 70 % and 80 % (Bertin et al. 2013; Margarita A. Dareioti et al. 2022; S. Liu et al. 2020; Nkemka et al. 2014).

Elemental analysis highlighted carbon (C) and nitrogen (N) as key parameters for evaluating substrate suitability for biological processes. As expected, CM and MWW showed higher nitrogen contents than FVW, reflecting their animal-based origin. Nevertheless, both substrates exhibited C/N ratios within ranges considered appropriate for DF and AD.

Table 4.1 Chemical and physical characterization of inoculum, fruit and vegetable waste (FVW), milk wastewater (MWW) and cow manure (CM).

	Inoculum	**FVW**	**MWW**	**CM**
TS (%)	8.85 ± 0.25	10.89 ± 0.36	0.51 ± 0.07	25.53 ± 0.24
VS/TS (%)	73.24 ± 0.45	85.04 ± 0.31	96.68 ± 0.07	91.62 ± 3.24
N (%)	2.83 ± 0.22	1.52 ± 0.13	2.90 ± 0.02	3.89 ± 0.68
C (%)	36.33 ± 0.77	41.65 ± 0.74	53.74 ± 3.98	61.23 ± 9.83
H (%)	4.15 ± 0.02	6.35 ± 0.18	7.40 ± 0.28	5.79 ± 0.34
S (%)	0.57 ± 0.02	0.21 ± 0.01	0.34 ± 0.04	0.78 ± 0.06
O (%)	56.13 ± 0.54	50.27 ± 0.99	35.63 ± 4.23	28.32 ± 10.76
C/N	12.91 ± 1.22	27.49 ± 2.14	18.54 ± 4.30	15.79 ± 0.92

The experiment was carried out under three different configurations based on substrate composition: CM combined with FVW, CM alone, and CM combined with MWW. *Figure 4.1-a* and *-b* show the cumulative production of biogas and H_2 over a 4-day period for the three configurations. Clear differences in gas production trends were observed among the tested conditions.

When FVW was included as a co-substrate, higher biogas production was achieved compared to the other configurations. In addition, H_2 production showed a slight improvement in the presence of FVW, reaching 8 N mL/g_{VS}, whereas both CM and CM+MWW produced negligible amounts of H_2, with final yields close to 0 N mL/g_{VS}. These results indicate that the addition of FVW contributed to enhanced H_2 formation, likely due to its high content of readily fermentable carbohydrates. In contrast, substrates of animal origin appeared to strongly limit H_2 production. Despite the positive effect of FVW, the overall H_2 yield remained too low to be considered satisfactory for DF.

CO_2 production (*Figure 4.1-d)* followed trends like those observed for H_2. The CM+FVW configuration showed the highest cumulative biogas and CO_2 yields, reaching 120 and 100 N mL/g_{VS}, respectively. Lower values were

measured for CM+MWW (23 and 20 N mL/g_{VS}) and CM alone (15 and 13 N mL/g_{VS}). Notably, CH_4 production did not display a flat or negligible profile in any of the tested conditions. Instead, all configurations showed a continuous increase in CH_4 concentration from day 0 to day 4, suggesting that methanogenic activity was not fully suppressed *Figure 4.1-c*. Although final CH_4 yields remained below 7 N mL/g_{VS}, the increasing trends indicate that methanogenesis was progressively developing and beginning to compete with H_2-producing pathways.

Gas composition analysis further supports these observations. Only the CM+FVW configuration showed a detectable H_2 fraction, accounting for approximately 7 % of the total biogas, followed by 6 % CH_4, while CO_2 represented the dominant component (87 %). Similarly high CO_2 proportions were observed in CM and CM+MWW, accounting for 84 % and 89 %, respectively, with CH_4 representing most of the remaining fraction (approximately 15 and 11 %).

Overall, the results indicate that DF was not effectively established under the tested conditions, as reflected by the very low H_2 yields. While the addition of FVW slightly improved H_2 production due to its favorable substrate characteristics, co-digestion with CM was insufficient to sustain an efficient DF process. The poor performance can be attributed to the intrinsic nature of CM and MWW, which are likely to contain active methanogenic populations due to their animal origin. Although pretreatments were applied to both substrates, they were not sufficient to fully inhibit methanogens. It is likely that these microorganisms survived the pretreatment, remained metabolically active, and eventually outcompeted H_2-producing bacteria. For this reason, the second stage of TSAD was not performed.

The low H_2 yields observed in this study are consistent with previous literature on DF of cow manure. Xing et al. (2010), Wang et al. (2013) and Yokoyama et al. (2007) reported maximum H_2 yields of 18, 10, and 0.09 N mL/g_{VS}, respectively. Additional experiments were conducted to confirm these findings; additional experiments were conducted on this process but are not reported here to maintain a focused scope and manageable length of the thesis. However, they further indicated that animal-based biomasses may not be suitable substrates for DF, primarily due to their microbial composition. Nevertheless, such substrates have demonstrated good performance in conventional AD, despite certain limitations. Accordingly, the second part of this chapter focuses on the intensification of AD applied to substrates rich in lignocellulosic compounds, such as primary sludge and cow manure, to improve CH_4 yields and overall biodegradability of biomass waste.

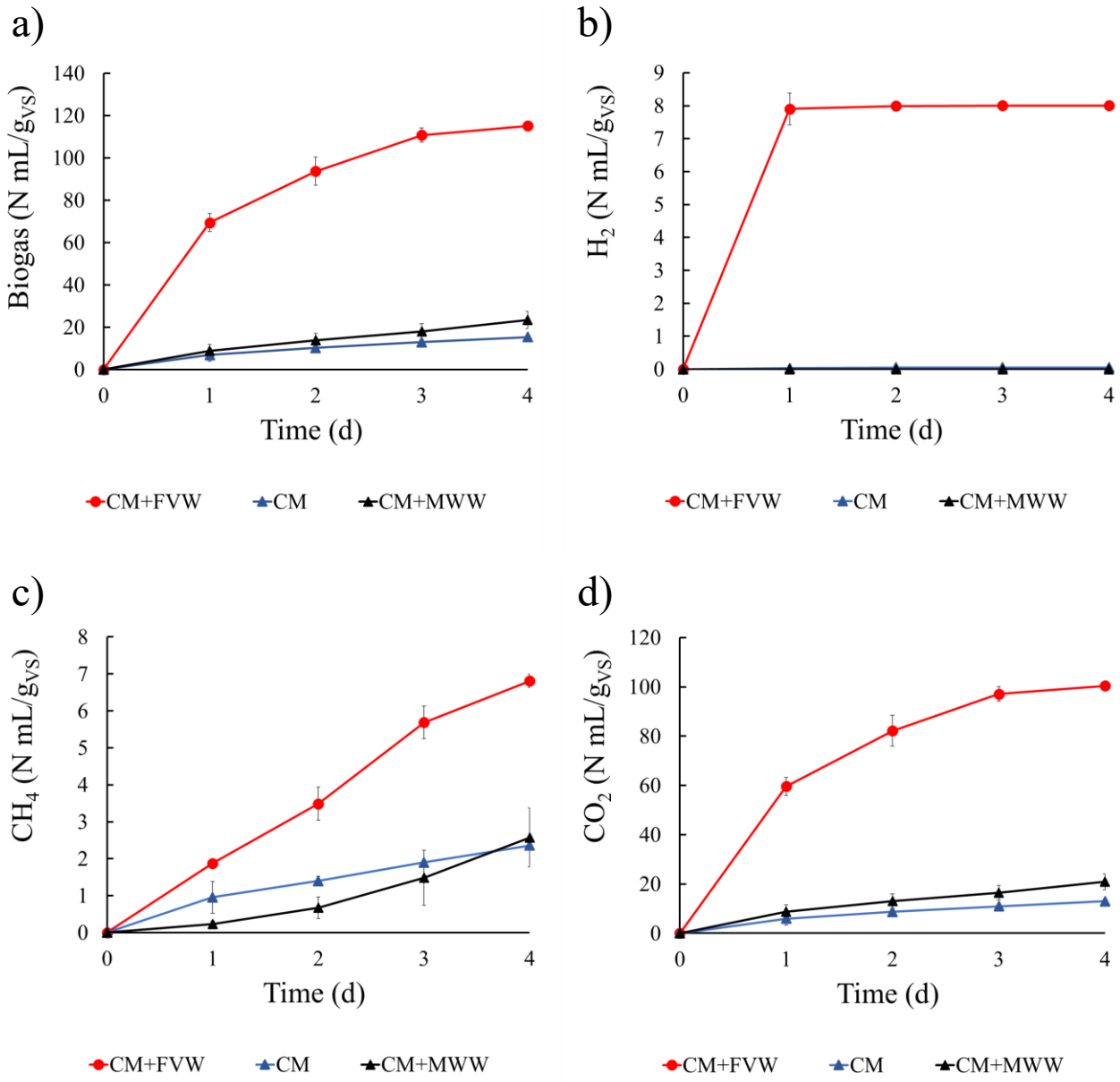

Figure 4.1 Results from the DF: a) biogas yield, b) H_2 yield, c) CH_4 yield and d) CO_2 yield.

4.2 Mesophilic anaerobic digestion of primary sludge: impact of feeding mode and post hyper-thermophilic hydrolysis process

As mentioned before, animal-based biomasses have gained interest as renewable resources for energy production. Among them, manure is an important feedstock due to its abundance and relatively high calorific value. On the other hand, its good management is essential due to its CH_4 emissions as well as the contamination of soil with pathogens (Samoraj et al. 2022). Another interesting biomass waste is primary sludge (PS), which is collected at the bottom of the primary clarifier in wastewater treatment plants (Sakaveli et al. 2024). Primary sludge has a high energy content due to the presence of biodegradable compounds such as proteins, carbohydrates, cellulose, and other organic material. Cellulose originated from toilet paper flushed in public sewers and represents 30-50% of suspended solids in wastewater (Crutchik et al. 2018). Both manure and primary sludge can be employed as substrate for AD but even though they contain some easily biodegradable matter, they also contain recalcitrant materials. Manure, which is an agricultural biomass waste, contains lignocellulosic compounds that are refractory to AD due to the cross-linked structure between lignin, cellulose, and hemicellulose. This structure hinders the enzymatic activity during fermentation, allowing just 40-50 % of its conversion. Enhancing the hydrolysis stage is essential to address current limitations, and this can be achieved through various pretreatment strategies (J. R. Kim and Karthikeyan 2021; S. R. Paudel et al. 2017; Ahring et al. 2015). Among them, thermal pretreatments have been extensively studied as they are associated with relatively simple operative conditions and low investments as well as high efficiency. However, thermal hydrolysis of lignocellulosic biomass usually takes place at approximately 160 °C and 6.1 atm, causing high operational costs (S. Kim et al. 2023). Moreover, the digestion substrate usually contains a portion of readily biodegradable matter, which makes pretreatment just a resource an energy waste. As an alternative to pretreatment, post-digestion treatment has recently gained interest as a lower volume of biomass is treated, allowing lower costs (Svensson, Kjørlaug, et al. 2018).

Several studies report that post-treatments can enhance organic matter solubilization or VS removal.

Hartmann and Ahring (2005) applied hyper-thermophilic post-digestion to OFMSW and achieved a substantial increase in VS removal (from 74 % to 89 %). However, this did not translate into higher CH_4 yields and resulted in reduced methane production in the second stage. Similarly, Kaparaju and Rintala (2005) tested mechanical, thermal, chemical, and freeze–thaw post-treatments on the solid fraction of digested cow manure. Despite reductions in TS and VS, no significant improvement in CH_4 yield was observed, indicating limited benefits of post-treatment for manure-based digestate. Negative or negligible effects were also reported by Sambusiti et al. (2015), where thermal and alkaline post-

treatments reduced CH_4 production, likely due to the formation of inhibitory compounds or changes in soluble COD composition. Axelsson Bjerg et al. (2024) further showed that moderate thermal post-treatment was not suitable for digestate rich in manure, as it led to process instability and VFAs accumulation.

Other studies demonstrate that post-treatment can be effective, particularly for digestates with lower manure content. Boe et al. (2009) reported that thermal post-digestion at 55 °C and 37 °C of digested cow and pig manure led to additional biogas production (11.7% and 8.4%, respectively), while also improving process stability.

Svensson, Kjørlaug, et al. (2018) observed increased methane yields and solubilization after applying high-temperature thermal post-treatments (134-175 °C) to food waste and sludge digestates, with stronger effects at higher temperatures and longer treatment times. Nordell et al. (2022) confirmed that thermal post-treatment at 70 °C effectively increased dissolved organic carbon and methane potential across several digestates, while remaining more feasible for scale-up compared to higher-temperature options. Enzymatic post-treatment also showed positive effects in Sambusiti et al. (2015), enhancing biodegradability without the negative impacts observed for thermal and alkaline treatments.

Most studies on digestate post-treatment focus on batch configurations, where treated digestate is evaluated in separate reactors or through biochemical methane potential (BMP) tests. These works generally report improvements in methane yield and organic matter solubilization, but they do not represent fully integrated digestion systems. While useful for screening purposes, batch studies provide limited insight into long-term process performance and stability under continuous operation.

A limited number of studies have explored post-treatment coupled with digestate recirculation to the main digester, demonstrating potential benefits in terms of methane production and process stability.

Dohdoh (2019) showed that digestate recirculation can improve overall methane yield and stabilize anaerobic digestion. Takashima (2008) applied a thermal post-treatment at 120 °C to digested sewage sludge and recirculated the treated fraction into a continuous digester. This approach resulted in increased VS removal (6.3%) and a 21% increase in CH_4 production, confirming the effectiveness of moderate thermal post-treatment combined with recirculation.

Bolzonella et al. (2020) further investigated this concept using digestate from a manure-straw AD plant. Hyper-thermophilic post-treatment at 65 °C led to methane yield increases of 15% in BMP tests and up to 38% in semi-continuous experiments, with higher gains observed at longer post-treatment HRTs.

Operational parameters such as feeding strategy play a critical role in the stability and performance of anaerobic systems treating both sludges and manure. Excessive OLR can lead to VFAs accumulation and process inhibition, while pulse feeding strategies may overstimulate microbial activity and destabilize the system (Crutchik et al. 2018; Winter and Pearce 2008). Intermittent feeding has been proposed as an effective approach to enhance microbial resilience and maintain stable CH_4 production.

Intermittent feeding in anaerobic digestion has been examined in several studies. For example, the work presented in Nebot-Sanz et al. (1995) investigated wastewater from food processing industries treated in thermophilic anaerobic filters equipped with stationary packing material and operated at a working volume of 2.2 L. Wine vinasse was supplied either continuously or semi continuously, and in the latter case, the authors evaluated feeding frequencies of 1, 3, 6, 12, 24, and 48 doses per day while maintaining OLR between 3.5 and 4.4 g_{COD}/L d. The degradation efficiency increased progressively with higher feeding frequencies, reaching a maximum of 94.8 % under continuous operation. In contrast, VFA concentrations decreased as the number of daily doses increased, falling below 200 mg/L at the lowest point. Methane yield, however, was not affected by the feeding frequency. Although continuous mode achieved the highest removal efficiency, the authors noted that intermittent feeding may still provide operational benefits by enhancing process stability and enabling easier control during system disturbances.

Svensson, Paruch, et al. (2018) examined feeding frequency in the mesophilic digestion of steam-exploded food waste in a 6 L reactor operated at 10 d HRT and an OLR of 21 g_{COD}/L d. Feeding once per day and 10 times per day were compared, resulting in methane yields of 236 and 305 mL/$g_{CODadded}$, respectively, demonstrating the benefits of intermittent feeding. VFAs profiles supported this conclusion, particularly with respect to propionic acid, which accumulated to 636 mg_{COD}/L in the once per day system but only 56 mg_{COD}/L in the intermittently fed reactor, indicating that propionic acid oxidation was inhibited under low feeding frequency.

Food waste was used as substrate in AD by Pramanik et al., (2020) in a 160 L mesophilic CSTR operated under two feeding regimes: daily feeding at HRT values of 124, 62, 41, and 31 d, and feeding three times per week at HRT values of 124, 62, and 35 d. The highest biogas yields were observed at 124 d HRT in both cases, at 1.01 and 0.91 L/$g_{VSadded}$, respectively. VS removal reached 88% in the daily-fed system and 58% in the intermittently fed system, while COD removal was 92% and 60%, respectively. These results again illustrate that more frequent feeding improves both biogas production and organic matter removal.

The effect of intermittent feeding was also investigated by Ezieke et al., (2024) by digesting berry fruit waste in a 3 L mesophilic reactor operated at an HRT of 25 d and an OLR of 1 gVS/L d. Feeding once per week and three times per week were compared, and unlike several previous studies, no significant difference in methane yield was observed, with both regimes producing an average of 369 L/kg_{VS}.

Similar findings were reported by Rasit et al. (2024), who examined palm oil mill effluent digestion in two 1 L CSTRs operated at 35 °C with HRTs between 4 and 11 d and OLRs between 13 and 3.6 g_{COD}/L d. Feeding once or twice per day resulted in comparable performance in both digesters, with methane yields of 0.14 L/$g_{CODremoved}$ and CH_4 concentrations of 57 % and 60 % in the biogas, respectively.

Winter and Pearce (2008) investigated the AD of PS through two mesophilic 60 L digesters fed several times per day with either surplus activated sludge (SAS) or PS. While the feeding regime involved multiple daily inputs, the study did not provide specific data on process stability in relation to feeding frequency.

Although literature does not present a fully unanimous perspective regarding the impact of intermittent feeding, most studies highlight advantages associated with pulse feeding. These benefits include improved process stability, reduced shock loading, lower VFAs accumulation, enhanced organic removal, and, in many cases, increased methane production. Collectively, these findings suggest that intermittent feeding can serve as an effective operational strategy for maintaining stable and efficient anaerobic digestion, particularly in systems susceptible to overload or inhibition.

4.2.1 Goal

In this paragraph, advanced anaerobic strategies for the valorization of organic residues are proposed with a specific focus on enhancing bioenergy recovery through targeted thermal interventions and optimized process configurations. To address the challenges associated with sludge stabilization and CH_4 production, the experiment focuses on the anaerobic digestion of PS generated in wastewater treatment plants. First, the influence of the feeding mode was investigated to assess the effectiveness of intermittent feeding on system stability and process performance. Subsequently, considering the high content of complex and slowly biodegradable organic matter in PS, a post-digestion intensification strategy was examined with the aim of enhancing overall biogas yields. Specifically, hyper-thermophilic hydrolysis of digestate sludge was applied at 75 °C with a solid retention time (SRT) of 2 days, followed by recirculation of the treated digestate back to the anaerobic digester. This approach was designed to enhance the solubilization and biodegradability of recalcitrant compounds, thereby increasing methane production without additional external substrates.

Overall, by exploring the anaerobic digestion and post-treatment of PS, this work demonstrates how tailored anaerobic process configurations and thermal strategies can be applied to recalcitrant organic waste matrices. The results contribute to the development of sustainable bioenergy systems that support waste minimization, renewable energy generation, and circular resource management.

4.2.2 Materials and method

4.2.2.1 Substrate and inoculum characterization

Inoculum was the waste activated sludge (WAS) from a wastewater treatment plant. Both WAS and PS were collected from *Greenway Wastewater Treatment Center* (London, Ontario, Canada). After collection, they were stored at 4 °C. Total COD (TCOD), soluble COD (SCOD), ammonia, VFAs, total nitrogen (TN), soluble nitrogen (SN), total suspended solids (TSS), volatile suspended solids (VSS), TS, and VS were analyzed periodically to monitor system performance.

4.2.2.2 Set-up and operative conditions

Two identical anaerobic digestion systems were operated in parallel as CSTRs and are hereafter referred to as the control and test reactors (*Figure 4.2*). Both systems were run under mesophilic conditions (37 °C) and monitored across four consecutive operational phases. Each system consisted of a 10 L anaerobic digester fed with PS at an OLR of 2.7 g COD/L/d and a SRT of 15 d. The digesters were coupled to a dedicated 1 L hyper-thermophilic hydrolysis (HTH) reactor operated at 75 °C with an SRT of 2 d. The digesters were designed for semi-continuous operation and equipped with dedicated ports for feeding, effluent withdrawal, and biogas sampling. Temperature control was ensured through a circulating water jacket connected to a thermostatic water bath, maintaining stable mesophilic conditions throughout the experiment. Mechanical mixing was provided by a high-speed impeller at 3000 rpm to ensure complete homogenization. Anaerobic conditions were established by purging the reactor headspace with nitrogen gas prior to start-up. The experimental campaign aimed to assess (i) the impact of feeding strategy on digester stability and performance and (ii) the effectiveness of HTH as a post-treatment step for digested PS. The study was structured into four operational phases. During the first phase (day 0-75), both digesters were operated under conventional feeding conditions, receiving a single daily feed of PS corresponding to an average organic input of 27 g COD/d. In the second phase (day 76-171), an intermittent feeding regime was implemented, in which the daily PS load was divided into three equal feedings per day. This feeding strategy was maintained during the third phase (day 172-206) to allow the systems to reach steady-state conditions, typically achieved after approximately three hydraulic retention time turnovers. In the final phase (day 207-265), hyper-thermophilic hydrolysis was introduced as a post-digestion intensification step. A portion of the digested sludge was treated in the HTH reactor and subsequently recirculated to the main digester. The recirculation ratio was set at 75%, corresponding to a feed mixture of 500 mL of HTH effluent combined with 667 mL of fresh PS.

4.2.2.3 Analytical methods and data elaboration

TCOD, SCOD, ammonia, VFAs, TN, and SN were analyzed using HACH methods and test kits (HACH Odyssey DR/2500 spectrophotometer manual). TSS, VSS, TS, and VS were analyzed according to Standard Methods for the Examination of Water and Wastewater (Rice et al. 2012). Daily biogas production was measured using a wet-tip gas meter (Rebel Wet-Tip Gas Meter Company, Nashville, TN, USA) while biogas composition including methane and carbon dioxide was characterized using a gas chromatograph (Model 310, SRI Instruments, Torrance, CA) equipped with a thermal conductivity detector (TCD) and a molecular sieve column (Mole sieve 5 A, mesh 80/100, 6 ft. 1/8 in). Argon was used as a carrier gas at a flow rate of 30 mL/min, and the temperature of the column and thermal conductivity detector (TCD) were 90 °C and 105 °C, respectively. Lignin, cellulose, and hemicellulose were characterized weekly for

raw PS, DPS, and HTHs effluent according to NREL methods (Sluiter et al. 2008).

a)

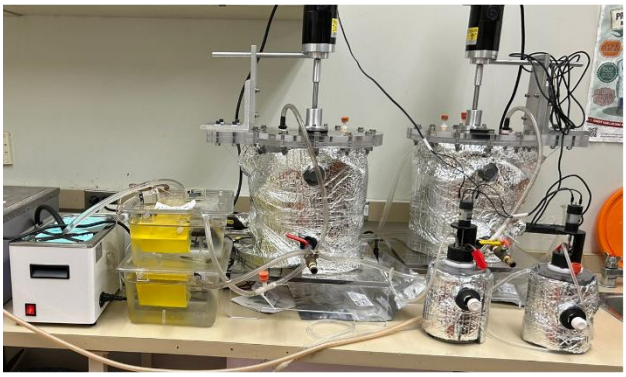

b)

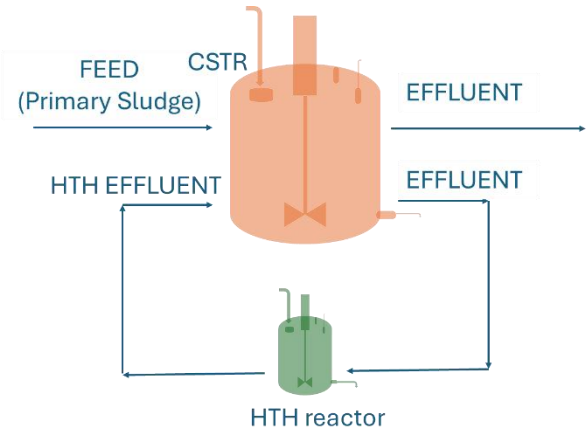

Figure 4.2 a) Experimental setup and b) schematic representation of the system, featuring a 10 L CSTR connected to a 1 L hyper-thermophilic hydrolysis (HTH) reactor.

4.2.3 Results

4.2.3.1 Influence of intermittent feeding on performance of PS-fed digesters

The performance of the two 10 L CSTRs is presented in *Figure 4.3-a* expressed as liters of CH_4 per gram of COD added. The discussion in this section focuses primarily on the effect of intermittent feeding on overall process stability.

During the initial feeding phase, the PS fed to the reactors had average TS and VS concentrations of 27200 and 20500 mg/L, respectively, while the average TCOD and SCOD values were 39677 and 5109 mg/L, as shown in *Table 4.2*. The initial pH of the PS was 5.4, and the alkalinity was 2.6 g_{CaCO3}/L, which are typical values for primary sludge and are likely related to its VFAs concentration of approximately 1.6 g/L (Abdelrahman et al. 2023). From day 0 to 75, the system exhibited marked instability, which is clearly reflected in the fluctuations of the curve. CH_4 production averaged 0.14 ± 0.09 L/$g_{CODadded}$, with a biodegradability of 34 ± 21 %, indicating substantial variability in reactor performance. The large standard deviation highlights alternating phases of elevated CH_4 generation followed by periods of nearly no production. The instability of the system is further reflected in the SCOD removal efficiencies, which were only 20% in CSTR 1 and nearly 0% in CSTR 2, indicating clear accumulation of soluble organics in the reactors due to insufficient methanogenic activity. This is consistent with the average SCOD concentrations measured during the period, which were 4037 mg/L in CSTR 1 and 5141 mg/L in CSTR 2.

This behavior is further supported by the temporal profile of VFAs shown in *Figure 4.3-b*, where both CSTRs display highly variable VFAs concentrations throughout the 244 day evaluation (with an average of 1.6 and 2.6 g/L in CSTR 1 and CSTR 2, respectively). In AD, VFAs produced during the acidogenesis and acetogenesis stages should be converted to CH_4 by methanogenic

microorganisms. Accumulation of VFAs is generally indicative of process imbalance or failure, as it reflects an interruption in their conversion. Moreover, excessive VFAs accumulation, typically above 8 g/L, can result in process inhibition (Cremonez et al. 2021). In the present study, the highest VFAs concentrations occurred during the first operational stage, when the reactors were fed once per day. Under these conditions, VFAs levels reached a maximum of 6 g/L in CSTR 1 and 3.7 g/L in CSTR 2. Although these values remained below the reported inhibition threshold and therefore did not lead to complete system failure, they were nonetheless associated with minimal CH_4 production, falling to only 0.04 and 0 $L/g_{CODadded}$ for CSTR 1 and CSTR 2, respectively.

Beginning on day 76, an intermittent feeding strategy was introduced to restore system stability and improve both CH_4 production and organic matter removal. The feeding frequency was increased from once per day to 3 times per day, while maintaining a total average organic loading of 27.7 g_{COD}/d. During this phase, the PS fed to the reactors had average TS and VS concentrations of 32500 and 24300 mg/L, respectively, and average TCOD and SCOD values of 37616 and 4792 mg/L. The initial pH of the PS was 6.1, and the alkalinity was 3.5 g_{CaCO3}/L.

Despite the change in feeding strategy, the reactors continued to exhibit signs of instability until approximately day 171, a behavior that can be attributed to the microbial community's need to adapt to the new operational regime. During this transitional phase, CH_4 production averaged 0.23 ± 0.09 $L/g_{CODadded}$, and biodegradability reached 57 ± 22 %, reflecting a substantial improvement relative to the initial period of the experiment, with increases of approximately 65 % in both CH_4 yield and biodegradability. Further enhancement was observed from day 172 to day 206, prior to the implementation of high-temperature hydrolysis (HTH) recycling, when CH_4 production increased to an average of 0.245 ± 0.014 $L/g_{CODadded}$ and biodegradability reached 61 ± 3 %. The modest yet steady 8 % increase observed in this phase suggests that the system was nearing steady-state conditions. This is further confirmed by the pronounced reduction in standard deviation values, indicating greater process stability under intermittent feeding. The evolution of VFAs concentrations provides an even clearer illustration of the beneficial effect of intermittent feeding. Whereas the once-per-day feeding regime resulted in VFAs accumulation, the transition to intermittent feeding led to a marked decrease, with average concentration dropping to 0.17 g/L in CSTR 1 and 0.18 g/L in CSTR 2. These reductions, corresponding to decreases of 90 and 93 %, respectively, are fully consistent with the improvements observed in CH_4 production and biodegradability. The positive impact of the new feeding strategy was further reflected in the removal efficiencies of organic matter: TCOD removal increased by 12 % in CSTR 1 and 25 % in CSTR 2 when compared with the first operational phase, while VS removal rose by 13 % and 23 %, respectively. The most notable enhancement, however, was observed in SCOD removal, which reached 80 % in CSTR 1 and 79 % in CSTR 2, representing a dramatic improvement over the performance recorded under the once per day feeding mode.

These results demonstrate the effectiveness of intermittent feeding in the anaerobic digestion of primary sludge. By increasing the rate of organic matter conversion to CH_4 and preventing the accumulation of VFAs, the strategy substantially improved overall system performance and contributed to a more stable and efficient digestion process.

Intermittent feeding in anaerobic digestion has been examined in several studies. For example, Ziels et al. (2017) investigated cattle manure and oleate digestion in three 5.5 L mesophilic CSTRs operated with feeding regimes ranging from once every two days to continuous feeding. VFA concentrations exceeded 3000 mg/L under continuous feeding but remained below 100 mg/L in pulse-fed reactors. These results aligned with the higher substrate conversion achieved in the intermittently fed system, where pulse feeding enhanced acetate utilization kinetics and increased tolerance to organic overloading.

A similar evaluation was conducted by Bombardiere et al. (2007) who operated a 40 m^3 thermophilic digester treating chicken litter slurry with loading frequencies of 1, 2, 6, and 12 times per day and a constant daily feed of 50.9 g_{COD}/L d. No statistically significant differences in methanogenic activity were observed across the feeding modes. Biogas production was highest when feeding occurred 6 or 2 times per day, reaching 20.5 and 19.6 m^3/d, respectively, whereas feeding once or 12 times per day resulted in lower production (17.1 and 17.2 m^3/d). The authors highlighted that more frequent feeding may offer operational advantages by facilitating system maintenance and improving process monitoring

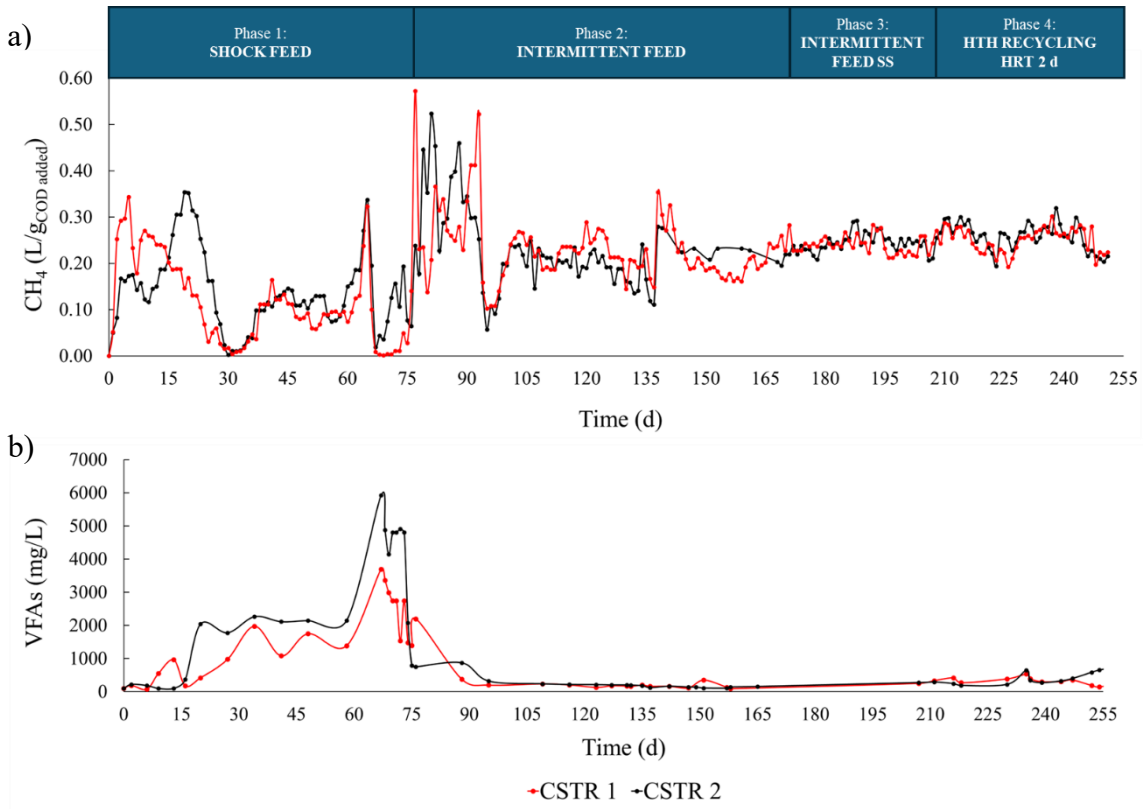

Figure 4.3 Performance of CSTR1 and CSTR 2: a) CH_4 yield as L/$g_{COD added}$ and b) VFAs concentrations as mg/L.

Table 4.2 Characterization of PS, CSTR 1, CSTR 2, HTH 1, HTH 2 during the four phases of the process.

Phase 1 (Day 0 – 75)	PS	CSTR 1	CSTR 2
pH	5.4 ± 0.4	7.5 ± 0.4	7.5 ± 0.4
Alkalinity (g/L)	2.6 ± 0.6	6.0 ± 2.2	6.1 ± 2.3
TCOD (mg/L)	39680 ± 5150	22870 ± 5980	26180 ± 9300
SCOD (mg/L)	5110 ± 1440	4040 ± 1440	5140 ± 3930
PCOD (mg/L)	34570 ± 3710	18830 ± 3710	21040 ± 5370
VFAs (mg/L)	1660 ± 1420	1630 ± 1170	2650 ± 2020
TN (mg/L)	1330 ± 210	1430 ± 200	1390 ± 260
SN (mg/L)	260 ± 90	670 ± 110	700 ± 110
Ammonia (mg/L)	190 ± 80	590 ± 120	610 ± 110
TS (g/L)	27.2 ± 2.9	18.2 ± 2.3	19.1 ± 2.7
VS (g/L)	20.5 ± 2.2	10.4 ± 1.6	11.6 ± 2.3
TSS (g/L)	24.0 ± 2.8	16.5 ± 2.2	17.2 ± 2.4
VSS (g/L)	18.9 ± 2.2	11.2 ± 1.9	11.2 ± 3.1

Phase 2 (Day 76 – 167)	PS	CSTR 1	CSTR 2
pH	6.1 ± 0.6	7.8 ± 0.2	7.7 ± 0.2
Alkalinity (g/L)	3.6 ± 1.2	5.7 ± 1.2	5.6 ± 0.9
TCOD (mg/L)	36800 ± 13530	15550 ± 5930	15690 ± 5700
SCOD (mg/L)	4800 ± 1370	970 ± 110	1030 ± 110
PCOD (mg/L)	32010 ± 12160	14580 ± 5820	14660 ± 5520
VFAs (mg/L)	2850 ± 290	170 ± 30	190 ± 40
TN (mg/L)	1230 ± 200	1420 ± 180	1390 ± 150
SN (mg/L)	270 ± 70	740 ± 70	760 ± 130
Ammonia (mg/L)	290 ± 110	730 ± 60	760 ± 100
TS (g/L)	32.6 ± 7.0	19.8 ± 2.4	18.4 ± 2.1
VS (g/L)	24.3 ± 6.7	10.5 ± 1.5	10.4 ± 1.7
TSS (g/L)	26.7 ± 2.1	16.8 ± 2.1	17.3 ± 2.9
VSS (g/L)	20.8 ± 4.4	9.9 ± 0.9	9.9 ± 1.2

Phase 3-4 (Day 168 – 265)	PS	CSTR 1	CSTR 2	HTH 1	HTH 2
pH	5.5 ± 0.2	7.7 ± 0.1	7.8 ± 0.2	7.9 ± 0.1	8.1 ± 0.1
Alkalinity (g/L)	0.9 ± 0.1	3.8 ± 0.1	3.8 ± 0.1	3.8 ± 0.1	3.8 ± 0.1
TCOD (mg/L)	44650 ± 4950	13780 ± 880	13750 ± 1160	13140 ± 9000	13600 ± 1510
SCOD (mg/L)	4740 ± 1440	620 ± 270	900 ± 660	3000 ± 400	2100 ± 400
PCOD (mg/L)	36910 ± 3510	13160 ± 610	11040 ± 540	11040 ± 500	11640 ± 1110
VFAs (mg/L)	1670 ± 400	320 ± 100	370 ± 170	660 ± 190	610 ± 110
TN (mg/L)	780 ± 570	760 ± 520	820 ± 580	890 ± 610	810 ± 550
SN (mg/L)	290 ± 230	460 ± 370	870 ± 730	590 ± 480	730 ± 600
Ammonia (mg/L)	160 ± 120	430 ± 280	450 ± 300	500 ± 350	520 ± 320
TS (g/L)	29.3 ± 5.0	14.4 ± 3.8	13.3 ± 3.1	12.9 ± 3.8	12.6 ± 3.6
VS (g/L)	24.6 ± 5.4	9.4 ± 2.2	9.1 ± 2.5	8.4 ± 2.0	8.3 ± 1.6
TSS (g/L)	27.4 ± 4.5	13.3 ± 3.5	12.3 ± 2.7	11.7 ± 3.5	11.2 ± 3.5
VSS (g/L)	20.9 ± 3.9	7.9 ± 0.9	7.2 ± 0.7	6.6 ± 0.3	6.8 ± 1.1

4.2.3.2 Application of hyper-thermophilic hydrolysis at 2d HRT

This section examines the application of HTH as a post-treatment step for digested primary sludge (DPS) at an HRT of 2 d. After the post-treatment, the

sludge produced in HTH 1 and HTH 2 was recirculated back into the main digesters, CSTR 1 and CSTR 2.

Both HTH reactors produced biogas containing 30-35 % of CH_4. From day 206 to day 244, 42.9 mL/d of CH_4 was formed, corresponding to 0.12 $g_{CODremoved}$/d. The physicochemical characteristics of the effluents from CSTR 1 and CSTR 2 are compared with those from HTH 1 and HTH 2. In CSTR 1 and CSTR 2, the degrees of solubilization were 80 ± 36 and 124 ± 87 mg_{SCOD}/g_{VSS}, respectively, while substantially higher values were observed in HTH 1 and HTH 2, reaching 319 ± 61 and 289 ± 90 mg_{SCOD}/g_{VSS}. A similar trend was observed for acidification, expressed as mg_{VFAs} per g_{VSS}: values of 80 ± 19 and 41 ± 36 mg_{VFAs}/g_{VSS} were recorded in CSTR 1 and CSTR 2, whereas HTH 1 and HTH 2 achieved 100 ± 20 and 90 ± 25 mg_{VFAs}/g_{VSS}. These results indicate that the recirculation of HTH-treated sludge introduces a higher fraction of soluble compounds back into the main reactors, supplying material that is more readily biodegradable by methanogens and therefore expected to enhance overall reactor performance.

Further insights are obtained by evaluating TCOD, SCOD, and VS removal. During the previous phase, when intermittent feeding was applied to stabilize the reactors and improve CH_4 production, TCOD removal reached 53 % in both CSTR 1 and CSTR 2, respectively. SCOD removal was 80 % and 79 %, while VS removal was 54 % in both reactors. All these parameters improved after the introduction of HTH post-treatment, consistent with the increase in soluble compounds entering the system. TCOD removal rose to 67 % in both CSTR 1 and CSTR 2, SCOD removal reached 87 % in CSTR 1 and 81 in CSTR 2, and VS removal increased by 9 and 12 % in CSTR 1 and CSTR 2, respectively.

These improvements are also reflected in CH_4 production and biodegradability. As previously described, the implementation of intermittent feeding produced an initial adaptation phase in which performance improved compared to the first stage of the experiment, although full stability had not yet been established. Steady-state conditions were reached around day 171. The addition of the HTH post-treatment further enhanced system performance, with CH_4 yields reaching 0.3 ± 0.0 $L/g_{CODadded}$ and biodegradability increasing to 64 ± 4 % in CSTR 1, while CSTR 2 achieved the same CH_4 yield and a biodegradability of 63 ± 5 % during the last 20 days of operation. These values represent increases of 22 % and 9 % in CH_4 yield and biodegradability for CSTR 1, and 25 % and 12 % for CSTR 2.

To better assess the influence of implementing HTH post-treatment and the subsequent recirculation, cellulose and hemicellulose concentrations were analyzed, and the results are summarized in *Table **4.3***. The PS contained, on average, 7340 ± 360 mg/L of cellulose and 2150 ± 160 mg/L of hemicellulose. Prior to the introduction of HTH, cellulose removal reached 70.3 % and 71.5 % in CSTR 1 and CSTR 2, respectively.

Once the HTH-treated sludge was recirculated into the system, clear differences in cellulose and hemicellulose concentrations emerged between CSTR 1 and CSTR 2, while the concentrations within the CSTRs themselves remained

comparable to previous levels. In contrast, HTH 1 and HTH 2 showed substantial reductions, with cellulose and hemicellulose decreasing by 43 % and 73 %, respectively. These reductions were consistent with the improved removal efficiencies measured in the main digesters. Cellulose removal increased to 84.3 % and 86.2 % in CSTR 1, and 84.1 % and 88 % in CSTR 2. Overall, this corresponds to an increase in cellulose removal of 20 % and 18 % in CSTR 1 and CSTR 2, respectively, and a similar enhancement of 20 % and 18 % in hemicellulose removal.

Because cellulose and hemicellulose are inherently recalcitrant, a significant fraction of these compounds typically remain unconverted to CH_4. Their transformation into more readily degradable polymers through HTH post-treatment can therefore improve digester performance, contributing to both process stability and CH_4 yield (Kim and Karthikeyan, 2021).

The use of HTH as a post-treatment strategy has also been evaluated in the anaerobic digestion of cattle manure, as reported by Haroun et al. (2025) who extensively investigated the application of 1 or 2 d HRT. The composition of cattle manure differs notably from that of PS due to its substantial lignin content, which represents approximately 59 % of TCOD. Nevertheless, similar to the results obtained for PS, the implementation of HTH post-treatment led to marked improvements in the degradation of recalcitrant fractions. Increases of 69 %, 4 %, and 468 % were observed in the degradation rates of lignin, cellulose, and hemicellulose, respectively. These improvements were reflected in higher biodegradability, which reached 46 % following the introduction of HTH. Overall, this post-treatment strategy facilitated the breakdown of resistant lignocellulosic components and enhanced their conversion within the digester.

Post-treatment processes have emerged as an attractive alternative to improve anaerobic digestion performance without significantly increasing energy demand.

A relevant comparison can be drawn with the study by Takashima (2008), who applied thermal post-treatment to digested sewage sludge in a continuous AD system. Sludge was heated at 120 °C for one hour weekly and returned to the digester, resulting in a 6.3 % increase in VS removal and a 21 % increase in methane production, confirming the effectiveness of moderate thermal post-treatment.

Further evidence supporting the benefits of post-treatment and recirculation is provided by Bolzonella et al. (2020), who evaluated a hyper-thermophilic post-treatment step (65 °C) applied to digestate from a full-scale AD plant treating manure and straw. A control CSTR (5 L) treating untreated digestate was compared with a system combining a hyper-thermophilic reactor (HRT 1–5 d) and a 4 L CSTR. Both digesters operated at a 14-day HRT. CH_4 production increased by 20 %, 33 %, and 38 % for HTH HRTs of 1, 3, and 5 d, respectively, demonstrating the substantial performance gains achievable through hyper-thermophilic post-treatment and recirculation.

Table 4.3 Cellulose and hemicellulose content and removal in PS, CSTR1, CSTR 2, HTH 1, and HTH 2.

	Cellulose (mg/L)					% Removal			
	Primary Sludge	**CSTR 1**	**CSTR 2**	**HTH 1**	**HTH 2**	**CSTR 1**	**CSTR 2**	**HTH 1**	**HTH 2**
Before HTH recirculation	7094	2104	2023	1348	1312	70.3	71.5	-	-
After HTH recirculation	7598	2103	2130	1190	1208	72.3	72.0	84.3	84.1
	Hemicellulose (mg/L)					**% Removal**			
	Primary Sludge	**CSTR 1**	**CSTR 2**	**HTH 1**	**HTH 2**	**CSTR 1**	**CSTR 2**	**HTH 1**	**HTH 2**
Before HTH recirculation	2037	913	874	239	202	55.2	57.1	-	-
After HTH recirculation	2263	1073	1052	313	271	52.6	53.5	86.2	88.0

4.3 Integration of *Caldicellulosiruptor bescii* into post-hyper-thermophilic hydrolysis for enhanced anaerobic digestion of PS

As discussed previously, cellulose is inherently recalcitrant due to its high degree of crystallinity, which limits enzymatic accessibility and microbial degradation. Nevertheless, certain anaerobic microorganisms are capable of effectively utilizing cellulose, with degradation efficiency generally increasing at elevated temperatures. Among extremely thermophilic anaerobes, *Caldicellulosiruptor bescii* (*C. bescii*) is notable for its ability to grow at approximately 75 °C under neutral pH conditions (S. J. Yang et al. 2009). This organism can ferment a wide range of substrates, including cellobiose, crystalline cellulose, pectin, α- and β-linked glucans, and xylan, producing lactate, ethanol, acetate, CO_2, and H_2 as metabolic end products (Yasemin D. Yilmazel et al. 2015). Unlike several other members of the *Caldicellulosiruptor* genus, *C. bescii* has demonstrated the capacity to degrade untreated switchgrass, highlighting its potential for the conversion of complex lignocellulosic biomass in addition to simple carbohydrates (Basen et al. 2014). Although *C. bescii* received limited attention in the decades following its discovery, increasing research efforts over the past 15 years have focused on evaluating its suitability for lignocellulosic biomass solubilization. Early work by Yang et al. (2009) demonstrated that *C. bescii* grows efficiently on both defined carbohydrates (cellulose and xylan) and untreated lignocellulosic substrates such as switchgrass and poplar at 75 °C, reaching cell densities above 10^8 cells/mL. Hydrogen and acetate were the main fermentation products, although initial biomass solubilization was limited. Successive fermentations of residual biomass substantially increased cumulative solubilization, confirming the organism's capacity to progressively deconstruct lignin-rich substrates.

Subsequent studies confirmed and extended these findings at larger scales. Kataeva et al. (2013) reported up to 85% solubilization of water-insoluble switchgrass after three sequential fermentations in a 20 L reactor, with lignin solubilized concurrently with polysaccharides. Basen et al. (2014) showed that *C. bescii* tolerates high concentrations of untreated cellulose and switchgrass (up to 200 g/L for cellulose), though solubilization efficiency declined at higher loads and growth was inhibited by pretreatment-derived compounds. Comparative studies within the *Caldicellulosiruptor* genus consistently identified *C. bescii* as one of the most effective species for cellulose and lignocellulosic biomass degradation (Zurawski et al. 2015).

Beyond plant biomass, *C. bescii* has also demonstrated strong performance on complex waste substrates. Fermentation of wastewater biosolids yielded high hydrogen production at low substrate concentrations, with inhibition observed only above 2.5 g VS/L (Yilmazel et al. 2015). Studies on manure and mixed organic wastes further confirmed its ability to degrade both plant- and animal-

derived materials, often achieving hydrogen yields comparable to those obtained with pure cellulose (Yasemin Dilsad Yilmazel and Duran 2021).
Importantly, *C. bescii* has been successfully integrated as a pretreatment step prior to anaerobic digestion. Mulat et al. (2018) and Hansen et al. (2021) demonstrated that introducing *C. bescii* fermentation before AD significantly enhances volatile solids reduction and methane yields. Pilot-scale trials treating dairy manure reported biogas yield increases of up to 74%, highlighting the organism's scalability and practical relevance for waste-to-energy applications. An in-depth analysis of the characteristics and applications of *C. Bescii* can be found in Appendix B.

4.3.1 Goal

Overall, the literature indicates that *C. bescii* can enhance the solubilization of recalcitrant biomass under extreme thermophilic conditions, although conversion efficiencies are highly dependent on substrate properties and operational parameters. In continuous or semi-continuous systems, the retention of an active *C. bescii* population remains challenging, as short hydraulic retention times can promote microbial washout and compromise process stability.
Based on these considerations, integrating *C. bescii* into anaerobic digestion could potentially improve CH_4 production from substrates such as primary sludge and digested cattle manure, where unconverted recalcitrant biomass remains a limiting factor. Its application in HTH units may enhance substrate biodegradability prior to digestion; however, the effectiveness of this approach is likely constrained by washout risks and the need for adequate biomass retention.
In this context, the present study evaluates the long-term impact of treating mesophilically digested primary sludge with *C. bescii* and recirculating the hyper-thermophilic effluent back to the main digester. Following the results obtained in paragraph 4.2.3, the same system was employed to test the performance of hyper-thermophilic fermentation operated with and without *C. bescii* was assessed at HRT of 2 and 4 days, focusing on COD and VS removal, cellulose, and hemicellulose solubilization, as well as on methane production.

4.3.2 Materials and method

4.3.2.1 Substrate and inoculum characterization

Inoculum and PS were provided and stored as reported in paragraph 4.2.2.1 of this thesis. *C. bescii* was obtained as a lyophilized pure culture from the DSMZ (medium 516). The culture was revived and enriched under strict anaerobic conditions in 100 mL serum bottles flushed with nitrogen. Cellobiose (2.0 g/L) was used as the sole carbon source, supplemented with nutrients, trace metal, and vitamin solutions. Enrichments were incubated at 75 °C in a shaking incubator. Gas production, optical density, VFAs, and pH were monitored daily. Once gas production ceased, the culture was sequentially subcultured by tenfold dilution into fresh medium, first in 100 mL and then in 1 L bottles. Biogas volume was

measured three times daily using a syringe. All media, glassware, and consumables were autoclaved at 121 °C for 30 min to prevent contamination.

4.3.2.2 Set-up and operative conditions

The two systems were operated identically as described in paragraph 4.3.2.2 except for the inoculation of C. bescii in the test HTH reactor in phases 5-6 as follows. Phases 1-2-3-4 are the same described in paragraph 4.2.2.2 while C. Bescii was introduced from phase 5. In phase 5 (day 266-320), the HTH reactor was bioaugmented with *C. bescii*, whereas the control reactor remained without inoculation. The HTH was operated at 2 d HRT, with recirculation rates unchanged. This phase assessed the effect of *C. bescii* addition on hydrolysis efficiency and subsequent mesophilic digestion under conditions of high washout pressure. In phase 6, C. Bescii was reinoculated in the control reacor and HRT was changed to 4 d to improve biomass retention. The recirculation rate was fixed to 0.25 L/d while CSTRs HRT was reduced to 10.9 d. In phase 6 (days 320–363), the effect of extending the HRT was evaluated to determine whether it could improve *C. bescii* persistence and enhance system performance.

Analytical methods, and data processing were carried out in accordance with the procedures described in Sections 4.2.2.3 of this thesis.

4.3.3 Results

The performance of the two 10 L CSTRs over the entire experimental period is shown in *Figure 4.4*, expressed as liters of CH_4 per gram of COD added. This section focuses on the results obtained during the final two operational phases (phases 5 and 6).

As previously discussed in paragraph 4.2, the introduction of HTH post-treatment initially resulted in a modest improvement in reactor performance, with biodegradability increasing from approximately 61 % to 63-64 %. Based on this observation, *C. bescii* was introduced into HTH 2 at the beginning of Phase 5, while HTH 1 continued operating without bioaugmentation, effectively representing a continuation of phase 4.

Contrary to expectations based on literature, phase 5 was characterized by a marked decline in system performance, as reported in *Table 4.4*. CH_4 production decreased by approximately 11 %, accompanied by a reduction in biodegradability to 57 ± 11 % and 55 ± 11 % in CSTR 1 and CSTR 2, respectively. This deterioration was also reflected in total COD removal, which dropped from 67 % to 58 % in CSTR1 and to 51 % in CSTR2. Notably, this negative trend was observed in both reactors, regardless of the presence of *C. bescii*, indicating that no clear positive or negative effect of bioaugmentation could be detected under the applied HTH conditions with an HRT of 2 d.

To enhance solubilization of recalcitrant compounds and improve biomass retention, the HRT of both HTH reactors was increased to 4 d during phase 6. However, this modification further compromised system stability, leading to increased fluctuations in both CH_4 production and biodegradability. Variability

during phases 5-6 was approximately three times higher than that observed during phases 3-4. CH_4 yield declined to about 0.21 L/g_{COD} in both reactors, while biodegradability decreased to values between 53 ± 11 % and 55 ± 8 %.

Effluent recirculation can have competing effects: while it may reintroduce readily biodegradable compounds, it can also effectively reduce the HRT of the system, potentially leading to a deterioration of overall process performance.

Overall, the behavior of CSTR 1 and CSTR 2 following the introduction of HTH post-treatment and *C. bescii* suggests that post-digestion may provide short-term benefits, as observed during phase 4, but prolonged operation led to reduced stability and performance. Similarly, *C. bescii* bioaugmentation did not result in measurable improvements, likely due to insufficient retention, kinetic limitations and washout of the microorganisms under the tested operating conditions.

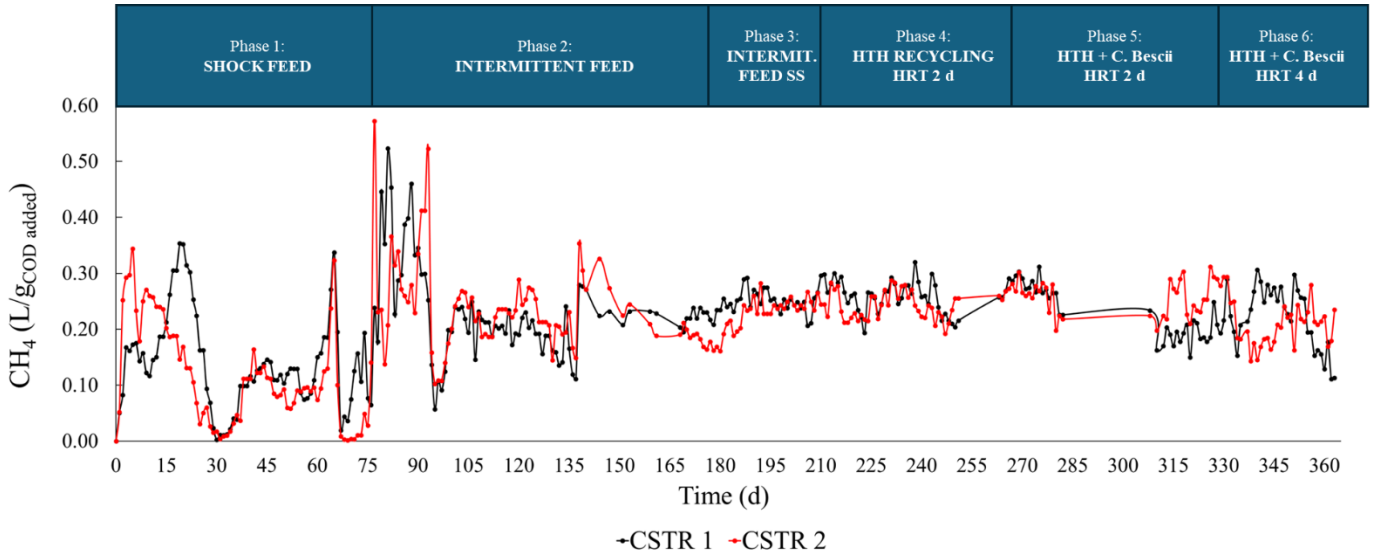

Figure 4.4 Methane yield of CSTR1 and CSTR 2 as $L/g_{COD_{added}}$ during phase 1,2,3,4,5, and 6 of the process.

Table 4.4 Methane yield, TCOD reduction, and VSS reduction in the control CSTR 1 vs. C. Bescii CSTR 2 at different phases of the experiment.

	Feed PS (Average ± STD)	**CSTR_1_Control (Average ± STD)**	**% Conversion to CH_4**	**CSTR_2_*C. Bescii* (Average ± STD)**	**% Conversion to CH_4**
			CH_4 yield (mL/g_{COD})		
Stage _1	-	140±90	34±21.3	140±90	28±22.5
Stage _2	-	230±90	57±21.8	230±90	57±16
Stage _3	-	245±14	61±3.5	242±9.3	60.5±2.3
Stage _4	-	256±16	64±4.0	252±18	63±4.5
Stage_5	-	227±44	57±11.0	219±44	55±11
Stage_6	-	212±46	53±11.0	218±31	55±8
			TCOD (mg/L)		
Stage _1	39677±5148	22871±5977	47.4±9.6	26179±9303	42.6±14.7
Stage _2	37616±12776	15501±5477	56.1±13.3	15642±5393	53.2±6.9
Stage _3	41734±5207	19365±1612	53.0±6.0	19303±1892	53.0±6.7
Stage _4	42205±5232	13857±948	67.2±4.2	13884±1219	67.1±4.5
Stage_5	36102±2574	15086±664	58.2±1.12	17718±5017	51±12.9
Stage_6	42100±1398	18608±1713	55.8±2.1	22917±1972	52.2±1.3
			VS (mg/L)		
Stage _1	20500±220	10700±1600	47.8±8.0	11600±2300	44.4±9.0
Stage _2	24300±670	10500±1500	56.3±13.5	10400±1700	59.1±10.4
Stage _3	24254±6450	10455±1410	54.1±12.6	10373±1630	54.7±11.6
Stage _4	24492±5049	9983±2217	59.2±10.18	9267±2254	62.2±6.3
Stage_5	21420±1836	8400±932	60.8±3.1	10000±3394	53.3±8.2
Stage_6	25529±2710	11038±1114	56.8±3.8	12763±1177	50.0±1.9

References

Abdelrahman, Amr Mustafa, Sadiye Kosar, Hazal Gulhan, et al. 2023. "Impact of Primary Treatment Methods on Sludge Characteristics and Digestibility, and Wastewater Treatment Plant-Wide Economics." *Water Research* 235 (May): 119920. https://doi.org/10.1016/j.watres.2023.119920.

Ahring, Birgitte K., Rajib Biswas, Aftab Ahamed, Philip J. Teller, and Hinrich Uellendahl. 2015. "Making Lignin Accessible for Anaerobic Digestion by Wet-Explosion Pretreatment." *Bioresource Technology* 175: 182–88. https://doi.org/10.1016/j.biortech.2014.10.082.

Axelsson Bjerg, Mette, Eva Maria Ekstrand, Ingrid Sundgren, Sepehr Shakeri Yekta, Jan Moestedt, and Annika Björn. 2024. "Moderate Thermal Post-Treatment of Digestate to Improve Biomethane Production from Agricultural- and Food Waste." *Bioresource Technology Reports* 27 (February). https://doi.org/10.1016/j.biteb.2024.101887.

Basen, Mirko, Amanda M. Rhaesa, Irina Kataeva, et al. 2014. "Degradation of High Loads of Crystalline Cellulose and of Unpretreated Plant Biomass by the Thermophilic Bacterium Caldicellulosiruptor Bescii." *Bioresource Technology* 152: 384–92. https://doi.org/10.1016/j.biortech.2013.11.024.

Bertin, Lorenzo, Selene Grilli, Alessandro Spagni, and Fabio Fava. 2013. "Innovative Two-Stage Anaerobic Process for Effective Codigestion of Cheese Whey and Cattle Manure." *Bioresource Technology* 128: 779–83. https://doi.org/10.1016/j.biortech.2012.10.118.

Boe, Kanokwan, Dimitar Karakashev, Eric Trably, and Irini Angelidaki. 2009. "Effect of Post-Digestion Temperature on Serial CSTR Biogas Reactor Performance." *Water Research* 43 (3): 669–76. https://doi.org/10.1016/j.watres.2008.11.037.

Bolzonella, D., F. Battista, A. Mattioli, C. Nicolato, N. Frison, and S. Lampis. 2020. "Biological Thermophilic Post Hydrolysis of Digestate Enhances the Biogas Production in the Anaerobic Digestion of Agro-Waste." *Renewable and Sustainable Energy Reviews* 134 (July): 110174. https://doi.org/10.1016/j.rser.2020.110174.

Bombardiere, John, Teodoro Espinosa-Solares, Max Domaschko, and Mark Chatfield. 2007. *Thermophilic Anaerobic Digester Performance under Different Feed-Loading Frequency*. 136.

Cremonez, Paulo André, Joel Gustavo Teleken, Thompson Ricardo Weiser Meier, and Helton José Alves. 2021. "Two-Stage Anaerobic Digestion in Agroindustrial Waste Treatment: A Review." *Journal of Environmental Management* 281 (March). https://doi.org/10.1016/j.jenvman.2020.111854.

Crutchik, Dafne, Nicola Frison, Anna Laura Eusebi, and Francesco Fatone. 2018. "Biorefinery of Cellulosic Primary Sludge towards Targeted Short Chain Fatty Acids, Phosphorus and Methane Recovery." *Water Research* 136: 112–19. https://doi.org/10.1016/j.watres.2018.02.047.

Dareioti, Margarita A., Konstantina Tsigkou, Aikaterini I. Vavouraki, and Michael Kornaros. 2022. "Hydrogen and Methane Production from Anaerobic Co-Digestion of Sorghum and Cow Manure: Effect of pH and Hydraulic Retention Time." *Fermentation* 8 (7). https://doi.org/10.3390/fermentation8070304.

Dohdoh, Ayman. 2019. "Effect of Sludge Recirculation on Sewage Sludge Anaerobic Digester Performance." *International Journal of Current Engineering and Technology* 9 (5): 661–68.

Ezieke, Arinze Hycienth, Antonio Serrano, Miriam Peces, William Clarke, and Denys Villa-Gomez. 2024. "Effect of Feeding Frequency on the Anaerobic Digestion of Berry Fruit Waste." *Waste Management* 178 (April): 66–75. https://doi.org/10.1016/j.wasman.2024.02.011.

Font-Palma, Carolina. 2019. "Methods for the Treatment of Cattle Manure—A Review." *C* 5 (2): 27. https://doi.org/10.3390/c5020027.

Hansen, Jaron C, Zachary T Aanderud, Lindsey E Reid, et al. 2021. "Enhancing Waste Degradation and Biogas Production by Pre-Digestion with a Hyperthermophilic Anaerobic Bacterium Enhancing Waste Degradation and Biogas Production by Pre-Digestion with a Hyperthermophilic Anaerobic Bacterium Enhancing Waste Degradation and Biogas Production by Pre-Digestion with a Hyperthermophilic Anaerobic Bacterium." *Biofuel Research Journal* 31: 1433–43. https://doi.org/10.18331/BRJ2021.8.3.

Haroun, Basem, Mohamed El-Qelish, Mina Nayebi Shahabi, et al. 2025. "Enhanced Energy Recovery from Lignin-Rich Cattle Manure: Impact of Coupling Mesophilic Anaerobic Digestion with Hyperthermophilic Hydrolysis." *Chemical Engineering Journal* 523 (November): 167965. https://doi.org/10.1016/j.cej.2025.167965.

Hartmann, Hinrich, and Birgitte K. Ahring. 2005. "A Novel Process Configuration for Anaerobic Digestion of Source-Sorted Household Waste Using Hyper-Thermophilic Post-Treatment." *Biotechnology and Bioengineering* 90 (7): 830–37. https://doi.org/10.1002/bit.20485.

Kaparaju, P. L.N., and J. A. Rintala. 2005. “The Effects of Post-Treatments and Temperature on Recovering the Methane Potential of >2 Mm Solid Fraction of Digested Cow Manure.” *Environmental Technology* 26 (6): 625–32. https://doi.org/10.1080/09593330.2005.9619502.

Kataeva, Irina, Marcus B. Foston, Sung Jae Yang, et al. 2013. “Carbohydrate and Lignin Are Simultaneously Solubilized from Unpretreated Switchgrass by Microbial Action at High Temperature.” *Energy and Environmental Science* 6 (7): 2186–95. https://doi.org/10.1039/c3ee40932e.

Kim, Joonrae Roger, and K. G. Karthikeyan. 2021. “Solubilization of Lignocellulosic Biomass Using Pretreatments for Enhanced Methane Production during Anaerobic Digestion of Manure.” *ACS ES and T Engineering* 1 (4): 753–60. https://doi.org/10.1021/acsestengg.0c00226.

Kim, Joonrae Roger, and K.G. Karthikeyan. 2021. “Effects of Severe Pretreatment Conditions and Lignocellulose-Derived Furan Byproducts on Anaerobic Digestion of Dairy Manure.” *Bioresource Technology* 340 (November): 125632. https://doi.org/10.1016/j.biortech.2021.125632.

Kim, Seunghwan, Changmin Lee, Junhyeon Kim, and Jae Young Kim. 2023. “Feasibility of Thermal Hydrolysis Pretreatment to Reduce Hydraulic Retention Time of Anaerobic Digestion of Cattle Manure.” *Bioresource Technology* 384 (June): 129308. https://doi.org/10.1016/j.biortech.2023.129308.

Köninger, Julia, Emanuele Lugato, Panos Panagos, Mrinalini Kochupillai, Alberto Orgiazzi, and Maria J.I. Briones. 2021. “Manure Management and Soil Biodiversity: Towards More Sustainable Food Systems in the EU.” *Agricultural Systems* 194 (December): 103251. https://doi.org/10.1016/j.agsy.2021.103251.

Lembo, Giuseppe, Antonella Signorini, Antonella Marone, Claudio Carbone, and Alessandro Agostini. 2022. “Hydrogen and Methane Production by Single- and Two-Stage Anaerobic Digestion of Second Cheese Whey: Economic Performances and GHG Emissions Evaluation.” *Energies* 15 (21). https://doi.org/10.3390/en15217869.

Liu, Shuang, Wenzhe Li, Guoxiang Zheng, Haiyan Yang, and Longhai Li. 2020. “Optimization of Cattle Manure and Food Waste Co-Digestion for Biohydrogen Production in a Mesophilic Semi-Continuous Process.” *Energies* 13 (15): 3848. https://doi.org/10.3390/en13153848.

Martínez-Mendoza, Leonardo J., Octavio García-Depraect, and Raúl Muñoz. 2023. “Unlocking the High-Rate Continuous Performance of Fermentative Hydrogen Bioproduction from Fruit and Vegetable Residues by Modulating Hydraulic Retention Time.” *Bioresource Technology* 373 (April). https://doi.org/10.1016/j.biortech.2023.128716.

Mulat, Daniel Girma, Silvia Greses Huerta, Dayanand Kalyani, and Svein Jarle Horn. 2018. “Enhancing Methane Production from Lignocellulosic Biomass by Combined Steam-Explosion Pretreatment and Bioaugmentation with Cellulolytic Bacterium Caldicellulosiruptor Bescii.” *Biotechnology for Biofuels* 11 (1). https://doi.org/10.1186/s13068-018-1025-z.

Nebot-Sanz, Enrique, Luis Isidoro Romero-García, José María Quiroga Alonso, and Diego Sales-Márquez. 1995. *Effect of the Feed Frequency on the Performance of Anaerobic Filters*. 1 (2): 113–20. https://doi.org/10.1006/anae.1995.1006.

Nkemka, Valentine Nkongndem, Jorge Arenales-Rivera, and Marika Murto. 2014. “Two-Stage Dry Anaerobic Digestion of Beach Cast Seaweed and Its Codigestion with Cow Manure.” *Journal of Waste Management* 2014 (July): 1–9. https://doi.org/10.1155/2014/325341.

Nordell, E., A. Björn, S. Waern, S. Shakeri Yekta, I. Sundgren, and J. Moestedt. 2022. “Thermal Post-Treatment of Digestate in Order to Increase Biogas Production with Simultaneous Pasteurization.” *Journal of Biotechnology* 344 (December 2021): 32–39. https://doi.org/10.1016/j.jbiotec.2021.12.007.

Paudel, Shukra Raj, Sushant Prasad Banjara, Oh Kyung Choi, Ki Young Park, Young Mo Kim, and Jae Woo Lee. 2017. “Pretreatment of Agricultural Biomass for Anaerobic Digestion: Current State and Challenges.” *Bioresource Technology* 245: 1194–205. https://doi.org/10.1016/j.biortech.2017.08.182.

Pramanik, Sagor Kumar, Fatihah Binti Suja, and Biplob Kumar Pramanik. 2020. “Effect of Substrate Feeding Strategy of a Semi-Pilot-Scale Single-Stage Reactor under Different Hydraulic Retention Time and Multiple Kinetic Models Analysis.” *Desalination and Water Treatment* 207 (December): 420–36. https://doi.org/10.5004/dwt.2020.26241.

Rasit, Nazaitulshila, Wan Azlina Wan Ab Karim Ghani, Mohammad Hakim Che Harun, Sofiah Hamzah, Roslinda Seswoya, and Md Nurul Islam Siddique. 2024. “Feeding Frequency Efficacy on Biogas Yield of Oily Substrate Anaerobic Digestion in Continuous Stir Tank Reactor.” *Water Science & Technology* 89 (10): 2796–811. https://doi.org/10.2166/wst.2024.153.

Rice, Eugene W., Rodger B. Baird, Andrew D. Eaton, Lenore S. Clesceri, and Laura Bridgewater. 2012. *Standard Methods for the Examination of Water and Wastewater*.

Sakaveli, Foteini, Maria Petala, Vasilios Tsiridis, and Efthymios Darakas. 2024. "Enhancing Methane Yield in Anaerobic Co-Digestion of Primary Sewage Sludge: A Comprehensive Review on Potential Additives and Strategies." *Waste* 2 (1): 29–57. https://doi.org/10.3390/waste2010002.

Sambusiti, C., F. Monlau, E. Ficara, et al. 2015. "Comparison of Various Post-Treatments for Recovering Methane from Agricultural Digestate." *Fuel Processing Technology* 137 (May): 359–65. https://doi.org/10.1016/j.fuproc.2015.04.028.

Samoraj, Mateusz, Małgorzata Mironiuk, Grzegorz Izydorczyk, et al. 2022. "The Challenges and Perspectives for Anaerobic Digestion of Animal Waste and Fertilizer Application of the Digestate." *Chemosphere* 295 (January). https://doi.org/10.1016/j.chemosphere.2022.133799.

Sluiter, Amie D., Bonnie Hames, R. Ruiz, et al. 2008. "Determination of Structural Carbohydrates and Lignin in Biomass."

Svensson, Kine, Oda Kjørlaug, Matthew J. Higgins, Roar Linjordet, and Svein J. Horn. 2018. "Post-Anaerobic Digestion Thermal Hydrolysis of Sewage Sludge and Food Waste: Effect on Methane Yields, Dewaterability and Solids Reduction." *Water Research* 132: 158–66. https://doi.org/10.1016/j.watres.2018.01.008.

Svensson, Kine, Lisa Paruch, John Christian Gaby, and Roar Linjordet. 2018. "Feeding Frequency Influences Process Performance and Microbial Community Composition in Anaerobic Digesters Treating Steam Exploded Food Waste." *Bioresource Technology* 269 (December): 276–84. https://doi.org/10.1016/j.biortech.2018.08.096.

Takashima, Masanobu. 2008. "Examination on Process Configurations Incorporating Thermal Treatment for Anaerobic Digestion of Sewage Sludge." *Journal of Environmental Engineering* 134 (7): 543–49. https://doi.org/10.1061/(asce)0733-9372(2008)134:7(543).

Wang, Kuen-Sheng, Jung-Hsing Chen, Yu-Hsiang Huang, and Shir-Ly Huang. 2013. "Integrated Taguchi Method and Response Surface Methodology to Confirm Hydrogen Production by Anaerobic Fermentation of Cow Manure." *International Journal of Hydrogen Energy* 38 (1): 45–53. https://doi.org/10.1016/j.ijhydene.2012.03.155.

Winter, P, and P Pearce. 2008. "Parallel Digestion of Secondary and Primary Sludge." *15th European Biosolids and Organic Resources Conference*, no. 2009: 1–10.

Xing, Yan, Zhuo Li, Yaoting Fan, and Hongwei Hou. 2010. "Biohydrogen Production from Dairy Manures with Acidification Pretreatment by Anaerobic Fermentation." *Environmental Science and Pollution Research* 17 (2): 392–99. https://doi.org/10.1007/s11356-009-0187-4.

Yang, Sung Jae, Irina Kataeva, Scott D. Hamilton-Brehm, et al. 2009. "Efficient Degradation of Lignocellulosic Plant Biomass, without Pretreatment, by the Thermophilic Anaerobe 'Anaerocellum Thermophilum' DSM 6725." *Applied and Environmental Microbiology* 75 (14): 4762–69. https://doi.org/10.1128/AEM.00236-09.

Yilmazel, Yasemin D., David Johnston, and Metin Duran. 2015. "Hyperthermophilic Hydrogen Production from Wastewater Biosolids by Caldicellulosiruptor Bescii." *International Journal of Hydrogen Energy* 40 (36): 12177–86. https://doi.org/10.1016/j.ijhydene.2015.06.140.

Yilmazel, Yasemin Dilsad, and Metin Duran. 2021. "Biohydrogen Production from Cattle Manure and Its Mixtures with Renewable Feedstock by Hyperthermophilic Caldicellulosiruptor Bescii." *Journal of Cleaner Production* 292 (April). https://doi.org/10.1016/j.jclepro.2021.125969.

Yokoyama, Hiroshi, Miyoko Waki, Akifumi Ogino, Hideyuki Ohmori, and Yasuo Tanaka. 2007. "Hydrogen Fermentation Properties of Undiluted Cow Dung." *Journal of Bioscience and Bioengineering* 104 (1): 82–85. https://doi.org/10.1263/jbb.104.82.

Ziels, Ryan M., David A.C. Beck, and H. David Stensel. 2017. "Long-Chain Fatty Acid Feeding Frequency in Anaerobic Codigestion Impacts Syntrophic Community Structure and Biokinetics." *Water Research* 117 (June): 218–29. https://doi.org/10.1016/j.watres.2017.03.060.

Zurawski, Jeffrey V., Jonathan M. Conway, Laura L. Lee, et al. 2015. "Comparative Analysis of Extremely Thermophilic Caldicellulosiruptor Species Reveals Common and Unique Cellular Strategies for Plant Biomass Utilization." *Applied and Environmental Microbiology* 81 (20): 7159–70. https://doi.org/10.1128/AEM.01622-15.

Chapter 5

5. Two-Stage Anaerobic Digestion of Fruit and Vegetable Waste Using Jam Wastewater as a Sugar and Water Source

5.1 Introduction

5.1.1 Biochar as an additive in DF and AD

As discussed in Chapter 2, a mixture of fruit and vegetable waste (FVW) and jam wastewater (JWW) can be effectively used as substrate for two-stage anaerobic digestion (TSAD). A S:I ratio equal to 1 of 1 was identified as optimal to prevent microbial overstimulation. However, in previous experiments, JWW was primarily considered as a co-substrate due to its high content of readily biodegradable sugars, and its proportion in the reactors remained relatively low (12-37 % on a wet weight basis). Under these conditions, the potential of JWW as a water source was not fully exploited.

Increasing the proportion of JWW in the feed mixture could reduce or eliminate the need for freshwater addition to achieve the target TS content, which was fixed at 6 % for the experiments presented in this chapter. This approach would enhance process sustainability by further promoting wastewater reuse.

Moreover, Chapter 2 demonstrated that thermal pretreatment of FVW improved system performance, resulting in approximately a 30% increase in H_2 yield due to enhanced solubilization of complex organic compounds and increased availability of simple sugars for microbial metabolism. In addition to thermal pretreatment, the use of additives represents another strategy to further improve process efficiency by enhancing microbial activity, substrate conversion, and energy recovery.

Additives can be classified as inorganic or organic. Inorganic additives, such as metals and metal nanoparticles (e.g., iron-based materials), can stimulate enzymatic activity and electron transfer processes. Organic additives, including yeast extract, peptone, and tryptone, primarily promote microbial growth, while materials such as activated carbon, biochar, and hydrochar can enhance microbial attachment, improve syntrophic interactions, and stabilize the anaerobic digestion process (Hidalgo et al. 2024). As discussed in Chapter 1, biochar (BC) is a solid carbonaceous material produced through thermochemical conversion of biomass under oxygen-limited or oxygen-free conditions at temperatures typically ranging from 300 to 1000 °C. A wide variety of feedstocks can be used for biochar production, particularly organic residues such as plant-derived wastes (e.g., corn straw, rice husks, algae), animal-derived wastes (e.g., manure and crustacean shells), and municipal solid wastes (Lou et al. 2024).

Biochar is characterized by a highly porous structure, large specific surface area, good electrical conductivity, ion-exchange capacity, and the presence of numerous surface functional groups. These physicochemical properties strongly depend on both the biomass feedstock and the thermochemical conversion technique employed. Owing to these characteristics, biochar has found broad application in water and wastewater treatment, soil remediation, energy conversion, and pollutant removal processes (S. Tang et al. 2020).

In recent years, biochar has gained increasing attention as an additive in AD and DF processes due to its ability to enhance energy yields and improve process stability. Its microporous structure and surface chemistry, enriched with functional groups, minerals, and trace metals, promote microbial attachment and biofilm formation, thereby creating favorable microenvironments for the growth of H_2- and CH_4-producing microbial consortia. Moreover, the redox-active surfaces of biochar facilitate direct and indirect extracellular electron transfer, enhancing syntrophic interactions among microbial populations. Biochar also contributes to process stabilization by buffering pH fluctuations and adsorbing inhibitory compounds such as VFAs, ammonia, and heavy metals (Y. Zhao et al. 2025).

Consistent with these mechanisms, several studies have reported significant improvements in biogas production following biochar addition. In AD, biochar acts as both a conductive medium and a microbial support, mitigating inhibition from ammonia and VFAs while stabilizing methanogenic activity. For instance, Ding et al. (2024) reported a 35.7 % increase in CH_4 yield with the addition of 10 g/L of cattle manure–derived biochar. Similarly, Shen et al. (2015) demonstrated that corn-derived biochar enhanced CH_4 content by 42.4 % and achieved CO_2 removal efficiencies of up to 86.3 %, thereby improving overall biogas quality.

In DF systems, biochar has also shown promising results. Yang et al. (2024) reported that the use of iron-modified biochar (Fe-L600) in thermophilic DF of food waste increased H_2 yield by more than 30 %, reduced the time required to reach process stability from 18 to 12 h, and altered the VFAs profile, as evidenced by a decrease in the acetic-to-butyric acid ratio from 3.09 to 2.69.

Biochar dosage in DF and AD has not been standardized, as a wide range of operational conditions and concentrations have been reported in the literature (*Table 5.1*). For this study, intermediate biochar concentrations were selected for application in DF and AD.

Table 5.1 Examples of biochar applications in dark fermentation processes and associated operating conditions.

DF					**Pyrolysis**		
Substrate	**Op. Cond.**	**H_2 Yield**	**T (°C)**	**Time**	**Biomass**	**Concentration**	**Reference**
Glucose	Batch, 100 mL pH = 7 37 °C	18 mL/g $_{glu}$	600	3 h	Sugarcane leaves (SL) and bagasse (SB)	SB = 6.09 g/L SL+Fe = 5.38 g/L SL+Ni = 7.66 g/L	Wongfaed et al. (2025)
Food Waste	Batch 100 mL pH =5.5 35 °C	116 mL/g $_{VS}$	650	20 min	Pine sawdust	8.3 g/L	Sunyoto et al. (2016)
Glucose	Batch 55 mL pH =7.8 55 °C	240 mL/g $_{VS}$	600		Corn bran residue	0.6 g/L	Lou et al. (2024)
Sugarcane bagasse	Batch 100 mL pH =7 37 °C	320 mL/g $_{VS}$	600	1 h	Fallen leaves	7 g/L	Huang et al. (2022)
Grass biomass	Batch 100 mL pH =5.5 35 °C	31 mL/g $_{VS}$	500	2 h	Sawdust	0.6 g/L	Yang and Wang (2019)

Moreover, as discussed in Section 1.4.4, anaerobic digestates can be further valorized through the extraction of humic acids (HA) and fulvic acids (FA). Alkaline treatments are commonly recommended for this purpose, as they represent a simple and effective approach for recovering these valuable bio stimulants.

5.1.2 Goal

To the best of the authors' knowledge, no previous studies have specifically investigated the application of TSAD in which JWW is used as the primary water source to achieve the desired TS content. In addition, the role of biochar across the different stages of TSAD remains insufficiently explored.

To address these gaps, this study aims to evaluate the feasibility of using JWW as a water substitute in the DF stage. This is tested under three different inoculum thermal pretreatments. Subsequently, the second stage of TSAD was

carried out with and without biochar addition to assess its influence on CH_4 production from DF digestate. In the second experiment, the effect of biochar on process performance was also examined during the DF stage, followed by AD to evaluate its combined impact on overall CH_4 recovery. Moreover, the influence of process temperature was investigated by conducting DF of FVW and JWW under thermophilic conditions (55 °C), both in the presence and absence of biochar, to further elucidate the role of temperature on system performance. Finally, HA extraction was performed on the digestate to assess the effectiveness of alkaline treatment as a valorization strategy and to evaluate its efficiency in recovering humic-like substances from anaerobically treated biomass.

The findings of this work provide insight into the potential integration of biochar and wastewater reuse within TSAD systems. In particular, the use of JWW as a water source may reduce the need for freshwater input while maintaining process functionality. Overall, this approach aligns with circular economy principles by promoting resource recovery and more efficient use of waste-derived materials within anaerobic treatment systems.

5.2 Materials and method

5.2.1 Substrates and inoculum characterization

The inoculum employed in DF and AD was the mesophilic digestate of cow-agricultural sludge (CAS) provided by "Cascina La Speranza" (Fossano, Cuneo, Italy). FVW was collected from household residue (mass composition of 75% vegetables and 25 % fruits) and chopped through a kitchen blender. JWW was supplied by a local agricultural cooperative (Piedmont, Italy) as the water employed to wash jam production equipment. Both FVW and JWW were frozen at -18 °C after their collection to avoid natural decomposition. Then they were defrosted before being fed into the fermentation system. JWW, FVW and inoculum characterization are presented *Table 5.2*. All the experiments have been performed with the same lot of JWW and FVW, while fresh inoculum was supplied at different times to ensure adequate microbial activity. Consequently, the reported inoculum characterization represents the average values obtained from the different batches used throughout the experimental campaign. The biochar employed was the commercial WSP770 produced from wheat straw pellets pyrolyzed at 700 °C.

5.2.2 Inoculum thermal pretreatment

In the present study, inoculum was thermally pretreated at 80, 100, and 120 °C (depending on the experiment) for 30 min to eliminate H_2-consumers and favor sporulation of H_2-producers. The inoculum was heated through heating plates and an anchor stirrer to ensure uniform temperature and adequate mixing.

5.2.3 Process setup and operative condition

DF and AD were performed in 500 mL Pyrex glass bottles (Duran, Germany) with a working volume of 80 %. The heating was controlled by a 55 L thermostatic water-bath (Julabo-Corio-C, Merck, Germany). Reactors were operated in batch feeding mode with 3 % of total solids and shaken manually to keep the mixture homogeneous inside the reactor. Each reactor was sealed with a two-port cap. Through one of the ports, anaerobic conditions were assured by purging N_2 directly inside the biomass to change the volume of the reactor three times and closing the port. The second port was connected to a 1 L Teddlar gas bag where biogas was collected. The duration of each assay depended on biogas or H_2 production: testing was stopped when daily H_2 (for DF tests) and biogas (for AD tests) production was less than 1% of the overall production recorded during the period of preparation (VDI 4630 2006). The experimental campaign consists of three main experiments, and all the campaigns were studied in replicates. The pH of each reactor was measured daily. When necessary, NaOH or HCl were added to the reactors to lower the pH to around 6-7 in DF and to maintain AD pH between 7 and 8.

In the first experimental campaign, TSAD of FVW and JWW was investigated by first determining the optimal thermal pretreatment temperature for DF inoculum. Three DF configurations were operated at 35 °C, with inoculum pretreated at 80, 100, or 120 °C. Effluents from the two best-performing DF pretreatments were subsequently used as substrates for a second-stage mesophilic AD. In this stage, four configurations were tested, including reactors operated with and without biochar addition (1 g/L).

The second experimental campaign focused on assessing the role of biochar during the first stage of TSAD. DF was conducted at 35 °C using inoculum thermally pretreated at 80 or 100 °C. Five DF configurations were evaluated: inoculum pretreated at 80 °C; inoculum pretreated at 100 °C; inoculum pretreated at 80 °C with 1 g/L biochar; inoculum pretreated at 100 °C with 1 g/L biochar; and inoculum pretreated at 100 °C with 2 g/L biochar. The resulting DF digestates were then subjected to a second-stage mesophilic AD.

For both the first and second experimental campaigns, the performance of TSAD was compared with that of single-stage mesophilic AD treating FVW and JWW.

Finally, a third experimental campaign investigated DF under thermophilic conditions (55 °C). Inoculum was thermally pretreated at 80 and 100 °C, and DF was carried out with and without the addition of biochar at a concentration of 1 g/L, to evaluate the combined effects of temperature and biochar on DF performance.

A summary of configuration characteristics is presented in *Table 5.3*.

5.2.4 Humic acid extraction

For HA extraction, the effluent from the second stage of TSAD without biochar addition and using DF inoculum pretreated at 100 °C was selected, as this configuration demonstrated the best overall performance in the preceding experiments. Digestates were subjected to alkaline extraction at pH 12 for 24 h at 35 °C under continuous agitation (150 rpm), following the method described by Guilayn et al. (2020). pH was adjusted using KOH pellets (>85 % purity, Sigma-Aldrich). After extraction, samples were centrifuged at 4000 RFC for 5 min at 20 °C. The resulting supernatant, containing soluble organic compounds, was collected as the humic-like substances extract.

The HA fraction was then precipitated by acidifying the supernatant to pH 2 using 37 % HCl. The suspension was centrifuged again at 4000 RFC for 5 min at 20 °C to recover the pellet containing HA. The recovered solids were dried at 90 °C for at least 24 h, until constant weight was achieved. Subsequently, the dried samples were combusted in a muffle furnace at 500 °C for 6 h to obtain ash. The humic acid weight was quantified as the difference between the dried residue mass and the ash mass after combustion (Cristina et al. 2020).

5.2.5 Analytical methods and data elaboration

DF design, analytical methods, and data processing were carried out in accordance with the procedures described in Sections 2.2.4 and 2.2.5 of this thesis.

Functional groups of HA were detected by Attenuated Total Reflectance Fourier-transform infrared spectroscopy (ATR-FTIR) on a Bruker Alpha Platinum spectrometer. 64 spectra from 4000 to 400 cm^{-1} with resolution of 4 cm^{-1} were automatically collected and their average was given as result.

5.3 Results

5.3.1 Characterization of inoculum and substrates

As observed in paragraph 2.3.1, the characterization of the inoculum and substrates (*Table 5.2*) confirms their suitability for biological conversion processes. The inoculum and FVW showed higher TS content compared to JWW that was highly diluted, with a TS content below 1%. The inoculum exhibited a lower VS fraction due to its higher inorganic content, while both FVW and JWW were rich in VS, indicating a high proportion of readily biodegradable organic matter. Despite the TS content of FVW being slightly lower than typical literature values, its VS/TS ratio remained consistent with reported data, supporting its biodegradability. Elemental analysis further showed that the combined use of FVW and JWW resulted in a C/N ratio within the optimal range for microbial activity and eliminates the need for nutrient supplementation.

Table 5.2 Chemical and physical characterization of inoculum, fruit and vegetable waste (FVW) and jam wastewater (JWW).

	Inoculum	**FVW**	**JWW**
TS (%)	5.97 ± 1.57	9.40 ± 0.10	0.82 ± 0.14
VS/TS (%)	88.56 ± 8.06	96.54 ± 0.41	97.20 ± 1.70
N (%)	3.21 ± 0.52	2.38 ± 0.29	0.21 ± 0.04
C (%)	38.40 ± 2.25	46.23 ± 0.62	33.21 ± 6.62
H (%)	4.59 ± 0.30	6.30 ± 0.05	5.27 ± 1.12
S (%)	0.48 ± 0.13	0.15 ± 0.03	0.36 ± 0.02
O (%)	53.32 ± 2.93	44.95 ± 0.41	60.95 ± 7.76
C/N	12.10 ± 1.23	19.63 ± 2.66	158.19 ± 0.44

Table 5.3 Configurations tested across three experiments: (i) first, varying inoculum pretreatment temperature in DF and application of BC in AD, (ii) second, application of biochar in DF and AD performance and (iii) third, application of thermophilic conditions in DF.

Configuration	T (°C)	Inoculum pretreatment T (°C)	BC concentration (g/L)
First experiment: Dark Fermentation			
TH_80	35	80	/
TH_100	35	100	/
TH_120	35	120	/
First experiment: Anaerobic Digestion			
DF80	35	/	/
DF80_B1	35	/	1
DF100	35	/	/
DF100_B1	35	/	1
SingleAD	35	/	/
Second experiment: Dark Fermentation			
TH_80	35	80	/
TH_80_B1	35	80	1
TH_100	35	100	/
TH_100_B1	35	100	1
TH_100_B2	35	100	2
Second experiment: Anaerobic Digestion			
DF80	35	/	/
DF80+B1	35	/	1
DF100	35	/	/
DF100+B1	35	/	1
DF100+B2	35	/	2
SingleAD	35	/	/
Third experiment: Dark Fermentation			
TH_80	55	80	/
TH_80_B1	55	80	1
TH_100	55	100	/
TH_100_B1	55	100	1

5.3.2 Two-stage anaerobic digestion of FVW and JWW: evaluation of thermal pretreatment for dark fermentation

This experimental campaign assessed the feasibility of integrating DF and AD in a sequential process by applying TSAD to FVW and JWW. In the first stage, three DF configurations were evaluated by varying the inoculum thermal pretreatment temperature to 80, 100, and 120 °C, hereafter referred to as TH_80, TH_100, and TH_120, respectively.

Biogas production started on day 1 in all configurations (*Figure 5.1-a*). TH_100 and TH_120 showed similar production trends, characterized by a steep initial increase, whereas TH_80 exhibited a delayed response. In TH_100 and TH_120, the highest production rate occurred during the first day, as indicated by the sharp initial slope of the cumulative curves. Conversely, TH_80 reached its maximum production rate between days 2 and 3, reflecting a slower start-up. From day 2 onward, biogas production in TH_100 and TH_120 declined markedly and progressively approached a plateau, indicating reduced microbial activity, with steady-state conditions reached by day 3 in all configurations. Among the tested conditions, TH_100 achieved the highest cumulative biogas production (194 N

mL/g_{VS}), followed by TH_80 (179 N mL/g_{VS}) and TH_120 (157 N mL/g_{VS}). Notably, 65-75 % of total biogas production in TH_100 and TH_120 occurred within the first day, whereas only 11 % of the total biogas in TH_80 was produced during this period, suggesting that higher pretreatment temperatures promoted faster biogas generation. Despite this delay, TH_80 surpassed TH_120 in cumulative production, and all configurations reached their maximum yields at similar times.

H_2 production (*Figure 5.1-b*) followed a comparable temporal pattern. In TH_100 and TH_120, the highest H_2 production rates occurred within the first day, accounting for approximately 60-73 % of the total H_2 generated. In contrast, TH_80 exhibited lower H_2 production during the initial phase, followed by a rapid increase after day 2, ultimately exceeding the maximum H_2 yield of TH_120. H_2 production reached a plateau by day 3 in all cases. Overall, the highest H_2 yields were obtained in TH_100 and TH_80 (75 N mL/g_{VS}), while TH_120 achieved a slightly lower value (67 N mL/g_{VS}).

CH_4 production displayed a different behavior (*Figure 5.1-c*). After a modest increase during the first day, CH_4 production rapidly stabilized and remained nearly constant throughout the experiment, with cumulative yields below 0.25 N mL/g_{VS} for all configurations. This indicates effective suppression of methanogenic activity under the applied DF conditions.

CO_2 production (*Figure 5.1-d*) closely mirrored total biogas trends. TH_100 and TH_120 exhibited the highest CO_2 production rates during the first day, followed by a gradual increase until day 3, after which production plateaued. The highest cumulative CO_2 yield was observed in TH_100 (119 N mL/g_{VS}), followed by TH_80 (105 N mL/g_{VS}) and TH_120 (89 N mL/g_{VS}).

The composition of the produced biogas is reported in *Figure 5.1-e*. H_2 reached maximum concentrations of 43 % in TH_120 and 41 % and 38 % in TH_80 and TH_100, respectively. In all configurations, CO_2 was the dominant gas, accounting for approximately 57-61 % of the total biogas volume. Methane was detected only in trace amounts, with maximum concentrations of 0.12 % in TH_80, followed by 0.05 % in TH_100 and 0.01 % in TH_120, confirming effective suppression of methanogenic activity. Thermal pretreatment proved effective under all tested conditions. No substantial differences in overall biogas production were observed among the three pretreatment temperatures, indicating comparable fermentability of the substrate ($p > 0.05$). This result suggests that lower pretreatment temperatures (80 and 100 °C) may be sufficient for DF, offering potential advantages in terms of reduced energy demand when considering scale-up applications.

Digestates from the DF stage were further analyzed for VFAs, namely acetic, propionic, and butyric acids, to elucidate the dominant metabolic pathways (*Figure 5.1-f*). Overall, VFA profiles were similar across all configurations. Acetic and butyric acids were the predominant compounds, while propionic acid was almost negligible in all configurations. Acetic acid concentrations ranged from 1.02 to 1.96 g/L, whereas propionic acid, when detected, remained below 0.02 g/L. Butyric acid was the dominant VFA in all cases, reaching 3.9 g/L in

TH_80, 2.5 g/L in TH_100, and 2.8 g/L in TH_120. As a result, total VFAs concentrations were 5.8, 3.6, and 4.8 g/L for TH_80, TH_100, and TH_120, respectively. None of these values exceeded the commonly reported inhibitory threshold of 8 g/L. Although VFAs accumulated during DF, regular pH monitoring and adjustment likely contributed to process stability by preventing acidification-induced inhibition. Overall, thermal pretreatment was confirmed as an effective strategy to suppress methanogens and promote H_2-producing microbial populations. Among the tested conditions, pretreatment at 80 and 100 °C appeared adequate, as increasing the temperature to 120 °C did not provide additional benefits in terms of gas production or VFAs profiles, while potentially increasing energy requirements. These findings are consistent with the study by Pascualone et al. (2019), who reported effective hydrogen production (63.2 mL/g_{VS}) using a 100 °C thermally pretreated vermicompost inoculum for vegetable waste fermentation, with biogas containing 46 % H_2 and no detectable CH_4.

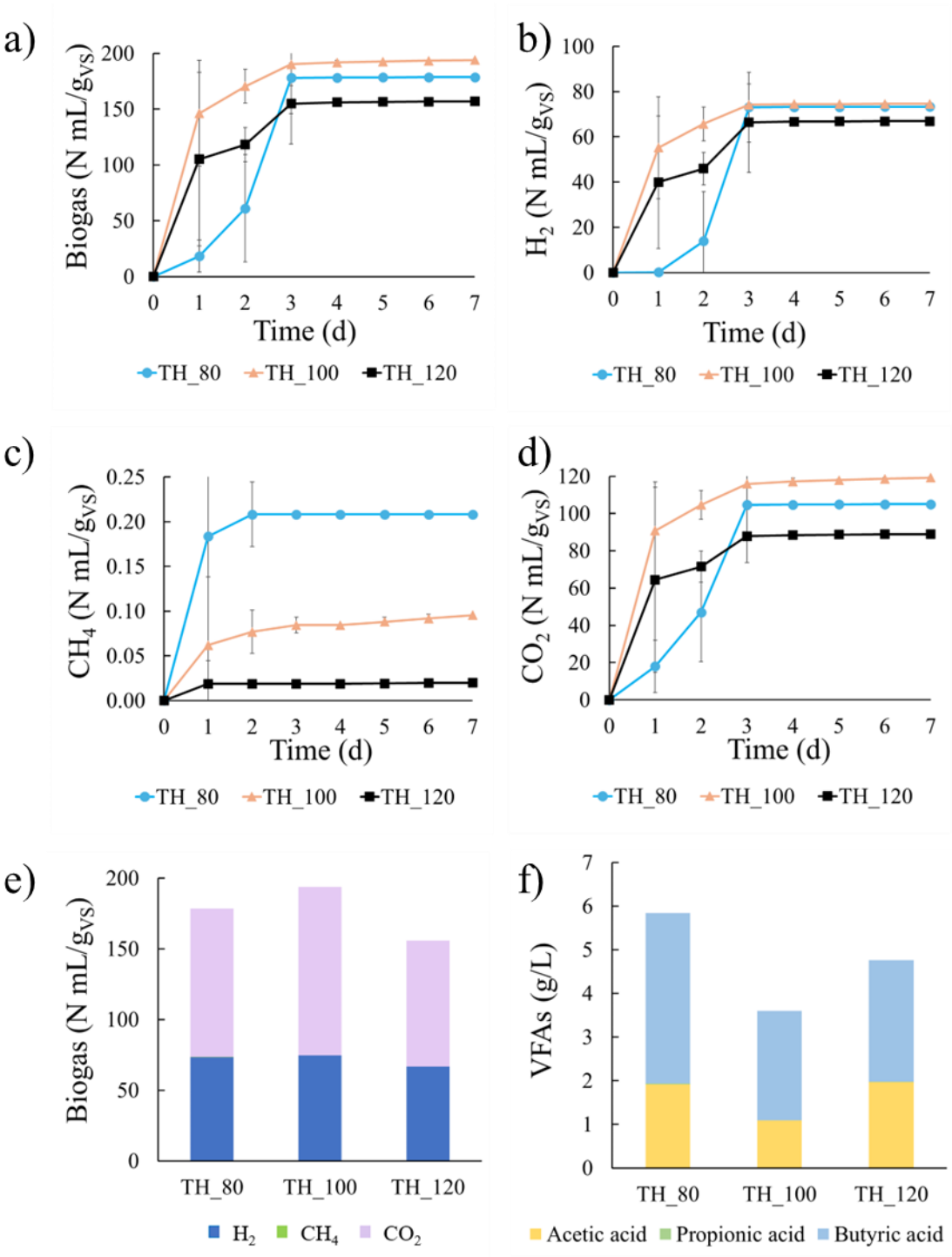

Figure 5.1 Results from the DF of the first experiment: a) biogas yield, b) H_2 yield, c) CH_4 yield, d) CO_2 yield, e) composition of total biogas produced during dark fermentation considering H_2, CH_4 and CO_2, f) VFAs concentration in the three configurations as g/L.

5.3.3 Two-stage anaerobic digestion of FVW and JWW: application of biochar in anaerobic digestion

The second stage of the process (AD) utilized the digestate from the DF stage as substrate. Four experimental configurations were evaluated during the AD, based on the DF with inoculum thermally pretreated at 80 or 100 °C since they achieved similar process performance while requiring lower pretreatment temperatures, thereby reducing energy consumption. For each digestate, AD was conducted either without additives or with the addition of biochar at a concentration of 1 g/L. The configurations were therefore defined as follows: DF80 (digestate from DF with 80 °C pretreatment), DF80_B1 (DF80 with 1 g/L biochar), DF100 (digestate from DF with 100 °C pretreatment), and DF100_B1 (DF100 with 1 g/L biochar). These digestates were combined with non-pretreated CAS inoculum at a 1:1 ratio while maintaining a TS content of 3 %. The performance of the second stage of AD was compared with that of a conventional single-stage AD applied directly to FVW and JWW (defined as SingleAD).

Biogas and CH_4 production over the 34-day experimental period are shown in *Figure 5.2-a* and *-b*. All configurations generated biogas, with broadly similar trends except for the SingleAD control. During the initial phase (days 0-6), biogas production rates were high, as indicated by the steep slope of the cumulative curves. Between days 6 and 10, production slowed across all reactors, resulting in a gentler slope, and a plateau was reached in the final phase until the end of the experiment. Cumulative biogas yields were 246, 266, 235, and 253 N mL/g_{VS} for DF80, DF80_B1, DF100, and DF100_B1, respectively. In contrast, SingleAD exhibited a sharp increase until day 5, reaching only 35 % of its maximum biogas yield. A plateau occurred from days 6 to 12, after which biogas production resumed, reaching a final cumulative yield of 402 N mL/g_{VS}.

CH_4 production followed trends like total biogas. An initial phase of rapid accumulation occurred until day 6, followed by slower production through the remainder of the experiment. Maximum CH_4 yields were 193 N mL/g_{VS} for DF100, 208 N mL/g_{VS} for DF80, 227 N mL/g_{VS} for DF100_B1, and 241-240 N mL/g_{VS} for DF80_B1 and SingleAD, respectively. CO_2 production *Figure 5.2-d* exhibited comparable trends, with SingleAD peaking during the first 4 days (138 N mL/g_{VS}) and other configurations reaching lower yield: DF80 and DF100 at 42 N mL/g_{VS}, and DF80_B1 and DF100_B1 at 26 N mL/g_{VS}.

Biogas composition is presented in *Figure 5.2-e*. CH_4 was the dominant component, accounting for 90 % in DF80_B1 and DF100_B1, 82-84 % in DF80 and DF100, and 60 % in SingleAD. CO_2 concentrations ranged from 9-34 %, with the lowest in the biochar-supplemented reactors. H_2 was detected only in SingleAD (6 %). Statistical analysis indicated no significant differences in cumulative biogas production among the four TSAD configurations during the second stage ($p > 0.05$). As observed in the DF stage, inoculum pretreatment temperature (80 or 100 °C) and biochar addition (1 g/L) had limited influence on biogas or CH_4 yields in the subsequent AD stage.

However, it is noteworthy that the configurations supplemented with biochar exhibited a substantially higher CH_4 fraction in the biogas compared to SingleAD, together with a correspondingly lower CO_2 content. This shift in biogas composition suggests a beneficial role of biochar in enhancing biogas quality rather than increasing total gas production. The reduced CO_2 fraction may be attributed to the ability of biochar to adsorb CO_2, as well as to promote more efficient conversion of intermediate compounds toward methanogenesis. In addition, the conductive surface and porous structure of biochar may facilitate direct or indirect interspecies electron transfer, favoring methane formation over CO_2 accumulation. Although the overall CH_4 yields were not significantly different, the improvement in CH_4 concentration highlights the potential of biochar as an effective additive for upgrading biogas composition and improving downstream energy recovery.

A notable observation is the difference in production dynamics between the second stage of TSAD and SingleAD. While SingleAD ultimately produced the highest total biogas (402 N mL/gVS), CH_4 yields were similar across all configurations. The main advantage of TSAD lies in production rate: 90 % of maximum CH_4 yield was achieved within 10 days in DF80, DF100, DF80_B1, and DF100_B1, compared to day 28 for SingleAD, almost three times longer. This acceleration highlights the potential industrial relevance of TSAD, where faster attainment of peak yields can significantly improve process efficiency and throughput. These results are consistent with observations discussed in Section 2.3.6, confirming that while single-stage AD can maximize total biogas, TSAD enhances CH_4 production kinetics without compromising final yields.

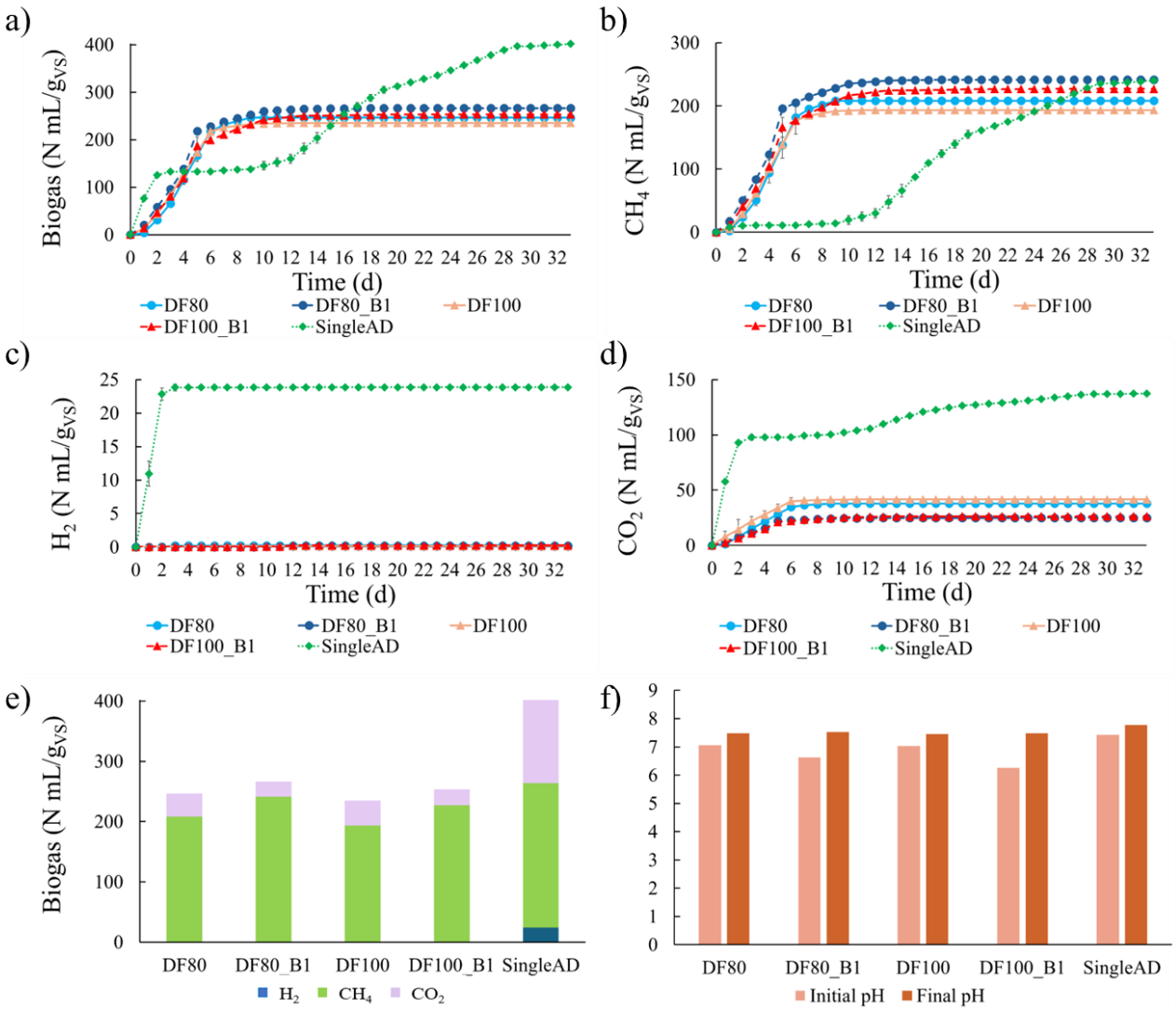

Figure 5.2 Results from the second stage of the first experiment: a) biogas yield, b) CH_4 yield, c) H_2 yield, d) CO_2 yield, e) composition of total biogas produced during AD considering H_2, CH_4 and CO_2 and f) initial and final pH of each configuration.

5.3.4 Two-stage anaerobic digestion of FVW and JWW: evaluation of biochar effect in dark fermentation

This experimental campaign assessed the feasibility of integrating DF and AD in a sequential process by applying TSAD to FVW and JWW. In the first stage, five DF configurations were evaluated by varying the inoculum thermal pretreatment temperature between 80 and 100 °C and investigating biochar role in process performance. The configurations were therefore defined as follows: TH_80 (80 °C pretreatment), TH_80_B1 (80 °C pretreatment with 1 g/L biochar), TH_100 (100 °C pretreatment), TH_100_B1 (100 °C pretreatment with 1 g/L biochar), and TH_100_B2 (100 °C pretreatment with 2 g/L biochar).

Biogas production began immediately in all configurations, as shown in *Figure 5.3-a*, although the production kinetics differed markedly among treatments. The configurations with inoculum pretreated at 100 °C (TH_100, TH_100_B1, and TH_100_B2) exhibited a rapid start-up, characterized by a steep initial increase in biogas production. Among these, TH_100_B2 reached a plateau as early as day 2, whereas TH_100 and TH_100_B1 continued producing biogas until day 3. In contrast, the configurations pretreated at 80 °C (TH_80 and TH_80_B1) displayed a slower initial production rate, as indicated by gentler slopes, but ultimately surpassed TH_100_B1 and TH_100_B2 in terms of cumulative biogas yield. Specifically, TH_80 and TH_80_B1 achieved final biogas yields of 179 and 190 N mL/g_{VS}, respectively. The highest cumulative biogas production was observed for TH_100 (194 N mL/g_{VS}), whereas lower yields were obtained for TH_100_B1 and TH_100_B2 (163 and 175 N mL/g_{VS}, respectively). These results indicate that higher pretreatment temperatures favored faster biogas production kinetics but did not necessarily result in higher final biogas yields.

H_2 production (*Figure 5.3-b*) followed a different temporal pattern. All configurations with inoculum pretreated at 100 °C initiated H_2 production immediately, whereas those pretreated at 80 °C showed a one-day lag before H_2 generation began. Consistent with biogas trends, the 100 °C pretreatment promoted faster H_2 production, as reflected by steeper cumulative curves. In all cases, H_2 production ceased by day 3, when a plateau was reached. The highest hydrogen yield was achieved by TH_100_B2, reaching 93 N mL/g_{VS}, while all other configurations yielded approximately 75 N mL/g_{VS}.

CH_4 production remained negligible throughout the experiment (*Figure 5.3-c*). Only TH_80 and TH_100 exhibited trace CH_4 formation, with cumulative yields below 0.2 N mL/g_{VS}, most of which occurred during the first day. This confirms effective suppression of methanogenic activity under the applied DF conditions.

CO_2 production trends (*Figure 5.3-d*) differed from those of both biogas and H_2. Configurations with inoculum pretreated at 100 °C showed a faster CO_2 production rate compared to those pretreated at 80 °C. TH_100_B2 reached a plateau by day 2, whereas the remaining configurations plateaued by day 3. Despite a slower start-up, TH_80_B1 achieved the highest cumulative CO_2 production (123 N mL/g_{VS}), closely followed by TH_100 (119 N mL/g_{VS}).

Intermediate yields were observed for TH_80 (105 N mL/g_{VS}), while lower values were obtained for TH_100_B1 and TH_100_B2 (91 and 83 N mL/g_{VS}, respectively).

The biogas composition is reported in *Figure 5.3-e*. H_2 reached a maximum concentration of 53 % in TH_100_B2, followed by 46 % in TH_100_B1 and 39 % in TH_80. The lowest H_2 concentrations (38%) were observed in TH_80_B1 and TH_100. CO_2 accounted for 47–62% of the biogas volume, while CH_4 was detected only in trace amounts, further confirming successful inhibition of methanogens. No statistically significant differences in total biogas production were observed among the five configurations ($p > 0.05$), suggesting that biochar addition in the tested range (1-2 g/L) did not substantially affect overall biogas yields. However, the higher H_2 yield and fraction observed in TH_100_B2 may indicate a potential positive effect of biochar on H_2 production, although this cannot be conclusively established due to the high variability of the results, as reflected by the large error bars.

VFAs in the DF digestates were analyzed to elucidate the dominant metabolic pathways (*Figure 5.3-f*). The VFAs profiles varied across configurations, although acetic and butyric acids consistently dominated, while propionic acid remained negligible. Acetic acid concentrations ranged from 0.09 to 3.32 g/L. Butyric acid was the predominant acid in all configurations except TH_100_B2, where it accounted for 47% of total VFAs and reached 3.0 g/L. Higher butyric acid concentrations were measured in TH_80 (4.16 g/L) and TH_80_B1 (3.32 g/L), while lower values were observed in TH_100 (2.41 g/L) and TH_100_B1 (2.79 g/L). Consequently, total VFAs concentrations were 7.0, 3.4, 3.5, 4.9, and 6.3 g/L for TH_80, TH_80_B1, TH_100, TH_100_B1, and TH_100_B2, respectively, all remaining below the commonly reported inhibitory threshold of 8 g/L. Although VFAs accumulated during DF, regular pH monitoring and adjustment likely prevented acidification-related inhibition and contributed to process stability.

Overall, the role of biochar in enhancing DF performance could not be clearly established under the tested conditions, as process variability and statistical analysis did not indicate a significant effect. This contrasts with the findings of W. Li et al. (2020), who reported a 114% increase in H_2 yield during glucose DF with biochar additions of 3–12 g/L. The discrepancy may be attributed to the higher biochar dosages and the use of a simpler substrate in their study, suggesting that biochar effectiveness may be strongly dependent on both concentration and substrate complexity.

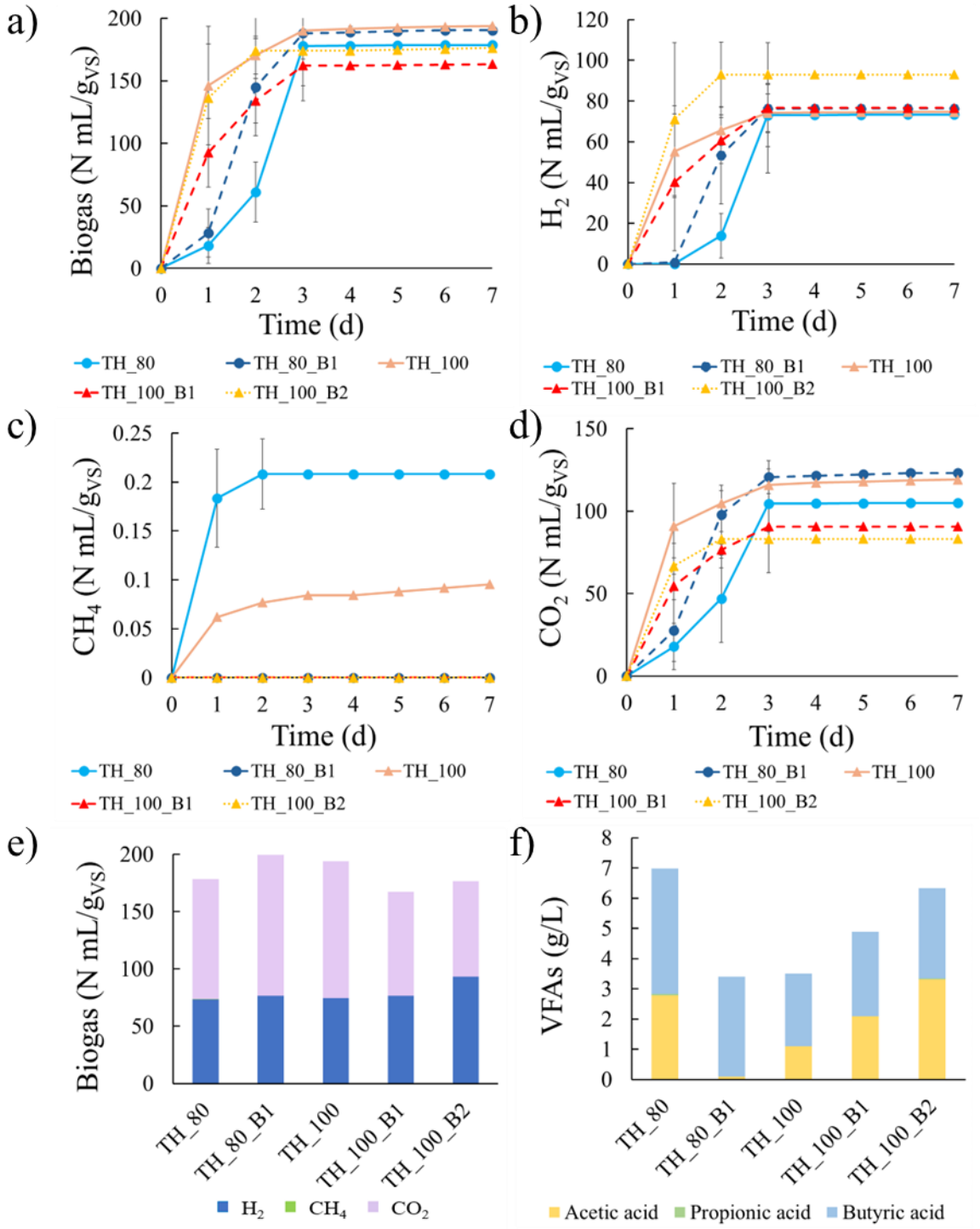

Figure 5.3 Results from the DF of the second experiment: a) biogas yield, b) H_2 yield, c) CH_4 yield, d) CO_2 yield, e) composition of total biogas produced during dark fermentation considering H_2, CH_4 and CO_2, f) VFAs concentration in the five configurations as g/L.

5.3.5 Two-stage anaerobic digestion of FVW and JWW: effects of biochar-amended DF on anaerobic digestion

The second stage of the process (AD) utilized the digestate from the DF stage as substrate. Five experimental configurations were evaluated during the AD corresponding to the configurations tested in the first stage (paragraph 5.3.4). They were defined as: DF80 (digestate from TH_80), DF80+B1 (digestate from TH_80_B1), DF100 (digestate from TH_100), DF100+B1 (digestate from TH_100_B1) and DF100+B2 (digestate from TH_100_B2). Each effluent was mixed with fresh, non-pretreated CAS inoculum at a S:I ratio of 1:1, maintaining a TS content of 3 %. The performance of the second stage of TSAD was compared with that of a conventional single-stage AD process applied directly to FVW and JWW (hereafter referred to as SingleAD).

Cumulative biogas and CH_4 production over the 34-day experimental period are shown in *Figure 5.4-a* and *-b*. All TSAD configurations produced biogas and exhibited similar overall trends, whereas SingleAD showed a distinct production pattern. During the initial phase (days 0–6), biogas production rates were high in all TSAD reactors, as indicated by the steep slopes of the cumulative curves. After day 6, production gradually slowed, and a stable plateau was reached from day 9 until the end of the experiment. Final cumulative biogas yields were 246, 283, 235, 117, and 164 N mL/g_{VS} for DF80, DF80+B1, DF100, DF100+B1, and DF100+B2, respectively. In contrast, SingleAD exhibited a rapid increase in biogas production until day 5, followed by a temporary plateau between days 6 and 12, after which production resumed, reaching a final cumulative yield of 402 N mL/g_{VS}.

CH_4 production followed trends similar to those observed for total biogas. A rapid accumulation phase occurred during the first six days, followed by a plateau for the remainder of the experimental period. The highest CH_4 yield among the TSAD configurations was obtained with DF80+B1 (230 N mL/g_{VS}), followed by DF80 (208 N mL/g_{VS}), DF100 (193 N mL/g_{VS}), DF100+B2 (131 N mL/g_{VS}), and DF100+B1 (95 N mL/gVS). SingleAD reached a comparable CH_4 yield of 240 N mL/g_{VS}. CO_2 production (*Figure 5.4-d*) showed a similar temporal trend across all reactors, although SingleAD exhibited higher CO_2 production, peaking at 138 N mL/g_{VS}, whereas TSAD configurations ranged between 18 and 53 N mL/g_{VS}.

Biogas composition is presented in *Figure 5.4-e*. CH_4 was the dominant component in all TSAD configurations, accounting for 80-85 % of the biogas, whereas SingleAD contained a lower CH_4 fraction (approximately 60 %). CO_2 concentrations ranged from 14 to 34 %, with the lowest values observed in biochar-amended reactors. H_2 was detected only in trace amounts in DF100+B1 (4 %), DF100+B2 (7 %), and SingleAD (6 %). Statistical analysis revealed significant differences in total biogas production among the six configurations. In particular, SingleAD significantly outperformed all other configurations in terms of biogas yield, whereas DF100+B1 showed markedly lower performance. Interestingly, this trend was not observed for methane production: SingleAD achieved methane yields comparable to DF80+B1, indicating an improvement in

process performance resulting from the application of TSAD. Overall, results regarding the effect of biochar addition during the first stage on the performance of the second AD stage are not easy to interpret. While DF80+B1 showed improved performance compared to DF80, this trend was not confirmed for the 100 °C pretreatment, where the biochar-amended configurations performed worse than DF100 in AD. This variability may be attributed to the inherent complexity of the system, which is influenced by factors such as feedstock composition, seasonal variations, and operational conditions.

Nevertheless, a key outcome of this study is the marked difference in production kinetics between TSAD and SingleAD, as discussed in paragraphs 2.3.6 and 5.3.3. Although SingleAD achieved the highest total biogas production, CH_4 yields were comparable to DF80 and DF80+B1. The principal advantage of TSAD lies in the substantially faster CH_4 production: approximately 99 % of the final CH_4 yield was reached within 10 days in all TSAD configurations, whereas SingleAD required up to 32 days to achieve the same level. This acceleration is particularly relevant for industrial applications, where reduced retention times and higher process throughput can significantly enhance overall efficiency. These results demonstrate that TSAD improves CH_4 production kinetics without compromising final yields, confirming its potential as an effective alternative to conventional single-stage AD.

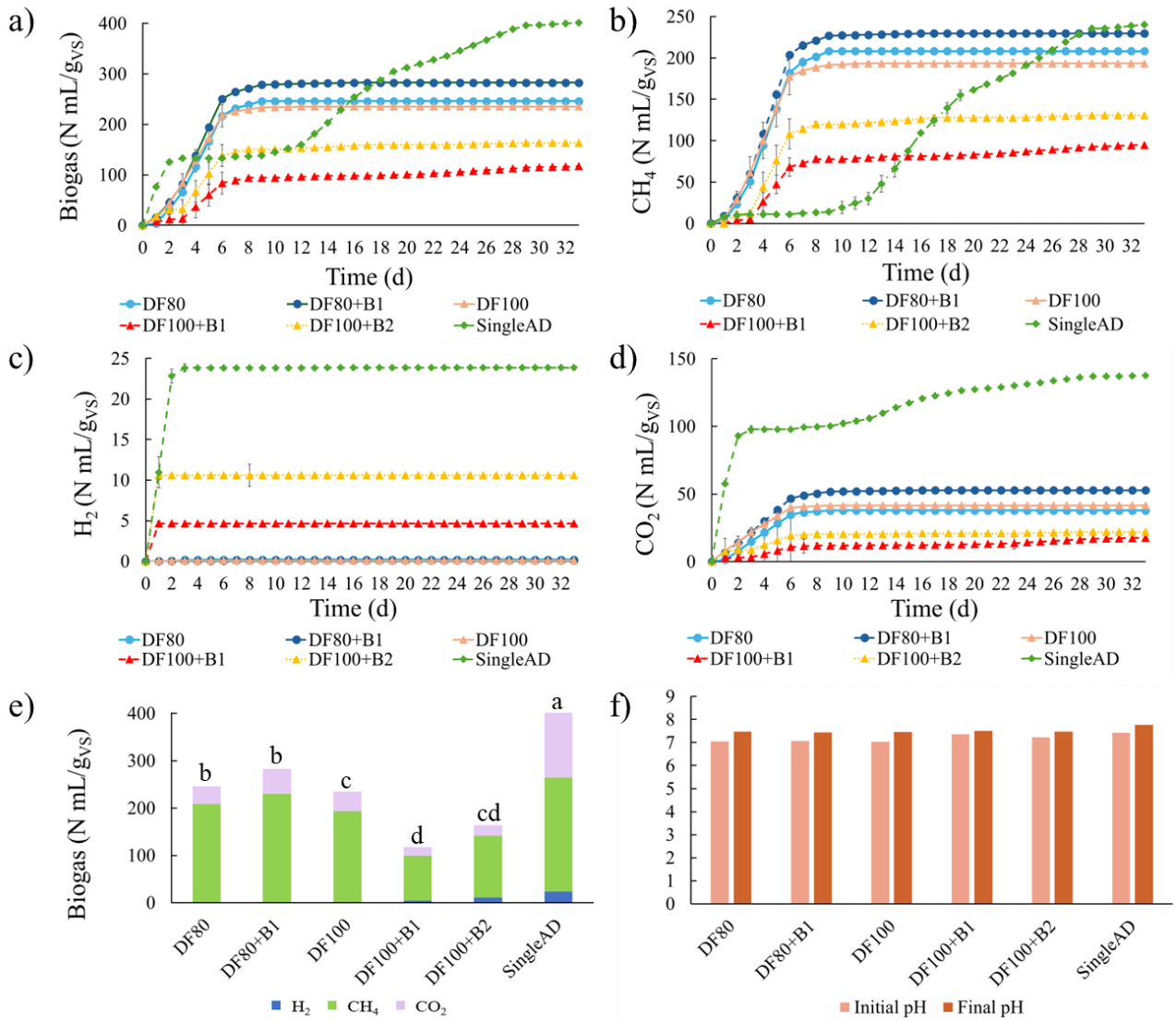

Figure 5.4 Results from the second stage of the second experiment: a) biogas yield, b) CH_4 yield, c) H_2 yield, d) CO_2 yield, e) composition of total biogas produced during AD considering H_2, CH_4 and CO_2 and f) initial and final pH of each configuration.

5.3.6 Thermophilic dark fermentation of FVW and JWW: evaluation of biochar effect

This experimental campaign assessed the feasibility of thermophilic DF applied to FVW and JWW. Four configurations were evaluated by varying the inoculum thermal pretreatment temperature between 80 and 100 °C and investigating on biochar role in process performance. The configurations were therefore defined as follows: TH_80 (80 °C pretreatment), TH_80_B1 (80 °C pretreatment with 1 g/L biochar), TH_100 (100 °C pretreatment), and TH_100_B1 (100 °C pretreatment with 1 g/L biochar).

Biogas production started immediately in all configurations, as shown in *Figure 5.5-a*. Similar production kinetics were observed for TH_80, TH_80_B1, and TH_100_B1, all characterized by a steep initial slope indicating the highest production rate within the first day of operation. From day 2 onward, the rate of biogas production progressively decreased, reaching a plateau by day 4. In contrast, TH_100 exhibited a high production rate during the first two days, followed by a lag phase that persisted until the end of the experiment. Final cumulative biogas yields of 224 and 198 N mL/g_{VS} were obtained for TH_80 and TH_80_B1, respectively. The highest biogas production was achieved by TH_100_B1 (243 N mL/g_{VS}), while the lowest yield was observed for TH_100 (152 N mL/gVS).

H_2 production followed trends comparable to those of total biogas (*Figure 5.5-b*). In TH_80, TH_80_B1, and TH_100_B1, between 75 % and 97 % of the total H_2 yield was produced within the first day of fermentation. Conversely, TH_100 reached its maximum H_2 production by day 2, after which production ceased. The highest H_2 yield was recorded in TH_100_B1 (128 N mL/g_{VS}), while the other configurations achieved values ranging between 78 and 101 N mL/g_{VS}.

CH_4 production remained negligible throughout the experiment (*Figure 5.5-c*). Only TH_80 and TH_100_B1 exhibited trace CH_4 formation, with cumulative yields below 0.21 N mL/g_{VS}. CH_4 production occurred mainly during the first day in TH_100_B1 and by day 8 in TH_80, confirming the effective suppression of methanogenic activity under the applied dark fermentation conditions.

CO_2 production trends are presented in *Figure 5.5-d*. Like biogas and H_2, most CO_2 production occurred within the first day in TH_80, TH_80_B1, and TH_100_B1, whereas TH_100 maintained a relatively high production rate during the second day as well. Despite achieving the highest biogas and H_2 yields, TH_100_B1 did not exhibit the highest CO_2 production, reaching 114 N mL/g_{VS} compared to 123 N mL/g_{VS} in TH_80. TH_80_B1 reached 106 N mL/g_{VS}, while TH_100 showed the lowest CO_2 yield (74 N mL/g_{VS}).

Biogas composition is reported in *Figure 5.5-e*. H_2 reached a maximum concentration of 53 % in TH_100_B1, followed by 51 % in TH_100 and 46 % in TH_80_B1. The lowest H_2 concentration (45 %) was observed in TH_80. CO_2 accounted for 47-55 % of the biogas, while CH_4 was present only in trace amounts, further confirming effective inhibition of methanogens.

Statistical analysis revealed significant differences in total biogas production among the four configurations. Biochar addition (1 g/L) significantly enhanced biogas production in the 100 °C pretreated inoculum, whereas no substantial effect was observed for the 80 °C pretreatment. The higher H_2 yield and fraction observed in TH_100_B1 may indicate a possible influence of biochar on hydrogen production; however, this effect should be interpreted with caution, as it may also reflect intrinsic process variability. Under these conditions, the observed increase in biogas production was approximately 64 %.

VFAs in the DF digestates were analyzed to elucidate the dominant metabolic pathways (*Figure 5.5-f*). VFAs profiles differed among configurations; however, butyric acid consistently dominated, while acetic acid was detected only in three configurations. Propionic acid was not detected. Acetic acid concentrations ranged from 0.07 to 0.09 g/L. Butyric acid concentrations reached 2.41, 2.39, 2.45, and 2.57 g/L for TH_80, TH_80_B1, TH_100, and TH_100_B1, respectively. Consequently, total VFAs concentrations were 2.41, 2.47, 2.53, and 2.65 g/L, all well below the commonly reported inhibitory threshold of 8 g/L. Regular pH monitoring and adjustment likely prevented acidification and contributed to process stability.

Overall, process temperature had a strong influence on H_2 production. Thermophilic conditions (55 °C) substantially increased H_2 yields compared to the mesophilic conditions discussed in Section 5.3.4, where maximum yields of approximately 75 N mL/g_{VS} were obtained regardless of pretreatment temperature or biochar addition. In the present study, TH_80, TH_80_B1, and TH_100_B1 achieved H_2 yields of 101, 92, and 128 N mL/g_{VS}, corresponding to increases of 35 %, 23 %, and 71 %, respectively, compared to mesophilic operation.

The influence of operating temperature on DF performance is consistent with previous studies. Shin et al. (2004) investigated DF of food waste at 35 and 55 °C and reported a ninefold increase in H_2 yield under thermophilic conditions. Similarly, Zhang et al. (2019) observed a 20 % increase in CH_4 yield during AD of soybean curd at 55 °C compared to 35 °C. Zhang et al. (2023) further demonstrated that thermophilic conditions enhanced CH_4 yields by 8 % in food waste digestion, with biochar addition providing an additional 11 % increase and reducing digestion time. These findings confirm the critical role of temperature in improving anaerobic process performance.

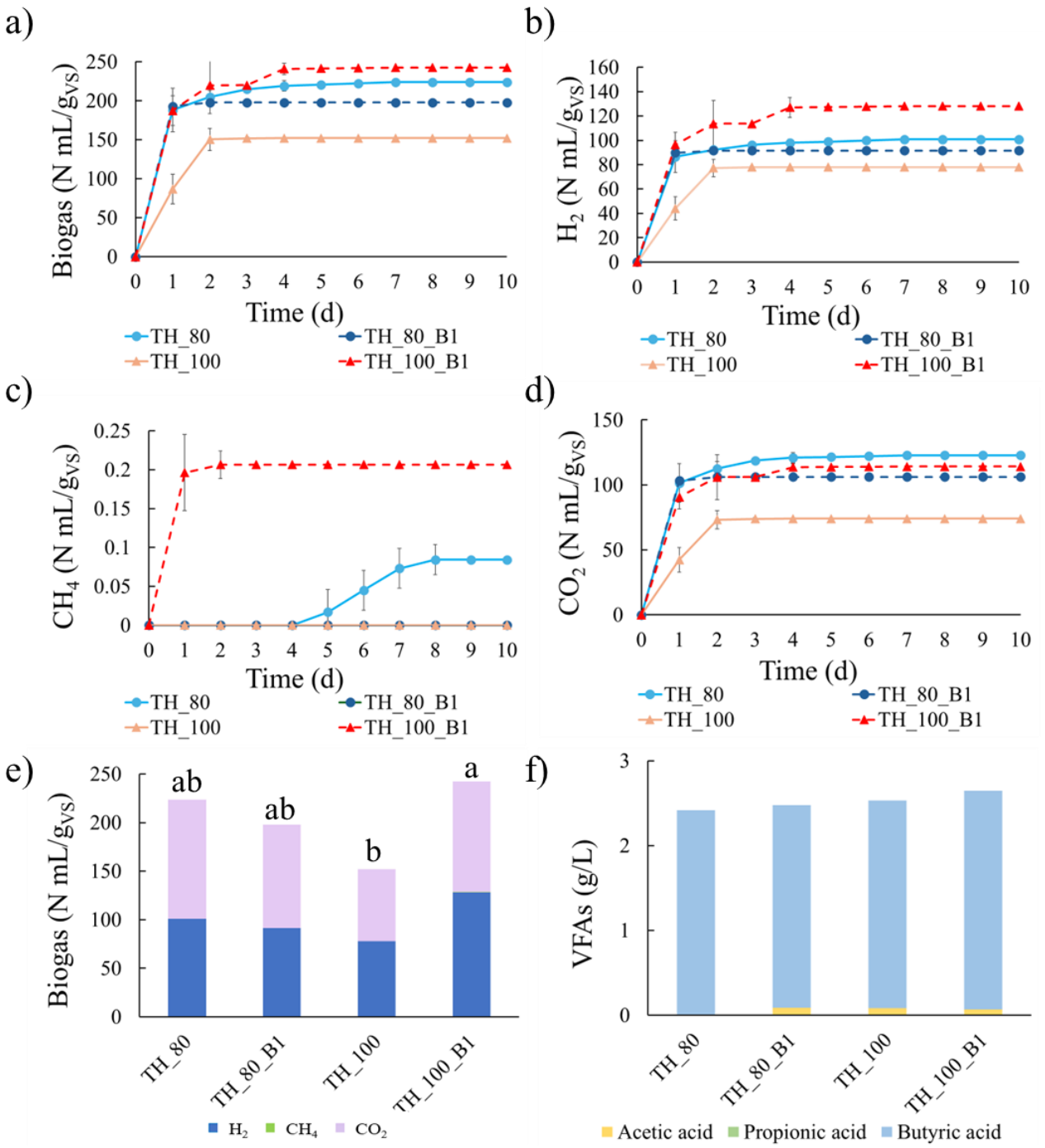

Figure 5.5 Results from thermophilic DF: a) biogas yield, b) H_2 yield, c) CH_4 yield, d) CO_2 yield, e) composition of total biogas produced during dark fermentation considering H_2, CH_4 and CO_2, f) VFAs concentration in the three configurations as g/L.

5.3.7 Humic acids extraction

As previously described, HA extraction was carried out on digestate obtained from the TSAD of FVW and JWW, using inoculum thermally pretreated at 100 °C. The quantification of HA was performed following the method proposed by Lamar et al. (2014). The extracted HA was first dried in a laboratory oven at 90 °C, then transferred to a ceramic crucible and combusted in a muffle furnace. After cooling, the crucible containing the ash was weighed to determine the ash content. The final HA mass was then calculated by correcting the measured mass for ash content. Results are presented in *Table 5.4*.

Table 5.4 Humic acids (HA) yield expressed as g HA/ g dry mass digestate.

Substrate	% HA (dry matter basis)	Standard deviation	Reference
Anaerobic sewage sludge from wastewater	12.53	± 1.60	Cristina et al. (2020)
Sewage sludge	7.33	N.A.	H. Li et al. (2017)
Digestate from TSAD of FVW and JWW	20.01	± 1.81	This study

The amount of HA extracted from the digestate represents the highest value among the studies considered in this work. However, the HA purity remains lower than that of commercial products, which typically reach values of about 77%. This difference is expected and can be attributed to the origin of the extracted material. In this case, HA is derived from waste-based digestate, which inherently contains a higher fraction of inorganic residues and non-humified organic compounds compared to commercial HA obtained from peat, lignite, or leonardite. These conventional sources are naturally richer in humic substances and undergo extensive industrial purification processes, resulting in higher purity levels (Cristina et al. 2020).

Elemental analysis showed carbon, nitrogen, and hydrogen contents of 38.36 ± 2.25 %, 3.68 ± 0.44 %, and 4.29 ± 0.44 %, respectively. These values are consistent with those reported in the literature for humic acids obtained from waste-derived substrates by Kambatyrov et al. (2025) and Spaccini and Piccolo (2009). The elemental composition reflects the heterogeneous and partially aromatic nature of the extracted organic matter.

Despite the lower purity, the HA recovered from digestate demonstrates a significant recovery potential and may still be suitable for applications such as soil amendment or organic fertilization, where extremely high purity is not strictly required.

5.3.7.1 FTIR spectroscopic analysis of humic acids

Infrared spectroscopy of the three powdered HA extract replicates confirmed the presence of functional groups characteristic of humic substances. *Figure 5.6*

shows the ATR–FTIR transmittance spectrum, which displays several bands commonly associated with HA.

A broad absorption band centered around 3728 cm^{-1} was observed and is attributed to O-H stretching vibrations of carboxylic acids, phenols, and alcohols. This feature reflects the high abundance of hydroxyl-containing functional groups typically found in humic materials (Kambatyrov et al. 2025). The spectrum also exhibits a characteristic doublet in the 2920-2850 cm^{-1}, corresponding to C-H stretching vibrations of aliphatic structures (Taha 2025; Spaccini and Piccolo 2009).

In the mid-infrared region, an intense band between 1650 and 1630 cm^{-1} can be assigned to C=O stretching of carboxylic and ketonic groups, as well as to aromatic C=C stretching vibrations, indicating the presence of both oxygenated and aromatic moieties (Taha 2025; Timofeevna Shirshova et al. 2006). A further peak at approximately 1533 cm^{-1} is associated with C=N stretching of amide groups, suggesting contributions from nitrogen-containing organic compounds. Additional bands at 1456 and 1418 cm^{-1} are characteristic of bending vibrations of aliphatic C-H groups, further confirming the aliphatic nature of part of the organic matrix (Spaccini and Piccolo 2009). The region between 1216 and 1031 cm^{-1} shows multiple overlapping peaks, which can be attributed to C-O stretching vibrations of alcohols, phenols, aliphatic ethers, and polysaccharides. This region is commonly reported as a fingerprint zone for oxygenated functional groups in humic substances (Timofeevna Shirshova et al. 2006; Kambatyrov et al. 2025; Taha 2025).

Finally, several bands observed at lower wavenumbers (832-456 cm^{-1}) are reasonably attributed to vibrations of aromatic carbon structures and alkyl substituents (Kambatyrov et al. 2025). Overall, the FTIR spectral features agree with those reported in the literature for humic substances, suggesting that the extracted material shares typical structural and functional features of humic acids.

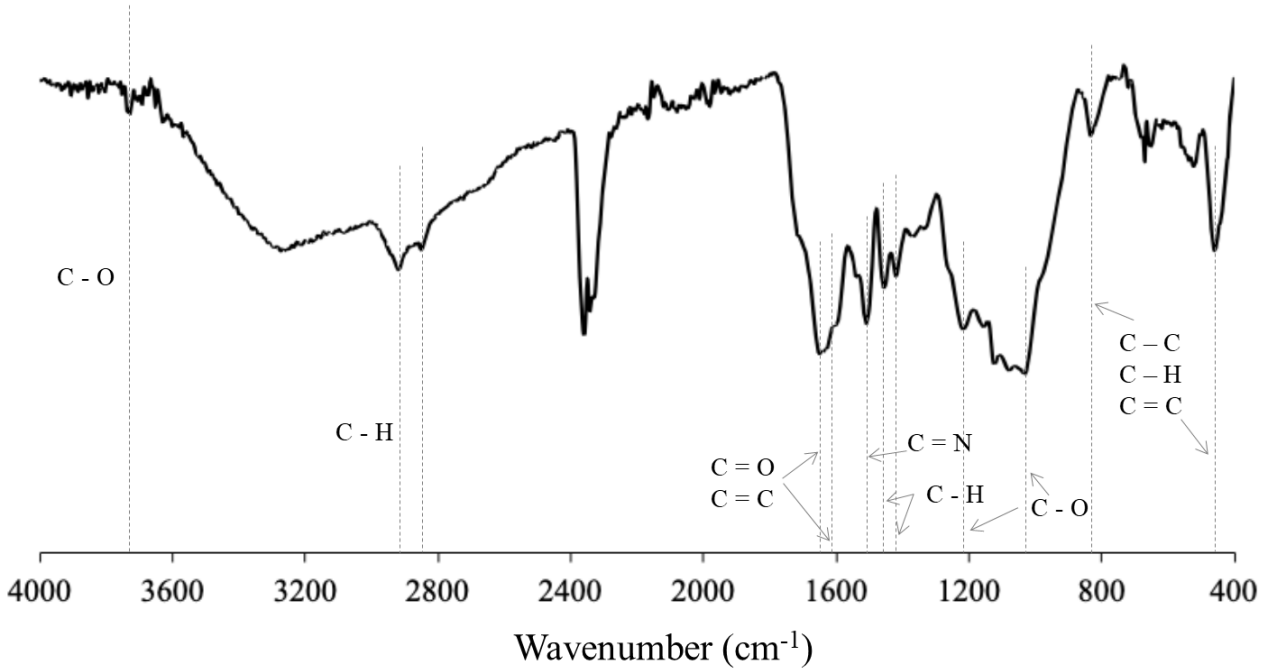

Figure 5.6 ATR-FTIR transmittance spectrum of powered HA extract.

References

Cristina, Giulio, Enrico Camelin, Carminna Ottone, et al. 2020. “Recovery of Humic Acids from Anaerobic Sewage Sludge: Extraction, Characterization and Encapsulation in Alginate Beads.” *International Journal of Biological Macromolecules* 164 (December): 277–85. https://doi.org/10.1016/j.ijbiomac.2020.07.097.

Ding, Jingran, Feng Zhen, Xiaoying Kong, Yunzi Hu, Yi Zhang, and Lang Gong. 2024. “Effect of Biochar in Modulating Anaerobic Digestion Performance and Microbial Structure Community of Different Inoculum Sources.” *Fermentation* 10 (3): 151. https://doi.org/10.3390/fermentation10030151.

Guilayn, F., M. Benbrahim, M. Rouez, M. Crest, D. Patureau, and J. Jimenez. 2020. “Humic-like Substances Extracted from Different Digestates: First Trials of Lettuce Biostimulation in Hydroponic Culture.” *Waste Management* 104 (March): 239–45. https://doi.org/10.1016/j.wasman.2020.01.025.

Hidalgo, Dolores, Enrique Pérez-Zapatero, Jesús M. Martín-Marroquín, Miguel A. Sánchez-Gatón, and Marta Gómez. 2024. “Comparative Analysis of Additives for Enhanced Biohydrogen Production via Dark Fermentation.” *JOM* 76 (1): 141–52. https://doi.org/10.1007/s11837-023-06231-5.

Huang, Jin-Rong, Xiong Chen, Bin-Bin Hu, Jing-Rong Cheng, and Ming-Jun Zhu. 2022. “Bioaugmentation Combined with Biochar to Enhance Thermophilic Hydrogen Production from Sugarcane Bagasse.” *Bioresource Technology* 348 (March): 126790. https://doi.org/10.1016/j.biortech.2022.126790.

Kambatyrov, Maksat, Perizat Abdurazova, Ulzhalgas Nazarbek, and Yerkebulan Raiymbekov. 2025. “Infrared Spectroscopic Study of the Mechanisms of Humic Acid Precipitation in Aqueous Acid Solutions.” *Engineering, Technology and Applied Science Research* 15 (3): 23527–36. https://doi.org/10.48084/etasr.10976.

Lamar, Richard T., Daniel C. Olk, Lawrence Mayhew, and Paul R. Bloom. 2014. “A New Standardized Method for Quantification of Humic and Fulvic Acids in Humic Ores and Commercial Products.” *Journal of AOAC International* 97 (3): 721–30. https://doi.org/10.5740/jaoacint.13-393.

Li, Weiming, Lei He, Chi Cheng, Guangli Cao, and Nanqi Ren. 2020. “Effects of Biochar on Ethanol-Type and Butyrate-Type Fermentative Hydrogen Productions.” *Bioresource Technology* 306 (June): 123088. https://doi.org/10.1016/j.biortech.2020.123088.

Lou, Tianru, Yanan Yin, and Jianlong Wang. 2024. “Recent Advances in Effect of Biochar on Fermentative Hydrogen Production: Performance and Mechanisms.” *International Journal of Hydrogen Energy* 57 (February): 315–27. https://doi.org/10.1016/j.ijhydene.2024.01.039.

Pascualone, María J., Marcos B. Gómez Costa, and Pablo R. Dalmasso. 2019. “Fermentative Biohydrogen Production from a Novel Combination of Vermicompost as Inoculum and Mild Heat-Pretreated Fruit and Vegetable Waste.” *Biofuel Research Journal* 6 (3): 1046–53. https://doi.org/10.18331/BRJ2019.6.3.5.

Shen, Yanwen, Jessica L. Linville, Meltem Urgun-Demirtas, Robin P. Schoene, and Seth W. Snyder. 2015. “Producing Pipeline-Quality Biomethane via Anaerobic Digestion of Sludge Amended with Corn Stover Biochar with in-Situ CO2 Removal.” *Applied Energy* 158 (November): 300–309. https://doi.org/10.1016/j.apenergy.2015.08.016.

Shin, Hang Sik, Jong Ho Youn, and Sang Hyoun Kim. 2004. “Hydrogen Production from Food Waste in Anaerobic Mesophilic and Thermophilic Acidogenesis.” *International Journal of Hydrogen Energy* 29 (13): 1355–63. https://doi.org/10.1016/j.ijhydene.2003.09.011.

Spaccini, Riccardo, and Alessandro Piccolo. 2009. “Molecular Characteristics of Humic Acids Extracted from Compost at Increasing Maturity Stages.” *Soil Biology and Biochemistry* 41 (6): 1164–72. https://doi.org/10.1016/j.soilbio.2009.02.026.

Sunyoto, Nimas M.S., Mingming Zhu, Zhezi Zhang, and Dongke Zhang. 2016. “Effect of Biochar Addition on Hydrogen and Methane Production in Two-Phase Anaerobic Digestion of Aqueous Carbohydrates Food Waste.” *Bioresource Technology* 219 (November): 29–36. https://doi.org/10.1016/j.biortech.2016.07.089.

Taha, Nancy A. 2025. “Chemical and Spectroscopic Studies on a Humic Acid Extracted from Clover Straw.” *Journal of Agricultural Chemistry and Biotechnology* 0 (0): 73–76. https://doi.org/10.21608/jacb.2025.379159.1110.

Tang, Shuai, Zixin Wang, Zhidan Liu, Yuanhui Zhang, and Buchun Si. 2020. “The Role of Biochar to Enhance Anaerobic Digestion: A Review.” *Journal of Renewable Materials* 8 (9): 1033–52. https://doi.org/10.32604/jrm.2020.011887.

Timofeevna Shirshova, Ludmila, Elham A. Ghabbour, and Geoffrey Davies. 2006. "Spectroscopic Characterization of Humic Acid Fractions Isolated from Soil Using Different Extraction Procedures." *Geoderma* 133 (3–4): 204–16. https://doi.org/10.1016/j.geoderma.2005.07.007.

Wongfaed, Nantharat, Sureewan Sittijunda, Sompong O-Thong, et al. 2025. "Enhancement of Dark Fermentative Hydrogen Production Using Metal-Modified Biochar from Sugarcane Residues: Optimization, Characterization, and Metabolic Analysis." *Journal of Environmental Management* 380 (April): 125047. https://doi.org/10.1016/j.jenvman.2025.125047.

Yang, Guang, and Jianlong Wang. 2019. "Synergistic Enhancement of Biohydrogen Production from Grass Fermentation Using Biochar Combined with Zero-Valent Iron Nanoparticles." *Fuel* 251 (September): 420–27. https://doi.org/10.1016/j.fuel.2019.04.059.

Yang, Yongjun, Jie Bu, Yong Wei Tiong, et al. 2024. "Enhanced Thermophilic Dark Fermentation of Hydrogen Production from Food Waste by Fe-Modified Biochar." *Environmental Research* 244 (March): 117946. https://doi.org/10.1016/j.envres.2023.117946.

Zhang, Le, Kai-Chee Loh, Suseeven Sarvanantharajah, Yen Wah Tong, Chi-Hwa Wang, and Yanjun Dai. 2019. "Mesophilic and Thermophilic Anaerobic Digestion of Soybean Curd Residue for Methane Production: Characterizing Bacterial and Methanogen Communities and Their Correlations with Organic Loading Rate and Operating Temperature." *Bioresource Technology* 288: 121597.

Zhang, Rong, Min Zhang, Huaqian Mou, et al. 2023. "Comparation of Mesophilic and Thermophilic Anaerobic Co-Digestion of Food Waste and Waste Activated Sludge Driven by Biochar Derived from Kitchen Waste." *Journal of Cleaner Production* 408: 137123.

Zhao, Yawen, Yuhao Wang, Chengjie Wen, et al. 2025. "Biochar-Mediated Enhancement of Dark Fermentative H2 Production from Xylose Wastewater: Insight into the Microbial Community Structure Succession to Metabolic Performance." *Biomass and Bioenergy* 203 (December): 108297. https://doi.org/10.1016/j.biombioe.2025.108297.

Chapter 6

6. Techno-economic and environmental assessment

6.1 Introduction

Industrial scale-up refers to the transition of a process from laboratory or pilot-scale conditions to full-scale industrial application. This step is essential for translating scientific and technological advances into solutions that are economically viable and socially relevant. One of the main challenges associated with scale-up is reproducing the performance observed at small scale in large-volume systems, where operating conditions become more complex and are constrained by technical, regulatory, and economic requirements. Ensuring stable operation, comparable efficiencies, consistent product quality, and acceptable environmental and economic performance require careful adaptation of laboratory conditions to industrial realities.

In conventional development pathways, pilot-scale studies are typically employed to refine operating parameters and identify potential limitations before full-scale implementation. In the present work, however, a direct transition from laboratory-scale results to industrial scale was considered. This approach was adopted because the objective was not to develop a detailed engineering design, but rather to provide a preliminary evaluation of process feasibility, plant configuration, and associated cost implications and environmental impacts at an industrial scale.

Accordingly, this chapter addresses the conceptual design, economic and environmental evaluation of a TSAD industrial plant. The analysis includes the definition of the main process units and operating assumptions, followed by an assessment of capital and operating costs and the calculation of key economic performance indicators, with particular attention to the role of economies of scale. Furthermore, the economic evaluation is complemented by an environmental assessment based on Life Cycle Assessment (LCA), allowing a comprehensive evaluation of both the economic and environmental sustainability of the proposed

system. The configuration selected for this analysis corresponds to the system described in Sections 5.3.2 and 5.3.3. It includes inoculum thermal pretreatment at 100 °C and excludes biochar addition, as no significant performance improvements were observed with the use of this additive. In contrast, the 100 °C thermal pretreatment resulted in the highest H_2 yield and was therefore retained.

6.2 Materials and methods

6.2.1 Technological assessment

Before starting the detailed design, the purpose of the process was clearly defined in terms of the raw material to be used and the desired final products. Then, existing technologies used in similar processes were reviewed to select the most suitable option. After the technology was chosen, the design activities began.

The equipment design approach adopted in this thesis is based on two main phases.

6.2.1.1 Matter and energy balances

Each piece of equipment is defined by one or more inlet material streams and one or more outlet streams. Identifying these flows is essential to accurately quantify the mass moving through the process, as this directly affects plant sizing.

When a unit involves heat transfer or electricity use, energy balances must also be considered. Energy consumption can be classified as electrical or thermal, depending on the operation. Electrical consumption refers to the amount of electricity used, expressed in kWh. Thermal consumption is related to heating or cooling requirements and is often quantified through the flow rate of a heating or cooling medium.

For heating operations, steam is commonly used; it releases heat as it condenses, while for cooling, water may be sufficient. In these cases, the flow rate of steam or cooling fluid represents the thermal energy demand of the process.

By knowing the enthalpy of vaporization or the specific heat capacity of the fluid, the thermal energy requirement can be easily calculated and expressed in kWh.

6.2.1.2 Sizing

As mentioned before, once the material flow rates and energy requirements of the plant are known, it is possible to estimate the size of the equipment. There is no single, universal method for this evaluation. For some units, sizing can be performed using established calculation procedures based on theoretical or empirical approaches. These methods rely on assumptions and formulas that allow reasonably accurate estimates of equipment dimensions.

In other cases, such calculation methods are not available or are not suitable. When this occurs, equipment selection is based on process requirements and practical considerations, often using technical catalogs to identify commercially available units that meet the plant’s needs.

Some general assumptions were made regarding the utilities used in the process. Heating and cooling operations are achieved through the supply of saturated steam, cooling water or chilling water. Unless otherwise specified, the properties of these utility streams are reported in *Table 6.1*. Based on these assumptions, saturated steam is assumed to release heat and fully condense at the same temperature while chilling water is assumed to increase in temperature by (ΔT) of 13 °C.

Table 6.1 Characteristics of fluids used in cooling and heating operations.

Fluid	Components	Status	Tin (°C)	Tout (°C)	Pressure (atm)
Water vapor	Water	Saturated Steam	125	125	1.68
Chilling water	Water	Liquid	7	20	1

Further considerations concern process pressure. Unless otherwise specified, all operations are assumed to occur at atmospheric pressure. When different pressures are required, the operating conditions are explicitly stated.

6.2.2 Economic assessment

Economic analysis evaluates all cost components that contribute to the total expense of the plant. These costs depend on earlier design choices, such as equipment sizing and energy optimization. For this reason, economic analysis represents the final step of the preliminary techno-economic assessment and allows verification of the project's technical and financial feasibility.

This analysis compares investment and operating costs with the expected revenues from product sales, providing an estimate of process profitability. Based on this comparison, realistic assumptions can be made about the practical implementation of the proposed system, considering both design simplifications and current market prices.

Plant costs are generally divided into fixed (FC) and variable costs (VC). FC are independent of production rate and include equipment investment, insurance, maintenance, and fixed personnel. VC depends on production and includes raw materials, energy consumption, packaging, and variable labor. The sum of fixed and variable costs at a given production level defines the total costs (TC) of the process.

Many of the decisions that are made during design are influenced by economic indicators. The purpose of economic analysis is to determine the convenience of certain choices to have maximum profit.

The indicators useful in the evaluation of these parameters are:

- Revenue (R)

$$R = p * q \tag{6.1}$$

where p is price and q is sales level.

- Helpful (U)

$$U = R - TC \tag{6.2}$$

where U can be negative (loss) or positive (gain).

These quantities are fundamental in the evaluation of the production levels that must be achieved in a company. For this purpose, a diagram is used where profitability is shown on the x-axis while costs and revenues are shown on the y-axis.

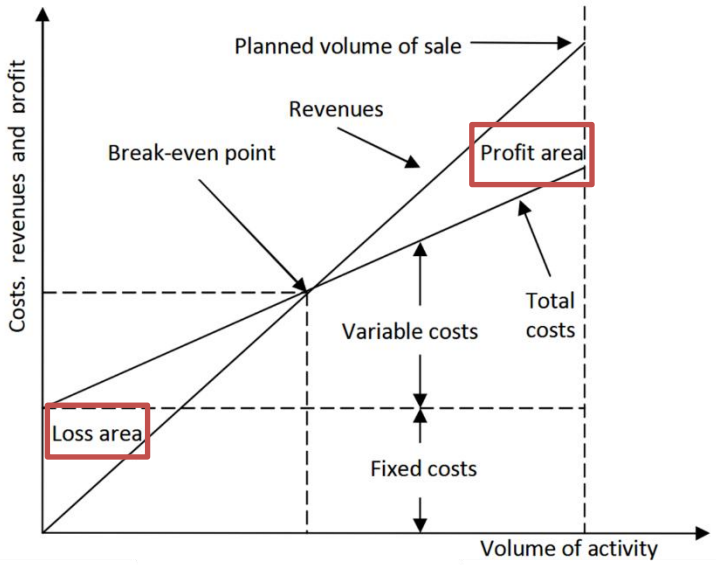

Figure 6.1 Profitability diagram as a function of production intensity modified from Janjić et al. (2010).

From *Figure 6.1* you can see the break-even point (BEP). The BEP is the point at which total costs and revenue equalize each other in a defined time. Before this point, there is no gain, so U is negative (loss area). On the contrary, beyond the BEP, U is positive (profit area). The increase in production of a plant is always associated with an increase in costs due to the management of the high level of production.

Plant design involves technical decisions guided by two main considerations. On one side, technological innovation is attractive because it can offer higher yields and improved process efficiency. On the other side, advanced technologies are often associated with higher costs compared to conventional solutions. For this reason, it is essential to evaluate whether the performance benefits justify the additional investment.

A key concept in process economic analysis is the economy of scale. This principle states that the specific cost per unit of product generally decreases as plant productivity increases. In other words, total costs do not increase

proportionally with production capacity. Instead, the relationship between cost and scale is less than linear, as described by the following equation:

$$C = C_0 \left(\frac{P}{P_0}\right)^m \tag{6.3}$$

where P and P_0 are the two levels of productivity, C and C_0 are the relative costs, and m is the scale factor (number less than or equal to 1).

Economies of scale arise from the different ways in which costs increase with plant size. For example, capital costs are often related to the surface area of equipment, while production capacity increases with volume, leading to a more efficient use of materials as size increases.

This principle also applies to operating costs such as maintenance and labor, which are more closely linked to the number of operators than to the size of the equipment itself. Energy consumption likewise tends to increase less than proportionally with productivity, as larger plants usually operate more efficiently (with scaling exponents typically in the range of m = 0.2–0.3).

As a result, economies of scale generally favor larger plants or the centralization of processes, as these configurations can achieve lower overall unit costs (Singh et al. 2015).

The economic evaluation of a plant can be carried out by calculating the cost of the different components that take part in the process. On the one hand, it is necessary to estimate the capital cost of the system, i.e. the one associated with the main equipment required. On the other hand, the operating cost of the process necessary to allow a good operation of the plant and therefore to ensure an intense production is evaluated.

6.2.2.1 Capital cost

The capital cost was estimated based on the equipment included in the process flow diagram. Equipment sizing was derived from material and energy balances. Once the required calculations were completed and the dimensions of each unit were defined, the main pieces of equipment were economically evaluated. The cost estimation was performed according to:

$$C_{BM} = C_p^0 F_{BM} = C_p^0 (B_1 + B_2 F_M F_P) \tag{6.4}$$

where C_{BM} is the total cost of a piece of equipment (*Bare Module Cost*), C_p^0 is the cost of equipment at atmospheric pressure and made of carbon steel (*Purchased Cost*) and F_{BM} is the factor that considers changes in pressure and materials of construction (*Bare Module Factor*). The latter can be either a unique value associated with a certain type of equipment or it can be evaluated according to four parameters: B_1 and B_2 are two constants, F_M is a factor associated with the

material of construction (*Material Factor*) and F_P is associated with the operating pressure of the equipment (*Pressure Factor*).

The value of C_p^0 is evaluated according to:

$$log_{10}C_p^0 = K_1 + K_2 log_{10}(A) + K_3[log_{10}(A)]^2$$

(6.5)

where K_1, K_2 and K_3 are three characteristic constants of each equipment and A is the characteristic size of the section (e.g. a heat exchanger is evaluated according to the exchange area). This relationship is associated with certain ranges of characteristic dimensions. Where the equipment does not fall within these values, the value of C_p^0 is assessed according to:

$$\frac{C_p^0}{C_{p,min}^0} = \left(\frac{A_p^0}{A_{p,min}^0}\right)^n$$

(6.6)

where $C_{p,min}^0$ is the cost of a piece of equipment with a size equal to the minimum of the relationship validity interval, $A_{p,min}^0$ is the minimum size of the interval and A_p^0 is the actual size of the equipment. The coefficient n has been evaluated as 0.6 as the average of the typical values that normally range between 0.3 and 0.84.

As previously mentioned, for some equipment the F_{BM} factor is provided directly, independently of construction material and operating pressure. In other cases, the F_{BM} must be calculated using the constants B_1 and B_2, together with the material factor F_M and the pressure factor F_P. Depending on the type of equipment, F_P is evaluated differently.

For pressure tanks, F_P is calculated according to:

$$F_{P,vessel} = \frac{\frac{PD}{2SE - 1.2P} + CA}{t_{min}}$$

(6.7)

where P is the operating pressure in *barg*, D is the diameter of the tank, CA is the corrosion factor (equal to 0.00315 m), S is the maximum stress sustained by carbon steel (equal to 944 bar), E is the welding efficiency (equal to 0.9) and t_{min} is the minimum thickness required for the tank wall (equal to 0.0063 m). If F_P is lower than 1, it is set equal to 1. For operating pressures below −0.5 barg, F_P is assumed to be 1.25.

For all other cases, F_P is calculated as:

$$log_{10}F_P = C_1 + C_2 log_{10}P + C_3[log_{10}P]^2$$

(6.8)

where C_1, C_2, and C_3 are constants associated with the equipment and P is the operating pressure in *barg* (Turton 1998).

For some equipment, it was not possible to estimate the values of the constants mentioned above. The C_{BM} value was then estimated from graphs in which this value is given as a function of the characteristic size (as in the case of the blade mill) or from data present in the literature (as in the case of the digesters) (Ulrich and Vasudevan 2004).

The value of C_{BM} is first calculated in $ and then converted into € with a conversion factor of 0.873 €/$.

Once the total cost of your main equipment has been calculated, inflation must be accounted for via the Chemical Engineering Plant Cost Index (CEPCI) factor. This index takes on a different value every year, so it is necessary to normalize the total cost of the plant to the year in which its construction is planned. C_{BM} values were evaluated using factors associated with the year 2001 when the CEPCI was worth 397. To update the design, the CEPCI of the year 2023 was considered equal to 801.

$$C_{BM,2023} = C_{BM,2001} \left(\frac{CEPCI_{2023}}{CEPCI_{2001}}\right)$$

(6.9)

Following the calculation of the total cost of the plant, the values of the contributions due to various operations were derived. The value of C_{BM} is worth 68 % of the total cost of building a plant (*Bare Erected Cost*) which also includes installation costs (24 % of the total) and materials, equipment and labor costs (8 % of the total). An additional cost equal to 17.5 % of the Bare Erected Cost was included to account for contractor services (*Engineering Procurement and Construction contractor services*). The sum of the latter term and the *Bare Erected Cost* constitutes the total *Engineering Procurement and construction cost*. This value is added to the costs due to process and project contingencies (17.6 % and 15 % of the *Bare Erected Cost*, respectively) to obtain the *Total Plant Cost (FCI).* Finally, the *Total Overnight Cost* is calculated as the sum of the *Total Plant Cost* and the start-up costs, inventory, financing and overhead (respectively 2 %, 0.5 %, 2.7 % and 15 % of the *Total Plant Cost*). All values calculated so far will be expressed in k€.

6.2.2.2 Operating costs

Following the evaluation of the total cost of the plant represented by *Total Overnight Cost*, it is necessary to calculate the costs due to the operation of the plant. This quantity differs from the first in that it is a time-dependent value and is therefore measured in k€/y.

Cost of Manufacturing (*COM*) can be divided into three categories:

- *Direct Manufacturing Cost* (*DMC*): these depend on the speed of production and consist of the cost of raw materials, cooling water, heating steam, labor, administration and support personnel, maintenance and repair, consumables, laboratory fees, patents, and royalties.

A brief in-depth analysis of the calculation of labor costs is necessary. It is based on the calculation of the operators needed to monitor the plant during production. It can be assumed that an operator works 49 weeks a year (thus considering 3 weeks for holidays and leave). Each week consists of 5 shifts of 8 hours for a total of 245 shifts per year per operator. Assuming that the plant is in operation 24 hours a day, 365 days a year, the total number of shifts to be covered can be calculated by multiplying the working days by three, i.e. the number of shifts per day. Dividing this value by the number of shifts per year assigned to an operator, we get about 4 operators hired for each operator present in the plant at any given time. The number of operators present in each shift (NOL) can be evaluated as:

$$N_{OL} = \left(6.29 + 0.23\, N_{np}\right)^{0.5} \tag{6.10}$$

where N_{np} is the number of equipment. Considering an annual salary of 40000 € for each operator, the cost of labor is obtained as:

$$C_{OL} = 4 * N_{OL} * 40000 \tag{6.11}$$

- *Fixed Manufacturing Costs* (*FMCs):* These are not affected by the level of production and are associated with depreciation, local taxes and insurance, and costs due to ancillary operations to support production.
- *General Expenses* (*GEs*): These are not associated with production because they consider expenses due to administration and management activities. This cost item includes expenses due to the distribution and sale of the product as well as those associated with research and development.

Table 6.2 shows the relationships used in the calculation of the various cost items (Turton 1998).

Table 6.2 Relationships used in the evaluation of the total cost of productivity of a plant.

Direct Manufacturing Cost	
Raw Materials	CRM
Waste Treatment	CWT
Utilities	CUT
Operating Labor	COL
Direct Supervisory and clerical labor	0.18 COL
Maintenance and Repairs	0.06 FCI
Operating Supplies	0.009 FCI
Laboratory Charges	0.15 COL
Patents and Royalties	0.03 COM
Fixed Manufacturing Cost	
Depreciation	0.1 FCI
Local Taxes and Insurance	0.032 FCI
Plant Overhead Costs	0.708 COL + 0.036 FCI
General Manufacturing Expenses	
Administration costs	0.177 COL + 0.009 FCI
Distribution and selling costs	0.11 COM
Research and Development	0.05 COM

The total manufacturing cost is therefore the sum of the three terms mentioned above and is a value expressed in k€/y. This value is referred to the production of all products on the process taken into considerations that in this case involve the production of bioH_2 (accounting for 9 % of the revenues), bioCH_4 (accounting for 0.56 % of the revenues), CO_2 (accounting for 0.51 % of the revenues) and HA (accounting for 0.37 % of the revenues).

Once the revenues from product sales are known, the profitability of the investigated processes can be evaluated using a set of economic indicators: Net Present Value (NPV), payback time (PBT), and Return on Investment (ROI).

NPV expresses the overall profitability of the plant over its lifetime, assumed to be 20 years. It is calculated by discounting future cash flows to their present value using a discount rate of 5 %. A positive NPV (NPV > 0) indicates that the process is economically profitable. It is calculated according to:

$$NPV\ (€) = \sum_{t-1}^{T} \frac{C_t}{(1+d)^t} - C_0 \tag{6.12}$$

PBT is the time required to regain the investment cost, calculated as:

$$PBT\ (y) = \frac{C_0}{Net\ cash\ flow\ per\ period} \tag{6.13}$$

ROI was defined according to:

$$ROI\ (\%) = \frac{Annual\ net\ profit}{Initial\ total\ investment} \cdot 100$$

(6.14)

Specifically, ROI is the annual net profit referred to the annual net profit after 5 years of amortization (Francesca Demichelis et al. 2018, 2024).

6.2.3 Environmental analysis

Life Cycle Assessment (LCA) is a standardized methodology (ISO 14040-44:2006) used to quantify the environmental impacts of a process or product alongside their life cycle. It evaluates the effects of material and energy flows, identifies critical points or bottlenecks, and allows comparison between different processes by using the same functional unit and system boundaries (Mazzanti et al. 2025). When applied to an industrial facility, LCA provides a comprehensive evaluation of the environmental footprint generated during all stages of the system, including construction, operation, maintenance, and end-of-life decommissioning.

The primary objective of LCA is to identify and quantify the environmental impacts associated with each life-cycle stage to support resource optimization, minimize environmental burdens, and promote more sustainable and environmentally responsible industrial practices.

The LCA procedure begins with the definition of the system boundaries and the scope of the analysis. For industrial applications, this step involves the identification and quantification of all relevant inputs, such as raw materials, chemicals, water, and energy, and outputs, including emissions, waste streams, and by-products. The collected data are then analyzed to determine which stages or processes contribute most significantly to the overall environmental impact, thereby highlighting opportunities for improvement.

The LCA process includes four main stages:

• Goal and scope definition
• Life Cycle Inventory (LCI)
• Life Cycle Impact Assessment (LCIA)
• Interpretation.

LCA was conducted using the SimaPro 9.4 software, with the Ecoinvent 3.10 and Agri-footprint 5 databases serving as the primary data sources.

6.2.3.1 Goal and scope

LCA was applied considering a grave-to-gate approach. The functional unit (FU) is defined as one year of process operation; therefore, the required energy, the consumed reagents, and emissions were referred to the FU. The analysis is geo-referred in the North of Italy, particularly in the Piedmont region, where the experimental wastes were sourced, and time-referred to 2025. Two configurations were compared: the first included a biogas purification unit for the separation of CH_4 and CO_2, while the second excluded this unit.

6.2.3.2 Life Cycle Inventory (LCI)

LCI phase, corresponding in this study to the plant design described in previous paragraphs, involved the systematic collection of data on material and energy exchanges between the system and the environment. This included inputs such as raw materials, water, chemicals, and energy, as well as outputs in the form of emissions, by-products, and waste as shown in *Table 6.3*.

Table 6.3 Life Cycle Inventory (LCI). The data are referred to the FU.

Step 1: Waste collection		**Input**	**Unit**
	FVW	6029	t/y
	JWW	43971	t/y
	Transport	47	km
		Output	
	Waste transport	50000	t/y
Step 2: Mechanical pretreatment		**Input**	**Unit**
	FVW	6029	t/y
	Crushing energy	60294	kWh
		Output	
	Greens wastes	6029	t/y
Step 3: Dark fermentation		**Input**	**Unit**
	Substrate (FVW+JWW)	50000	t/y
	Mixing energy	10419	kWh
	Heating energy	12411513	kWh
		Output	
	m H_2	5706	kg/y
	m CO_2	1198340	kg/y
	Digestate	50000	t/y
Step 4: Purification Hydrogen		**Input**	**Unit**
	Biogas from DF	1.64E+11	mL/y
	Chilling energy	24608161	kWh
	Heating energy	24846077	kWh
		Output	
	m H_2	5706	kg/y
	m CO_2	1190651	kg/y
Step 5: Anaerobic digestion		**Input**	**Unit**
	Digestate from DF	50000	t/y
	Mixing energy	27083	kWh
	Heating energy	59331	kWh

		Output	
	m CH_4	127900	kg/y
	m CO_2	440379	kg/y
	Digestate	50000	t/y
		Input	**Unit**
	Biogas from AD	2.21E+11	t/y
	Chilling energy	32850409	kWh
	Heating energy	40471766	kWh
Step 6: Purification Methane		**Output**	
	V CH_4	181714005017	mL/y
	m CH_4	120802	kg/y
	V CO_2	37365465831	mL/y
	m CO_2	68311	kg/y
		Input	**Unit**
	Digestate	50000	t/y
	KOH	28	t/y
Step 7: Recovery HA -> Basification	Electricity energy	106847	kWh
		Output	
	Liquid fraction	37521	t/y
	Humins (solid fraction)	12507	t/y
		Input	**Unit**
	Liquid fraction	37521	t/y
	HCl	74	t/y
Step 8: Recovery HA -> Acidification	Electricity energy	12802	kWh
		Output	
	Liquid fraction (waste)	28197	t/y
	HA (solid fraction)	9399	t/y
		Input	**Unit**
	HA (solid fraction)	9399	t/y
	Heating energy	6512469	kWh
Step 9: Drying HA	Electricity energy	43177	kWh
		Output	
	Liquid fraction (waste)	9011	t/y
	HA (solid fraction)	388	t/y

6.2.3.3 Life Cycle Impact Assessment (LCIA) and interpretation

LCIA converted the energy and material flows into potential environmental impacts. The evaluation was performed using the ReCiPe Midpoint 2016 (H) method, with particular emphasis on climate change (kg CO_2 eq).

In the interpretation phase, results from the inventory and impact assessment were integrated to identify the most significant environmental hotspots and to highlight possible strategies for mitigation.

6.3 Results

6.3.1 Design of process scale-up

This section will present the design of a TSAD plant at full scale. As mentioned before, the plant is intended to be in Piedmont with a potential input flow of 50000 t/y of waste, composed of 12 % FVW and 88 % JWW, following the substrates mass ratios presented in Chapter 5. Raw material production is not affected by seasonality, so the plant can be considered to operate year-round. The operating period amounts to 8760 hours per year and the process is assumed to operate 24 hours a day. Specifically, 7509 hours per year were considered for the normal operation of the plant, including DF, AD, and HA extraction, corresponding to six days of operation per week. The seventh day was reserved for purification activities, inoculum pretreatment in DF, and routine maintenance.
The plant is divided into two principal sections:

- TSAD section involves the biological treatment of FVW and JWW through DF and AD, as well as the purification of biogas from both processes. After FVW size reduction, the substrates are fed into a DF digester, followed by an AD unit. Two absorption–stripping systems are included for the recovery of H_2 and CH_4.
- HA extraction section utilizes AD digestate for the extraction of HA, following the procedure described in paragraph 5.3.7. Digestate is treated with KOH and centrifuged, then subjected to acid treatment and a second centrifugation. A final drying step produces HA powder.

Process diagram is presented in *Figure **6.2** Process flow diagram for two-stage anaerobic digestion process and humic acids extraction.Figure 6.2*.

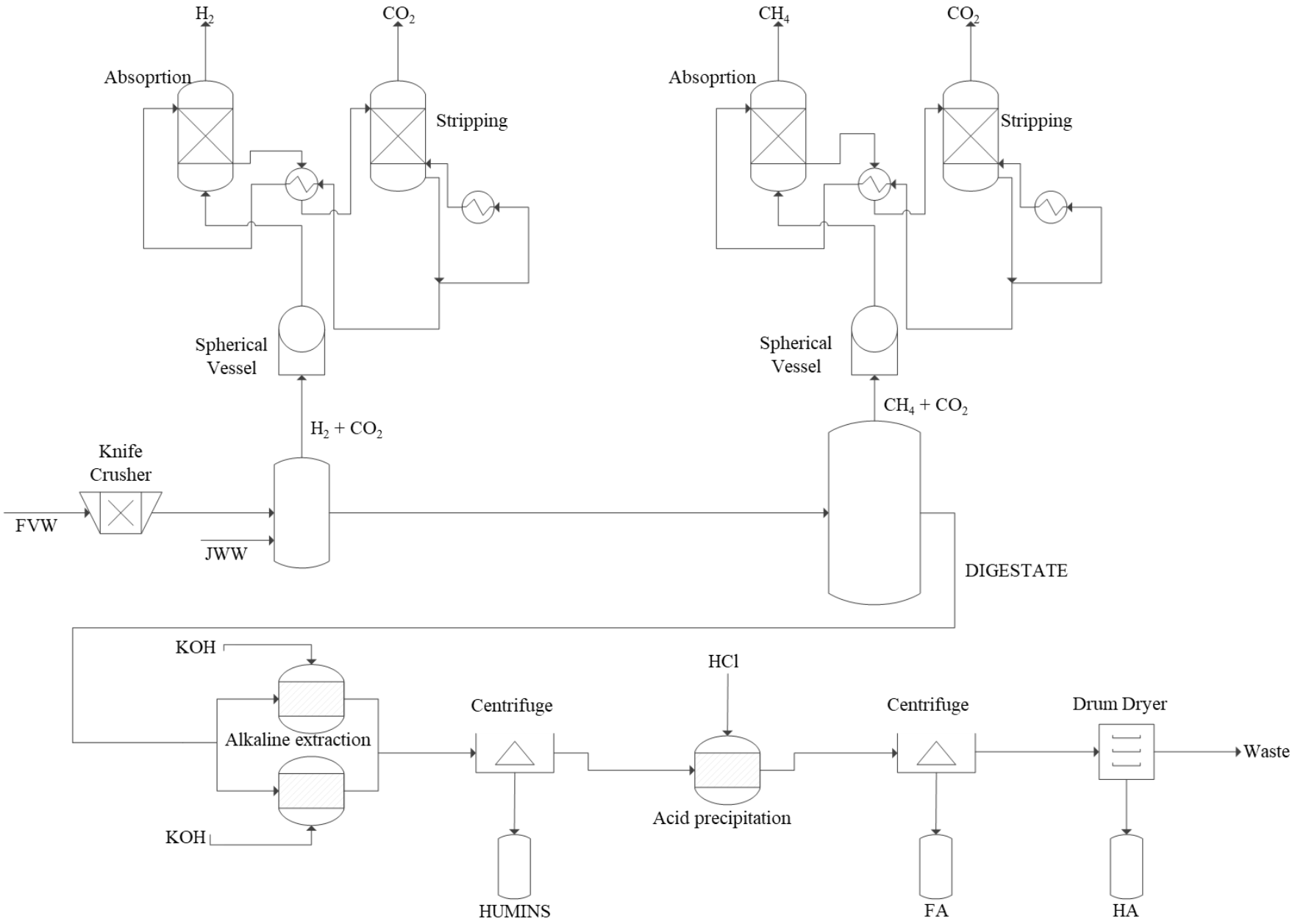

Figure 6.2 Process flow diagram for two-stage anaerobic digestion process and humic acids extraction.

6.3.1.1 Knife crusher

Before DF, FVW undergoes mechanical pretreatment through particle size reduction to increase substrate accessibility for microorganisms. A S710 shredder by the company *WaliShredder* was selected, as it is specifically designed for the processing of kitchen waste (Anhui Wali Environmental Protection Equipment Co.). The unit has a nominal capacity of 3000 kg/h and operates for approximately 6.4 h per day to process the daily FVW input. The resulting particle size of the treated feed ranges between 1 and 200 mm. Characteristics of the equipment are presented in *Table 6.4*.

Table 6.4 Characteristics associated with FVW size reduction using a shredder.

Q_{in} *(kg/d)*	19271
Load (kg/h)	3000
t (h)	6.4
Power (kW)	30
Mixing energy required (kWh)	60294

6.3.1.2 Dark fermentation

The digester was designed in accordance with the guidelines issued by "Agenzia per la Protezione dell'Ambiente e per i Servizi Tecnici - APAT" (Cecchi et al. 2005). Digester sizing can be performed using two main approaches. The first approach is based on the daily volumetric feed rate and considers the HRT as the primary design parameter. The second approach is based on the organic loading requirements of the process, allowing the reactor volume to be defined according to the amount of substrate needed to sustain the active biomass.

In this work, the HRT-based approach was adopted as a first-order approximation. The sizing procedure was carried out in the following steps:

- determination of the mass input flow rate, including TS and VS content;
- calculation of the organic load per unit reactor volume and estimation of the effective digester volume (V), defined as the ratio between the daily Total Volatile Solids (TVS) load and the OLR;
- Selection of the digester size based on standard reactor dimensions (Fischer and Krieg, n.d.).

Energy requirements were divided into two main categories: electrical energy and thermal energy.

Electrical energy was required for sludge mixing within the reactor and for pumping operations. Electricity consumption was estimated based on these two contributions following the approach proposed by Lu et al. (2008) according to:

$$E_{electricity} = E_{mixing} + E_{pumping} = Q_{in} \cdot \theta + V_{digester} \cdot \omega \quad (6.15)$$

where Q_{in} is the influent flowrate, m^3/d; θ is the electrical energy consumption for pumping, 1800 kJ/m^3; V is the volume of the digester, m^3; ω is the electrical energy consumption rate for stirring, 300 kJ/m^3 d.
Thermal energy requirements included: the heat necessary to maintain the digester at the operating temperature ($Q_{biomass}$), heat losses due to reactor interface (Q_{loss}) and heat losses associated with the piping system (Q_p), according to Demichelis et al. 2018):

$$E_{heating} = Q_{biomass} + Q_{loss} + Q_p \quad (6.16)$$

$Q_{biomass}$ was calculated following:

$$Q_{biomass} = \dot{m}_{biomass} \cdot c_p \cdot (T_{in} - T_{digetser}) \quad (6.17)$$

where $\dot{m}_{biomass}$ represents the biomass flow rate, kg/s; T_{in} and $T_{digester}$ are the inlet and digester temperatures, 15 and 35 °C respectively; c_p is the specific heat capacity (here considered equal to the value of water, as FVW dry matter is equal to 9.4 wt%), 4.18 kJ/kg °C.

Q_{loss} was calculated according to:

$$Q_{loss} = U_{ug} \cdot A_{ug} \cdot (T_{digester} - T_{gr}) + U_{ext} \cdot A_{ext} \cdot (T_{digester} - T_{ext}) \quad (6.18)$$

where U_{ug} and U_{ext} are the heat transfer coefficients for underground walls and non-ground walls, 2.33 and 0.93 W/m^2 °C, respectively (Mehr et al. 2017); A_{ug} and A_{ext} are the areas of underground walls and partial walls, respectively, and roof, m^2; T_{gr} and T_{ext} are the temperatures of underground walls and partial walls, 7.5 and 13.1 °C respectively. Q_p is calculated as 5 % of Q_{loss}.

For the DF digester, an additional thermal demand was considered for the periodic thermal pretreatment of the biomass used as inoculum. This pretreatment, applied once per week, was implemented to suppress methanogenic activity and promote the sporulation of H_2-producing microorganisms. The energy required for inoculum pretreatment ($Q_{pretreatment}$) was calculated according to:

$$Q_{pretreatment} = q_{biomass} \cdot t \quad (6.19)$$

where $q_{biomass}$ represents the heat required to raise the sludge mass inside the digester to the target temperature, kJ; t is the heating time, which depends on the temperature difference and the applied heating rate.

The biogas produced during the process was collected in a spherical storage vessel, a configuration widely used in anaerobic digestion plants due to its

structural efficiency and suitability for gas storage. The vessel volume was sized to accommodate the biogas produced over six consecutive days of operation, as the seventh day is dedicated to biogas purification. The spherical geometry was selected because it allows uniform stress distribution, minimizes material requirements for a given volume, and is well suited for low-pressure gas storage applications (Ulrich and Vasudevan 2004).
The characteristics and dimensions of the digester and spherical vessel are given in *Table 6.5*.

Table 6.5 Characteristics of dark fermentation digester and spherical vessel.

Q_{in} *(kg/d)*	1.60e05
HRT (d)	4
V (m^3)	884
OLR (kg_{VS}/m^3 *d)*	4.23
T (°C)	35
D (m)	7.5
H (m)	20
$E_{electricity}$ *(kWh)*	1.04e04
$E_{heating}$ *(kWh)*	1.24e07
$V_{Sphericalvessel}$ (m^3)	4000
$D_{Sphericalvessel}$ *(m)*	20

6.3.1.3 Hydrogen purification

Biogas produced during the DF stage is mainly composed of H_2 (39 %) and CO_2 (61 %), based on the experimental results presented in Section 5.3.2. The objective of this section is to propose a purification strategy by separating H_2 from CO_2 through water scrubbing in an absorption column.

The target H_2 purity at the column outlet was set to 99 %, while the absorption system was designed to capture more than 98 % of the CO_2 using water as the solvent operating at 25 °C. In the design of the absorption column, the molar fraction of CO_2 in the gas phase at the column outlet was fixed according to the desired separation performance.

The McCabe–Thiele graphical method was applied to determine the minimum number of theoretical stages required for the separation. An efficiency factor (0.8) was then used to estimate the actual number of stages. Since the process requires discrete stages, a tray (plate) absorption column was selected. The total column height was calculated based on the spacing between trays, which typically ranges from 0.15 to 1.0 m. A tray spacing of 1 m was adopted in this study. The overall column height was therefore obtained by multiplying the tray spacing by the actual number of trays.

Finally, the maximum allowable superficial gas velocity in the column was calculated to avoid flooding and ensure stable operation. This value was estimated using the following relationship:

$$u_v = (-0.171 l_t^2 + 0.27 l_t - 0.047) \left[\frac{\rho_L - \rho_v}{\rho_v}\right]^{\frac{1}{2}} \tag{6.20}$$

where l_t is the space between the plates, ρ_L is the density of the liquid and ρ_v is the density of the vapor.
The column diameter Dc is then calculated as:

$$D_c = \sqrt{\frac{4\, V_w}{\pi\, \rho_v\, u_v}} \tag{6.21}$$

where V_w is the maximum mass flow rate of vapor (Sinnott and Towler 2020).

After H_2 purification, a CO_2 stripping step was designed to release CO_2 from the absorption water and recover it as an additional product of the plant. The stripping process uses water vapor to remove CO_2 from the liquid stream exiting the absorption unit. This stream was heated in a heat exchanger until it reached 90 °C, corresponding to the operating temperature of the stripping unit.

In the stripping design, the target molar fraction of CO_2 in the liquid phase at the column outlet was fixed. As for the absorption unit, the McCabe–Thiele graphical method was applied to determine the required number of stages for

effective stripping. The column height and diameter were then calculated following the same design criteria used before.

Inside the column, CO_2 is transferred from liquid water to the rising steam, which carries the gas toward the top of the column. At the same time, heat exchange occurs between the liquid and vapor phases, leading to condensation of the steam near the column head. As a result, a liquid mixture of water and condensed steam accumulates at the bottom of the column.

To minimize water losses and promote internal recirculation, part of this liquid is sent to a reboiler, where it is vaporized to regenerate the steam required for stripping. The remaining liquid stream is cooled with chilling water to 25 °C, corresponding to the operating temperature of the absorption unit, and then recycled as the absorbent for H_2 purification. Characteristics of the system are presented in *Table 6.6*.

Table 6.6 Characteristics of absorption and stripping units employed for H_2 and CO_2 recovery.

ABSORPTION	
Q_{in} (N m^3/d)	3149
$T_{Absorption}$ (°C)	25
P (atm)	1.00
$y_{CO2,in}$	0.61
$y_{CO2,out}$	0.01
H_2 purity (%)	99
N° stages	7
Q_{Heater} (kW)	1.97e04
m_{Steam} (t/y)	2.03e04
Plate spacing (m)	1
H (m)	7
u_v (m/s)	2.14
D_c (m)	0.17
STRIPPING	
Q_{in} (N m^3/d)	6249
$T_{Stripping}$ (°C)	90
P (atm)	1.00
$x_{CO2,in}$	2.51e-04
$x_{CO2,out}$	5.00e-06
CO_2 purity (%)	98
N° stages	5
$Q_{Condenser}$ (kW)	1.97e04
$m_{ChilledWater}$ (t/y)	1.62e06
Q_{Heater} (kW)	190
m_{Steam} (t/y)	197
Plate spacing (m)	1
H (m)	5
u_v (m/s)	2.14
D_c (m)	2.1

6.3.1.4 Anaerobic digestion

The anaerobic digester was designed following the same procedure used for DF, as described in Section 6.3.1.2. In this case, occasional thermal treatment was not required because the inoculum was already adapted for methanogenesis, so no additional heating for this purpose was included in the energy requirements. Since the plant operates continuously and the HRT for DF is typically shorter than for anaerobic digestion, the AD was assigned an HRT of 20 days. At the same input flow rate, this longer retention time resulted in a larger digester volume.
The characteristics and dimensions of the digester and spherical vessel are given in *Table 6.7*.

Table 6.7 Characteristics of anaerobic digester and spherical vessel.

Q_{in} *(kg/d)*	1.60e05
HRT (d)	20
V (m^3)	4021
OLR (kg_{VS}/m^3 *d)*	0.94
T (°C)	35
D (m)	15
H (m)	25
$E_{electricity}$ *(kWh)*	2.71e04
$E_{heating}$ *(kWh)*	5.93e07
$V_{Sphericalvessel}$ (m^3)	5300
$D_{Sphericalvessel}$ *(m)*	21.6

6.3.1.5 Methane purification

For CH_4 purification, water scrubbing in an absorption column was selected, similar to the method used for H_2. The design procedure described in Section 6.3.1.3 was applied here to size both the absorption and stripping columns. Biogas from the anaerobic digester consisted of 82 % CH_4 and 18 % CO_2. Characteristics of the system are presented in *Table 6.8*.

Table 6.8 Characteristics of absorption and stripping units employed for CH_4 and CO_2 recovery.

ABSORPTION	
Q_{in} *(N* m^3*/d)*	4236
$T_{Absorption}$ *(°C)*	25
P (atm)	1.00
$y_{CO2,in}$	0.18
$y_{CO2,out}$	0.01
H_2 *purity (%)*	99
N° stages	9
Q_{Heater} *(kW)*	2.62e04
m_{Steam} *(t/y)*	2.71e04
Plate spacing (m)	1
H (m)	9
u_v *(m/s)*	2.14
D_c *(m)*	0.2
STRIPPING	
Q_{in} *(N* m^3*/d)*	8340
$T_{Stripping}$ *(°C)*	90
P (atm)	1.00
$x_{CO2,in}$	7.40e-05
$x_{CO2,out}$	5.00e-06
CO_2 *purity (%)*	93
N° stages	4
$Q_{Condenser}$ *(kW)*	2.62e04
$m_{ChilledWater}$ *(t/y)*	2.16e06
Q_{Heater} *(kW)*	6090
m_{Steam} *(t/y)*	1.25e04
Plate spacing (m)	1
H (m)	4
u_v *(m/s)*	2.14
D_c *(m)*	0.38

6.3.1.6 Humic acids extraction

After AD, digestate is further valorized in the second section of the plant which involves the extraction of HA, according to the procedure described in section 5.3.7.

As a first step, the digestate must be adjusted to strongly alkaline conditions (pH 12). For this purpose, it is fed into a continuously stirred tank reactor (CSTR), where potassium hydroxide (KOH) is added to achieve the target pH. The alkaline treatment is maintained for 24 h to allow effective solubilization of humic substances. To ensure continuous plant operation and facilitate charging and discharging procedures, two parallel treatment lines were designed. Each line consists of two stirred vessels operating alternately. While one line processes digestate for 24 h, the second line remains available for feeding or emptying operations. This alternating configuration guarantees uninterrupted treatment

while accommodating the required residence time. Each vessel was sized to accommodate half of the daily digestate throughput. Mixing was ensured by installing one impeller per vessel, and the corresponding electrical power demand was included in the energy balance (Sinnott and Towler 2020). After the alkaline treatment, the CSTR effluent is sent to a centrifuge to separate the solid fraction (humins, discharged as waste) from the liquid phase (supernatant containing humic and fulvic substances), which is forwarded to subsequent processing steps. A *Flottweg* AC100 centrifuge was selected for this operation. A phase split of 25 % solids and 75 % liquid was assumed. A dedicated storage vessel was designed to collect solid waste, sized to accommodate the daily solids production. The main design parameters of the vessels, the selected impellers and centrifuge are reported in *Table 6.9*.

Table 6.9 Characterization of HA alkaline extraction system.

Alkaline extraction	
Q_{in} *(kg/d)*	1.60e05
$t_{process}$ *(h)*	24
V_{Vessel} *(m^3)*	100
D_{Vessel} *(m)*	3.2
H_{Vessel} *(m)*	11.5
Nr. vessels	4
Nr. parallel lines	2
$D_{impeller}/D_{vessel}$	0.6
$D_{impeller}$ *(m)*	1.9
$P_{single\ impeller}$ *(kW)*	7
First Centrifugation	
Q_{in} *(kg/d)*	1.60e05
Model	AC100
Load (L/h)	10000
P (kW)	5.5
$V_{VesselWaste}$ *(m^3)*	50
D_{Vessel} *(m)*	3
H_{Vessel} *(m)*	6.5

The supernatant obtained from the first centrifugation is sent to an acidification step carried out in a stirred vessel, where HCl is added to adjust the pH to 2. This acidic condition promotes the precipitation of humic acids, allowing their separation from fulvic acids remaining in solution. One acidification vessel was designed for each basification line, resulting in two identical stirred reactors equipped with impellers.

Following acidification, the slurry is processed in a second centrifugation step to separate the solid humic acids from the liquid phase. The liquid supernatant is collected in a dedicated storage vessel for discharge, while the solid fraction, rich in humic acids, is sent to a drying unit to obtain a powdered product.

The main design parameters of the vessels, the selected impellers and centrifuge are reported in *Table 6.10*.

Table 6.10 Characterization of HA acid precipitation system.

Acid precipitation	
Q_{in} *(kg/d)*	1.20e05
V_{Vessel} *(m³)*	100
D_{Vessel} *(m)*	3.2
H_{Vessel} *(m)*	11.5
Nr. vessels	2
Nr. parallel lines	2
$D_{impeller}/D_{vessel}$	0.6
$D_{impeller}$ *(m)*	1.9
$P_{single\ impeller}$ *(kW)*	4
Second Centrifugation	
Q_{in} *(kg/d)*	1.20e05
Model	AC100
Load (L/h)	10000
P (kW)	5.5
$V_{VesselWaste}$ *(m³)*	100
D_{Vessel} *(m)*	3.2
H_{Vessel} *(m)*	11.5

6.3.1.7 Humic acids drying

The final unit operation in the process is a drum dryer, designed to remove residual moisture from the extracted HA. The dryer consists of two concentric cylinders, with saturated steam circulating around the rotating inner drum. Heat is transferred through the drum wall to the solid material, promoting solvent evaporation and reducing the moisture content of the product to the target value of 3%.

The thermal demand of the drying process was calculated as the sum of two contributions: the sensible heat required to raise the temperature of the material to the boiling point of the solvent ($Q_{Sensible}$) and the latent heat required for solvent evaporation ($Q_{Evaporation}$). The total heat duty (Q_{Tot}) exchanged between the product and the saturated steam was therefore determined as the sum of these two terms. Based on this total heat requirement, the corresponding steam flow rate necessary to sustain the drying operation was calculated.

The total heat exchanged between the biomass and the saturated steam is given by:

$$Q_{Tot} = Q_{Sensible} + Q_{Evaporation} \quad (6.22)$$

$$Q_{Sensible} = \dot{m}_{H2O} \cdot c_{P,H2O} \cdot (T_{in} - T_{wb})$$

(6.23)

$$Q_{Evaporation} = \dot{m}_{H2O} \lambda_{H2O}$$

(6.24)

where $\dot{m}_{H2O}$ is the mass of heated substance (water, in this case), kg/s; c_p is the specific heat capacity of water, J/kg K; T_{in} is the initial temperature of the slurry, K; T_{wb} is the temperature of boiling water, K.

The mass vapor required for the process is calculated as follows:

$$\dot{m}_{steam} = \frac{Q_{Tot}}{\lambda_{vap}}$$

(6.25)

The dimensions of the drum dryer were selected based on data provided in an Andritz technical brochure, which reports standard equipment diameters, lengths, and typical energy consumption values (*Andritz*). Using these reference specifications, an appropriate dryer size was chosen to meet the process requirements. Finally, the specific energy consumption of the dryer was calculated with respect to the mass flow rate of the dried product, and the results are reported in *Table 6.11* together with three auxiliary vessels designed for the collection of powdered humic acids, stream generated during the drying process, and emergency storage purposes.

Table 6.11 Characteristics of drum dryer employed for humidity removal from HA.

Q_{in} *(kg/d)*	30040
Drum Diameter (m)	0.5
Drum Length (m)	0.5
Min Drive power (kW)	4
Max Drive power (kW)	7.5
Average Drive power (kW)	5.75
m_{Steam} *(t/y)*	1.07e04
$E_{Electricity}$ *(kWh)*	4.32e04
Nr. vessel	3
$V_{VesselWaste}$ *(m³)*	1
D_{Vessel} *(m)*	0.9
H_{Vessel} *(m)*	1.5

6.3.2 Economic analysis

6.3.2.1 Capital cost estimation

After sizing the equipment, the system capital cost was estimated. As shown in *Figure **6.3** Distribution of plant equipment costs.*, the equipment costs were allocated across the main sections of the plant: FVW mechanical pretreatment, dark fermentation, H_2 purification, anaerobic digestion, CH_4 purification, and HA extraction. The anaerobic digestion section accounted for the largest share, representing 48 % of the total cost due to the high expense of the digester. Dark fermentation followed for the same reason. The HA extraction unit ranked third, contributing 17 % of the total cost because of the numerous machines required for the process.

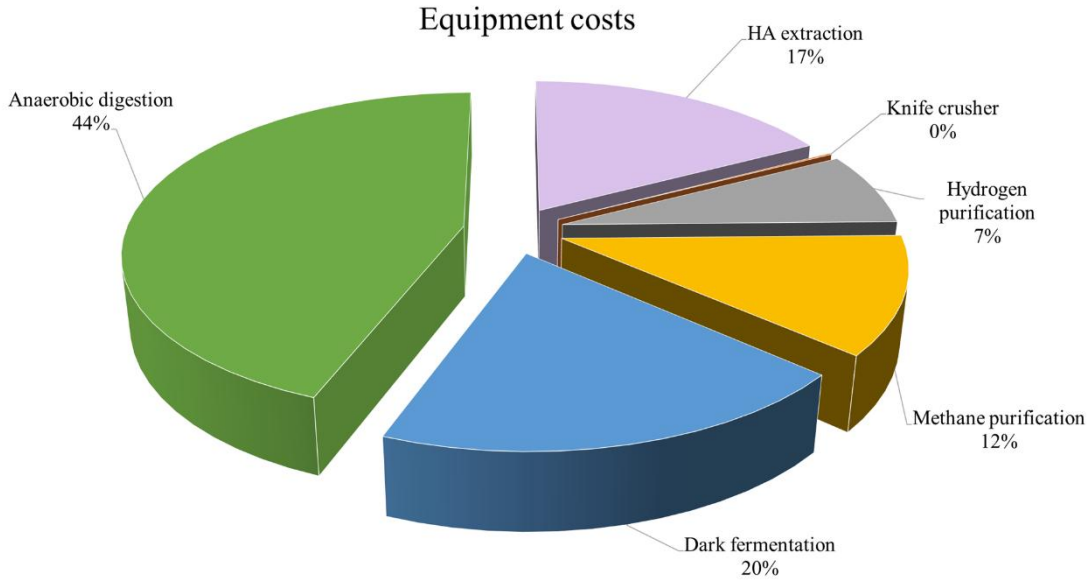

Figure 6.3 Distribution of plant equipment costs.

Table 6.12 presents the results of the total installation cost assessment, which includes all cost items related to plant installation. The cost of the equipment alone was calculated to be over 22.6 million euros. When adding expenses for installation, materials, and contingencies, the total cost of the plant rises to 50.7 million euros. Further inclusion of inventory, start-up costs, and other overheads brings the overall total installation cost to 60.9 million euros.

This analysis highlights that while the equipment itself represents a substantial portion of the investment, additional costs related to installation, auxiliary materials, and operational preparation significantly increase the total financial requirement. These values provide a comprehensive overview of the capital needed to establish the plant and serve as a critical reference for evaluating project feasibility, planning financial resources, and guiding decision-making for industrial-scale implementation.

Table 6.12 Results of the calculation of capital costs associated with TSAD and HA extraction plant.

CAPITAL COST ESTIMATION				
Bare Module Cost			k€	22558
Installation labour	%	24.0%	k€	7962
Buildings, material and labour	%	8.0%	k€	2654
Bare Erected Cost			k€	33174
EPC contractor services	%	17.5%	k€	5805
Engineering Procurement and Construction cost			k€	38979
Process contingencies	%	17.6%	k€	5839
Project contingencies	%	15.0%	k€	5852
Total Plant Cost			k€	50670
Start-up cost	%	2.0%	k€	1013
Inventory	%	0.5%	k€	253
Financing costs	%	2.7%	k€	1368
Other costs, overheads	%	15.0%	k€	7600
Total Overnight Cost			k€	60905

6.3.2.2 Operating and maintenance cost estimation

Figure 6.4 illustrates the distribution of direct operating costs for the plant. The largest single contributor is low-pressure (LP) steam, accounting for 46 % of the total, which is used in heaters for the thermal treatment of process streams. This is followed by ordinary maintenance costs at 23 %, chilling water at 12 % (used in condensers) and operating labor at 15 %. Smaller contributions come from waste treatment (8 %) and electricity consumption (1%). Waste generation is primarily associated with the effluent from the HA extraction section. The cost of raw materials, specifically HCl and KOH, is negligible relative to the other operating expenses. Feedstock materials, namely FVW and JWW, were treated as zero-cost inputs, as they are by-products from other processes. This distribution highlights the dominance of energy-related expenses in the plant's operation and underscores the importance of efficient thermal management in controlling overall operating costs.

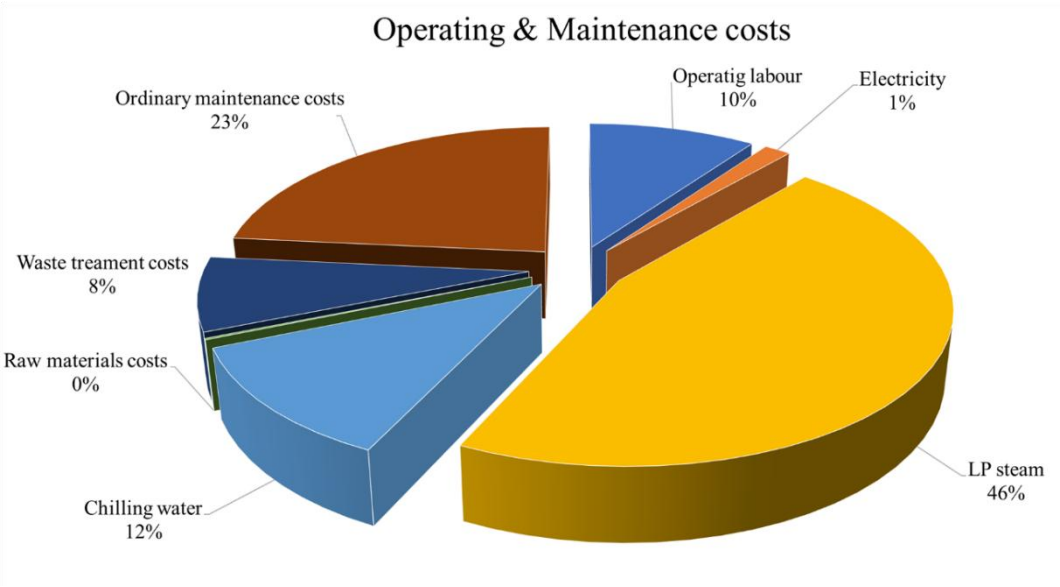

Figure 6.4 Distribution of direct operating costs associated with the production of H_2, CO_2, CH_4 and HA.

Table 6.13 summarizes the operating costs of the TSAD plant, which includes 32 pieces of equipment. Costs directly associated with production and routine maintenance amount to 6.5 million euros per year. When additional items such as supervisory and clerical labor, extraordinary maintenance, laboratory analyses, and patent costs are included, the Direct Manufacturing Costs increase to 9.34 million euros per year.

Fixed Manufacturing Costs, which are independent of the production rate and include depreciation, taxes, insurance, and overheads, amount to 8.9 million euros per year. General Manufacturing Costs, covering administrative, sales, and research activities, contribute an additional 4.2 million euros per year. *Figure 6.5* shows the distribution of the total production costs for the plant. Total Direct Manufacturing Costs represent the largest single component, accounting for 42 % of the total costs. Total Fixed Manufacturing Costs contribute a similarly significant share, approximately 40 % while General Manufacturing Costs (18 %) remain an important component.

Overall, the Total Cost of Production is estimated at 22.5 million euros per year. The analysis highlights that fixed and indirect costs collectively represent a substantial portion of the total expenses, emphasizing their critical role in determining the economic feasibility and sustainability of the plant. These results suggest that both operational efficiency and careful management of fixed overheads are essential for maximizing profitability.

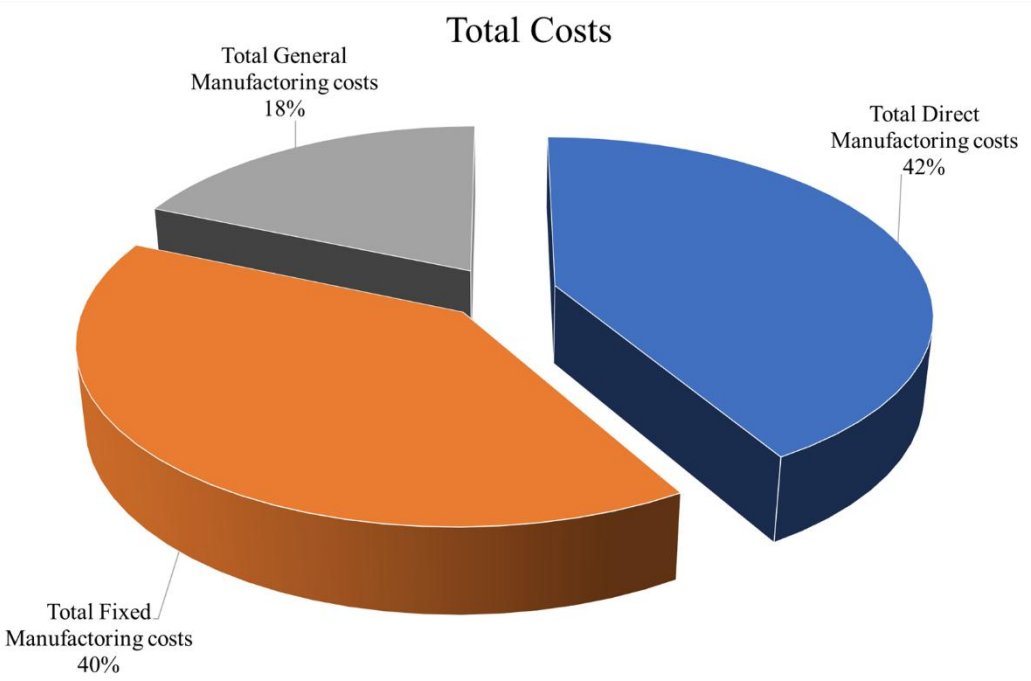

Figure 6.5 Distribution of Total Costs divided in Total Direct Manufacturing costs, Total Fixed Manufacturing costs and Total General Manufacturing costs.

Table 6.13 Results of the calculation of operating costs associated with the production of H_2, CO_2, CH_4 and HA.

OPERATING COST ESTIMATION				
Pieces of equipment in the whole plant			#	32
Operating labor	€/y	40000	k€/y	635.47
Electricity	€/kWh$_{el}$	0.15	k€/y	99.94
LP steam	€/t	16	k€/y	2960.51
Chilling water	€/t	0.2	k€/y	757.28
Utility costs			k€/y	3817.73
FVW	€/t	0	k€/y	0.00
JWW	€/t	0	k€/y	0.00
KOH	€/t	244	k€/y	6.85
HCl	€/t	34.5	k€/y	2.57
Raw materials costs			k€/y	9.41
Waste and disposal	€/t	10	k€/y	497.15
Waste treatment costs			k€/y	497.15
Ordinary maintenance costs	%	3.00%	k€/y	1520.10
Operating & Maintenance costs			k€/y	6479.86
Scenario	%	0.0%	Realistic	
Raw Materials			k€/y	9
Waste Treatment			k€/y	497
Utilities			k€/y	3818
Operating labor			k€/y	635
Direct Supervisory and clerical labor	%	18.0%	k€/y	114
Maintenance and repairs	%	6.0%	k€/y	3040
Operating supplies	%	0.9%	k€/y	456
Laboratory charges	%	15.0%	k€/y	95
Patents and royalties	%	3.0%	k€/y	674
Total Direct Manufacturing costs			k€/y	9340
Depreciation	%	10%	k€/y	5067
Local taxes and insurance	%	3.2%	k€/y	1621
Plant overhead costs	%	70.8%	k€/y	2274
Total Fixed Manufacturing costs			k€/y	8962
Administration costs	%	17.7%	k€/y	569
	%	0.9%	k€/y	
Distribution and selling costs	%	11.0%	k€/y	2471
Research and development	%	5.0%	k€/y	1123
Total General Manufacturing costs			k€/y	4163
Cost of Manufacturing			k€/y	22465
Total Costs			k€/y	22465
Revenues from Products (H_2, CH_4, CO_2, HA)			k€/y	25935

6.3.2.3 Revenue Estimation and Key Financial Indicators

The revenues generated by the plant depend on the annual production rates of the products and their respective selling prices. H_2 produced via DF can be positioned between conventional grey H_2, obtained from fossil fuels (e.g., steam CH_4 reforming), and green H_2 produced by water electrolysis. Grey H_2 benefits from high availability and therefore has a relatively low market price, estimated at 1.29 €/kg (Curcio 2025). In contrast, the selling price of green H_2 is highly dependent on the electricity mix of the country considered. In Italy, the current electricity mix leads to relatively high production costs, with estimated prices reaching up to 10.17 €/kg when wholesale electricity is used ("European Hydrogen Observatory" 2024). Other studies report lower values, around 5.17 €/kg. To provide a balanced and conservative estimate, an intermediate value of 7.67 €/kg was adopted in this analysis.

The selling price of biomethane was set at 0.75 €/m^3, in agreement with literature data (Ferella et al. 2019). CO_2 recovered from the process was assumed to be sold at 0.08 €/kg, based on current market prices. HA were classified as a product with applications between fertilizers and soil amendments. Fertilizers are typically sold at approximately 709 €/t (Y. Li et al. 2020), while soil amendments have a significantly lower market value, around 43 €/t (L. Lin et al. 2019). An average value of 376 €/t was therefore selected to represent the selling price of HA.

Based on the estimated annual production of H_2 (5.706 t/y), CH_4 (195026 m^3/y), CO_2 (1639 t/y), and HA (253 t/y), the total annual revenue of the plant is estimated at 25.9 million of euros.

Using these revenues together with the total annual production costs, NPV, PBT and ROI were calculated. The results of this economic evaluation are reported in *Table **6.14***.

Table 6.14 NPV, PBT and ROI values associated with TSAD and HA extraction plant.

NPV (k€)	-262528518
PBT (y)	-2.98
ROI (%)	-33.55%

The results of the economic assessment indicate that, under the assumptions adopted in this study, the integrated TSAD and humic acid extraction process applied to FVW and JWW is not economically feasible. Despite the theoretical potential of the proposed configuration, the calculated economic indicators do not support its financial sustainability at the considered scale and operating conditions.

A major limitation of the proposed process is linked to the intrinsically low H_2 yields typically achieved by DF, which remains a technology with a low TRL. This limitation is reflected in laboratory-scale experimental results, where H_2 production is generally modest. Since DF represents the primary source of revenue in the proposed configuration, its limited H_2 yields significantly constrain the overall economic performance of the system.

Furthermore, the process is characterized by high capital and operating costs, especially associated with reactor volumes, gas purification units, thermal energy demand, and downstream humic acid extraction. These costs outweigh the revenues generated under the assumed market prices for H_2, CH_4, CO_2, and HA, even when optimistic selling prices are considered.

A H_2 selling price of 3753 €/kg would result in a positive economic outcome, with an NPV of 4,000,000 €, a payback time of 12 years, and an ROI of 8.7 %. However, such a price is clearly unrealistic in practice. This highlights that improving the efficiency of the process, rather than relying on high product prices, is essential to achieve economic feasibility.

It should also be noted that several assumptions were required regarding equipment costs, operating hours, energy consumption, and product prices. While these assumptions were based on literature and market data, uncertainties related to scale-up, biological process stability, and market variability further reduce confidence in the economic viability of the system.

Overall, the present analysis suggests that, in its current configuration and based on laboratory-scale performance, the proposed TSAD and humic acid extraction process cannot be considered economically viable. Significant improvements in process efficiency, particularly in dark fermentation yields, as well as cost reductions through process simplification, technological optimization, or alternative valorization pathways would be necessary before real-scale implementation could be realistically considered.

6.3.3 Life cycle analysis

6.3.3.1 LCA of an integrated biorefinery

As mentioned previously, the LCA was conducted using one year of plant operation as the functional unit, to evaluate the environmental impact of the process in terms of climate change (kg CO_2 eq). The first scenario considered corresponds to the full plant configuration analyzed in the economic assessment, including the TSAD section followed by the extraction of HA. Both heat and electricity consumption were analyzed to quantify their contribution to the total environmental impacts. In the LCA representation, arrows of varying thickness were used to indicate the relative magnitude of each contribution (*Figure 6.6*).

Among the two energy sources, electricity was the dominant contributor, responsible for 64.7 % of total emissions, corresponding to 8.26×10^6 kg CO_2 eq per year out of a total of 1.28×10^7 kg CO_2 eq. Heat accounted for the remaining 36.7 %, corresponding to 4.68×10^6 kg CO_2 eq per year.

Examining individual stages of the process, the largest contributions to total impacts were associated with gas purification operations. CH_4 purification accounted for 38.4 % of total impacts, while CO_2 recovery following AD contributed 27.1 %. Drying of HA also contributed significantly, representing 21.1 % of total emissions. Other process steps had lower impacts: CO_2 purification after DF accounted for 18.3 % of total impacts, while the alkaline and acid pretreatments for HA recovery contributed 13.4 % and 14.4 %, respectively.

The direct contributions of DF and AD themselves were similar, together accounting for 24.9 % of total impacts.

Overall, these results indicate that electricity consumption and gas purification steps are the primary drivers of climate change impacts in the plant. In contrast, the core biological processes, while essential for production, have a smaller direct effect on total emissions.

To evaluate an alternative and more conventional operating configuration, a second LCA scenario was analyzed in which the biogas produced from AD was not purified. This assumption reflects common industrial practice, where raw biogas is often directly fed to a cogeneration unit for combined heat and power production rather than being upgraded to biomethane (Aui et al. 2019). All other process steps, including TSAD and HA extraction, were kept unchanged to ensure a consistent comparison between scenarios.

As shown in *Figure 6.7*, the exclusion of biogas purification has a strong influence on the overall environmental performance of the system, leading to a reduction of total climate change impacts by approximately 64 % compared to the reference scenario. This result confirms that gas upgrading operations are among the most energy-intensive stages of the process and it is associated with high environmental impacts.

A substantial reduction in electricity-related emissions was observed in this scenario, with electricity now accounting for only 38.9 % of the total greenhouse gas emissions. In contrast, heating has become the dominant contributor, representing 60.8 % of total emissions. Within this category, the purification of CO_2 during H_2 recovery is the most significant source, contributing 51 % of the overall emissions. This indicates that even when CH_4 upgrading is bypassed, H_2 purification remains a critical environmental hotspot and a key factor driving the plant's climate impact. The drying of HA also represents a notable contribution, accounting for approximately 48 % of total emissions. The relatively high impact of this stage is largely due to the energy-intensive nature of the drying process, which requires significant thermal input to remove moisture from the product. This highlights the importance of evaluating process efficiency and exploring potential optimization strategies, such as waste heat recovery or alternative drying technologies, to reduce the environmental footprint.

Although the removal of biogas purification substantially improves the environmental profile of the process, the overall emissions remain relatively high. This outcome indicates that further mitigation strategies are required, particularly targeting electricity-intensive operations such as H_2/CH_4 purification and HA drying. Any efforts to improve sustainability should focus on these two stages, as they dominate the plant's climate change impact and offer the greatest potential for mitigation. Potential improvements could include the integration of renewable electricity sources, optimization of separation processes, or heat and energy recovery strategies. Overall, achieving a low-carbon configuration will require additional process optimization beyond the exclusion of methane upgrading.

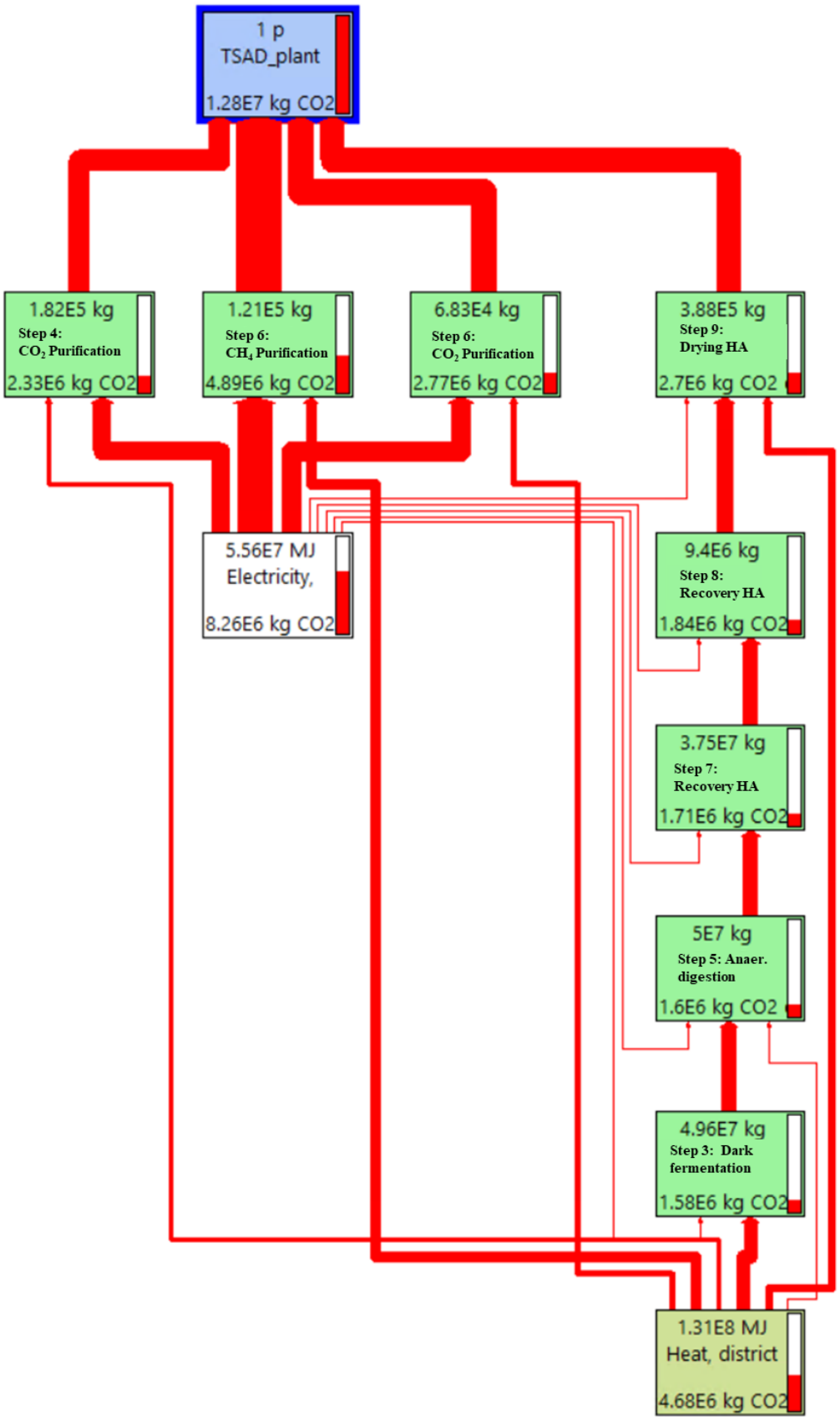

Figure 6.6 Environmental impact, expressed as kg CO_2 eq/FU associated with TSAD and HA extraction plant.

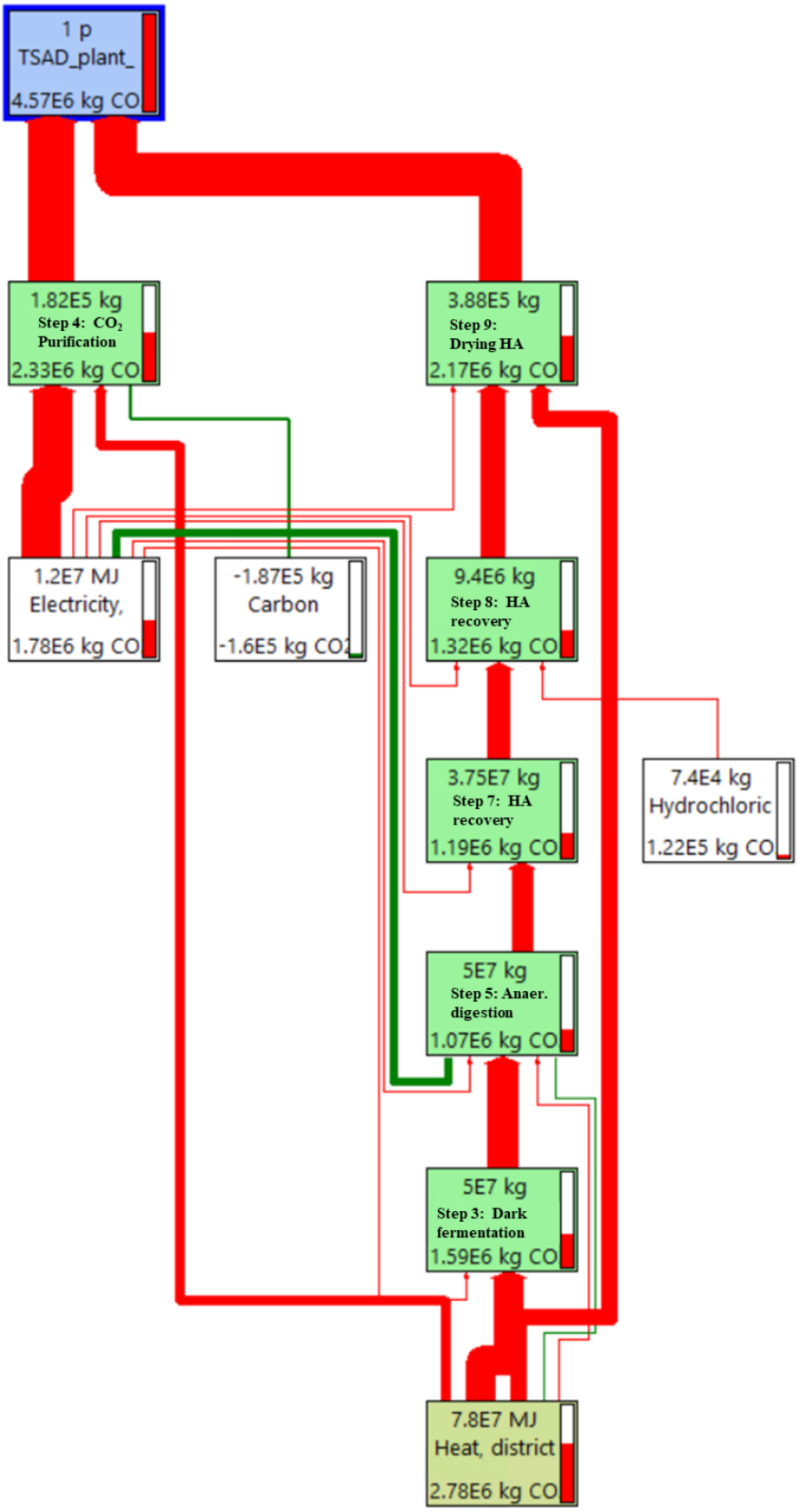

Figure 6.7 Environmental impact, expressed as kg CO_2 eq/FU associated with TSAD and HA extraction plant without considering a CH_4 purification unit.

Table 6.15 The environmental evaluation of anaerobic digestion (AD), two-stage anaerobic digestion (TSAD), and digestate conversion. The adopted acronyms are Global warming (GW), Pyrolysis (PY), and Incineration (INC). FU considered was 1 ton of substrate treated.

Process	Biomass	Capacity	Scale of the system	Approach	Impact methods	Impact category	Impactful phase	Reference
AD	Olive mill wastewater	N.A.	Lab-scale. 6.2 L	Cradle-to-grave	ReCiPe 2016 Midpoint (H)	GW	89.3 $kgCO_2$ eq/FU	Manthos et al. (2023)
TSAD	Pig slurry and cow dung	10950 t/y	30 L	Gate-to-Gate	CML-baseline 2001	GW	1.16×10^{-6} $kgCO_2$ eq/FU	Sinsuw et al. (2024)
AD+PY/ INC	Food waste	10000 t/y	N.A.	Cradle-to-gate	TRACI	GW	AD: 3.4×10^{-4} $kgCO_2$ eq/FU PY: 5.6×10^{-4} $kgCO_2$ eq/FU AD+PY: 4.2×10^{-4} $kgCO_2$ eq/FU AD+INC: 4.1×10^{-4} $kgCO_2$ eq/FU	Inalegwu Okopi et al. (2024)
TSAD	FVW+JWW	50000 t/y	Industrial scale	Grave-to-gate	ReCiPe 2016 Midpoint (H)	GW	256 $kgCO_2$ eq/FU	This study

6.3.3.2 LCA benchmarking of AD

The environmental impact estimated in this study was compared with results reported in other studies that investigated AD systems for renewable energy production. For this purpose, the results were normalized to a different functional unit, namely 1 ton of treated substrate, corresponding to an impact of 256 kg CO_2 eq per FU.

This value was first compared with an environmental assessment conducted on the anaerobic digestion of olive mill wastewater (Manthos et al. 2023), as reported in *Table 6.15*. Although the same LCIA method was adopted, the overall approach differed substantially. In particular, the referenced study applied a cradle-to-grave system boundary, whereas the present analysis followed a different boundary definition. Moreover, the investigated process operated at laboratory scale, which can significantly influence the results due to non-optimized energy use and scale-related inefficiencies. In that study, a global warming impact of 89.3 kg CO_2 eq per FU was reported. However, it should be noted that no biogas purification or upgrading stages were included in their system boundaries, which substantially reduces the associated energy demand and, consequently, the environmental impact. In addition, the authors employed an UASB reactor, a technology generally recognized for its higher efficiency and lower specific energy requirements compared to conventional continuous stirred tank reactors. This choice likely contributed to the lower emissions reported. Overall, the comparison shows that differences in system boundaries, operating scale, reactor technology, and the inclusion of downstream purification steps strongly influence the estimated environmental impacts. Consequently, the higher impact observed in this study is mainly driven by energy-intensive gas purification and product recovery stages, rather than by the anaerobic digestion process itself.

Significantly lower environmental impacts have been reported by Sinsuw et al. (2024) and Inalegwu Okopi et al. (2024). The first one investigated an AD process applied to pig slurry and cow dung at commercial scale, using a reactor volume of 30 L and an annual treatment capacity of approximately 10950 t/y. Their LCA followed a gate-to-gate approach and employed the CML Baseline 2001 impact assessment method. Inalegwu Okopi et al. (2024), on the other hand, presented an LCA of an integrated waste-to-energy system combining AD and pyrolysis applied to food waste. Four scenarios were evaluated, namely AD alone, pyrolysis alone, AD coupled with pyrolysis, and AD coupled with incineration. Although the reactor volume was not specified, the treatment capacity was reported to be about 10,000 t/y. Their study adopted a cradle-to-gate approach and applied the TRACI impact assessment method.

Both studies reported GW impacts that are several orders of magnitude lower than those estimated in the present work, with values ranging from 1.16×10^{-6} kg CO_2 eq/FU in the first study to 3.4-5.6 $\times 10^{-4}$ kg CO_2 eq/FU in the second. These substantial differences can be largely explained by key methodological and process-related choices. In particular, neither study included biogas upgrading or

separation of CH_4 and CO_2 following AD, as both systems assumed direct utilization of biogas in cogeneration units. Furthermore, digestate management in those studies was limited to land application, which typically entails lower energy and environmental burdens.

In contrast, the present study proposes an enhanced valorization pathway for digestate through HA extraction, aiming at the production of higher value-added products. While this approach increases resource recovery and potential economic value, it also introduces additional processing steps, chemical inputs, and energy demand, which inevitably lead to higher environmental impacts. Therefore, the higher GW values observed in this work should be interpreted as a trade-off between increased product valorization and environmental performance, rather than as an indication of lower intrinsic sustainability of anaerobic digestion itself.

A final comparison can be made with the emissions associated with the most widely adopted route for H_2 production today, namely steam methane reforming (SMR). The life-cycle environmental performance of SMR has been extensively investigated and is well documented in the literature. For instance, Spath and Mann (2000) and Cetinkaya et al. (2012) reported a global warming potential (GWP) of approximately 11.9 kg CO_2 eq/kgH_2, while Dufour et al. (2009) reported a slightly lower value of 10.6 kg CO_2 eq/kgH_2.

These reference values are substantially lower than the emissions estimated in the present study, which amount to 2243 kg CO_2 eq/kgH_2. At first glance, this large discrepancy might suggest a significantly poorer environmental performance; however, such a comparison must be interpreted with caution. Indeed, LCA results are highly sensitive to the definition of system boundaries, functional unit, allocation criteria, and methodological assumptions.

In the case of SMR, most literature studies adopt relatively narrow system boundaries and typically consider SMR followed by pressure swing adsorption (PSA) as the sole purification step. In contrast, the system investigated in this work encompasses multiple processing steps and multiple co-products, including CH_4 and humic acids, resulting in a considerably more complex process configuration. This complexity is associated with higher electricity and thermal energy demands, as well as additional upstream and downstream operations that are not usually included in conventional SMR assessments. Moreover, differences in allocation methods, energy mix assumptions, and treatment of by-products can lead to variations in GWP estimates of several orders of magnitude. As a result, direct numerical comparisons between studies employing different LCA approaches should be regarded as indicative rather than definitive.

Although some of the observed discrepancy stems from differences in boundary conditions, modeling approaches, and system complexity, the results underscore the need to improve the process environmentally. Future efforts should reduce energy use, optimize integration, enhance co-product valorization, and explore lower-carbon energy sources. Without these improvements, the system's environmental impact would limit large-scale implementation.

References

Anhui Wali Environmental Protection Equipment Co. n.d. "WaliShredder." Accessed May 14, 2024. https://www.walirecycling.com/it/product/wls/#.

Aui, Alvina, Wenqin Li, and Mark M. Wright. 2019. "Techno-Economic and Life Cycle Analysis of a Farm-Scale Anaerobic Digestion Plant in Iowa." *Waste Management* 89 (April): 154–64. https://doi.org/10.1016/j.wasman.2019.04.013.

Cetinkaya, E., I. Dincer, and G.F. Naterer. 2012. "Life Cycle Assessment of Various Hydrogen Production Methods." *International Journal of Hydrogen Energy* 37 (3): 2071–80. https://doi.org/10.1016/j.ijhydene.2011.10.064.

Curcio, Eliseo. 2025. "Techno-Economic Analysis of Hydrogen Production: Costs, Policies, and Scalability in the Transition to Net-Zero." *International Journal of Hydrogen Energy* 128 (May): 473–87. https://doi.org/10.1016/j.ijhydene.2025.04.013.

Demichelis, Francesca, Robotti Elisa, Deorsola Fabio Alessandro, Marengo Emilio, Tommasi Tonia, and Fino Debora. 2024. "Modelling of Technical, Environmental, and Economic Evaluations of the Effect of the Organic Loading Rate in Semi-Continuous Anaerobic Digestion of Pre-Treated Organic Fraction Municipal Solid Waste." *Environmental Pollution* 344 (March): 123417. https://doi.org/10.1016/j.envpol.2024.123417.

Demichelis, Francesca, Silvia Fiore, Daniel Pleissner, and Joachim Venus. 2018. "Technical and Economic Assessment of Food Waste Valorization through a Biorefinery Chain." *Renewable and Sustainable Energy Reviews* 94 (October): 38–48. https://doi.org/10.1016/j.rser.2018.05.064.

Dufour, J, D Serrano, J Galvez, J Moreno, and C Garcia. 2009. "Life Cycle Assessment of Processes for Hydrogen Production. Environmental Feasibility and Reduction of Greenhouse Gases Emissions." *International Journal of Hydrogen Energy* 34 (3): 1370–76. https://doi.org/10.1016/j.ijhydene.2008.11.053.

"European Hydrogen Observatory." 2024. https://observatory.clean-hydrogen.europa.eu/.

Ferella, Francesco, Federica Cucchiella, Idiano D'Adamo, and Katia Gallucci. 2019. "A Techno-Economic Assessment of Biogas Upgrading in a Developed Market." *Journal of Cleaner Production* 210 (February): 945–57. https://doi.org/10.1016/j.jclepro.2018.11.073.

Fischer, Torsten, and Andreas Krieg. n.d. *FARM-SCALE BIOGAS PLANTS*.

Inalegwu Okopi, Solomon, Jianfei Zeng, Xuetong Fan, et al. 2024. "Environmental Sustainability Assessment of a New Food Waste Anaerobic Digestion and Pyrolysis Hybridization System." *Waste Management* 179 (April): 130–43. https://doi.org/10.1016/j.wasman.2024.01.038.

Janjić, Vesna, Mirjana Todorović, and Dejan Jovanović. 2010. *CVP ANALYSIS -THE IMPACT OF COST STRUCTURE ON THE RESULT OF THE COMPANY*.

Li, Yangyang, Yiyu Han, Yiran Zhang, Wenhai Luo, and Guoxue Li. 2020. "Anaerobic Digestion of Different Agricultural Wastes: A Techno-Economic Assessment." *Bioresource Technology* 315 (November): 123836. https://doi.org/10.1016/j.biortech.2020.123836.

Lin, Long, Ajay Shah, Harold Keener, and Yebo Li. 2019. "Techno-Economic Analyses of Solid-State Anaerobic Digestion and Composting of Yard Trimmings." *Waste Management* 85 (February): 405–16. https://doi.org/10.1016/j.wasman.2018.12.037.

Lu, Jingquan, Hariklia N. Gavala, Ioannis V. Skiadas, Zuzana Mladenovska, and Birgitte K. Ahring. 2008. "Improving Anaerobic Sewage Sludge Digestion by Implementation of a Hyper-Thermophilic Prehydrolysis Step." *Journal of Environmental Management* 88 (4): 881–89. https://doi.org/10.1016/j.jenvman.2007.04.020.

Manthos, Georgios, Dimitris Zagklis, Constantina Zafiri, and Michael Kornaros. 2023. "Comparative Life Cycle Assessment of Anaerobic Digestion, Lagoon Evaporation, and Direct Land Application of Olive Mill Wastewater." *Bioresource Technology* 388 (November): 129778. https://doi.org/10.1016/j.biortech.2023.129778.

Mazzanti, Gaia, Francesca Demichelis, Debora Fino, and Tonia Tommasi. 2025. "A Closed-Loop Valorization of the Waste Biomass through Two-Stage Anaerobic Digestion and Digestate Exploitation." *Renewable and Sustainable Energy Reviews* 207 (September 2024): 114938. https://doi.org/10.1016/j.rser.2024.114938.

Mehr, A.S., M. Gandiglio, M. MosayebNezhad, et al. 2017. "Solar-Assisted Integrated Biogas Solid Oxide Fuel Cell (SOFC) Installation in Wastewater Treatment Plant: Energy and Economic Analysis." *Applied Energy* 191 (April): 620–38. https://doi.org/10.1016/j.apenergy.2017.01.070.

Singh, R. P., D. R. Heldman, and G. Giovanelli. 2015. *Principi Di Tecnologia Alimentare*. Rozzano: CEA.

Sinnott, Ray, and Gavin Towler. 2020. *Chemical Engineering Design Specifications*. Butterworth-Heinemann.

Sinsuw, Alicia Amelia Elizabeth, Tsung Hsien Chen, Pannipha Dokmaingam, Hendrik Suryo Suriandjo, and Chen Yeon Chu. 2024. "Life Cycle Assessment of Environmental Impacts for Two-Stage Anaerobic Biogas Plant between Commercial and Pilot Scales." *International Journal of Hydrogen Energy* 52 (January): 58–70. https://doi.org/10.1016/j.ijhydene.2023.06.331.

Spath, P L, and M K Mann. 2000. *Life Cycle Assessment of Hydrogen Production via Natural Gas Steam Reforming*. NREL/TP-570-27637, 764485. https://doi.org/10.2172/764485.

Turton, R. 1998. *Analysis, Synthesis and Design of Chemical Processes*. Upple Saddle River: Prentice-Hall PTR.

Ulrich, G., and P. Vasudevan. 2004. *Chemical Engineering Process Design and Economics*. Process Publishing.

7. Conclusion

The depletion of fossil fuels and the urgent need for renewable energy sources continue to drive research into alternative, sustainable technologies. In this context, biomass and organic waste have gained significant attention as renewable, carbon-neutral feedstocks. The integration of TSAD with HA extraction represents a promising approach to valorize organic waste while generating energy carriers such as H_2 and CH_4.

In this study, TSAD was applied to a mixture of FVW and JWW to explore the potential of this underutilized substrate. Thermal pretreatment effectively promoted H_2-producing microorganisms during the dark fermentation stage, allowing the process to proceed without the addition of costly culture media and supporting the scalability of the system. JWW was successfully processed both alone and in combination with FVW. Compared to conventional single-stage AD, TSAD improved CH_4 output, confirming that JWW can serve as a low-cost alternative to commercial sugars in supporting DF and TSAD, in line with circular economy principles.

The approach was also applied to sugar-rich wastewater from the starch syrup industry but H_2 and CH_4 yields remained lower than those reported in comparable studies. This limitation is likely due to constraints inherent to laboratory-scale experiments and variability in inoculum composition. Differences in microbial communities can significantly influence metabolic pathways, underscoring the need for further optimization of operating conditions and reactor configurations to improve process stability and enhance energy recovery.

When TSAD was applied to animal-based biomasses such as CM and PS, DF was ineffective, producing very low H_2 yields. This poor performance is attributed to the inherent presence of active methanogens in animal-derived wastes, which survived pretreatment and outcompeted H_2-producing bacteria. Consequently, the focus shifted to single-stage continuous AD for these substrates, investigating feeding strategies and post-digestion HTH to improve the biodegradability of recalcitrant lignocellulosic compounds. Intermittent feeding significantly enhanced CH_4 conversion rates and prevented VFAs accumulation, leading to a more stable and efficient digestion process. Post-digestion HTH and the bioaugmentation with the hyper-thermophilic microorganism *Caldicellulosiruptor bescii* provided short-term benefits in lignocellulose degradation, but prolonged operation revealed limitations due to microbial washout, kinetic constraints, and reduced system stability.

Further experiments explored JWW as a water source rather than a sugar source and tested the addition of biochar in both TSAD stages in the conversion of JWW and FVW. Overall, biochar did not show a significant effect on DF performance under the tested conditions. However, in the second-stage AD, while overall CH_4

yields remained similar, the improvement in CH_4 concentration suggested that biochar may enhance biogas quality and downstream energy recovery. Importantly, TSAD continued to improve CH_4 production kinetics without compromising final yields, demonstrating its potential as an effective alternative to conventional single-stage AD.

Finally, preliminary TEA and LCA of a TSAD plant fed with FVW and JWW and coupled with HA extraction were performed. Results indicate that while the integrated process offers potential for resource valorization and revenue generation, its current economic and environmental performance is limited by low H_2 yields and energy-intensive operations. The additional valorization of digestate into HA adds value but increases environmental impacts, primarily due to electricity and heat consumption in purification and drying steps.

Overall, these findings highlight several key considerations for future development:

1. Dark fermentation optimization is critical, as H_2 production is currently the main limitation for both economic viability and environmental performance.
2. Energy efficiency improvements in gas purification and HA drying are necessary to reduce operational costs and environmental impacts.
3. Process scale-up and robust sensitivity analyses are required to validate laboratory-scale results and ensure the feasibility of full-scale implementation.
4. Targeted substrate selection and pretreatment strategies must be tailored to suppress competing methanogens and maximize H_2 yields, particularly when using animal-based biomasses.

In conclusion, TSAD coupled with HA extraction demonstrates potential for integrating energy and value-added chemical production from organic waste. However, further research and optimization are required to overcome current limitations in H_2 yields, energy demand, and operational stability before the process can be considered economically and environmentally sustainable at industrial scale.

A. Appendix A

TS, VS and CHNSO elemental composition of the digestates obtained from DF and AD are reported.

Table A.1 Chemical and physical characterization of digestates from the DF configurations discussed in paragraph 2.3.2.

	G	S	G_M	S_M	G_T	S_T	G_M_T	S_M_T
TS (%)	6.85 ± 0.02	3.61 ± 0.84	5.79 ± 0.35	5.01 ± 0.10	7.03 ± 1.30	4.76 ± 0.02	6.14 ± 4.10	4.17 ± 0.23
VS/TS (%)	82.71 ± 1.78	84.89 ± 0.05	88.92 ± 4.90	89.40 ± 2.82	92.67 ± 1.21	88.45 ± 4.80	89.09 ± 4.90	84.06 ± 7.38
N (%)	3.26 ± 0.27	3.07 ± 0.23	4.12 ± 0.57	3.96 ± 0.01	3.83 ± 0.11	3.68 ± 0.42	3.43 ± 0.39	3.66 ± 0.28
C (%)	37.72 ± 0.56	38.07 ± 1.78	36.40 ± 5.07	38.50 ± 0.54	42.08 ± 1.45	40.56 ± 1.36	34.32 ± 5.09	36.68 ± 0.23
H (%)	5.75 ± 0.12	4.63 ± 0.17	4.27 ± 0.21	4.46 ± 0.06	4.92 ± 0.15	4.41 ± 0.29	4.06 ± 0.39	4.04 ± 0.08
S (%)	0.35 ± 0.02	0.41 ± 0.04	0.28 ± 0.12	0.42 ± 0.04	0.25 ± 0.08	0.35 ± 0.01	0.19 ± 0.11	0.75 ± 0.16
O (%)	52.93 ± 0.73	53.84 ± 2.23	54.93 ± 5.30	52.66 ± 0.56	48.92 ± 1.79	50.99 ± 2.06	57.99 ± 5.98	54.87 ± 0.74
C/N	11.62 ± 0.79	12.43 ± 0.37	8.84 ± 0.01	9.72 ± 0.12	10.98 ± 0.06	11.06 ± 0.89	10.01 ± 0.30	10.04 ± 0.70

Table A.2 Chemical and physical characterization of digestates from the DF configurations discussed in paragraph 2.3.3.

	SUCR_A	SUCR_B	JWW_A	JWW_B	SUCR_FVW_A	SUCR_FVW_B	JWW_FVW_A	JWW_FVW_B
TS (%)	5.18 ± 0.52	4.98 ± 0.83	6.01 ± 0.07	3.82 ± 0.02	6.23 ± 0.26	5.98 ± 0.09	4.84 ± 1.20	3.55 ± 0.23
VS/TS (%)	85.56 ± 1.57	84.19 ± 4.30	85.98 ± 3.97	86.24 ± 3.94	90.63 ± 1.36	92.80 ± 0.22	92.24 ± 0.44	87.47 ± 3.25
N (%)	3.63 ± 0.12	3.71 ± 0.36	3.99 ± 0.14	3.53 ± 0.21	3.54 ± 0.14	3.36 ± 0.31	4.77 ± 0.14	5.34 ± 0.93
C (%)	39.70 ± 1.19	40.18 ± 1.30	42.21 ± 0.36	41.50 ± 1.34	41.75 ± 0.52	43.80 ± 1.88	47.62 ± 1.93	49.58 ± 7.78
H (%)	4.95 ± 0.45	5.33 ± 0.33	5.48 ± 0.17	5.39 ± 0.06	5.70 ± 0.05	6.13325 ± 0.09	5.77 ± 0.21	5.95 ± 0.56
S (%)	4.29 ± 1.40	2.17 ± 0.58	1.49 ± 0.11	1.19 ± 0.19	0.94 ± 0.03	0.85 ± 0.12	0.74 ± 0.04	0.84 ± 0.21
O (%)	47.43 ± 0.36	48.61 ± 2.58	46.85 ± 0.50	48.38 ± 1.79	48.08 ± 0.40	45.85 ± 1.53	41.10 ± 2.32	38.29 ± 9.48
C/N	10.94 ± 0.03	10.88 ± 0.71	10.60 ± 0.47	11.76 ± 0.31	11.81 ± 0.61	13.11 ± 1.79	9.99 ± 0.12	9.30 ± 0.17

Table A.3 Chemical and physical characterization of digestates from the DF configurations discussed in paragraph 2.3.4.

	JWW_FVW_1:1	JWW_FVW_2:1	JWW_FVW_T_1:1	JWW_FVW_T_2:1
TS (%)	5.92 ± 0.02	6.36 ± 0.04	5.42 ± 0.06	5.99 ± 0.17
VS/TS (%)	90.73 ± 2.94	91.80 ± 2.06	92.48 ± 0.76	94.39 ± 0.44
N (%)	3.17 ± 0.06	3.00 ± 0.02	3.39 ± 0.02	3.04 ± 0.08
C (%)	37.05 ± 0.95	39.45 ± 0.84	38.01 ± 0.25	40.73 ± 0.23
H (%)	4.67 ± 0.18	4.98 ± 0.14	4.54 ± 0.03	5.04 ± 0.11
S (%)	0.73 ± 0.01	0.63 ± 0.05	0.67 ± 0.02	0.59 ± 0.02
O (%)	54.39 ± 1.06	51.96 960.02	53.40 ± 0.18	50.60 ± 0.24
C/N	11.69 ± 0.51	13.17 ± 0.19	11.23 ± 0.014	13.40 ± 0.45

Table A.4 Chemical and physical characterization of digestates from the DF configurations discussed in paragraph 2.3.5.

	JWW_FVW_1:1	JWW_FVW_2:1	JWW_FVW_T_1:1	JWW_FVW_T_2:1
TS (%)	4.70 ± 0.43	6.06 ± 2.22	4.79 ± 0.02	5.48 ± 0.82
VS/TS (%)	88.04 ± 2.94	80.67 ± 2.06	80.54 ± 0.76	80.67 ± 0.44
N (%)	5.295 ± 0.11	7.18 ± 0.76	6.61 ± 0.43	6.52 ± 0.59
C (%)	57.79 ± 8.56	64.86 ± 9.42	61.07 ± 8.99	64.39 ± 9.20
H (%)	6.08 ± 0.36	6.05 ± 0.33	6.02 ± 0.35	5.58 ± 0.3
S (%)	0.81 ± 0.24	1.08 ± 0.08	0.97 ± 0.16	0.87 ± 0.12
O (%)	30.03 ± 9.28	20.84 ± 10.59	25.33 ± 9.93	22.64 ± 10.26
C/N	10.90 ± 1.40	9.02 ± 0.36	9.24 ± 0.88	9.88 ± 0.62

Table A.5 Chemical and physical characterization of digestates from the DF configurations discussed in paragraph 2.3.7.

	OLR 1.8	OLR 3.6	OLR 7.9
TS (%)	1.14 ± 0.02	2.09 ± ± 0.33	4.98 ± 0.34
VS/TS (%)	96.57 ± 0.15	95.75 ± 1.13	98.12 ± 1.25
N (%)	4.21 ± 0.03	4.14 ± 0.09	4.02 ± 0.04
C (%)	38.34 ± 0.27	40.37 ± 3.80	39.90 ± 1.75
H (%)	4.70 ± 0.23	4.97 ± 0.35	4.99 ± 0.09
S (%)	0.70 ± 0.03	0.59 ± 0.07	0.57 ± 0.01
O (%)	47.95 ± 0.50	50.07 ± 4.00	49.47 ± 1.89
C/N	9.11 ± 0.00	9.76 ± 1.14	9.92 ± 0.33

Table A.6 Chemical and physical characterization of digestates from the DF configurations discussed in paragraph 3.3.2.

	Permeate	Retentate	Aliment
TS (%)	4.49 ± 0.82	5.92 ± 1.48	4.92 ± 0.17
VS/TS (%)	99.1 ± 0.00	94.43 ± 0.40	90.32 ± 2.24
N (%)	3.03 ± 0.74	3.32 ± 0.08	3.41 ± 0.13
C (%)	42.37 ± 3.56	39.62 ± 1.62	37.89 ± 1.20
H (%)	3.60 ± 0.70	4.34 ± 0.56	3.36 ± 0.16
S (%)	0.95 ± 0.26	0.50 ± 0.05	0.70 ± 0.00
O (%)	50.06 ± 3.26	52.23 ± 2.05	54.63 ± 1.16
C/N	14.55 ± 4.71	11.94 ± 0.79	11.11 ± 0.06

Table A.7 Chemical and physical characterization of digestates from the DF configurations discussed in paragraph 3.3.3.

	Permeate	Retentate	Aliment
TS (%)	1.61± 0.82	1.55 ± 1.48	1.99 ± 0.17
VS/TS (%)	91.7 ± 0.00	94.25 ± 0.40	92.21 ± 2.24
N (%)	2.48 ± 0.74	2.64 ± 0.08	2.79 ± 0.13
C (%)	24.99 ± 3.56	22.61 ± 1.62	30.00 ± 1.20
H (%)	2.07 ± 0.70	0.26 ± 0.56	3.31 ± 0.16
S (%)	0.62 ± 0.26	1.09 ± 0.05	0.62 ± 0.00
O (%)	69.84 ± 3.26	73.41 ± 2.05	63.29 ± 1.16
C/N	10.08 ± 4.71	8.58 ± 0.79	10.75 ± 0.06

Table A.8 Chemical and physical characterization of digestates from the DF configurations discussed in paragraph 3.3.4.

	Permeate 6%	Permeate 3%	Retentate 6%	Retentate 3%	Aliment 6%	Aliment 3%
TS (%)	4.83 ± 0.67	3.43 ± 0.64	4.46 ± 1.32	2.41 ± 1.41	4.41 ± 0.88	2.06 ± 0.17
VS/TS (%)	96.00 ± 0.68	96.72 ± 0.35	94.97 ± 2.08	96.41 ± 2.51	96.43 ± 1.09	97.22 ± 0.49
N (%)	3.86 ± 0.19	3.80 ± 0.09	3.85 ± 0.29	4.17 ± 0.49	3.93 ± 0.21	4.28 ± 0.21
C (%)	40.85 ± 2.82	41.82 ± 1.32	39.53 ± 4.32	37.13 ± 9.54	38.01 ± 4.60	38.62 ± 0.94
H (%)	4.65 ± 0.42	4.96 ± 0.28	4.78 ± 0.57	4.33 ± 1.17	4.76 ± 0.67	4.81 ± 0.11
S (%)	0.65 ± 0.03	0.67 ± 0.04	0.76 ± 0.02	0.91 ± 0.10	0.97 ± 0.01	1.03 ± 0.20
O (%)	50.00 ± 3.40	48.75 ± 1.65	51.09 ± 5.15	53.47 ± 10.12	52.34 ± 5.49	51.27 ± 1.24
C/N	10.58 ± 0.21	11.02 ± 0.08	10.27 ± 0.35	9.11 ± 3.36	9.67 ± 0.67	9.04 ± 0.21

Table A.9 Chemical and physical characterization of digestates from the DF configurations discussed in paragraph 5.3.2.

	TH_80	TH_100	TH_120
TS (%)	2.33 ± 0.13	2.09 ± 0.20	2.55 ± 0.52
VS/TS (%)	88.44 ± 5.55	91.61 ± 2.69	92.12 ± 3.61
N (%)	2.83 ± 0.59	2.96 ± 0.66	3.36 ± 0.31
C (%)	37.93 ± 5.07	34.59 ± 4.61	39.55 ± 2.33
H (%)	5.24 ± 0.52	3.84 ± 0.89	4.19 ± 0.61
S (%)	0.45 ± 0.12	0.66 ± 0.26	0.55 ± 0.11
O (%)	53.56 ± 6.25	57.95 ± 6.40	52.35 ± 3.17
C/N	13.54 ± 0.95	11.88 ± 1.13	11.82 ± 0.64

Table A.10 Chemical and physical characterization of digestates from the DF configurations discussed in paragraph 5.3.3.

	DF80	DF80_B1	DF100	DF100_B1	SingleAD
TS (%)	2.63 ± 0.09	2.35 ± 0.15	1.90 ± 0.42	2.08 ± 0.17	2.11 ± 0.13
VS/TS (%)	95.76 ± 0.06	91.74 ± 0.80	91.52 ± 1.00	90.71 ± 0.85	95.41 ± 0.90
N (%)	3.23 ± 0.14	2.23 ± 0.33	3.62 ± 0.13	1.81 ± 0.26	3.15 ± 0.23
C (%)	39.39 ± 2.70	23.66 ± 3.64	40.93 ± 1.89	20.43 ± 2.09	37.32 ± 1.48
H (%)	5.07 ± 0.35	2.58 ± 0.70	5.24 ± 0.22	2.06 ± 0.19	5.07 ± 0.17
S (%)	0.61 ± 0.06	5.70 ± 1.36	0.65 ± 0.04	0.15 ± 0.00	0.52 ± 0.04
O (%)	51.70 ± 3.25	65.84 ± 5.76	49.57 ± 2.26	75.56 ± 2.54	53.94 ± 1.74
C/N	12.19 ± 0.30	10.59 ± 0.50	11.31 ± 0.24	11.35 ± 0.49	11.88 ± 0.71

Table A.11 Chemical and physical characterization of digestates from the DF configurations discussed in paragraph 5.3.4.

	TH_80	TH_80_B1	TH_100	TH_100_B1	TH_100_B2
TS (%)	2.33 ± 0.13	2.37 ± 0.04	2.09 ± 0.20	2.43 ± 0.39	2.64 ± 0.40
VS/TS (%)	88.44 ± 5.55	82.92 ± 1.65	91.61 ± 2.69	96.17 ± 0.83	95.97 ± 0.99
N (%)	2.83 ± 0.59	3.04 ± 0.08	2.96 ± 0.66	3.26 ± 0.44	3.20 ± 0.36
C (%)	37.93 ± 5.07	39.25 ± 0.49	34.59 ± 4.61	39.33 ± 1.13	39.22 ± 4.67
H (%)	5.24 ± 0.52	5.08 ± 0.31	3.84 ± 0.89	4.49 ± 0.62	4.46 ± 0.46
S (%)	0.45 ± 0.12	0.65 ± 0.07	0.66 ± 0.26	0.55 ± 0.06	0.53 ± 0.03
O (%)	53.56 ± 6.25	51.99 ± 0.54	57.95 ± 6.40	52.37 ± 1.61	52.59 ± 5.45
C/N	13.54 ± 0.95	12.92 ± 0.42	11.88 ± 1.13	12.24 ± 1.76	12.27 ± 0.65

Table A.12 Chemical and physical characterization of digestates from the DF configurations discussed in paragraph 5.3.5.

	DF80	DF80+B1	DF100	DF100+B1	DF100+B2	SingleAD
TS (%)	2.63 ± 0.09	1.80 ± 0.76	1.90 ± 0.42	2.68 ± 0.25	3.06 ± 0.34	2.11 ± 0.13
VS/TS (%)	95.76 ± 0.06	94.90 ± 1.95	91.52 ± 1.00	93.01 ± 0.53	92.85 ± 0.77	95.41 ± 0.90
N (%)	3.23 ± 0.14	3.71 ± 0.11	3.62 ± 0.13	3.37 ± 0.13	3.12 ± 0.13	3.15 ± 0.23
C (%)	39.39 ± 2.70	42.91 ± 1.07	40.93 ± 1.89	36.03 ± 2.29	36.83 ± 2.09	37.32 ± 1.48
H (%)	5.07 ± 0.35	5.59 ± 0.08	5.24 ± 0.22	3.61 ± 0.28	3.24 ± 0.25	5.07 ± 0.17
S (%)	0.61 ± 0.06	0.66 ± 0.02	0.65 ± 0.04	0.56 ± 0.05	0.58 ± 0.04	0.52 ± 0.04
O (%)	51.70 ± 3.25	47.13 ± 1.27	49.57 ± 2.26	56.43 ± 2.75	56.23 ± 2.50	53.94 ± 1.74
C/N	12.19 ± 0.30	11.57 ± 0.19	11.31 ± 0.24	10.69 ± 0.27	11.80 ± 0.26	11.88 ± 0.71

Table A.13 Chemical and physical characterization of digestates from the DF configurations discussed in paragraph 5.3.6.

	TH_80	TH_80_B1	TH_100	TH_100_B1
TS (%)	1.71 ± 0.30	2.03 ± 0.24	1.78 ± 0.02	1.48 ± 0.25
VS/TS (%)	93.63 ± 2.52	94.51 ± 3.82	97.44 ± 3.52	97.13 ± 1.90
N (%)	2.60 ± 0.01	2.41 ± 0.09	2.89 ± 0.14	2.67 ± 0.02
C (%)	35.20 ± 2.02	37.55 ± 0.21	38.15 ± 2.33	38.86 ± 1.48
H (%)	3.61 ± 0.14	3.76 ± 0.01	3.82 ± 0.23	3.87 ± 0.41
S (%)	0.37 ± 0.02	0.33 ± 0.00	0.35 ± 0.02	0.33 ± 0.01
O (%)	58.23 ± 2.13	55.95 ± 0.32	54.79 ± 2.69	54.28 ± 1.86
C/N	13.57 ± 0.82	15.62 ± 0.51	13.20 ± 0.16	14.58 ± 0.67

B. Appendix B

Caldicellulosiruptor bescii: Characteristics and Applications in Biomass Conversion

Recently, depletion of fossil fuels has risen as a global concern arising research on alternative resources for energy and chemicals production. In this context, biomass waste has gained interest as raw material for renewable energy production due to its high content of biodegradable matter. Agricultural residues are particularly appealing for this purpose as they don't take part in the "Food vs. Fuel" dilemma, which considers the issues related to diverting crops for biofuel production pauperizing the food supply. This conflict arises from the limited availability of land on Earth to be intended for food or energy crops cultivation (Muscat et al. 2020). Agricultural residues include crop and plant residues, fruit and vegetable waste, grass and forest residues, manure and many others (S. R. Paudel et al. 2017). Among them, manure is an important feedstock due to its abundancy and relatively high calorific value. On the other hand, its good management is essential due to its CH_4 emissions as well as the contamination of soil with pathogens (Samoraj et al. 2022). Another interesting biomass waste is primary sludge which is collected at the bottom of the primary clarifier in wastewater treatment plants (Sakaveli et al. 2024). Primary sludge has a high energy content due to presence of biodegradable compounds such as proteins, carbohydrates, cellulose and other organic material. Cellulose originated from toilet paper flushed in public sewers and represents 30-50 % of suspended solids in wastewater (Crutchik et al. 2018). Both agricultural residues and primary sludge can be employed as substrate for AD but, even though they contain some easily biodegradable matter, they also contain recalcitrant materials. Agricultural biomass waste is mostly composed of lignocellulosic compounds which are refractory to AD due to the cross-linked structure between lignin, cellulose and hemicellulose. This structure hinders the enzymatic activity during fermentation (J. R. Kim and Karthikeyan 2021; S. R. Paudel et al. 2017). The cellulosic fiber in primary sludge is refractory to AD which hinders the complete degradation of the substrate (Crutchik et al. 2018; B. Liu et al. 2022). Cellulose removal has been reported to be between 2-99 % depending on different conditions. However, most of the studies are carried out in batch system, at relatively low cellulose concentration (less than 10 g/L) and, when continuous system are considered, solid residence time in the digester was short compared to real cases (Bolaji and Dionisi 2021).

As mentioned before, cellulose is not easy to be degraded due to its high order of crystallinity which hinder the enzymatic activity of microorganisms. However, some anaerobic bacteria can effectively grow on cellulose, with an increase in the substrate degradation with temperature. Among the most thermophilic anaerobic bacteria, *Caldicellulosiruptor bescii* (*C. bescii*) grows at 75 °C at neutral pH (S. J. Yang et al. 2009). It can ferment cellobiose, crystalline cellulose, pectin, α- and β-linked glucans and xylan producing lactate, ethanol, acetate, CO_2 and H_2 as fermentation products (Yasemin D. Yilmazel et al. 2015). Moreover, unlikely other species in *Caldicellulosiruptor genus, C. bescii* was able to degrade switchgrass demonstrating its suitability for not only simple sugars but also real plant biomass (Basen et al. 2014). Although it has not been extensively studied since its discovery three decades ago, in the last 15 years some tests have been conducted in order to assess *C. Bescii* suitability in lignocellulosic biomass solubilization.

Yang et al. (2009) investigated the ability of *C. bescii* to grow on complex lignocellulosic substrates in comparison to defined carbohydrates. The bacterium was cultivated at 75 °C on crystalline cellulose and xylan (5 g/L) in 50 mL serum bottles, achieving cell densities of 1.5×10^8 and $\sim 1.0 \times 10^8$ cells/mL, respectively, after 20 hours. The primary fermentation products were hydrogen and acetate, with molar ratios of 2.0 and 1.4 for cellulose and xylan, respectively. These results were compared with growth on lignin-rich biomass substrates, including switchgrass and hardwood poplar (5 g/L), under batch conditions in 0.5 L bottles. Both substrates supported microbial growth comparable to that observed with cellulose and xylan, with final cell densities of 1.3×10^8 and $\sim 1.1 \times 10^8$ cells/mL, respectively. The major fermentation products were again hydrogen and acetate, with molar ratios of 0.97 for switchgrass and 1.3 for poplar, which likely reflects differences in biomass acetylation. However, initial biomass solubilization was limited, reaching only 26 % for switchgrass and 15 % for poplar. The spent residues from the first fermentation were used in two consecutive fermentations to determine whether this was due to substrate recalcitrance. Remarkably, *C. bescii* maintained similar growth rates and cell densities, and cumulative solubilization after 10 days increased to 65.2 % for switchgrass and 36.6 % for poplar. These results demonstrate the organism's capacity to progressively solubilize lignin-rich biomass while producing hydrogen, a promising biofuel.

Kataeva et al. (2013) further evaluated switchgrass solubilization in a 20 L batch reactor, using the water-insoluble fraction of switchgrass (wSG) pretreated at 78 °C at a concentration of 5 g/L. The resulting cell densities exceeded 10^8 cells/mL, consistent with those reported by Yang et al. (2009). The insoluble residues from each fermentation were reused as substrates in two additional cultures. After three sequential fermentations, 85 % of the wSG was solubilized, substantially higher than the 17 % achieved from abiotic incubation, highlighting *C. bescii*'s efficiency in deconstructing recalcitrant biomass. Additionally, lignin metabolism was assessed throughout the fermentation process. The relative lignin content remained constant, indicating that lignin was solubilized concurrently with polysaccharides. These findings underscore the potential of extreme

thermophiles like *C. bescii* for consolidated bioprocessing of lignocellulosic biomass into biofuels.

Basen et al. (2014) investigated the growth of *C. bescii* on high substrate concentrations in a 10 L batch fermenter. The substrates evaluated included crystalline cellulose, water-insoluble switchgrass (wSG), and thermochemically pretreated switchgrass (treated with 0.05 g H_2SO_4 per g dry switchgrass at 190 °C for 5 minutes). *C. bescii* could grow on cellulose concentrations up to 200 g/L, maintaining cell densities above 10^8 cells/mL, although pH control was critical to prevent acidification from lactate and acetate production. Complete cellulose solubilization was observed at concentrations up to 10 g/L, but efficiency declined significantly at higher loads, with only 20 % solubilization achieved at 50 g/L. When grown on wSG at concentrations up to 50 g/L, *C. bescii* demonstrated the ability to degrade 27-33 % of the biomass while sustaining cell densities above 10^8 cells/mL. In contrast, growth on pretreated switchgrass was markedly inhibited at higher concentrations. While *C. bescii* could grow at lower concentrations, its cell density decreased as the substrate concentration increased from 10 to 50 g/L, likely due to the accumulation of inhibitory compounds generated during thermochemical pretreatment. These findings highlight *C. bescii*'s robust capacity to utilize high concentrations of untreated cellulose and wSG, but also its sensitivity to pretreatment-derived inhibitors.

Zurawski et al. (2015) further examined the degradation of cellulose and unpretreated switchgrass by three species of the *Caldicellulosiruptor* genus: *C. bescii*, *C. kronotskyensis*, and *C. saccharolyticus*. Batch cultures (50 mL) were incubated with 5 g/L of switchgrass at 70 °C for 7 days. All three species achieved cell densities exceeding 10^8 cells/mL. However, *C. saccharolyticus* exhibited a slower growth rate, requiring approximately 250 hours to reach this density compared to the ~200 hours needed by *C. bescii* and *C. kronotskyensis*. Cellulose solubilization efficiencies were highest in *C. bescii* and *C. kronotskyensis*, reaching 77.1 % and 71.7 %, respectively, while *C. saccharolyticus* achieved only 58 %. A similar trend was observed for switchgrass solubilization: *C. bescii* and *C. kronotskyensis* solubilized 40.3 % and 39.6 %, respectively, whereas *C. saccharolyticus* reached only 23.5 %, marginally higher than the abiotic thermal solubilization control (19.6 %). These results suggest that *C. saccharolyticus* has limited efficacy in biomass degradation while *C. bescii* demonstrated superior performance in both cellulose and lignocellulosic biomass solubilization, reinforcing its potential as a key organism for the bioconversion of recalcitrant substrates and enhancement of biofuel production processes.

C. bescii was also applied to the fermentation of wastewater biosolids in the study by Yilmazel et al. (2015). Batch fermentations were carried out in 30 mL serum bottles at 78 °C for 15 days, and performance was compared to fermentations using crystalline cellulose. Additionally, co-digestion of biosolids with cellulose was evaluated. Biosolids were tested at concentrations of 5, 2.5, and 1.25 g_{VS}/L, and the production of hydrogen, lactate, and acetate was monitored. At the highest concentration (5 g_{VS}/L), biosolids caused complete inhibition of hydrogen production. At 2.5 g_{VS}/L, inhibition persisted but was less severe, with hydrogen

detected in both biosolids-only and co-digestion configurations. When biosolids were reduced to 1.25 g_{VS}/L, the inhibitory effect was minimal, and hydrogen production was comparable between cellulose-only and co-digested systems. Notably, the maximum hydrogen yield from biosolids alone reached 98.5 mL/g_{VS}, a value considered high relative to other reports in the literature. Regarding organic acid production, lactic acid was not detected when biosolids were fermented alone. In contrast, both lactic and acetic acids were produced in cellulose-containing setups, with acetic acid concentrations peaking at 8.5 mM in the 1.25 g_{VS}/L biosolids co-digestion condition. These results suggest that biosolids are a suitable substrate for hydrogen production by *C. bescii* at concentrations below 2.5 g_{VS}/L, offering high yields and the potential for efficient waste valorization.

The performance of *C. bescii* was also compared with *Clostridium thermocellum* and *Caldicellulosiruptor obsidiansis* in the fermentation of dilute acid-pretreated poplar (Yee et al. 2015). The substrate (5 g/L dry biomass) was added to 2 L batch reactors. *C. thermocellum* operated at 58 °C, while *C. bescii* and *C. obsidiansis* were cultured at 78 °C. The pretreated substrate was predominantly composed of glucan derived from cellulose (600 mg/g dry biomass). Glucan content was reduced to 25 %, 10 %, and 16 % of the initial value by *C. thermocellum*, *C. obsidiansis*, and *C. bescii*, respectively. Although *C. thermocellum* achieved slightly lower overall glucan removal, it exhibited a shorter lag phase and a faster hydrolysis rate. All three organisms effectively hydrolyzed the dilute acid poplar, each offering unique advantages for biomass conversion.

In another study, *C. bescii* was evaluated alongside *C. saccharolyticus* in the fermentation of lignocellulosic garden waste (Abreu et al. 2016). Batch fermentations were conducted in 160 mL bottles at 70 °C for 15 days. Co-cultivation of *C. bescii* and *C. saccharolyticus* led to improved process performance compared to monocultures, enhancing both stability and tolerance to elevated hydrogen partial pressures. The highest hydrogen yield was achieved with the co-culture (98.3 L/kg_{VS}), surpassing the yields from *C. saccharolyticus* (82 L/kg_{VS}) and *C. bescii* (84.6 L/kg_{VS}) alone. This enhanced performance was associated with increased acetate production relative to lactate in the co-culture. The study demonstrates the synergistic potential of mixed cultures in improving lignocellulosic biomass conversion and biohydrogen production.

Traditional and genetically modified switchgrass were fermented using *C. bescii* in 60 mL batch cultures incubated at 70 °C for 12 days. The genetically modified (transgenic) switchgrass contained a lower lignin content compared to the wild-type variety. Both raw and hydrothermally pretreated substrates (treated at 180 °C for 25 minutes) were tested at a concentration of 5 g/L. Across five different switchgrass types, hydrothermal pretreatment consistently enhanced carbohydrate solubilization, with increases ranging from 1.3- to 3.7-fold. The highest degree of solubilization (50 %) was observed for hydrothermally treated, field-grown, non-transgenic switchgrass. This substrate also supported rapid cell growth and high *C. bescii* cell density. Despite its higher lignin content, the unmodified switchgrass was efficiently fermented, underscoring *C. bescii*'s capacity to

degrade recalcitrant biomass. These results also confirm that hydrothermal pretreatment facilitates microbial accessibility and conversion of lignocellulosic substrates (Zurawski et al. 2017).

The effectiveness of *C. bescii* was further investigated in combination with methanogens for anaerobic digestion of birch biomass. Birch was pretreated via steam explosion (210 °C, 10 minutes), and *C. bescii* was introduced into the AD culture at concentrations of 2 %, 5 %, 10 %, and 15 % (v/v) to assess its impact on biogas production. Batch digesters (70 mL working volume) were incubated at 62 °C for 50 days with a substrate-to-inoculum ratio of 2:1 on a volatile solids basis. The highest methane yield (197 mL/g_{VS}) was achieved with the addition of 2% *C. bescii*, although variations between different dosages were minimal. This yield was slightly higher than that from pretreated birch without *C. bescii*, while unpretreated birch yielded only 81 mL/g_{VS}. These findings demonstrate that both steam explosion and the addition of *C. bescii* enhance methane production by improving biomass degradability (Mulat et al. 2018).

In a separate study, traditional and genetically modified poplar lines (with reduced lignin content) were again tested to evaluate *C. bescii*'s capacity to degrade recalcitrant biomass. Fermentations were performed in 150 mL bottles at 65 °C using 5 g/L of substrate. A sharp contrast was observed in solubilization: while traditional switchgrass showed 20-25 % solubilization, the transgenic lines exhibited over 90 % solubilization of both total mass and carbohydrates. These results highlight the synergistic effect of lignin-reducing genetic modifications and *C. bescii* fermentation in achieving high biomass degradation efficiencies (Straub et al. 2019).

C. bescii was also applied to animal-based substrates in a study by Yilmazel and Duran (2021), which investigated its activity on cattle manure (CM). Six combinations of substrates were tested in 30 mL batch cultures at 78 °C for 15 days: (1) CM + biosolids + switchgrass, (2) CM + switchgrass, (3) CM + biosolids, (4) biosolids + switchgrass, (5) CM alone, and (6) switchgrass alone. Hydrogen production in these configurations was 15.0, 11.2, 12.8, 10.7, 9.2, and 6.6 mM, respectively. The highest yield was obtained from the mixture of all three substrates, comparable to yields from crystalline cellulose fermentation. No clear synergistic effect was detected among the three biomass types. Notably, fermentation of cattle manure alone yielded 82.5 mL/g_{VS} of hydrogen which was 1.1 to 36 times higher than values typically reported for conventional dark fermentation processes. These findings reaffirm *C. bescii*'s effectiveness in degrading both plant-based and animal-based lignocellulosic materials.

All the studies discussed so far have examined *Caldicellulosiruptor bescii* in systems ranging from 30 mL to 20 L, which can be categorized as laboratory scale. Hansen et al. (2021) expanded on this by investigating *C. bescii* fermentation at laboratory, bench, and pilot scales. The primary objectives were to identify challenges in scaling up the process and to assess the impact of *C. bescii* fermentation prior to anaerobic digestion on biogas yield enhancement.

In the lab-scale setup, two 1 L pre-digestion reactors inoculated with *C. bescii* (75 °C, retention time = 4 days) were connected in series to a 10 L anaerobic

digester (37 °C, retention time = 12 days). The substrates tested were waste activated sludge (WAS) and anaerobically digested WAS (DWAS). Volatile suspended solids were reduced by 52 % and 69 %, respectively, demonstrating the effectiveness of *C. bescii* in substrate solubilization.

At the bench scale, a batch configuration included two identical systems, each consisting of a 30 L *C. bescii* fermenter (75 °C, retention time = 3-5 days) and a 60 L AD vessel (37 °C). Substrates included WAS, dairy manure, giant king grass (stems and leaves), grass clippings, green waste, grass silage, and corn mash. A second test focused solely on manure using a 2-day retention time in the fermenter. Across all tests, methane and biogas yields increased by an average of 95 % and 87 %, respectively, compared to control systems. In the manure-specific trial, biogas production doubled, and the methane content increased by 10 %, likely due to elevated acetate levels in the effluent from the *C. bescii* fermenter. Volatile solids reduction was also improved, with 44% reduction in the *C. bescii* system versus 24 % in the control.

In the continuous pilot-scale system, *C. bescii* fermentation was carried out in a 1875 L fermenter (75 °C, retention time = 2-4 days), followed by a 1875 L continuously stirred tank reactor (CSTR, 41 °C, retention time = 4-8 days) and a 1875 L induced bed reactor (IBR, 37 °C, retention time = 4-8 days) for AD. Dairy manure was the feedstock for this process. The impact of *C. bescii* on biogas production was measured via VS reduction, which was 19 % and 5 5% higher for 2- and 4-day fermenter retention times, respectively, compared to the control. COD reduction was marginal for the 2-day retention time but increased by 15 % at 4 days. Corresponding biogas yields were significantly enhanced, increasing from 493 to 584 L/kg_{VS} and from 283 to 493 L/kg_{VS} for 2- and 4-day fermentations, respectively, relative to the control.

Across all scales and substrates tested, the integration of *C. bescii* fermentation consistently enhanced biogas production and methane content. These improvements are attributed to the production of acetate and lactate by *C. bescii*, which serve as favorable intermediates for methanogenesis. In the specific case of cattle manure, *C. bescii* enabled greater volatile solids degradation and biogas yield.

Overall, the literature demonstrates the beneficial role of *C. bescii* in the fermentation of recalcitrant biomass. This thermophilic bacterium produces enzymes capable of breaking down lignocellulosic materials, resulting in a gaseous phase rich in hydrogen and a liquid phase enriched in acetate and lactate, both of which enhance subsequent anaerobic digestion and energy recovery.

Given these considerations, *C. bescii* is a valuable bacterium for waste stabilization, solubilization of recalcitrant biomass, and hydrogen production, while also minimizing contamination from hydrogen-consuming microorganisms. Although its potential has been recognized, relatively few studies have investigated its performance on real lignocellulosic waste materials. *C. bescii* is known to utilize a broad range of carbon sources, including crystalline cellulose, and has also demonstrated the ability to degrade actual biomass waste such as

switchgrass and cattle manure. However, research on the kinetics of *C. bescii* remains limited.

Bacterial growth is generally influenced by substrate availability and follows a non-linear relationship described by the Monod equation:

$$\mu = \mu_{max} \frac{[S]}{k_s + [S]} \tag{B.1}$$

where μ is the net specific growth rate (g_{VSS}/g_{VSS} d), μ_{max} is the maximum specific biomass growth rate (g_{VSS}/g_{VSS} d), k_s is the half velocity constant (g/m^3), and *[S]* is the substrate concentration (g/m^3). This model is based on 5 assumptions: when the maximum growth rate is reached, the addition of substrate will not influence this value; at low substrate concentration, the growth rate depends on substrate concentration; the model is not valid when there is substrate inhibition; it is ignored the need of substrate for cell maintenance during stationary phase; kinetic does not take into consideration the lag, stationary and death phase (Owoade et al. 2025).

Concerning the kinetics of *C. bescii*, and within the framework of the Monod equation, some data are available on specific growth rates (μ_{max}) and doubling times, the latter defined as the time required for a microbial population to double in size. Reported μ_{max} values (in h^{-1}) are 0.67 for glucose, 0.57 for cellobiose, 0.24 for C5 xylose, 0.43 for xylan, 0.40 for crystalline cellulose, 0.34 for unpretreated switchgrass, and 0.37 for pretreated switchgrass. Doubling times have also been reported for crystalline cellulose and unpretreated switchgrass, at 1.7 and 1.9 hours, respectively (Poudel et al. 2018). As substrate complexity increases, specific growth rates tend to decrease, as expected. Additionally, the growth rate on unpretreated switchgrass is slightly lower than its pretreated counterpart. Although the available data are consistent, comprehensive kinetic studies on *C. bescii* remain limited, leaving a promising area for further investigation.

An additional research gap concerns the transition from batch to continuous *C. bescii* fermentation systems. This shift is particularly important for the design of large-scale processes, where continuous operation is essential to maintain system stability. In *C. bescii* fermentation, substrates are converted into a hydrogen-rich gas phase and volatile fatty acids (VFAs), which can lead to a decline in pH. Since *C. bescii* requires a neutral pH for optimal growth, the accumulation of acids can inhibit microbial activity if not properly controlled. Therefore, the system's buffering capacity becomes a critical parameter for efficient substrate conversion. A continuous configuration can help manage this challenge by facilitating the removal of VFAs, thereby optimizing the interaction between microorganisms and the substrate. Within this context, HRT emerges as a key variable, as it influences both the flow rates within the reactor and the fluxes of metabolites (Santhosh and Mohan 2025).

To date, most studies employing *C. bescii* have relied on batch configurations, ranging from small- to bench-scale setups. The only reported continuous system

was presented by Hansen et al. (2021), who tested *C. bescii* fermentation at pilot scales. In the experiment, cattle manure served as the substrate, and a higher VS reduction was observed following *C. bescii* treatment. However, the retention time in the digester proved to be a crucial parameter, as it significantly influenced the microbial metabolism of the manure. For optimal performance, the retention time must be sufficient to allow *C. bescii* to remain in an active growth phase, thereby enhancing metabolic and enzymatic activity. In Hansen's study, the fermenter retention time ranged between 2 and 4 days. At 2 days, microbial washout likely occurred, whereas at 4 days, *C. bescii* reached the stationary phase, limiting further metabolic activity. These findings suggest that an optimal HRT for efficient manure fermentation lies between 2 and 4 days.

These results contrast markedly with those from bench-scale batch tests, where retention times ranged from 15 to 20 days. This highlights the significant impact of system configuration on time-related parameters and underscores the importance of carefully selecting appropriate retention times during scale-up. Another critical factor is the interdependence between the retention time in the fermenter and that in the subsequent anaerobic digester. Because these parameters are tightly linked, adjustments in one necessitate corresponding changes in the other to ensure effective VS removal. Neglecting this interdependence can result in either overfeeding the anaerobic digester, potentially overwhelming the system, or underfeeding it, which would prevent methanogenic microorganisms from maintaining growth and activity due to insufficient substrate availability.

Based on the results obtained so far, several challenges have emerged regarding the integration of *C. bescii* into mesophilic anaerobic digestion systems. Much of the existing research has focused on the isolated application of *C. bescii* for the degradation of lignocellulosic biomass, such as switchgrass or poplar. While some studies have demonstrated its capacity to efficiently degrade these recalcitrant substrates, the complexity of the biomass has led researchers to propose sequential fermentation strategies to better manage refractory compounds (S. J. Yang et al. 2009; Kataeva et al. 2013). However, complete solubilization of the substrate has not been achieved; the highest reported solubilization of the water-insoluble fraction of switchgrass reached only 85 % (Kataeva et al. 2013). Implementing a system requiring multiple fermenters would add significant complexity and cost compared to conventional anaerobic digestion processes.

Another key challenge in *C. bescii*-based biomass fermentation is the accumulation of VFAs in the liquid phase as a result of microbial metabolism. Alongside hydrogen production, VFAs are generated during biomass conversion, leading to pH reduction. This acidification can inhibit microbial activity and potentially cause process failure if not properly controlled (Basen et al. 2014). Additionally, substrate concentration can influence *C. bescii* growth, as certain feedstocks may contain inhibitory compounds. For instance, biosolids fermented at various concentrations showed that hydrogen production by *C. bescii* only occurred at concentrations below 2.5 g/L, with peak production observed at 1.25 g/L. These findings were attributed to the toxic effects of biosolids, likely due to

the presence of heavy metals and antimicrobial agents (Yasemin D. Yilmazel et al. 2015).

Currently, many of the challenges in implementing *C. bescii* within anaerobic digestion systems arise from the limited scope of fermentation studies, particularly with respect to substrate diversity and operational conditions. While crystalline cellulose and switchgrass have been frequently studied, substrates such as manure and primary sludge remain largely unexplored in the context of *C. bescii* metabolism.

Several studies have explored the use of *C. bescii* as a first-stage fermenter in a process analogous to two-stage anaerobic digestion. In this configuration, the substrate is initially fermented by *C. bescii* and subsequently fed into an anaerobic digester for methane production. Hansen et al. (2021) investigated this process across three different scales using various substrates. Overall, *C. bescii* fermentation was shown to positively influence methane yields, primarily through the release of acetate, a key precursor in methanogenesis. However, the lack of consistency in substrate choice across the lab-, bench-, and pilot-scale systems limits the ability to perform a proper scale-up analysis. Moreover, the pilot-scale experiments operated under continuous conditions, while the bench-scale setup was batch-operated and the lab scale was in semi-continuous mode, complicating any time-based comparisons.

In continuous systems, retention time was found to be a critical factor in maintaining *C. bescii* activity. Despite this, other important aspects, such as the fate of *C. bescii* in the downstream anaerobic digester, were not fully explored. Since a portion of the fermenter effluent containing *C. bescii* is transferred to the digester, understanding its interaction with the native methanogenic community is essential. Mulat et al. (2018) examined this interaction and demonstrated *C. bescii*'s role in enhancing methane production. Although microbial community analyses failed to detect *C. bescii* in the bioaugmented reactors, its beneficial impact was evident. When *C. bescii* was added at a concentration of 2%, methane yields improved; in contrast, higher concentrations or complete absence of the bacterium showed no such enhancement. In the optimal configuration, the microbial community was dominated by hydrogenotrophic *Methanothermobacter* and hydrolytic *Caldicoprobacter*, suggesting that *C. bescii* may have facilitated the development of a highly efficient microbiota capable of degrading recalcitrant biomass. Although *C. bescii*'s presence appeared to influence community composition, its persistence within the system remains unclear. The authors suggested that *C. bescii* remained active for approximately nine days before being surmounted by indigenous microorganisms. These findings indicate that *C. bescii* can survive temporarily within anaerobic digesters and contribute to improved substrate degradation during that period.

Based on the preceding assumptions, integrating *C. bescii* into anaerobic digestion systems could potentially optimize CH_4 production from both primary sludge and digested cattle manure, where unconverted recalcitrant biomass remains a limiting factor.

References

Abreu, Angela A., Fábio Tavares, Maria Madalena Alves, and Maria Alcina Pereira. 2016. "Boosting Dark Fermentation with Co-Cultures of Extreme Thermophiles for Biohythane Production from Garden Waste." *Bioresource Technology* 219 (November): 132–38. https://doi.org/10.1016/j.biortech.2016.07.096.

Basen, Mirko, Amanda M. Rhaesa, Irina Kataeva, et al. 2014. "Degradation of High Loads of Crystalline Cellulose and of Unpretreated Plant Biomass by the Thermophilic Bacterium Caldicellulosiruptor Bescii." *Bioresource Technology* 152: 384–92. https://doi.org/10.1016/j.biortech.2013.11.024.

Bolaji, I. O., and D. Dionisi. 2021. "Experimental Investigation and Mathematical Modelling of Batch and Semi-Continuous Anaerobic Digestion of Cellulose at High Concentrations and Long Residence Times." *SN Applied Sciences* 3 (9). https://doi.org/10.1007/s42452-021-04750-x.

Crutchik, Dafne, Nicola Frison, Anna Laura Eusebi, and Francesco Fatone. 2018. "Biorefinery of Cellulosic Primary Sludge towards Targeted Short Chain Fatty Acids, Phosphorus and Methane Recovery." *Water Research* 136: 112–19. https://doi.org/10.1016/j.watres.2018.02.047.

Hansen, Jaron C, Zachary T Aanderud, Lindsey E Reid, et al. 2021. "Enhancing Waste Degradation and Biogas Production by Pre-Digestion with a Hyperthermophilic Anaerobic Bacterium Enhancing Waste Degradation and Biogas Production by Pre-Digestion with a Hyperthermophilic Anaerobic Bacterium Enhancing Waste Degradation and Biogas Production by Pre-Digestion with a Hyperthermophilic Anaerobic Bacterium." *Biofuel Research Journal* 31: 1433–43. https://doi.org/10.18331/BRJ2021.8.3.

Kataeva, Irina, Marcus B. Foston, Sung Jae Yang, et al. 2013. "Carbohydrate and Lignin Are Simultaneously Solubilized from Unpretreated Switchgrass by Microbial Action at High Temperature." *Energy and Environmental Science* 6 (7): 2186–95. https://doi.org/10.1039/c3ee40932e.

Kim, Joonrae Roger, and K. G. Karthikeyan. 2021. "Solubilization of Lignocellulosic Biomass Using Pretreatments for Enhanced Methane Production during Anaerobic Digestion of Manure." *ACS ES and T Engineering* 1 (4): 753–60. https://doi.org/10.1021/acsestengg.0c00226.

Liu, Baojie, Lu Liu, Baojuan Deng, et al. 2022. "Application and Prospect of Organic Acid Pretreatment in Lignocellulosic Biomass Separation: A Review." *International Journal of Biological Macromolecules* 222 (December): 1400–1413. https://doi.org/10.1016/j.ijbiomac.2022.09.270.

Mulat, Daniel Girma, Silvia Greses Huerta, Dayanand Kalyani, and Svein Jarle Horn. 2018. "Enhancing Methane Production from Lignocellulosic Biomass by Combined Steam-Explosion Pretreatment and Bioaugmentation with Cellulolytic Bacterium Caldicellulosiruptor Bescii." *Biotechnology for Biofuels* 11 (1). https://doi.org/10.1186/s13068-018-1025-z.

Muscat, A., E. M. de Olde, I. J.M. de Boer, and R. Ripoll-Bosch. 2020. "The Battle for Biomass: A Systematic Review of Food-Feed-Fuel Competition." *Global Food Security* 25 (June). https://doi.org/10.1016/j.gfs.2019.100330.

Owoade, Ademola, Ali S. Alshami, Richard Sparling, and David Levin. 2025. "Kinetic Analysis of Phenotypic and Growth Variations in Clostridium Autoethanogenum across Two Xylose Concentration Ranges." *Biofuels, Bioproducts and Biorefining*, ahead of print, May 1. https://doi.org/10.1002/bbb.2748.

Paudel, Shukra Raj, Sushant Prasad Banjara, Oh Kyung Choi, Ki Young Park, Young Mo Kim, and Jae Woo Lee. 2017. "Pretreatment of Agricultural Biomass for Anaerobic Digestion: Current State and Challenges." *Bioresource Technology* 245: 1194–205. https://doi.org/10.1016/j.biortech.2017.08.182.

Poudel, Suresh, Richard J. Giannone, Mirko Basen, et al. 2018. "The Diversity and Specificity of the Extracellular Proteome in the Cellulolytic Bacterium Caldicellulosiruptor Bescii Is Driven by the Nature of the Cellulosic Growth Substrate." *Biotechnology for Biofuels* 11 (1). https://doi.org/10.1186/s13068-018-1076-1.

Sakaveli, Foteini, Maria Petala, Vasilios Tsiridis, and Efthymios Darakas. 2024. "Enhancing Methane Yield in Anaerobic Co-Digestion of Primary Sewage Sludge: A Comprehensive Review on Potential Additives and Strategies." *Waste* 2 (1): 29–57. https://doi.org/10.3390/waste2010002.

Samoraj, Mateusz, Małgorzata Mironiuk, Grzegorz Izydorczyk, et al. 2022. "The Challenges and Perspectives for Anaerobic Digestion of Animal Waste and Fertilizer Application of the Digestate." *Chemosphere* 295 (January). https://doi.org/10.1016/j.chemosphere.2022.133799.

Santhosh, J., and S. Venkata Mohan. 2025. "Self-Regulation of System Buffering through Flow Rate Optimization in Continuous Acidogenic Fermentation for Enhanced Biohydrogen

Production." *International Journal of Hydrogen Energy* 100 (January): 1315–28. https://doi.org/10.1016/j.ijhydene.2024.12.119.

Straub, Christopher T., Piyum A. Khatibi, Jack P. Wang, et al. 2019. "Quantitative Fermentation of Unpretreated Transgenic Poplar by Caldicellulosiruptor Bescii." *Nature Communications* 10 (1). https://doi.org/10.1038/s41467-019-11376-6.

Yang, Sung Jae, Irina Kataeva, Scott D. Hamilton-Brehm, et al. 2009. "Efficient Degradation of Lignocellulosic Plant Biomass, without Pretreatment, by the Thermophilic Anaerobe 'Anaerocellum Thermophilum' DSM 6725." *Applied and Environmental Microbiology* 75 (14): 4762–69. https://doi.org/10.1128/AEM.00236-09.

Yee, Kelsey L., Miguel Rodriguez, Choo Y. Hamilton, et al. 2015. "Fermentation of Dilute Acid Pretreated Populus by Clostridium Thermocellum, Caldicellulosiruptor Bescii, and Caldicellulosiruptor Obsidiansis." *Bioenergy Research* 8 (3): 1014–21. https://doi.org/10.1007/s12155-015-9659-1.

Yilmazel, Yasemin D., David Johnston, and Metin Duran. 2015. "Hyperthermophilic Hydrogen Production from Wastewater Biosolids by Caldicellulosiruptor Bescii." *International Journal of Hydrogen Energy* 40 (36): 12177–86. https://doi.org/10.1016/j.ijhydene.2015.06.140.

Yilmazel, Yasemin Dilsad, and Metin Duran. 2021. "Biohydrogen Production from Cattle Manure and Its Mixtures with Renewable Feedstock by Hyperthermophilic Caldicellulosiruptor Bescii." *Journal of Cleaner Production* 292 (April). https://doi.org/10.1016/j.jclepro.2021.125969.

Zurawski, Jeffrey V., Jonathan M. Conway, Laura L. Lee, et al. 2015. "Comparative Analysis of Extremely Thermophilic Caldicellulosiruptor Species Reveals Common and Unique Cellular Strategies for Plant Biomass Utilization." *Applied and Environmental Microbiology* 81 (20): 7159–70. https://doi.org/10.1128/AEM.01622-15.

Zurawski, Jeffrey V, Piyum A Khatibi, Hannah O Akinosho, et al. 2017. *Bioavailability of Carbohydrate Content in Natural and Transgenic Switchgrasses for the Extreme Thermophile Caldicellulosiruptor Bescii*. https://journals.asm.org/journal/aem.